The University of Nottingham

UNITED KINGDOM · CHINA · MALAYSIA

Tissue engineering in hostile environments:

The effects and control of inflammation

in bone tissue engineering.

Laura Sidney, MEng (Hons)

Thesis submitted to the University of Nottingham

for the degree of Doctor of Philosophy

May 2013

Abstract

The potential effects of introducing bone regeneration strategies into environments of disease and damage are often overlooked, despite the fact that many of the signalling pathways in inflammation have effects on bone development and healing. Embryonic stem cells (ESCs) are increasingly being used to develop models of disease and have potential in osteogenic-cell based therapies. Osteogenic differentiation strategies for ESCs are well established, but the response of these cells to tissue damage and inflammation has not yet been investigated, particularly in comparison to primary osteoblasts. Here, proinflammatory cytokines were used as part of an *in vitro* model to mimic elements of skeletal disease, such as rheumatoid arthritis and non-union fractures. The response of osteogenically differentiated mouse embryonic stem cells (osteo-mESCs) to the proinflammatory cytokines interleukin 1-β (IL-1β), tumour necrosis factor-α (TNF-α) and interferon-γ (IFN-γ), was compared to that of primary mouse calvarial osteoblasts, already well-described in literature and used as a "benchmark" in this study. Although histology, immunocytochemistry and PCR showed similarities in osteogenic differentiation of the osteo-mESCs and the primary calvarial cells, over 21 days in culture, there were marked differences in the response to the proinflammatory cytokines. Viability of the osteo-mESCs was maintained in response to cytokines, whereas viability of primary cells was significantly reduced. There were marked increases in nitric oxide (NO) and prostaglandin E_2 (PGE_2) production in primary calvarial cells over the entire 21-day culture period, but this was not seen with osteo-mESCs until day 21. The study then went on to look at the effects of proinflammatory signalling on the *in vitro* bone formation of the two cell types. Significant differences in the effects of proinflammatory cytokines on bone nodule

formation and matrix production were seen when comparing the osteo-mESCs and the calvarial cells. This study demonstrates that while osteo-mESCs share phenotypic characteristics with primary osteoblasts, there are some distinct differences in their biochemistry and response to cytokines. This is relevant to understanding differentiation of stem cells, developing *in vitro* models of disease, testing new drugs and developing cell therapies.

An additional objective in this investigation was to look at tissue engineering strategies as a means of controlling inflammation in bone disease. The primary calvarial osteoblasts were utilised as an *in vitro* inflammation model, and used to study the effects of anti-inflammatory mediators. Anti-inflammatory-releasing porous scaffolds were manufactured from poly(lactic-co-glycolic acid) (PLGA) and poly(ethylene glycol) (PEG). The calvarial osteoblast inflammation model was used successfully to show successful release of diclofenac sodium from the PLGA/PEG scaffolds. This study demonstrates that there is much to consider in the development of regenerative strategies for bone disease, particularly the role that the effect and control of inflammation will play in bone healing.

Acknowledgements

There are many people to whom I owe gratitude, and would like to thank, for helping me to reach this point.

I would like to begin by thanking my supervisor Dr Lee Buttery for the opportunity to undertake a project in which I had a great deal of interest, and for allowing me the freedom to work independently and take the investigation down the paths I found the most fascinating. I would also like to thank Professor David Walsh for guidance offered in the first year of my studies.

Thanks go to all involved in the EPSRC Doctoral Training Centre in Regenerative Medicine, for accepting me to be part of the “guinea pig” year, enabling me to be able to investigate this subject, and particularly for offering me the funding to be able to visit Toronto and Vienna.

Much appreciation goes to the members of Team Buttery, who have offered practical advice and support, as well as companionship and camaraderie. Particularly, Dr Glen Kirkham, who passed on so many words of wisdom and was responsible for the majority of my training. I’d like to acknowledge Adam Taylor, who shared the burden of the primary cell extractions, serum batch testing and allowed me to feel as if I too, had words of wisdom to pass on. Thanks to Sue Dodson for my initial training in mESC culture and Dr Cheryl Rahman for training, not only me, but also my students, in the PLGA/PEG scaffold manufacture.

From September to November 2011, I found myself welcomed into the lab at the University of Toronto, and I would like to give special thanks to Frieda Chen for taking

me under her wing. To Jane Aubin and the members of her lab: Kristen, Dana, Tanya, Marco, Ralph and Jonathan, for making it a brilliant two months and for introducing me to the delights of pumpkin pie.

Much appreciation goes to the students who have assisted in data gathering. The DTC mini-project students, Tom, Arif and Emily, who dealt admirably with the heavy workload, the endless scaffold manufacture and spur of the moment decisions. Thanks to Minu Anoop, for assisting with the optimisation of osteogenic differentiation.

I would like to thank all my friends in the Tissue Engineering group at the University of Nottingham and all my DTC compatriots for keeping me sane with much entertainment and many welcome distractions. Especially to Mike, Toby and Giles, who have been a constant support through the 3 years at Nottingham. Outside the world of Nottingham, I would like to acknowledge the support of Jules and Russ, who had the same experience, just in a different place. In addition, thanks to my friends outside the realm of science, particularly Amo, Kaylee, Helena, Sam, Sapna and Ollie.

Lastly, I would like to thank my family for their ongoing support. To my sister, Anne Sidney, I am grateful for all the support from afar and for allowing me escape when I needed it. Most importantly, I would like to thank my parents, Robert and Valerie Sidney, as without their encouragement, I'm not sure I would have made it anywhere near this far.

Table of Contents

List of Figures

Chapter 1: General Introduction

Chapter 2: Materials and Methods

Chapter 3: Effect of Proinflammatory Stimulus on Osteogenic Cell Response

Chapter 4: Effect of Proinflammatory Cytokines on Osteogenic Differentiation of mESCs and Primary Calvarial Cells

Chapter 5: Control of Inflammation: An In Vitro Osteoblast Model and Testing and Manufacture of Anti-Inflammatory Scaffolds

Appendices

List of Tables

List of Abbreviations

ALP	Alkaline Phosphatase
AP-1	Activator Protein-1
bFGF	Basic Fibroblast Growth Factor
BGP	β-GlyceroPhosphate
BMD	Bone Mineral Density
BMP	Bone Morphogenetic Protein
BSA	Bovine Serum Albumin
BSP	Bone Sialoprotein
Cad-11	Cadherin-11
Cbfa-1	Core Binding Factor a-1
cDNA	Complementary DNA
CEE	Columnar Epiblast Epithelium
CM	Conditioned Medium
Col-I	Collagen-1
COX(-1)(-2)	Cyclooxygenase (-1)(-2)
C_T	Threshold Cycle
DBM	Demineralised Bone Matrix
DMARD	Disease Modifying Anti-Rheumatic Drug
DMEM	Dulbecco's Modified Eagle's Medium
DMSO	Dimethyl Sulfoxide
DNA	Deoxyribonucleic Acid
dNTP	Deoxynucleotide triphosphate
E	Efficiency
EB	Embryoid Body
ECM	Extracellular Matrix
EDTA	Ethylenediaminetetraacetic Acid
EIA	Enzyme Immuno Assay
EMA	European Medicines Agency
eNOS	Endothelial Nitric Oxide Synthase
ESC	Embryonic Stem Cell

EthD-1	Ethylene Homodimer-1
FACS	Fluorescence Activated Cell Sorting
FBS	Foetal Bovine Serum
FDA	Food and Drug Administration (US)
g	Centrifugal G Force
GR	Glucocorticoid Receptor
GVHD	Graft Versus Host Disease
HA	Hydroxyapatite
HEPA filter	High Efficiency Particulate Air filter
hESC	Human Embryonic Stem Cell
HLA	Human Leukocyte Antigen
HRP	Horseradish Peroxidase
HSC	Haematopoietic Stem Cell
IFN	Interferon
IGF(-I,-II)	Insulin-like Growth Factors (-I,-II)
IKK	IκB Kinase
IL(-1)(-6)(-17)	Interleukin (-1)(-6)(-17)
IL-1ra	Interleukin-1 receptor antagonist
iNOS	Inducible Nitric Oxide Synthase
iPSC	Induced Pluripotent Stem Cell
JAK	Janus Kinase
LDH	Lactate Dehydrogenase
LIF	Leukaemia Inhibitory Factor
MACS	Magnetic Activated Cell Sorting
MAPK	Mitogen-Activated Protein Kinase
MEF	Mouse Embryonic Fibroblast
mESC	Mouse Embryonic Stem Cell
MHC	Major Histocompatibility Complex
MMP	Matrix Metalloproteinase
MSC	Mesenchymal Stem Cell
MTS	3-(4,5-dimethylthiazol-2-yl)-5-(3-carboxymethoxyphenyl)-2-(4-sulfonyl)-2H-tetrazolium
NAD+ (P)	Nicotinamide Adenine Dinucleotide (Phosphate)
NED	N-(1-napthyl)ethylenediamine
NF	Nuclear Factor

NK	Natural Killer
nNOS	Neuronal Nitric Oxide Synthase
NO	Nitric Oxide
NOS	Nitric Oxide Synthase
NSAID	Non-Steroidal Anti-Inflammatory Drug
OA	Osteoarthritis
OCN	Osteocalcin
OM	Osteogenic Medium
OPG	Osteoprotegerin
OPN	Osteopontin
Osteo-mESC	Osteogenically-differentiated mESC
OSX	Osterix
OTA	Orthopaedic Trauma Association
PBS	Phosphate Buffered Saline
PCR	Polymerase Chain Reaction
PDGF	Platelet Derived Growth Factor
PEG	Poly(ethylene glycol)
Pen-Strep	Penicillin-Streptomycin
PES	Phenazine Ethosulphate
PFA	Paraformaldehyde
PG(E_2)	Prostaglandin (E_2)
PGES	Prostaglandin E Synthase
PLGA	Poly(lactic-co-glycolic acid)
pNP(P)	p-Nitrophenyl (phosphate)
PTFE	Poly(tetrafluoroethylene)
RA	Rheumatoid Arthritis
RNA	Ribonucleic Acid
RT-qPCR	Real Time quantitative PCR
SCNT	Somatic Cell Nuclear Transfer
SDS	Sodium Dodecyl Sulphate
SIM	Sandoz Inbred Mice
SNL	STO Neomycin-resistant and LIF-transformed.
SSC	Saline Sodium Citrate
SSEA	Stage Specific Embryonic Antigen
STATs	Signal transducers and activators of transcription

STO	(SIM) Thioguanine-resistant and Ouabain-resistant
TAZ	Transcriptional co-activator with PDZ-binding motif
T_g	Glass transition temperature
TGF-β	Transforming Growth Factor-β
TLR	Toll-Like Receptor
TNF	Tumour Necrosis Factor
TRAP	Tartrate-Resistant Acid Phosphatase
U	Units
UV/Vis	Ultraviolet/Visible
w/v	Weight per Volume
αMEM	Minimum Essential Media Alpha

Chapter 1:
General Introduction

1.1 Tissue Engineering and Regenerative Medicine

1.1.1 Background and Overview

Tissue engineering is a discipline that aims to combine the principles of engineering and life sciences in the production of biological substitutes to restore, maintain or improve tissue function. A tissue engineering strategy may be applied *in vivo* to induce regeneration within the body, or can be developed *in vitro* to provide a functional alternative before implantation into the body [1]. Classically, tissue engineering strategies involve three general principles: the use of isolated cells or cell substitutes; tissue-inducing substances such as signal molecules and growth factors and supportive matrices or scaffolds, with and without the incorporation of cells [2] (see figure 1.1).

The field and term “regenerative medicine” has been more recently developed and encompasses the same final goal as tissue engineering: replacement or regeneration of human cells, tissues or organs. However, regenerative medicine tends to be more focused on biological principles, and revolves around the use of stem cells [3, 4]. The regenerative medicine term was originally embraced to distance researchers from the original “tissue engineering” moniker, after business failure of early tissue engineering

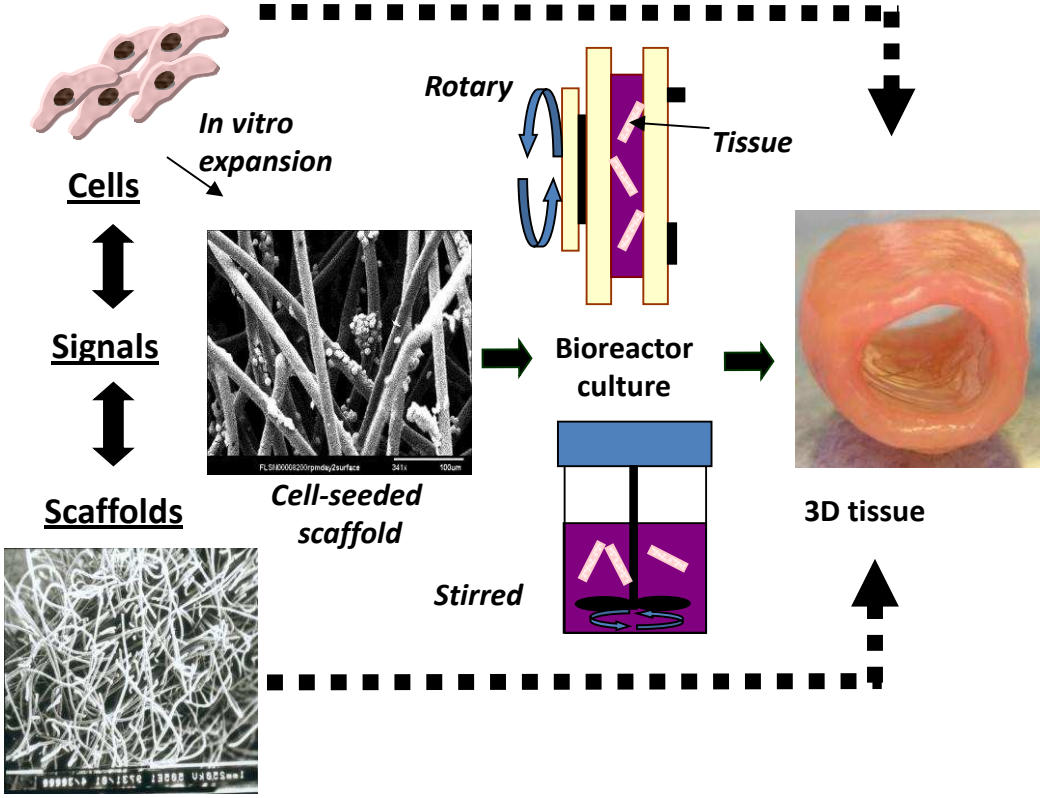

Figure 1.1: Tissue engineering. The premise of tissue engineering is centred around three core elements: cells, signals and scaffolds; designed to work together to produce a regenerative therapy for the body. There are several possible cell sources: primary sources, adult stem cells and embryonic/induced pluripotent cells. Cells may be combined with a scaffold that is designed to complement the biology of the cells and the tissue. Bioreactor culture can be used to produce a 3D-tissue before implantation into the body or alternatively, cells and scaffolds can be implanted with minimum *in vitro* culture, allowing the body to serve as a natural bioreactor.

products. However more recently, the term has been used to encompass pharmaceutical and biotech products, such as those containing growth hormones and bone morphogenetic proteins (BMPs), rather than the cell therapies it was originally aimed at [5]. Despite this, the terms “tissue engineering” and “regenerative medicine” are often used interchangeably.

1.1.2 Stem Cell Research and Cell Therapies

1.1.2.i Stem cell research

Stem cells exist as part of the developmental continuum, playing a crucial role in the progression of human life. The term “stem cell” can be a broad label. The basic definition incorporates cells that can continually divide and reproduce themselves, whilst maintaining the ability to differentiate into other cell types. A schematic of stem cell renewal can be seen in figure 1.2. This would include the totipotent stem cell that can give rise to all the cells of the developing embryo, including extra-embryonic tissues such as the placenta, the pluripotent embryonic stem cell (ESC), and the multipotent somatic adult stem cell, found within the mature human body.

Stem cell research is a comparatively modern phenomenon and has a short history featuring some very large technical advances. The first stem cell was proven to exist in 1961 when the haematopoietic stem cell (HSC) was identified in the bone marrow [6]. The discovery of the mouse embryonic stem cell (mESC) in 1981 generated much promise, and allowed a simple way of studying embryogenesis and development [7-9]. The first human embryonic stem cell (hESC) was isolated in 1998 [10] and with the development of induced pluripotent stem cells (iPSCs) in 2006, the field of stem cell research is ever expanding [11] .

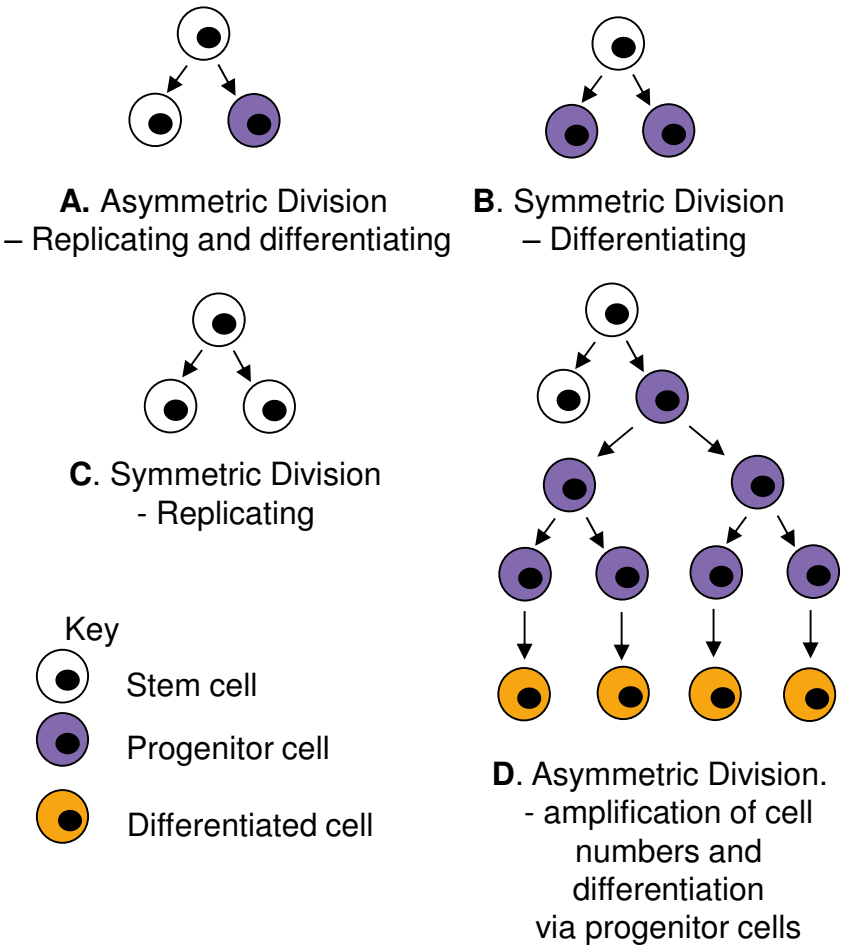

Figure 1.2: Stem cell renewal and differentiation. The purpose of stem cells is to give rise to specific differentiated cells, enabling our bodies to grow and function normally. Possible mechanisms of stem cell self-renewal are represented in figure A-C. **(A)** Asymmetric division, replicating and differentiating is the most classic process, with one stem cell giving rise to two daughter cells, one remaining identical to itself and the other going on to differentiate. **(B and C)** Symmetric division, one stem cell either giving rise to two differentiating cells or two more stem cells. **(D)** Generation of progenitor / transit amplifying cells. The role of progenitor cells is to enter into several rounds of division increasing cell numbers. With each division the progenitor may become progressively more differentiated and eventually stops dividing, having acquired the characteristics of a fully differentiated cell type.

1.1.2.ii The cell therapy industry

The cell therapy industry is considered by some to be distinct from regenerative medicine and is the therapeutic application of cells, regardless of cell type or clinical application [5]. Cell therapies have origins in blood transfusion, bone marrow transplantation and organ transplantation. Although the definition expresses that any cell type can be used, most often the cells are stem cell related. The market for cell therapies is rapidly expanding and clinical targets include heart disease, diabetes, neurodegenerative disorders, musculoskeletal disorders and spinal cord injury. The industry is now worth more than US$1 billion, and predicted to grow to more than US$3 billion by 2014 [12, 13]. Historically, the most successful cell therapies have been blood transfusions and bone marrow transplantations, but these were developed before a cell therapy industry existed. In recent times, progressing cell therapies to market can be difficult due to regulatory hurdles. Some therapies have been US Food and Drug Administration (FDA) and European Medicines Agency (EMA) approved, including Provenge (Dendreon Corporation), a cell-based cancer vaccine, and Carticel (Genzyme Biosurgery), an autologous cultured chondrocyte therapy [14]. Regulatory approval is not the only hurdle in getting cell therapies to market. The therapy needs to prove efficacy and improve upon existing medicine. This is where the importance of stem cell research is apparent. Knowledge of cell behaviour in different environments, and how control of cell behaviour may be integrated into a therapy, could play an important part in the success or failure of future cell-based products.

1.1.3 Bone Tissue Engineering

1.1.3.i Background and clinical need

Tissue engineering of bone is a rapidly expanding field and many different approaches are in creation. Clinical indications that call for a tissue-engineered bone substitute include defects caused by trauma, tumours and infections, non-union fractures and bone diseases such as osteoporosis and rheumatoid arthritis. The current “gold standard” treatments for defects are autologous or allogeneic bone grafts, or the use of metals and ceramics to fill the defect and support the bone as it attempts to heal [15, 16]. Although many of the current strategies for bone regeneration produce relatively satisfactory results, there are limitations and drawbacks to each treatment. In many cases, autologous bone grafts cannot be performed due to unavailability and donor site morbidity. Allogeneic grafts also carry disadvantages due to immune rejection and pathogen transmission [17]. The use of synthetic bone substitutes are disadvantageous because they rarely have superior or similar biological and mechanical properties, compared to natural bone.

1.1.3.ii Bone tissue engineering strategies

Due to lack of available treatments and successful cures for the diseases mentioned above, the tissue engineering and regenerative medicine fields are hoping to be able to create new and successful therapies. Strategies investigated thus far include biomaterial scaffolds alone, scaffolds loaded with growth factors, cell therapies and scaffolds loaded with cells [17-19].

1.1.3.ii.a Biomaterials Strategies

A biomaterial scaffold needs to attempt to replicate the natural extracellular matrix (ECM) of the tissue and therefore will influence cell attachment, migration, proliferation and differentiation. Scaffolds for bone regeneration require biocompatibility, porosity, correct mechanical properties, biodegradability, osteoconductive properties to promote osteogenic cell adhesion and proliferation, and osteoinductive properties to recruit stem and progenitor cells [17]. These properties can be achieved in several different ways, by adjusting materials selection, material processing, surface engineering and incorporation of cells or growth factors.

1.1.3.ii.b Growth Factor Therapies

Improved knowledge of bone healing and regeneration pathways has led to the identification of a number of key molecules that help to regulate the process. Some have been put into clinical use to enhance bone repair. The BMP family of molecules is one of the most extensively studied. BMPs are potent osteoinductive factors that can cause mitogenesis of mesenchymal stem cells (MSCs) and differentiation towards osteoblasts, inducing bone formation [20]. BMP-2 and BMP-7 have been licensed for clinical use since 2002 and 2001, respectively [21, 22]. The INFUSE® Bone Graft featuring BMP-2, manufactured by Medtronic, is used to treat degenerative disc disease. The OP-1 putty incorporating BMP-7, also a treatment for degenerative disc disease, was originally owned by Stryker but has since been sold to the Olympus Corporation [23]. Both Stryker and Medtronic have since encountered legal issues and have been indicted for encouraging doctors to use the product off-label, for purposes not approved by the FDA. The BMP-2 treatment has been associated with complications such as bony overgrowth, osteoclast activity, local

inflammation, systemic toxicity, airway compression and carcinogenicity [24]. Despite this, researchers are still looking for methods of incorporating and delivering factors, such as BMPs, as regenerative therapies [25-27]. The unseen complications caused by the use of these therapies highlights the need for better understanding of the biology of bone regulation, particularly in the hope of being able to influence and control bone regeneration.

1.1.3.ii.c Cell therapies

Cell therapies for bone repair have mostly been focused on the use of MSCs and bone marrow-derived osteoprogenitors and there have been some instances of use in animal studies and clinical trials, showing some success [28, 29]. The use of embryonic stem cells (ESCs) as cell-based therapies in bone regeneration is much further from clinical application but research has been initiated [18]. Human ESCs have been shown to produce mineralized "bone-like" tissue *in vitro* and in animal models [30, 31].

1.1.3.iii Cell sources for bone tissue engineering

1.1.3.iii.a Embryonic stem cells

ESCs are isolated from the inner cell mass of the blastocyst of a preimplantation embryo [7, 10]. This usually leads to the destruction of the embryo, provoking ethical objections from some sections of society, but there has been methods recently described that use a single cell biopsy from the embryo, that have less detrimental consequences [32]. The most common hESC lines have been derived from destruction of extraneous embryos from fertility treatment or embryos created from

somatic cell nuclear transfer (SCNT). The process of deriving ESCs from embryos and converting them to *in vitro* culture can be seen in figure 1.3.

ESCs are characterised by the ability to self-renew indefinitely and are capable of differentiating into any cell of the body; this ability is termed pluripotency. Literature describes both *in vivo* and *in vitro* differentiation of cells into all three of the primary germ layers: mesoderm, endoderm and ectoderm [33]. This includes differentiation into cardiomyocytes [34], haematopoietic cells [35], neuronal cells [36], muscle cells [37], chondrocytes [38] and pancreatic islet cells [39].

Continuous *in vitro* culture of ESCs requires the maintenance of pluripotency. This is performed in mESCs by culturing in the presence of leukaemia inhibitory factor (LIF).

LIF acts to suppress differentiation. In some cases, pluripotency can also be maintained by culturing upon a feeder layer of mouse embryonic fibroblasts (MEFs) with LIF [40]. LIF does not have the same effect upon hESCs. In this instance, maintenance of pluripotency is performed by culturing upon MEF feeder layers or on matrigel in MEF-conditioned media. In both situations, the presence of basic fibroblast growth factor (bFGF) is required [41]. Theoretically, ESCs can be put through infinite divisions *in vitro*, as long as pluripotency is maintained.

Markers used to identify pluripotent mouse and human ESCs include stage specific embryonic antigen (SSEA)-3, transcription factors Oct 3/4 and Sox-2, zinc finger protein Rex-1 and transcriptional activator UTF-1 [42-45]. The marker SSEA-4 is only found in hESCs and SSEA-1 only in mESCs. Expression of certain markers differs between mouse and human ESCs, as discussed by Ginis et al., but the conclusion reached was that overall strategies for maintenance of pluripotency and differentiation remain similar across species [45].

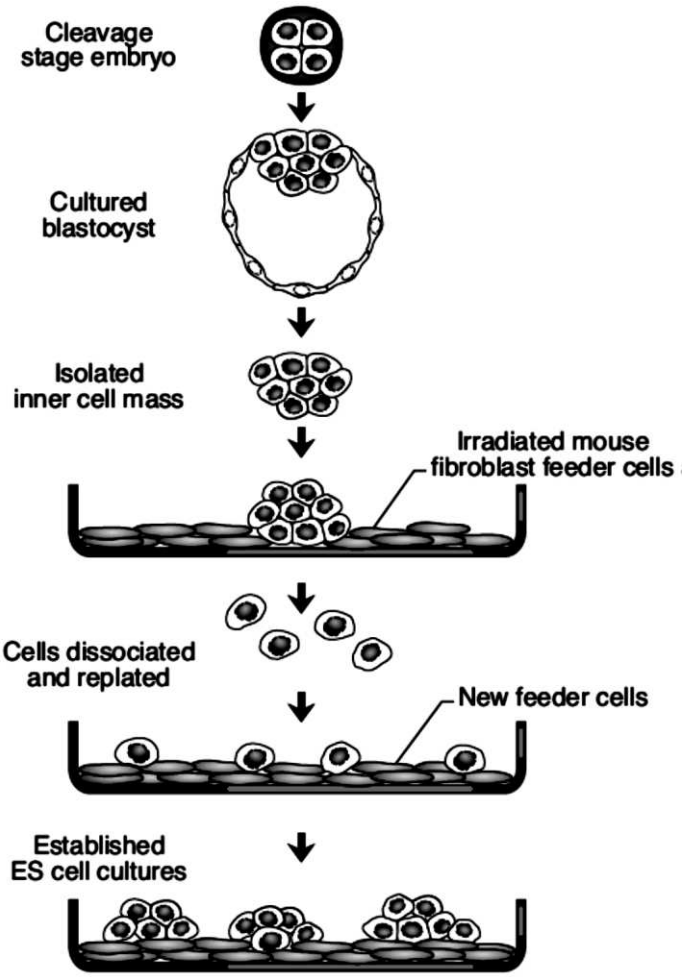

Figure 1.3: Derivation of ESC lines. The blastocysts are grown from *in vitro* fertilised embryos. Inner cell mass cells are separated from the blastocyst by immunosurgery and plated onto an inactivated mouse fibroblast feeder layer. Colonies can then be expanded and cloned. Taken from [46].

To date, there have been few ESC based products to reach clinical trial. The Geron Corporation started phase I clinical trials for their product involving oligodendrocytes derived from hESCs, in January 2009. This was the world's first hESC trial in humans. Since then, Geron have stopped stem cell research, due to economic concerns, but continue to monitor the patients that received the therapy. In 2011, Advanced Cell Technology started a phase I/II trial involving the injection of hESC-derived pigment epithelium cells to treat macular degeneration [47]. The trial is still ongoing [48].

The use of ESCs as transplantable cells in clinical trials has been hampered by several obstacles of a scientific nature. Current differentiation protocols are often unsatisfactory and can result in a final cell population that is heterogeneous in character, although with one cell type dominating. There can be considerable variation in final cell yield from batch-to-batch cultures, despite identical differentiation protocols. Due to the number of cell lineages that ESCs can spontaneously differentiate into, derivation of a homogenous cell population will ultimately rely upon consistent cell selection and purification techniques. It is also critical that the cells function physiologically when compared to cells of the body. Efficacy, safety and methods to prevent immunological rejection, will need to be demonstrated in order for further ESC-based cell therapies to reach human trials.

1.1.3.iii.b Adult stem cells

Adult stem cells, also known as somatic stem cells, can be isolated from several different tissue types. The most widely known example is the HSC, which can be found in the bone marrow. Clinically, the HSC has been utilised for many years in the

form of bone marrow transplants. HSCs can differentiate into all myeloid and lymphoid lineages [49].

In the field of tissue engineering, particularly bone and cartilage engineering, the MSC is of particular interest. MSCs are present in the early limb bud and migrate from the mesoderm. They can then differentiate through many stages into the osteoblast that goes on to produce the bone matrix [50]. *In vitro*, MSCs have been shown to differentiate into cells of mesodermal origin including osteoblasts, chondroblasts, adipocytes and myoblasts, and can be isolated from various tissues such as bone marrow, adipose tissue and skeletal muscle [51]. MSCs isolated from different tissues can vary in their activity and properties. MSCs may exhibit limited plasticity, differentiating into cells outside of the mesenchymal lineage. The most widely used MSCs originate from the bone marrow stroma and were first identified in 1970 [52]. The advantages of using MSCs for therapeutic applications are differentiation capacity, ease of isolation and ability to amplify *in vitro.* However*,* MSCs are more limited in the number of divisions that can be performed *in vitro* than ESCs, due to asymmetric division and being more advanced in the developmental continuum. MSCs are generally identified and defined via expression of markers such as CD29, CD44, CD73, CD90, CD105 and the ability to differentiate into osteoblasts, chondroblasts and adipocytes *in vitro*. They should not express the haematopoietic cell surface markers CD34, CD45, CD14 and human leukocyte antigen (HLA) class II [53, 54].

MSCs have had more success reaching therapeutic stage than ESCs and have been trialled as therapies for many clinical indications including graft-versus-host disease (GVHD), Crohn's disease, cardiovascular disease, diabetes and bone and cartilage defects [55].

1.1.3.iii.c Primary osteoblasts

Both primary osteoblasts and osteoclasts can be extracted from bone and cultured *in vitro*. There are also several bone cell lines that can be used for *in vitro* culture, including the mouse calvarial MC3T3-E1 line and the human osteosarcoma lines Saos-2 and MG-63. These cells are not generally useful for tissue engineering purposes, as primary cells have very limited proliferative capacity *in vitro* and others are essentially cancer cells. However, they can be very useful in disease modelling and *in vitro* testing.

1.1.3.iii.d Induced pluripotent stem cells

iPSCs are the most recent major development in stem cell research and are derived by nuclear reprogramming, a procedure that causes a switch in gene expression from one cell type to another [56]. The advance of iPSC development caused much excitement in the world of tissue engineering and stem cell research [11]. iPSCs can now be created from both murine and human somatic cells by retroviral delivery of transcription factor genes such as Oct-4, Sox2, Klf4, c-Myc [57]. Although iPSCs do not carry the ethical controversy that surrounds ESCs, there are still concerns and limitations with their use, particularly in the utilisation of transfection systems and the genes required to reprogram the cells [58]. iPSCs have shown the ability to differentiate down the osteogenic lineage and show promise in the fields of regenerative medicine and disease modelling [59].

1.1.3.iv Osteogenic differentiation strategies

When considering stem cells as a possible therapies or disease models for bone, osteogenic differentiation will need to be performed in order to create a cell that displays markers of osteoblasts and produces an ECM reminiscent of bone. Osteogenesis of stem cells is a complicated process, but has been reported *in vitro* using factors such as dexamethasone, ascorbic acid, beta-glycerophosphate, BMP-2, transforming growth factor-β (TGF-β) and 1,25 dihydroxy vitamin D_3 [30, 60-62]. The differentiation of ESCs is normally commenced with the formation of an embryoid body, a spheroid structure that mimics early development [63, 64]. Cells within the embryoid body will undergo morphological changes and differentiate into early cells of the three germ layers [33]. The embryoid body can then be dissociated and culture in monolayer continued. Osteogenesis of ESCs without the embryoid body step has been reported, as this allows an easier and quicker protocol to be followed and the study of direct osteogenesis, but is not commonly used [65].

1.2 Bone Physiology and Development

Bone is a highly dynamic organ. Throughout human life, bone is constantly remodelled, with matrix resorption and new matrix deposition occurring concurrently, in a complex and highly balanced cycle. In order to produce regenerative strategies for bone and to understand bone disease, a familiarity with bone biology and development is required.

1.2.1 Bone Structure and Biology

Bone is an organ composed of cortical and trabecular structures, cartilage, haematopoietic tissue and connective tissue. There are many functions of bone including support of the body, protection of internal organs, movement, a site for haematopoiesis and mineral storage [66, 67]. Figure 1.4 shows the structure of bone. Cortical bone, also known as compact bone, accounts for around 80% of the total bone mass of the skeleton. It has a mechanical function and a high mineral content. Cortical bone has a complex structure made up of cylindrical units called osteons. Each osteon runs parallel to the long axis of the bone and contains a ring structure of lamellae. The lamellae are made up of collagen fibres that run parallel to one another, providing the torsional strength of bone. Trabecular bone, also known as spongy or cancellous bone, has a fine lattice structure, filled with bone marrow, blood vessels and fat. The lattice structure allows a reduction in weight without compromising the strength of the bone. Long bones have a structure comprising the diaphysis or shaft, containing the bone marrow cavity, and the epiphyses, the bone ends. Short, irregular and flat bones all have simpler structures comprising both cortical and trabecular bone, but no bone marrow. Bone comprises both organic and inorganic components.

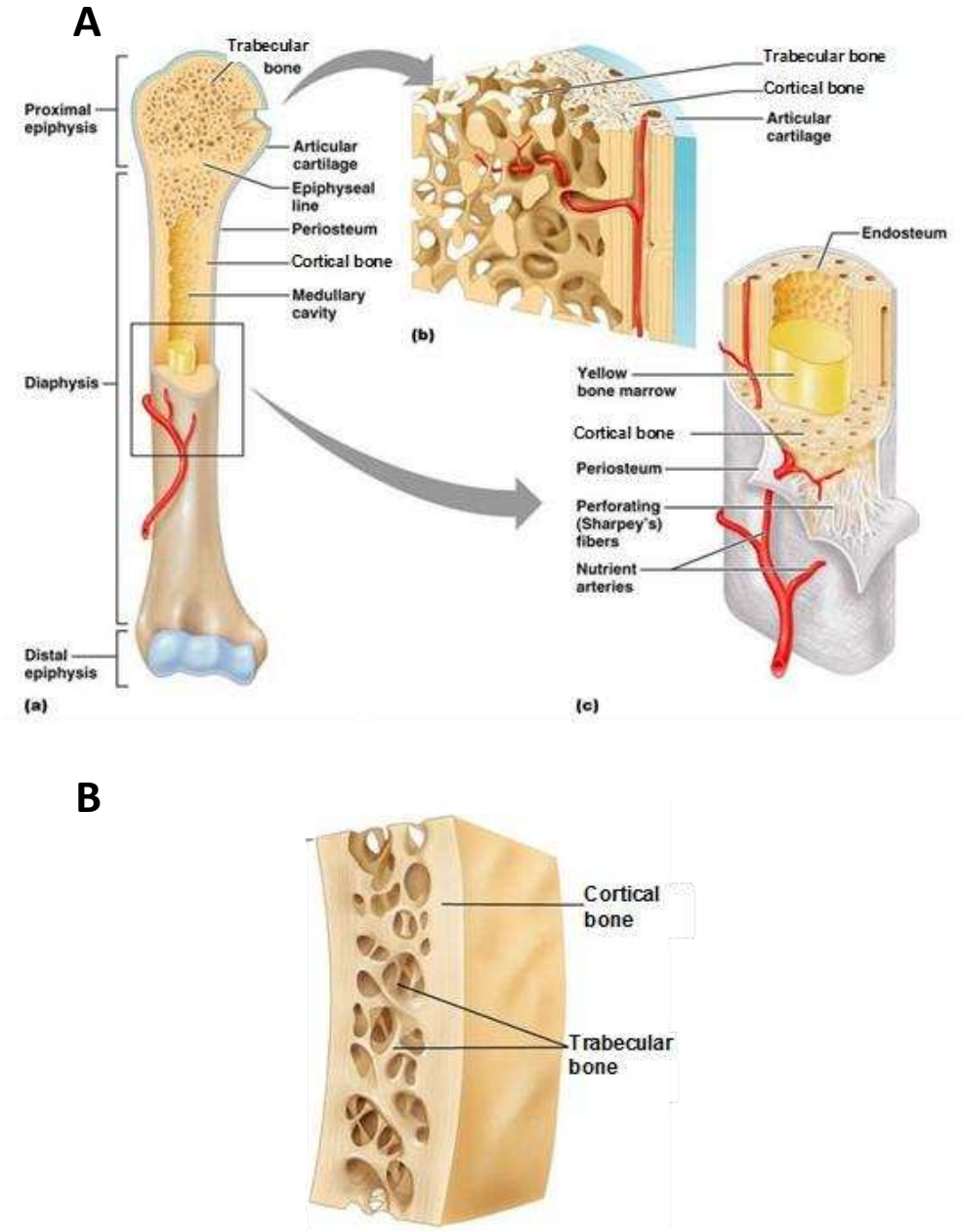

Figure 1.4: The structure of bone. (A) Structure of long bone: (a) bone sectioned frontally, (b) Enlarged view of trabecular (spongy) and cortical (compact) bone, (c) Cross-sectional view of diaphysis of bone. (B) Structure of flat bone, consisting of trabecular bone sandwiched between cortical bone. Taken from [67].

The organic components include the cells and the osteoid. Osteoid is predominantly made up of collagen but also contains other matrix proteins, proteoglycans and glycoproteins. The inorganic phase of bone consists of hydroxyapatites; calcium phosphates present in crystalline form surrounding the collagen fibres.

1.2.2 Bone Cells

There are a number of different cell types found in bone, including preosteoblasts, osteoblasts and osteocytes that originate from the mesenchymal line and osteoclasts that originate from HSCs. Figure 1.5 shows the stages of osteoblast differentiation from MSC to osteocyte.

1.2.2.i MSCs and osteoprogenitor cells

Osteoprogenitor cells are derived from multipotent MSCs that are found in the bone marrow stroma and resemble young fibroblasts. Osteoprogenitors retain a proliferative capacity but can also express proteins associated with the mature osteoblast phenotype [68]. During bone development or healing, these cells migrate and differentiate into the osteoblast. There is no definitive marker for the osteoprogenitor cell, causing them to be difficult to identify within a cell population. The genetic regulation of MSC differentiation to osteoblasts is in part regulated by the transcription factor Runx2 also known as core binding factor a-1 (cbfa-1) [69]. Runx2 plays an important role throughout skeletal development. Mice born without the *Runx2* gene die immediately after birth and show a complete lack of skeletal ossification [70]. More recently, the transcription factor TAZ (transcriptional co-activator with PDZ-binding motif) has been reported, which acts to specify osteoblast

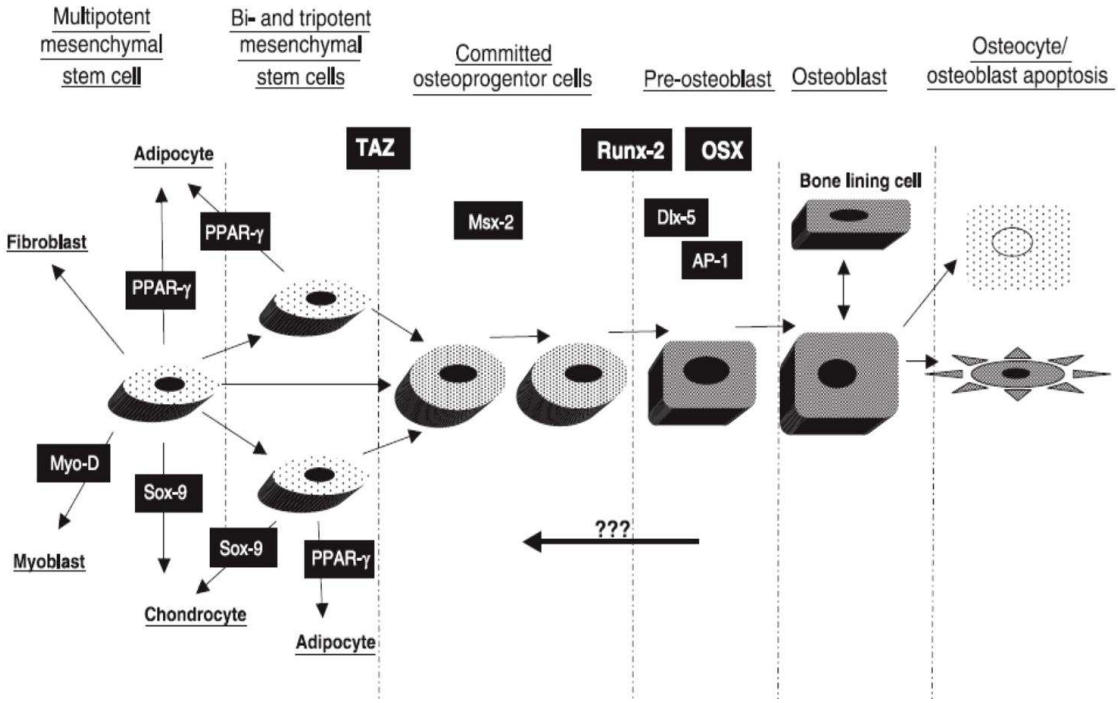

Figure 1.5: Stages in the osteoblast lineage. Schematic diagram showing stages in the osteoblast lineage and some of the transcription factors that lead to osteoblast production from MSCs. Adapted from Hughes et al. [71].

fate in bipotent osteoblast/adipocyte stem cells by leading to activation of Runx2 and repressing PPAR-γ, a transcription factor important in adipogenesis [72]. There are a number of other transcription factors that regulate differentiation to the osteoblast: Msx-2 acts upstream of Runx2, whereas Dlx-5, activator protein-1 (AP-1) and osterix (OSX) run downstream, and are involved in matrix synthesis and deposition .

1.2.2.ii Osteoblasts

Osteoblasts are the cells that originate from committed osteoprogenitor cells. Osteoblasts are responsible for the formation, organisation and subsequent mineralisation of bone ECM and are cuboid in shape [76]. A mature osteoblast will produce osteoid containing predominantly collagen I (col-I), but also a little collagen V and many bone specific proteins such as osteocalcin (OCN), osteopontin (OPN), osteonectin and bone sialoprotein (BSP) [66]. The secretory surface of osteoblasts runs close to the bone surface and is rich in the enzyme alkaline phosphatase (ALP). These proteins together have a calcium binding activity that leads to the hydroxyapatite crystal deposition seen in the mineralised matrix. Of these non-collagenous matrix proteins, OCN is considered to be the most bone-specific, as expression in the adult is restricted to bone dentin and cementum. Some osteoblasts eventually become bone-lining cells that cover bone surfaces but most become osteocytes. After producing bone matrix, osteoblasts may also die by apoptosis, this mechanism is partially controlled by BMP-2 and is a method of regulating osteoblast number and function [77].

1.2.2.iii Osteocytes

Osteocytes are terminally differentiated osteoblasts that have become trapped in lacunae inside the mineralized matrix of bone. They are the major cell type in mature bone. Osteocytes are connected by dendrites that reach through a system of canaliculi. Through these, they communicate with each other and the osteoblasts. This is believed to regulate the response of bone to the stresses of the external environment, communicating and maintaining electrical and metabolic activity [78].

1.2.2.iv Osteoclasts

Osteoclasts are responsible for bone matrix resorption. Unlike osteoblasts, they are not derived from mesenchymal progenitors but are of a haematopoietic lineage. Osteoclast progenitor cells are derived from the mononuclear phagocyte lineage. Preosteoclasts fuse to form giant multinucleated osteoclasts [79]. In bone, they are located in resorption pits known as Howship's lacunae, where they produce localised acidic environment that is conducive to bone resorption. The osteoclast cell surface when attached to bone forms a region known as the ruffled border, which is rich in vesicles, phagosomes and residual bodies. Bone resorption is caused by the synthesis of lysosymal enzymes, particularly tartrate-resistant acid phosphatase (TRAP) and matrix metalloproteinases (MMPs) [80].

1.2.3 Bone Development

Both the words osteogenesis and ossification refer to the development of bone. The embryonic origin of the bones of the skeleton are the limb buds, these are

mesodermal tissue covered by ectoderm. There are two types of ossification, endochondral and intramembranous. In endochondral ossification, MSCs condense at the limb bud and differentiate into chondroblasts. A matrix is secreted and a cartilage model of the bone is created surrounded by the perichondrium. The cartilage template grows and a vascular system develops, invading the perichondrium. Inner perichondrial cells differentiate into osteoblasts and a collar of bone is laid down around the mid-shaft. The osteoblasts also penetrate the centre of the shaft forming a diaphyseal ossification centre, where trabecular bone is deposited. The bone increases in width by appositional growth. In long bones, a secondary centre of ossification is developed at the cartilaginous ends of the bone, known as the epiphyseal ossification centre. This causes the ossification of the epiphyses of the bone. When completed, cartilage remains only at the ends of the bone and at the epiphyseal growth plate. It is from this growth plate that the bone can grow as a child matures. With the exception of the clavicles, endochondral ossification is responsible for the formation of most of the bones below the base of the skull.

Intramembranous ossification is important in the development of the bones of the skull and clavicles, and in the healing of bone fractures. Intramembranous ossification does not involve a cartilage step; the formation of bone comes directly from the condensed mesenchyme. The MSCs differentiate directly into preosteoblasts that then aggregate and undergo proliferation, then differentiation into osteoblasts, which begin to secrete bone matrix from an ossification centre. First, an irregular and disorganised woven bone matrix is formed; later this is remodelled to mature lamellar bone [66, 67].

1.2.4 Bone Remodelling

Changes in bone architecture occur continuously throughout a person's lifetime. This is known as bone remodelling and is a balance of bone resorption by osteoclasts and bone deposition by osteoblasts. The process is coordinated by groups of adjacent osteoblasts and osteoclasts known as the bone remodelling units. Local mediators of this process are various growth factors and cytokines. Osteoclasts resorb matrix from the erosion cavity and then mononuclear cells differentiate into osteoblasts and lay down new matrix. Bone is remodelled in response to mechanical loading and strain, in order to retain form and function. Reduced bone loading can lead to decreased bone mineral density (BMD) in fracture patients and people subjected to prolonged low gravity conditions, such as astronauts [81]. Bone remodelling is often initiated by the presence of microfractures that appear under everyday activity and strain. Signals produced during microdamage activate the remodelling units that then allow control over BMD and routine fatigue damage [82]. Bone remodelling appears to be governed by a feedback system in which bone cells can sense the environmental strain around them and react to produce or remove bone in accordance. Signalling molecules that have been implicated in the adaptive response of bone to mechanical strain include glutamate, nitric oxide, prostaglandins and calcium [83-85]

1.2.5 Regulation of Bone

A large number of growth factors and cytokines are involved in the regulation of bone growth, remodelling and the proliferation and differentiation of bone cells [86]. Tables 1.1 and 1.2 give brief descriptions of the effects of various growth factors and cytokines.

Table 1.1: Growth factor regulation of bone.

Factor	Regulatory Effect on Bone	References
Growth Factors		
Insulin-like growth factors (IGF-I & II)	Stimulates longitudinal bone growth by acting on growth plate chondrocytes. Stimulates osteoblast proliferation and differentiation. Upregulates OSX.	[87, 88]
Transforming growth factor-β (TGF-β)	Recruits and stimulates osteoprogenitors to proliferate during bone formation. In later stages of osteogenesis, can block differentiation and mineralisation. Regulates synthesis of collagen by growth plate chondrocytes. Inhibits *Runx2* and *Ocn* genes. Inhibits interleukin-1 and $1,25(OH)_2D_3$ (vitamin D) induced bone resorption and the formation of osteoclasts.	[89-93]
Fibroblast growth factors (FGF-1 and 2)	Stimulates osteoblast proliferation *in vitro.* No direct effect on osteoblast differentiation. Increases apoptosis with prolonged exposure.	[94-97]
Platelet derived growth factor (PDGF)	Synthesised by osteoblast and MSCs. Upregulates collagenase transcription in osteoblasts. Secreted by osteosarcoma cells. Mitogen for osteoblasts.	[66, 98, 99]
BMPs	Directs MSCs down the osteoblast pathway. Can upregulate Runx2 at certain stages of osteogenesis. Regulates bone formation. Can independently induce ossification from non-skeletal MSCs.	[100-102]
Wnt Signalling	Active in the early stages of osteoblast differentiation. Induces BMP-2 production and plays roles in BMP-induced osteogenic differentiation. Promotes osteogenesis indirectly through Runx2. Works with TGF-β to promote osteoblast proliferation. Has both stimulatory and inhibitory effects on TGF-β. Wnt-3a induces BMP-9	[103-109]

Table 1.2: Cytokine regulation of bone.

Factor	Regulatory Effect on Bone	References
Cytokines		
Interleukin-1 (IL-1) (α and β)	Produced by mesenchymal stem cells and osteoblasts. Can regulate both bone resorption and formation. Has been shown to inhibit osteoblast proliferation and enhance bone formation. Has also been shown to stimulate osteoblast proliferation and inhibit bone formation. Shown to inhibit col-I and OCN production. Increases production of other cytokines.	[110-116]
Interleukin-6 (IL-6)	Produced by osteoblasts Some inhibitory effect on osteogenic differentiation *in vitro*. May mediate some actions of IL-1 and regulate expression of other growth factors.	[117-119]
Tumour necrosis factor-α (TNF-α)	Produced by osteoblasts. Stimulates bone resorption and inhibits bone formation. Inhibits osteoblast differentiation Decreases production of col-I. Suppresses Runx2 and OSX expression.	[120-122]
Interferon-γ (IFN-γ)	Antagonist to IL-1 and TNF-α bone resorption. Inhibits osteoblast proliferation. Inhibits collagen synthesis. Inhibits osteoclastogenesis.	[121-123]

1.2.6 Bone Disease, Injury and Repair

During the course of a lifetime, bones are subject to many different forces. Fractures are produced in healthy bone from moments of exceptional trauma that can twist and break the bone. In old age, fractures are more common due to bones becoming thinner, weaker and more brittle. Fractures can be classified in many different ways according to the orthopaedic trauma association (OTA) classification system [124].

Normal bone repair, particularly in the case of fracture healing, involves four stages (table 1.3). In some cases, fractures fail to resolve themselves by healing in the normal way; these are commonly known as non-union fractures. Healing may also not occur when there is a large defect caused by blast injury, infection, surgical tumour resection or osteonecrosis. Bone diseases such as rheumatoid arthritis (RA), osteoarthritis (OA) and osteoporosis, can also disrupt bone healing and structure. RA is an inflammatory disorder, in which joints become inflamed, and is linked to autoimmunity. OA involves the degradation of joints of the skeleton and osteoporosis is a disease in which bone resorption occurs more efficiently than bone formation, disrupting the balance of bone remodelling. In addition, other disorders can cause a disruption to the bone balance including osteopetrosis, osteomalacia and rickets. There are many treatments available for all the above conditions but most are for pain management and containment of the disease. Although tissue engineering and regenerative medicine strategies can also be used for these purposes, the ultimate aim is to provide a cure and address the cause of the imbalance in bone healing.

Table 1.3: Stages of normal fracture healing.

Stage of Healing	Description
1. **Inflammation and haematoma formation**	Blood vessels in the periosteum are broken and torn by the trauma, causing a mass of clotted blood (haematoma) to form at the fracture site. Inflammatory exudate is released from blood vessels. Cells are deprived of nutrients and die. This attracts inflammatory cells and the tissue becomes painful and swollen.
2. **Fibrocartilaginous callus formation**	Formation of granulation tissue. Capillaries grow into haematoma and phagocytic cells begin cleaning up the area. Fibroblasts and osteoblasts occupy the area and begin the process of reconstruction. Chondrocytes begin to secrete cartilage matrix. Repair tissue is called fibrocartilaginous callus and bridges the fracture.
3. **Bony callus formation**	Fibrocartilaginous callus is converted to bony callus or trabecular bone. Can take months for a firm union to be developed. Compressive forces can be withstood.
4. **Bone Remodelling**	Complete healing occurs by remodelling of the bony callus Trabecular bone converted to cortical bone in shaft walls. Final structure should resemble that of unbroken bone.

1.3 The Inflammatory Response

1.3.1 Inflammation

Inflammation is a protective response against trauma, intense heat, chemicals or infection by foreign organisms, and is part of the immune response. The major clinical symptoms of inflammation include heat, redness, pain and swelling in the affected area. The beneficial effects of the inflammatory response include prevention of the spread of damaging agents to other tissues, disposal of cell debris and pathogens, and the provision of a foundation for healing [67].

1.3.1.i The acute inflammatory process

Inflammation is mediated by many local and systemic regulators. The inflammatory process after tissue injury begins with a flood of signals released into the extracellular fluid. Cells of the immune system play integral roles in inflammation and cells such as macrophages, monocytes and B-lymphocytes express surface membrane proteins called toll-like receptors (TLRs). Activation of certain TLRs, causes the release of cytokines that promote inflammation and can attract more cells of the immune system to the injured area [125]. Many cells produce these cytokines including injured tissue cells, macrophages, phagocytes, lymphocytes and mast cells. The released cytokines subsequently cause production of inflammatory mediators including additional cytokines, prostaglandins, histamine, kinins and complement proteins. The roles of these mediators can be found in table 1.4. One major effect of these mediators is vasodilation of the small blood vessels, causing more blood to flow into the area and

Table 1.4: Physiological effects of inflammatory mediators.

Mediator	Physiological Effect
Cytokines	Signalling molecules such as interleukins (IL)-1,-6, -17, tumour necrosis factors (TNFs) and interferons (IFNs). Orchestrate inflammatory response. Attract leukocytes. Stimulate production of further inflammatory mediators. [126-129]
Prostaglandins	Derived from arachidonic acid by most cells. Increases effects of other inflammatory molecules. Sensitises blood vessels. Leads to production of free radicals that can go on to cause inflammation and pain. [130-132]
Histamine	Produced in response to mechanical injury, presence of microorganisms and chemicals by basophils and mast cells. Promotes vasodilation and increases permeability of local capillaries, leading to heat, redness, pain and swelling. [133]
Kinins	Includes bradykinin and kallidin and can be produced by most cells. Promotes vasodilation, induces chemotaxis of leukocytes and generation of more kinins. Can induce production of eicosanoids, more cytokines and nitric oxide. Induces pain. [132].
Complement Proteins	Circulate in the blood. Causes lysis of microorganisms, enhances phagocytosis and intensifies inflammation. [134]
Nitric Oxide (NO)	Produced in large amounts during inflammation. Causes vasodilation, increasing temperature and swelling. [135]

the symptoms of redness and heat. The other major effect is permeabilisation of the local capillaries. This causes an exudate of fluid containing clotting proteins and antibodies to seep into tissue spaces. This exudate causes the swelling (oedema) that presses on the local nerve endings, causing pain sensation. Pain may also be caused by the sensitising effects of prostaglandins and kinins. The oedema allows dilution of harmful substances by the surge of fluids into the area, brings large quantities of nutrients and oxygen to help the repair process, and allows large clotting proteins to enter the area [67, 136].

The inflammatory mediators cause phagocytes, such as neutrophils and macrophages to migrate to the area, and depending on the cause of the inflammation, these cells then act to resolve the issue. The first stage is leukocytosis, the release of large amounts of neutrophils from the bone marrow into the blood stream. The neutrophils flow into the injured area and are caught by endothelial cells that have expressed selectins due to cytokine signalling, such as P-selectin and E-selectin. The neutrophils then bind to integrin receptors on the endothelial cells, arresting cell movement. The neutrophils migrate through capillary walls in a process called diapedesis and home to the area of injury through chemotaxis caused by the inflammatory mediators. This same process then attracts monocytes and macrophages. The function of these cells is to clear the injured area of pathogens, dead cells and other debris, so tissue repair can be initiated. The acute inflammatory response then ends [137].

1.3.1.ii Chronic Inflammation

If the condition causing acute inflammation is not resolved, the inflammatory process may continue, leading to long-term chronic inflammation. Whereas acute

inflammation should be over within days, chronic inflammation may last for weeks, months or years. During this process an imbalance in the inflammatory signalling means that monocytes and macrophages are still attracted to the wound site, and inflammatory mediators and cytokines are still being produced [138]. Hence, heat, swelling, redness and pain are still present at the site of injury. Due to the large amount of macrophages at the injury site, tissue damage is a common problem in chronic inflammation. Chronic inflammation is present in many disease states including RA, atherosclerosis, Crohn's disease, ankylosing spondylitis and dermatitis. In many chronic inflammatory conditions, such as inflammatory bowel disease, cystic fibrosis and periodontitis, increased rates of osteoporosis and fractures occurs due to systemic increases in circulating proinflammatory cytokines [139-141].

1.3.2 Inflammation and Bone

Many of the mediators of inflammation in bone, such as IL-1β and TNF-α, are also regulators of normal bone cell activity and bone development. Inflammatory effects in bone are due to changes in amounts, timings and combinations of cytokines. Due to the link between proinflammatory cytokines and bone development, inflammation can have great effect on bone structure, remodelling and growth. Systemic inflammatory effects throughout the body affect nutrient metabolism and hormone secretion, which can have knock-on effects on the skeleton.

1.3.2.i Signalling during inflammation in bone

A simplified diagram showing major pathways involved in inflammatory signalling in osteoblasts is shown in figure 1.6. Many of the effects of inflammation on osteoblasts

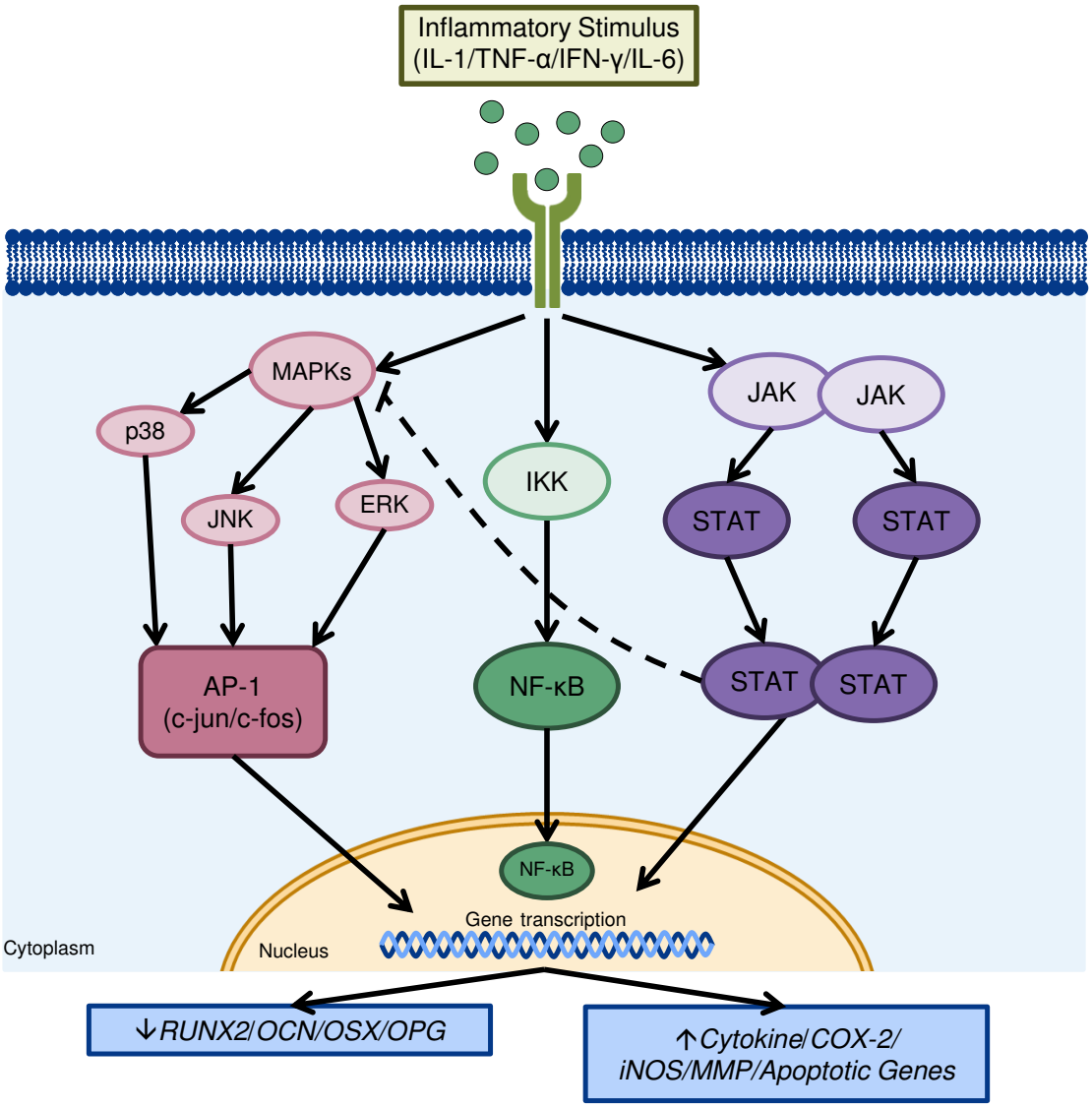

Figure 1.6: Signalling pathways in bone during inflammation. Simplified diagram showing major pathways involved in signalling in osteoblasts in response to inflammatory stimulus, such as proinflammatory cytokines. The major pathways involved include the MAPK, NF-κB and JAK/STAT pathways, leading to an overall downregulation of osteogenic genes such as *RUNX2, OCN, OSX* and osteoprotegerin (*OPG*) and an upregulation of genes involved in inflammation such as COX-2 and iNOS.

are mediated by the NF-κB transcription factor, produced through I-κB kinases (IKK). Activation of this transcription factor by proinflammatory cytokine stimulation leads to increased production of more proinflammatory cytokines, inducible enzymes such as cyclooxygenase-2 (COX-2) and inducible nitric oxide synthase (iNOS) and genes related to apoptosis [142]. The mitogen-activated protein kinase (MAPK) pathway, including p38, JNK and ERK, is also an important pathway during inflammation of bone, which plays a more complicated role, having both proinflammatory and anti-inflammatory effects [143-145]. A third pathway involved in inflammation in bone is the JAK/STATs (janus kinase/signal transducers and activators of transcription) system, that is activated by chemical inflammatory signals; this pathway goes to on to effect gene transcription including the production of apoptotic genes, additionally having an inhibitory effect on the MAPK pathway [145-147] .

Locally to bone, mediators of inflammation such as the proinflammatory cytokines and activation of the pathways described above, causes changes in cell proliferation, differentiation and activity, causing the process of bone remodelling to be affected [148]. The predominant mediators of this are the eicosanoids and the proinflammatory cytokines. Eicosanoids are signalling molecules derived from arachidonic acid, and include prostaglandins, prostacyclins, leukatrienes and thromboxins. There is evidence that prostaglandins have a role in bone remodelling, but expression and response to is very much altered during the inflammatory response [149]. The proinflammatory cytokines IL-1, TNF-α, IL-6 and IFN-γ all have regulatory roles in normal bone modelling as discussed above. During inflammation, these cytokines are produced in higher concentrations both systemically and locally and having an effect on bone healing and remodelling. The overall effects of inflammation on bone are very difficult to predict *in vitro* due to the large number of different factors involved [148].

1.3.3 Tissue Engineering and the Inflammatory Response

1.3.3.i Stem cells and inflammation

There has been more research into the effect of inflammation on MSCs than ESCs. MSCs have been described as having both anti-inflammatory and immunomodulatory effects [150]. They have been reported to inhibit T-lymphocyte activation and proliferation, secretion of IFN-γ and natural killer (NK) cell activity, leading to suppression of inflammation [151-153]. There has been less investigation into the effects of inflammation on ESCs, but like MSCs, ESCs have been described as being immunoprivileged, as they do not appear to provoke an immune response when implanted within a foreign body. An immune response to implanted cells is normally triggered by the presence of major histocompatibility complex (MHC) cell surface antigens such as class I and class II HLAs. On non-differentiated hESCs, levels of these antigens are minimal, but as cells differentiate, levels of expression increase [154-156]. Although the immune reaction and inflammation are separate phenomena, they are very much linked through the cells and proteins involved, and this immunoprivileged state may have an effect on ESC implantation into an inflammatory environment. ESCs are derived from the embryo and within embryos, wound healing occurs rapidly and perfectly, without scar formation. This is in part because the initial inflammatory signals are not released after embryonic wounding; and inflammation, particularly the role of macrophages, is not necessary for tissue repair [157, 158]. It remains to be discovered whether the lack of a role for inflammation in wound healing and the response of ESCs to inflammatory signalling is linked.

1.3.3.ii Modulation of inflammation through tissue engineering

Inflammation may play a large part in the success or failure of a regenerative medicine or tissue engineering strategy, particularly in bone regeneration. The process of implanting a therapy will induce a foreign body reaction, causing inflammation, which may help or hinder eventual regeneration. In the case of non-union fractures, large bone-defects or diseases such as RA or osteoporosis, the environment of implantation will likely be one of inflammation and imbalanced bone healing. Tissue engineering therapies are developed *in vitro,* and time and money is invested in refining growth, differentiation, scale-up and delivery of the final product. However, the effects of introducing this product into the damaged and diseased environment have not been investigated. For this reason, it is important to consider the effects that inflammatory signalling molecules will have on response and differentiation of implanted cells. There have been few strategies developed that aim to modulate the inflammatory response to aid bone regeneration, and to provide a level of control over inflammation. Providing this may help develop a more successful strategy for bone regeneration.

1.4 Aims and Objectives of the Study

There are two distinct aims of the research presented in this study, incorporating the general aim of looking at bone tissue engineering strategies in the context of inflammation. The first is to study the possible effect that an inflammatory environment (in the form of proinflammatory cytokines) may have on the response and osteogenic differentiation of cells postulated for bone repair. The second aim is to investigate the possibility of incorporating a level of control of the inflammatory response into bone regeneration strategies.

The specific objectives of this study are:

- Development of an *in vitro* simulation of an inflammatory environment using proinflammatory cytokine signalling.
- Assessment of the biochemical responses of osteogenically differentiated mESCs to proinflammatory cytokine signalling, and comparison to the responses of primary calvarial osteoblasts.
- Examination of mechanisms involved in any differences in responses between the two cell types.
- Assessment of osteogenic differentiation of mESCs compared to differentiation of primary calvarial osteoblasts.
- Examination of the effect of proinflammatory cytokine signalling on the osteogenic differentiation of mESCs and calvarial osteoblasts.
- Examination of the effect of anti-inflammatory mediators on the *in vitro* simulation of the inflammatory environment.
- Development of a bone regeneration strategy that offers some control over inflammation.

Chapter 2: Materials and Methods

This chapter focuses on the experimental methodologies used throughout the study. Many methods are utilised in more than one results chapter and form the basis for several of the experiments performed. The study focuses on the use of two cell types: primary calvarial osteoblasts extracted from neonatal mice, and osteogenically differentiated mESCs. General cell culture processes and osteogenic differentiation techniques for both cell types are described below. Assay and staining procedures used throughout the results are justified and explained. The processes of magnetic-activated cell sorting (MACS) of the mESCs and manufacture of porous anti-inflammatory releasing scaffolds are explained, despite only appearing in one chapter, as they are key techniques within the study. Further detail describing individual experimental design is available in the separate results chapters.

2.1 Materials

This section describes the origin of the major cell types and key chemicals, consumables and materials used throughout the study.

2.1.1 Cells

Neonatal CD-1 mice used to obtain the primary calvarial cells were obtained from the Biomedical Science Unit, University of Nottingham, UK. Mice were killed by qualified personnel using a physical method. The CD-1 mouse is an outbred albino mouse

strain described as suitable for multipurpose use and there is a history of use of this strain within the research group.

Mouse ESCs were a gift from Dr Vasso Episkopou, Imperial College, UK. The mESCs were originally derived from mouse columnar epiblast epithelium (CEE) [159, 160]. They are a well-characterised and immortalised cell line. All mESCs were used between passages 18-30 post receipt.

SNL fibroblasts were also a gift from Dr Vasso Episkopou. They are a well-established cell line, established by Dr Allan Bradley [161], predominantly utilised as feeder layers for the support of mESCs. Initial passage number was unknown; cells were not used past passage 20 post receipt.

2.1.2 General Chemicals, Cytokines and Primers

Most chemicals were purchased from Sigma-Aldrich (Poole, UK) unless otherwise stated in the methods section. Sterile preparation of cell culture medium and chemicals was performed by filtration through 0.22 µm filters or by autoclaving at 121℃ for 1 hour, using a Prestige Medical 20100 autoclave (Scientific Laboratory Supplies, Nottingham, UK).

2.1.2.i Foetal bovine serum

Foetal bovine serum (FBS) batch testing was carried out to determine optimal serum for growth and osteogenic differentiation of mESCs and mouse primary calvarial cells.

Description of the batch testing procedure and results can be found in Appendix I. Serum for mESC culture and differentiation was purchased from Biosera (East Sussex, UK), product code FB1001H, lot number S08670S1810. Serum for mouse primary calvarial cells was purchased from Sigma-Aldrich, product code F9665, lot number 070M3397.

2.1.2.ii Recombinant Cytokines

The proinflammatory cytokines IL-1β, TNF-α and IFN-γ were used throughout the study, forming the basis of the inflammatory signalling. Recombinant human IL-1β, recombinant human TNF-α and recombinant mouse IFN-γ were purchased from R&D Systems, Abingdon, UK. IL-1β and TNF-α have a cross-species reactivity between human and mouse that IFN-γ does not possess. Recombinant interleukin-1 receptor antagonist (IL-1ra), used as an anti-inflammatory mediator was also purchased from R&D Systems.

2.1.2.iii Antibodies

Various antibodies were used throughout the body of work, in immunocytochemical staining procedures and MACS. Table 2.1 lists all primary antibodies used, with species details and dilutions. Table 2.2 lists the secondary antibody used. The Alexa-Fluor antibodies are fluorescent conjugated, emitting at the stated value.

Table 2.1: List of primary antibodies.

Antigen	Source	Species	Working Dilution
iNOS	Thermo Scientific	Rabbit	1:4
COX-2	Millipore	Rabbit	1:500
PGES	Sigma	Rabbit	1:100
Osteocalcin	Millipore	Rabbit	1:200
Osteopontin	R&D Systems	Goat	1:588
Collagen-I	Millipore	Rabbit	1:200
Cadherin-11	R&D Systems	Goat	1:67 (Immuno) 2 µg/mL (MACS)

Table 2.2: List of secondary antibodies.

Antibody	Source	Species	Dilution
Anti-rabbit IgG (Alexa Fluor-488 and Alexa Fluor -516)	Invitrogen	Donkey	1:200
Anti-goat IgG (Alexa Fluor 516)	Invitrogen	Donkey	1:200
Anti-goat IgG (Biotinylated)	Vector	Rabbit	10 µg/mL (MACS)

2.1.2.iv Primers and primer design

Primers were required for the RT-qPCR procedures. Primer designs for the mouse genes *Rpl32, Runx2, Col1a1* and *Opn*, were kindly provided by Ms Frieda Chen, Aubin Lab, Centre for Skeletal Biology, University of Toronto. The primer for *NOS2* (iNOS) was designed using NCBI Primer-Blast online software. Validation and optimisation of this primer was performed at the University of Toronto with assistance from Ms Frieda Chen, using positive control RNA extracted from adult mouse spleen.

Table 2.3: List of PCR primers

Gene Name	Product Size (bp)	Sequences	Annealing Temperature
Rpl32	100	(Fwd) TTAAGCGAAACTGGCGGAAAC (Rvs) TTGTTGCTCCCATAACCGATG	59℃
Runx2	146	(Fwd) TGTTCTCTGATCGCCTCAGTG (Rvs) CCTGGGATCTGTAATCTGACTCT	59℃
Col1a1	103	(Fwd) GCTCCTCTTAGGGGCCACT (Rvs) CCACGTCTCACCATTGGGG	59℃
Opn	134	(Fwd) AGCAAGAAACTCTTCCAAGCAA (Rvs) GTGAGATTCGTCAGATTCATCCG	59℃
NOS2	131	(Fwd) AGGCTCATCCAGAGCCCGGAG (Rvs) AGGGTGGTGCGGCTGGACTT	56℃

2.1.3 Consumables

Consumable labware used for routine cell culture and experimental work included: tissue culture flasks (25 cm^2, 75 cm^2, 175 cm^2 and three layer 450 cm^2), (Nunc,

(Fisher, Loughborough, UK)); tissue-culture treated 6-well, 24-well, 12-well and 96-well plates (Falcon, Becton and Dickinson, Oxford, UK); polycarbonate 24-well transwell inserts (Corning, NY); 100 µm/70 µm cell strainers, cryovials, sterile steriological pipettes, pipette tips (1mL, 200 µL 20 µL and 10 µL), 0.22 µm filters (Fisher Scientific, Loughborough, UK); 7 mL bijoux, 100 mL sterile plastic containers, cell scrapers, 10 cm sterile petri dishes, glass Pasteur pipettes, syringes (various volumes) (Scientific Laboratory Supplies); 15 mL/50 mL centrifuge tubes (Grenier Bio One, Stonehouse, UK); and 30 mL universal tubes and 1.5 mL/0.5 mL Eppendorf tubes (Sarstedt, Leicester, UK).

2.2 Methods

2.2.1 Cell Culture

All cell culture was performed using aseptic technique, in a class II microbiological safety cabinet (Envair, Haslington, UK), fitted with high efficiency particulate air (HEPA) filters, unless otherwise stated. All cell cultures were kept in a Sanyo MCO-17AIC incubator (Sanyo Electric, Biomedical, Wood Dale, IL) at 37°C in a humidified atmosphere containing 5% CO_2.

2.2.1.i SNL fibroblasts

SNL fibroblasts are a mouse fibroblast STO (SIM (Sandoz Inbred Mice) Thioguanine-resistant and Ouabain-resistant) immortalised cell line, transformed with neomycin resistance and murine LIF genes. They are a well-established feeder layer for the *in vitro* support of mESC proliferation and maintenance of pluripotency.

SNL fibroblasts were maintained in SNL culture medium containing Dulbecco's Modified Eagle's Medium (DMEM) (Invitrogen, Paisley, UK) with 10% (*v/v*) FBS, 100 U/mL penicillin and 100 µg/mL streptomycin (Pen-Strep, Invitrogen), 2 mM L-Glutamine and 500 µM 2-mercaptoethanol. DMEM acts as a buffered liquid support for cell growth and contains amino acids, salts, glucose, vitamins, iron and phenol red as a pH indicator, providing an environment suitable for general cell maintenance and proliferation. FBS is added to supply nucleotides and various factors, including antibodies and growth factors, to support cell proliferation. L-Glutamine is added to cope with rate of cell growth, as it is a conditionally essential amino acid and Pen-

Strep acts to minimise bacterial infection. The supplement, 2-mercaptothanol is added to the medium as a reducing agent, to help to control the effects of harmful by-products of cell proliferation. This supplement is predominantly added for the purposes of mESC culture, for which the SNL culture medium is utilised as a base. SNL cultures were maintained as monolayers in T75 cm^3 flasks.

Cells were allowed to reach 80-90% confluency before detachment and passaging using a standard trypsinisation protocol. The cell monolayer was rinsed with phosphate buffered saline (PBS), before treatment with trypsin/ethylene diaminetetraacetic acid (EDTA), at 37℃ for 4 minutes (based on visual detachment). Trypsin is a serine protease that is used to detach cells from the tissue culture plastic. Trypsin predominantly cleaves peptide bonds and breaks cell-cell junctions and cell matrix attachments, as well as lifting cells from the flask surface. Trypsin was inactivated using an equal volume of serum-containing medium, the resulting cell suspension transferred to a universal tube and centrifuged for 5 minutes at 180 x g. Supernatant was aspirated and the cell pellet resuspended in the appropriate volume of medium and re-plated at the desired cell density. A typical passaging ratio was 1:5, to allow the cells to become confluent after 3-4 days. Medium was changed every 2-3 days.

2.2.1.ii Inactivated SNL fibroblast feeder layer preparation

Feeder layers of inactivated SNL fibroblasts were required for the successful growth and maintenance of pluripotent mESCs. The inactivation process involves treating the SNL fibroblasts with a solution of mitomycin-C that crosslinks DNA, halting cells in the G1 phase of the cell cycle.

T25 cm^2 flasks were prepared for feeder layers by coating in a solution of 0.1% (*w/v*) bovine gelatin in PBS for 1-2 hours at 37°C. Gelatin adsorbs to the flask and provides a base layer for the attachment of cell membrane integrins. Confluent cultures of SNLs were treated with a 10 mL solution of mitomycin-C (Merck Millipore, Frankfurt, Germany), and incubated for 2 hours at 37°C. Mitomycin-C solution was removed and the cell monolayer detached from the flask using trypsin/EDTA, as described above. The cell suspension was centrifuged at 180 x g for 5 minutes and the resulting cell pellet resuspended in an appropriate volume of medium and counted using an improved Neubauer haemocytometer, viewed under an inverted light microscope.

Excess gelatin was aspirated from T25 cm^2 flasks and replaced with 5 mL SNL culture medium. The correct volume of cell suspension was then added to each flask to produce a final cell density of 1.6 x 10^4 cells/cm^2. Flasks were incubated at 37°C overnight, to allow adhesion of the fibroblasts. Feeder layers were used for mESC culture within 1 week.

2.2.1.iii Mouse embryonic stem cell culture

Mouse ESCs were maintained on inactivated SNL feeder layers in mESC medium (SNL culture medium containing 500 U/mL LIF (Millipore, Watford, UK)). LIF was added to mESC culture medium to help maintain pluripotency of the cells during continuous culture. Cells were cultured until approximately 80% confluent. Confluency was judged by eye when individual cell colonies began to touch.

Cells were passaged using trypsin/EDTA treatment at room temperature with gentle agitation, until gaps appeared in the cell monolayer, indicating detachment from feeder layer. Cell suspension was transferred to a 25 mL universal tube and an equal

volume serum-containing medium added to inactivate the trypsin/EDTA. Suspension was centrifuged at 180 x g for 5 minutes, the cell pellet resuspended in the appropriate volume of culture medium and cells seeded at the desired cell density, on an SNL feeder layer. Typical passage ratio was 1:5 to achieve confluency in 2 days, but was adjusted as required. Cells were monitored closely for visual changes in morphology, indicating the beginnings of differentiation. Medium changes occurred daily.

2.2.1.iv Isolation and culture of mouse primary calvarial cells

Mouse primary calvarial cells are well described in literature, both in terms of response to proinflammatory cytokines and osteogenic differentiation [127, 162, 163]. Thus, they were chosen as a comparison to the less well-described mESCs.

Primary calvarial cells were isolated in-house from 1-3 day old CD-1 mice using a collagenase digestion technique. Calvaria were extracted from the skulls of the neonatal mice (see figure 2.1) and washed in PBS containing 100 U/mL penicillin, 25 µg/mL amphotericin B and 100 µg/mL streptomycin. Extraction was performed in a laminar flow hood (Envair, Haslingden, UK) using sterilised dissection equipment, viewed under a Nikon SMZ546 stereo dissection microscope illuminated with a KL 1500 portable light source. The antibiotics and antifungal were used to ensure that no infection was carried from the mice into cell culture.

Dissected calvariae were transferred in PBS containing antibiotic and antifungal, to a class II microbiological safety cabinet. PBS solution was removed and calvariae were cut up using sterile scissors to increase surface area. The calvaria were digested in a

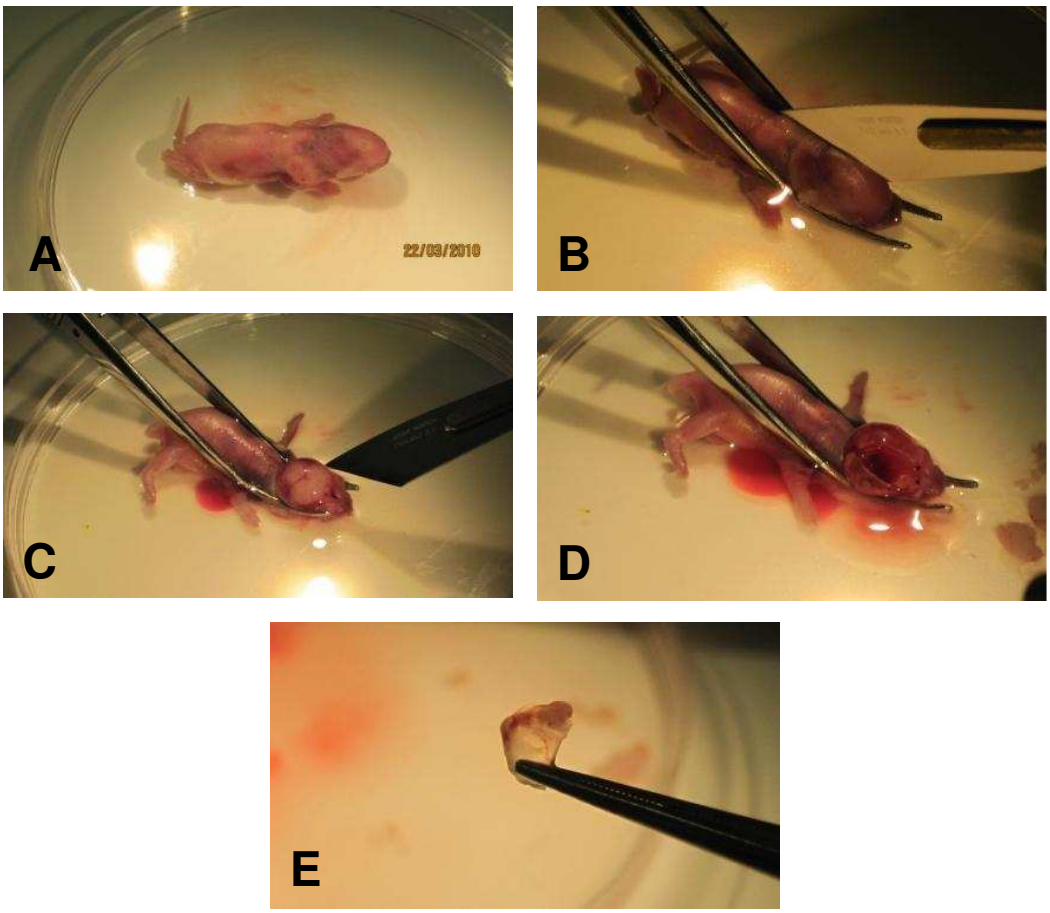

Figure 2.1: Extraction of the mouse calvariae. (A) One day old CD1 mouse (B) Initial skin incision (C) Skin pulled back to reveal skull and brain removed (D) View of neonatal skull (2 halves of calvaria with brain removed (E) Fully extracted neonatal mouse calvariae.

solution containing 1.4 mg/mL collagenase IA and 0.5 mg/mL trypsin II S for 12 minutes under constant agitation (Stuart Roller Mixer SRT6) at 37°C. The first population of cells released from the calvariae was aspirated and discarded. The calvariae were then suspended in a fresh aliquot of digestion solution and incubated for a further 12 minutes. This population of cells was also discarded. Fresh digestion solution was placed on the calvariae and digestion occurred for a further 12 minutes. This cell population was collected, an equal volume of FBS added and placed on ice. Two further cell populations were collected this way. The three populations on ice were pooled together. This serial digestion procedure was optimised to obtain a cell population rich in potential osteoblasts.

The resulting cell suspension in FBS was filtered through a 70 µm cell strainer, to remove tissue debris, and centrifuged for 5 minutes at 300 x g. The cell pellet was resuspended in primary calvarial cell medium containing Minimum Essential Medium Alpha (αMEM, Lonza) with 10% (*v/v*) FBS, 100 U/mL penicillin, 100 µg/mL streptomycin and 2 mM L-Glutamine. αMEM is an enriched minimal essential medium often used in the culture of osteoblasts. Cells were seeded in T75 cm^2 flasks, dependent on original number of calvariae, and incubated at 37°C for 24 hours. Removal of non-adherent haematopoietic cells was performed after 24 hours by washing with PBS twice before a medium change. Cells were allowed to become 80-90% confluent before a standard cryopreservation step (see Appendix II) at a density of 800,000 – 1,000,000 cells/mL.

Cell were reanimated from cryopreservation, maintained in cell culture flasks in primary calvarial cell medium, and used experimentally up to passage 3.

2.2.1.v Induction of osteogenic differentiation

2.2.1.v.a Embryonic stem cell osteogenic differentiation

To initiate the process of osteogenesis, the mESCs were induced to form embryoid bodies (EBs) by a mass suspension method. The mESCs were detached from the feeder layer by treatment with trypsin, as with passaging. After centrifugation, the cell pellet was resuspended in SNL culture medium, without LIF, and transferred to a non-adherent 10 cm petri dish at a density of 200,000 cells/mL, in 10 mL SNL culture medium. The cells were incubated under static conditions at 37°C for 3 days. Under these conditions, the mESC cells spontaneously aggregated to form EBs containing cells of the three germ layers.

After 3 days culture, the EBs were dissociated using trypsin treatment, to a single cell suspension, allowing culture as a cell monolayer. EBs were collected in a 15 mL falcon tubes, and allowed to settle under gravity. The supernatant was aspirated and EBs washed twice in PBS and allowed to settle again. EBs were resuspended in 10 mL trypsin and incubated under constant agitation, on a Stuart Roller Mixer SRT6, for 10 minutes at 37°C. This process breaks up the EBs gently, creating a single cell suspension. This suspension was centrifuged for 5 minutes at 180 x g, the cell pellet resuspended in SNL culture medium and passed through a 70 µm cell strainer to remove any remaining large aggregates and extraneous ECM. Viable cells were counted using a Neubauer haemocytometer and a trypan blue exclusion technique (see Appendix III). Viable cells were added at the cell density of 10,600 cells/cm^2, to tissue culture well-plates that had been pre-coated with 0.1% (*w/v*) gelatin. Plates were then incubated at 37°C overnight.

After 24 hours, dissociated EB cultures were changed to osteogenic medium by supplementing the SNL culture medium with 50 µg/mL ascorbate-2-phosphate, 50

mM β-Glycerophosphate (BGP) and in some cases 10 μM dexamethasone. Cells were incubated for the desired time-period with medium changes every 1-2 days. Throughout this study, from the moment the medium is changed to osteogenic, these cells are known as osteo-mESCs.

The supplements used to initiate osteogenic differentiation have been well described [60, 164]. Ascorbate 2-phosphate provides the ascorbic acid source that is vital for collagen production [165]. BGP provides an organic phosphate source allowing mineralisation of the ECM [162]. Dexamethasone is a glucocorticoid steroid. It is often used for *in vitro* osteogenic differentiation protocols, but the mechanism of action is not well understood. As dexamethasone is also an anti-inflammatory, it was used carefully throughout these studies, so as not to inhibit inflammatory signalling.

2.2.1.v.b Primary calvarial cell osteoinduction

Primary calvarial cells were reanimated from cryopreservation and cultured to passage 2, in standard tissue culture flasks. Trypsin/EDTA was used to detach the cells from the flasks. Cells were counted using trypan blue exclusion and a Neubauer haemocytometer. Primary calvarial cells were seeded in tissue-culture treated plates at a density of 10,600 cells/cm^2 and allowed to adhere overnight at 37°C. Culture was changed to osteogenic by supplementation of the primary calvarial medium with 50 μg/mL ascorbate-2-phosphate, 50 mM BGP and in some cases 10 μM dexamethasone. Cells were incubated for the desired time-period with medium changes every 1-2 days.

2.2.1.vi Proinflammatory cytokine stimulation

Throughout this study, the proinflammatory cytokines IL-1β, TNF-α, and IFN-γ were added to the cell culture medium, in varying concentrations and combinations, to simulate an inflammatory environment. Addition of the cytokines occurred at various times of osteogenic differentiation of both the osteo-mESCs and primary calvarial cells.

The cytokines arrived in lyophilised form and were reconstituted in PBS containing 0.1% (*w/v*) bovine serum albumin (BSA) and stored at -20℃ in aliquots of various concentrations, before dilution when used experimentally.

2.2.1.vii Anti-inflammatory mediator addition to culture medium

Several anti-inflammatory mediators were added to the culture medium and used during experiments to inhibit proinflammatory cytokine stimulation. Dexamethasone, prednisolone, piroxicam and ibuprofen had low solubility in water, so were first dissolved in dimethyl sulfoxide (DMSO). A mass of drug was weighed that would result in a concentration of 1 mM. Drug was fully dissolved in 1 mL DMSO, before medium added to make a total volume of 10 mL. This solution was then diluted further in medium to achieve the desired concentration. Control cultures that contained no drug in the media were adjusted to contain the same concentration of DMSO. Diclofenac sodium has solubility in water, so was dissolved in medium without DMSO at 37℃, to make a stock concentration of 1 mM, which could be further diluted. The recombinant protein IL-1ra was purchased lyophilised and reconstituted in PBS containing 0.1% (*w/v*) BSA, as per the manufacturer's instructions, before being further diluted in medium.

2.2.2 Viability, Proliferation and Cytotoxicity Assays

Several methods of detecting changing in cell viability, and cytotoxicity of agents added to the cell culture medium, were used throughout this investigation.

2.2.2.i MTS Assay

One method used to detect changes in cell viability, as well as the cytotoxic effects of adding proinflammatory agents to the culture medium, was the CellTiter AQ_{ueous} One Solution Proliferation® Assay (Promega, Southampton, UK), also known as the MTS assay. This assay detects viable cells in culture through a tetrazolium compound [3-(4,5-dimethylthiazol-2-yl)-5-(3-carboxymethoxyphenyl)-2-(4-sulfophenyl)-2H-tetrazolium, inner salt] (MTS), which with the help of an electron coupling reagent, phenazine ethosulphate (PES), is bioreduced by cells into a soluble coloured formazan product. This product can be detected by reading optical absorbance at 490 nm. Conversion is completed through NADH or NADPH produced by dehydrogenase enzymes in metabolically active cells. Thus, the optical absorbance is directly proportional to the number of metabolically active, viable cells.

To assess viability, osteo-mESCs and primary calvarial cells were grown in 96-well plates with various agents. At specific timepoints, 20 µL of MTS reagent was added to each cell-containing well, in 100 µL cell culture medium. Cells were incubated at 37℃ for 1 hour before the absorbance was read at 490 nm, with a wavelength correction of 690 nm, using a Tecan Infinite® 200 PRO plate reader. The wavelength correction accounts for variations in the optical properties across the assay plate, cell debris and fingerprints. Proliferation studies were performed using separate plates for each timepoint.

2.2.2.ii Lactate Dehydrogenase (LDH) Assay

This assay was used to measure levels of cytotoxicity, possibly caused by agents added to the cell culture medium. The assay measures levels of LDH in cell supernatants, an enzyme that is released upon cell lysis. The assay works on the principle that LDH present within the sample causes oxidation of lactate to pyruvate, which in turn, catalyses the reduction of NAD^+ to NADH. The second step of the reaction uses the NADH to catalyse the conversion of a tetrazolium salt to a coloured formazan product. Optical absorbance of the formazan at 492 nm is then directly proportional to the level of LDH within the sample.

To assess cytotoxicity of the proinflammatory cytokines or anti-inflammatory mediators using LDH production, the CytoTox 96® Non-Radioactive Cytotoxicity assay (Promega) was used. Cell culture medium supernatants were taken at certain timepoints of culture. Lysis of an identical cell monolayer, using the lysis solution provided in the kit, was performed at this timepoint, to determine maximum LDH release of the cells. LDH levels were determined by adding 50 µL of the substrate solution to 50 µL sample. Cell culture medium controls and LDH positive controls were also performed. The reaction was incubated for 30 minutes at room temperature, before a stop solution was added. The absorbance values were then determined by reading the plate at 492 nm on the plate reader (Tecan) with a wavelength correction of 690 nm.

Cytotoxicity values were determined by:

$$\text{Cytotoxicity (\%)} = \frac{\text{Experimental LDH release}}{\text{Maximum LDH release}} \times 100$$

2.2.2.iii Live/Dead™ Fluorescence Assay

The Live/Dead™ fluorescent stain was used to visualise changes in cell viability in response to cytotoxic agents. The Live/Dead® Viability/Cytotoxicity Assay kit contains two fluorescent probes: calcein AM; which is converted via intracellular esterase activity to the fluorescent calcein to indicate viable cells, that fluoresce green; and ethidium homodimer-1 (EthD-1), which enters non-viable cells with damaged membranes and binds to nucleic acids, fluorescing red. The assay can be used for imaging cells using fluorescent microscopy, as a quantitative assay using a fluorescent microplate reader or in flow cytometry.

To assess cell viability, cell culture medium was aspirated or collected for other assays, and cells were incubated with Live/Dead™ solution containing 2 μM calcein AM and 4 μM EthD-1 in PBS, for 30 minutes at room temperature. Cells were washed in PBS before imaging using an inverted fluorescent microscope, with excitation/emission wavelength of 495/515 nm for calcein AM and 495/635nm for EthD-1.

2.2.3 Nitric Oxide Production

NO is produced in response to proinflammatory cytokines, through the inducible nitric oxide synthase (iNOS) pathway and can give an estimate of the inflammatory response. Although both nitrite (NO_2^-) and nitrate (NO_3^-) are both stable end-products of NO, measurement of nitrite has been shown to be a good indicator of NO production *in vitro*, due to a strong correlation between the levels of nitrite and nitrate produced [166].

To determine nitrite release, the Griess Reagent System (Promega) was used. In the Griess reaction the acidified NO_2^- ion reacts with sulphanilamide to produce a diazonium ion, which then couples to N-(1-napthyl)ethylenediamine (NED) to form a chromophoric azo-derivative that absorbs light at 540-570 nm.

Cell supernatant samples were centrifuged to remove particulates and 50 µL was transferred to a 96-well plate. To perform the Griess assay, an equal volume of 1% (*v/v*) sulphanilamide in 5% (*v/v*) phosphoric acid was added to the samples and the plate incubated for 5 minutes at room temperature. NED (50 µL of 0.1% (*v/v*) in water) was added and the plate incubated at room temperature for 5 minutes. Absorbance at 540 nm was recorded immediately, using a plate reader, with a wavelength correction at 690 nm. Nitrite concentrations were determined using standard curves, prepared from serial dilutions of sodium nitrite, prepared each time the assay was performed.

2.2.4 Prostaglandin E_2 Production

Levels of prostaglandin E_2 (PGE_2) in the cell culture medium can be used as an indicator of the cellular response to proinflammatory cytokines. PGE_2 production was assessed using the Parameter™ PGE_2 Assay (R&D Systems), an enzyme immunoassay (EIA) based on competitive binding. The PGE_2 in the sample competes with horseradish peroxidase (HRP)-labelled PGE_2, for binding sites on a PGE_2 monoclonal antibody. A substrate solution determines the level of HRP-labelled PGE_2 bound to the antibody, causing a colour development. This colour is inversely proportional to the concentration of PGE_2 in the sample.

Cell supernatant samples were centrifuged to remove debris and a 3-fold dilution performed using assay buffer. Sample (150 µL) was added to a 96-well microplate

coated with a goat anti-mouse polyclonal antibody and a solution of PGE_2 monoclonal antibody was added. The plate was incubated at room temperature for one hour on an orbital microplate shaker at 500 rpm, to allow PGE_2 in the sample to bind to the antibody. HRP-conjugated PGE_2 was then added and the plate incubated at room temperature on the shaker for 2 hours, allowing the HRP-conjugated PGE_2 to bind to any remaining antibody. All antibody-bound material attaches to the coated microplate. The plate was washed three times with wash buffer, substrate solution added and a colour change developed. After 30 minutes static incubation at room temperature, a stop solution was added, causing another colour change, which was measured for optical absorbance at 450 nm, with wavelength correction at 570 nm. PGE_2 concentration within the sample was determined using standard curves, prepared each time the assay was performed.

2.2.5 DNA Quantification

DNA quantification was used to correct determined levels of nitrite and PGE_2 for cell number. Levels of DNA within a sample were determined via the Hoechst assay. Hoechst 33258 is a fluorescent bisbenzimide dye that binds to the A-T coupling in DNA. The more DNA within a sample, the more intense the fluorescence.

Hoechst 33258 was diluted to 1 mg/mL in saline sodium citrate buffer (SSC), aliquoted and stored at -20°C. DNA standards were prepared by dissolving calf thymus DNA in SSC to a 1 mg/mL stock that was aliquoted and stored at -20°C.

Samples were prepared by lysing a cell monolayer in 0.02% (*w/v*) sodium dodecyl sulphate solution (SDS) to release DNA. Samples were transferred to black 96-well plates. Standards were prepared from the calf thymus DNA, with a maximum of 20

µg/mL. A working solution of Hoechst 33258 was prepared at 2 µg/mL in distilled water. This was added to the sample and standards and thoroughly mixed. Fluorescence was recorded at excitation wavelength 360 nm and emission wavelength 460 nm. DNA concentration of the samples was determined using the standard curve prepared from calf thymus DNA.

2.2.6 Cell Fixation

Cell fixation at the end of an experiment ensures preservation of cell morphology and ECM architecture. Fixatives need to be suited to the end staining procedure. For the purposes of the histological stains used in this study, 10% (*w/v*) neutral-buffered formalin was used. Formalin is a good fixative for histology purposes as it forms cross-links between protein molecules and preserves a robust tissue structure. For formalin fixation, the cell monolayers were washed in PBS before incubation in formalin for 10 minutes. The formalin solution was then washed off three times with PBS and the fixed cell monolayers stored in PBS at 4℃, until staining.

For immunocytochemical procedures, 4% (*w/v*) paraformaldehyde (PFA) fixation was employed. The PFA recipe can be found in Appendix IV. PFA is polymerised formaldehyde and therefore is a larger molecule that does not form as many cross-links as formalin. This allows better tissue penetration of antibodies and the ability to perform steps such as permeabilisation and antigen retrieval that can improve immunocytochemical staining. The paraformaldehyde fixation protocol is similar to fixation with 10% (*w/v*) formalin although fixation time is increased to 15 minutes.

2.2.7 Immunocytochemistry

Immunocytochemistry is a technique in which antibodies are used to target specific proteins or peptides. These antibodies can be labelled to allow the protein to be visualised and imaged. In this study, an indirect method of immunocytochemistry was performed, using primary and secondary antibodies.

Fixed cell monolayers were washed in PBS and permeabilised in 0.1% (*v/v*) Triton-X100 in PBS for 15 minutes. Permeabilisation allows the antibody to penetrate the cell membrane and can create a more accurate final stain. Monolayers were washed 3 times in PBS for 5 minutes to remove Triton-X100 traces and a blocking step performed. The blocking solution is made up of PBS containing 1% (*w/v*) BSA and 3% (*v/v*) serum from the animal in which the secondary antibody was raised. The blocking step prevents non-specific binding of the secondary antibody and a sharper final image. Blocking solution was blotted and the primary antibody solution applied.

Primary antibodies used throughout this study can be found in Table 2.1. Antibodies were initially made-up to manufacturer's instructions then diluted in PBS containing 1% (*w/v*) BSA, at concentrations stated in Table 2.1. Cell monolayers were incubated with primary antibody solution at 4°C overnight. Primary antibody solution was washed off 3 times in PBS containing 1% (*w/v*) BSA, each wash for 5 minutes. Secondary antibody solution was then applied and incubated at room temperature for 1 hour. All secondary antibodies (see Table 2.1) were conjugated to a fluorescent tag and diluted in PBS containing 1% (*w/v*) BSA. After incubation, cell monolayers were washed 3 times in PBS and 1 µg/mL Hoechst 33258 applied for 30 minutes, to provide a nuclear stain, before final washing 3 times in PBS. Staining could then be imaged (see Section 2.2.11).

2.2.8 Real-time quantitative polymerase chain reaction (RT-qPCR)

RT-qPCR is based on the principle of the polymerase chain reaction (PCR) and allows a target DNA molecule to be amplified and quantified. To determine levels of a target gene within cell samples, ribonucleic acid (RNA) samples must first be extracted from cells and used to produce DNA via reverse transcription, creating complementary DNA (cDNA). PCR can then be performed using DNA polymerase, with specific primers, to amplify the target DNA. To achieve quantification of the level of amplification, a DNA binding fluorescent dye (in this case, SYBR green) can be used. This dye binds to the double stranded DNA whilst it is being created and with each amplification fluorescent intensity increases. This intensity can be recorded using a real-time PCR instrument. Using fluorescent intensity data, quantification can be performed. In this case, relative quantification is employed, using reference genes to determine fold-differences in expression of the target gene.

2.2.8.i RNA Isolation and purification

In this study, total RNA was harvested from the cells and extracted using an RNeasy kit (Qiagen, West Sussex, UK), according to the manufacturer's instructions. Samples were first lysed, and then an RNeasy mini spin column was used to extract the RNA using a variety of buffers and centrifugation steps. Extracted RNA was stored in 30 µL RNase free water at 80℃. Steps were performed on ice and utilising a temperature controlled centrifuge set at 4℃, to prevent RNA degradation. The concentration of RNA within the sample was measured using a NanoDrop spectrophotometer (Thermo Scientific NanoDrop 2000) at 260 nm.

2.2.8.ii Reverse Transcription

Reverse transcription of RNA into single stranded cDNA was performed using the Superscript II System (Invitrogen) and random hexamer primers, according to the manufacturer's instructions. The random hexamer primers anneal randomly to the RNA and the reverse transcriptase enzyme then synthesises cDNA from the primer sites using deoxynucleotide triphosphates (dNTPs). This process occurred using a PCR thermal cycler (Px2 Thermal Cycler, Thermo Scientific, Surrey, UK), that denatured the RNA at 85℃, allowing primer adhesion. The reaction is then heated at 55℃ to allow the reverse transcriptase to form the cDNA. Resulting cDNA transcripts were stored in RNase/DNase free water at -20℃.

2.2.8.iii RT-qPCR

RT-qPCR was performed on a MyiQ RT-PCR detection system (Bio-Rad, Ontario, Canada) using iQ SYBR Green supermix (Bio-Rad). To perform the reaction 6 µL cDNA sample, 5 µL of each of the forward and reverse primers (final concentration 300 nM) and 10 µL supermix were added to the wells of a qPCR plate. Preparation of samples was performed on ice. The thermal cycling protocol was then run on the RT-PCR detection system, according to manufacturer's instructions, with the annealing temperatures described in table 2.3. Forty amplification cycles were performed.

Data analysis was performed using online software based on a four parameter simple exponent model [167], that calculate efficiency (E) and threshold cycle (C_T). Expression levels were calculated using an efficiency corrected comparative threshold cycle (C_T) method ($E^{\Delta\Delta CT}$). All values were normalised to the *Rpl32* ribosomal protein gene, to get fold differences in gene expression.

2.2.9 Assessment of Mineralisation

Mineralisation of cell-secreted matrix was assessed via staining of calcium deposits by alizarin red S. The alizarin red dye chelates with calcium to give a bright red/orange colour. Fixed cell monolayers were washed twice in distilled water before being treated with 2% (*w/v*) alizarin red S solution in dH_2O for 4 minutes. Alizarin red solution was removed and cultures were washed repeatedly in dH_2O until no further colour leached out. Staining could then be imaged (see Section 2.2.11).

2.2.10 Assessment of Alkaline Phosphatase Activity

ALP is a membrane bound enzyme which catalyses the hydrolysis of phosphate monoesters and is found in abundance in bone, liver, kidney and placental tissue [168]. Levels of non-specific ALP can be assessed by the p-nitrophenyl phosphate (pNPP) assay. ALP acts as a catalyst for pNPP hydrolysis to p-nitrophenol (pNP). pNP is chromogenic and has a yellow appearance that can be read at an optical absorbance of 405 nm.

Cell monolayers were washed in 0.2 M tris buffer, and then lysed in a solution of 0.1% (*v/v*) Triton- X100 in 0.2 M tris buffer, and the cell layer collected using a cell scraper. Samples were centrifuged at 10,000 x g for 10 minutes and transferred to a 96-well plate. A pNPP solution of 1 mg/mL in 0.2 M tris buffer was added. Samples were incubated at room temperature for 20 minutes whilst the reaction occurred. Absorbance was then read at 405 nm. Assaying of ALP standards was also performed to derive a standard curve that could be used to extrapolate ALP concentration within the samples.

2.2.11 Microscopy and Imaging

2.2.11.i Microscopy

Fluorescently immunostained cell monolayers and Live/Dead™ stains were viewed using an inverted-microscope (Leica DM-IRB) and images captured using a Hamamatsu digital camera and Volocity imaging software (Improvision, Coventry, UK).

Alizarin red stained monolayers were viewed using a Nikon Eclipse 90i stereo dissection microscope and imaged as complete wells. Higher magnification images were taken using a Nikon Eclipse TS100 inverted microscope with Hoffman contrast and attached imaging screen and software (Nikon Digital Sight DS-L1).

2.2.11.ii Image Processing and Analysis

Image processing was performed to remove non-specific background of immunocytochemistry images, using Volocity imaging software. Secondary antibody only control images were used as a background subtraction.

Image analysis of the Alizarin Red stained monolayers, to determine area stained, was performed using ImageJ version 1.43U (NIH, USA). Images were thresholded to isolate the stained nodules, the image converted to 8-bit, and the percentage area stained quantified. Cell counts for Live/Dead™ images were also performed using ImageJ. Stained cells were identified, contrast was adjusted so the brightest part of each cell was visible, the image then converted to binary and a watershed applied. The number of particles could then be counted as a representative count of each cell.

2.2.12 Magnetic-Activated Cell Sorting

MACS is a method of isolating a cell population of interest or depleting a cell population of an unwanted cell type. Cells can be sorted via a particular antigen. An antibody is bound to this antigen and attached to a magnetic particle. After binding, the cells are passed through a column within a magnetic field. Cells labelled with the magnetic particle-conjugated antibody are held within the column and unlabelled cells pass through. The column can then be removed from the magnetic field and labelled cells eluted.

In this study, osteogenically differentiated mESCs were sorted for a cadherin-11 (cad-11) positive population. Osteo-mESCs were cultured in gelatin-coated flasks in osteogenic medium for 16 days. Cell monolayers were washed in PBS and cells incubated in trypsin for 10 minutes. Due to the high levels of ECM produced by the osteo-mESCs, trypsin incubation was not sufficient to remove all cells from the flask, so a cell scraper was utilised to ensure all cells had been detached. Trypsin was deactivated using serum-containing medium and the cell suspension transferred to a falcon tube. Cells were centrifuged at 180 x g for 5 minutes, resuspended in MACS buffer (PBS supplemented with 2 mM EDTA and 0.5% (*w/v*) BSA, degassed under vacuum) and passed through a 70 µm cell strainer to remove ECM. Cells were counted using a haemocytometer and centrifuged again at 180 x g for 5 minutes before being resuspended in primary antibody solution.

Primary antibody solution was goat anti-human cad-11 (see Table 2.1) at a concentration of 2 µg/mL in MACS buffer; 40 µL primary antibody was used per 1 x 10^6 cells. Cells were incubated in primary antibody solution for 5 minutes at room

temperature, diluted using 10x the volume of MACS buffer, before centrifugation for 5 minutes at 180 x g. Supernatant was removed carefully and secondary antibody added (biotinylated anti-goat, see Table 2.1), at 10 µg/mL in MACS buffer. Per 1 x 10^7 cells, 80 µL MACS buffer and 20 µL secondary antibody solution was added. Cells were incubated for 10 minutes at 4°C. Cells were then washed by adding 10x volume of MACS buffer and centrifuged for 5 minutes at 180 x g. Supernatant was removed and 80 µL MACS buffer and 20 µL MACS anti-biotin magnetic microbeads (Miltenyi Biotec, Surrey, UK), were added per 1 x 10^7 cells and incubated at 4°C for 15 minutes. MACS buffer (10x labelling volume) was added to wash cells and suspension centrifuged at 180 x g for 5 minutes, for the final time. Cells were then resuspended in 500 µL MACS buffer, up to a volume of 1 x 10^8 cells.

Separation of the cells took place on a MiniMACS™ magnetic separation unit (Miltenyi Biotech). This comprises a metal stand and a powerful magnet. The magnet holds a separation column (MS column, Miltenyi Biotech) to the stand, creating a magnetic field and magnetizing the column. The column was first washed by passing 500 µL MACS buffer through. Effluent was discarded and the magnetically-labelled cell suspension was passed through the column. Cad-11 positive cells would now be labelled with magnetic microbeads and remain in the column. The negative cell fraction passed through the column and was collected. The magnet was removed, demagnetizing the column and 1 mL MACS buffer added and the cell suspension forced through by plunger, creating a cad-11 positive cell fraction. The cad-11 positive and negative fractions were then cultured in gelatin-coated 6-well plates in osteogenic medium.

2.2.13 Production of PLGA/PEG Scaffolds

PLGA/PEG scaffolds were used in this study as a candidate for bone repair, they have previously been described by the Tissue Engineering group, University of Nottingham, UK (patent number: PCT/GB08/00329) [169-172]. The scaffolds are produced from sintered poly(lactic-*co*-glycolic) acid (PLGA) blended with poly(ethylene glycol) (PEG) microparticles (PLGA/PEG particles). Blending the PLGA with the correct ratio of PEG, a plasticiser, reduces the glass transition temperature (T_g) of PLGA to 37°C. The PLGA/PEG microparticles form a free-flowing powder at room temperature. When mixed with a carrier solution such as water or PBS, the microparticles form a particulate paste. This paste is of a consistency that can be injected or moulded into any shape or size. At body temperature (37°C), the paste solidifies as it sinters and forms a solid porous scaffold. During the sintering process, the microparticles soften and reach T_g, become cohesive and adhere to each other. At this stage, the hydrophilic PEG begins to leach out of the particles, reducing the PEG concentration, leading to an increase in T_g. This causes the particles to re-solidify forming porous strong scaffolds. A schematic of this process can be seen in figure 2.2. To manufacture scaffolds containing anti-inflammatory drugs, the drug is solubilised within the carrier solution.

2.2.13.i Production of temperature-sensitive PLGA/PEG particles

PLGA (53 kDA, 85:15 DLG 4CA, Lakeshore Biomaterials, USA) and PEG 400 were mixed at a ratio of 93.5:6.5, PLGA:PEG (w/v), on a poly(tetrafluoroethylene) (PTFE) sheet and melt blended at 80-90°C on a hotplate. The melted PLGA and PEG were thoroughly blended by hand using a PTFE spatula and once mixed were taken off the

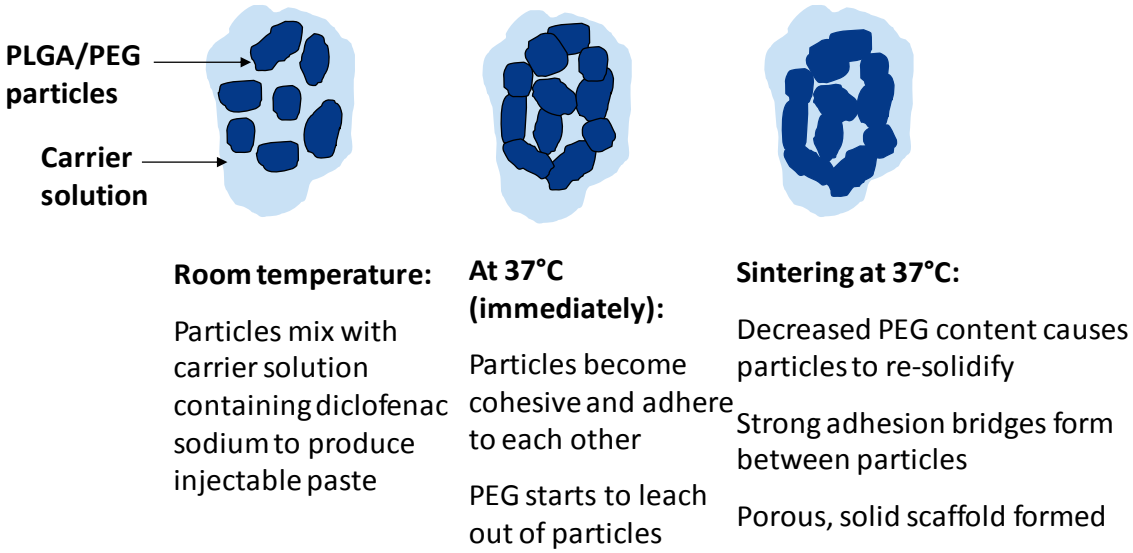

Figure 2.2: Schematic showing formation of PLGA/PEG scaffolds. The PLGA/PEG microparticles are mixed with a carrier solution (possibly containing anti-inflammatory drug) . This paste is then packed into moulds and sintered at 37°C, where the paste solidifies to become a porous scaffold.

heat and allowed to cool. Polymer blend sheets were cut into small pieces and ground into particles using a bench-top mill (Krups Mill F203), with liquid nitrogen cooling. Once ground, the particles were sieved to obtain a 100-200 µm size fraction.

2.2.13.ii Production of diclofenac sodium-loaded PLGA/PEG scaffolds

Scaffolds were prepared in PTFE moulds to produce cylindrical scaffolds of 12 mm length and 6 mm diameter. The PLGA/PEG particles were mixed manually at a ratio of 1:0.6, particles to PBS carrier solution. Diclofenac sodium loaded scaffolds were produced by mixing the particles in this ratio with PBS containing diclofenac sodium at various concentrations (see section 5.2.4) The microparticle/PBS paste was packed into the moulds. Moulds were placed at 37°C for 3 hours and allowed to sinter, forming a solid scaffold.

2.2.13.iii Measurement of drug release from PLGA/PEG scaffolds

Diclofenac sodium release from the scaffolds was measured by ultraviolet-visible (UV-Vis) spectrophotometry. After scaffolds had dry sintered at 37°C for 3 hours, they were removed from moulds and placed into bijoux. Release medium (1.5 mL) was added carefully to the bijoux and the scaffolds incubated at 37°C, for drug release to begin. In this study, the release medium was either phenol red-free αMEM (Invitrogen) or PBS. After certain time-periods, all release medium was removed from the scaffold for drug concentration measurements and fresh release medium added. Drug concentration measurements were taken using a microvolume UV-Vis spectrophotometer (Thermo Scientific NanoDrop 2000) at 276 nm. This wavelength was chosen after an absorbance scan was run, showing this as the peak. The

NanoDrop spectrophotometer was chosen rather than a conventional UV-Vis plate reader, as when reading from a 96-well plate at 276 nm, background absorbance caused by the polystyrene was very high. The NanoDrop does not require a plate to be used and allows smaller volumes of sample to be read (2 µL), so more readings could be taken. Standard diclofenac concentrations were determined, to enable a calibration curve to be drawn and to decipher minimum and maximum concentrations that could be measured. Concentrations of drug within the sampled release medium were determined using the calibration curve.

2.2.14 Statistical Analysis

Statistical significance between groups was analysed using PASW Statistics 18.0.3 software. Data sets were tested for normality and comparison tests chosen appropriately. Simple paired analysis was performed using unpaired Student's T-Test, with variances analysed by Levene's test. Multiple group comparisons were performed using one-way ANOVA, post hoc tests performed were Tukey, when variances were assumed equal, and Games-Howell in cases where variances were not assumed equal and sample sizes differed.

Chapter 3: Results
Effect of Proinflammatory Cytokines on Osteogenic Cell Response

3.1 Introduction

3.1.1 Overview

The investigation of cell differentiation *in vitro,* with possible applications to cell therapy, is typically performed in favourable environments, where nutrients and temperatures are controlled. However, the potential therapeutic target environment is characteristically one of tissue damage and inflammation. In order to mimic inflammation *in vitro*, proinflammatory cytokines such as IL-1β, TNF-α and IFN-γ, are often added to cell culture medium. When considering bone tissue engineering and osteogenic differentiation, it is important to consider the response of osteoblasts and osteogenic cells to these cytokines. Proinflammatory cytokines have *in vitro* effects on osteoblast proliferation, collagen synthesis, mineralisation and ALP activity [111, 112, 114, 173, 174]. Other measurements of osteoblast response to proinflammatory stimuli include increased prostaglandin and NO production, changes in cell viability and expression of various inducible enzymes including iNOS and COX-2 [128, 175, 176].

3.1.2 Proinflammatory cytokines

Proinflammatory cytokines are cell-signalling proteins that help to orchestrate local and systemic inflammation in response to traumatic injury or infection. This group contains IL-1, interleukin-6 (IL-6), interleukin-17 (IL-17), TNF-α and IFN-γ [126]. These cytokines are the major signalling molecules in both acute and chronic inflammation. This investigation focuses on the cytokines IL-1β, TNF-α and IFN-γ. IL-1β and TNF-α have similar *in vivo* inflammatory effects. The only major difference between the two cytokines is the involvement of TNF-α in the apoptotic pathway [126]. *In vivo*, the two cytokines work synergistically to attract leukocytes and stimulate production of mediators such as PGE_2 and NO [127, 128]. Prolonged production of IL-1β and TNF-α can cause extensive tissue remodelling and damage. The other cytokine concentrated on throughout this study, IFN-γ, is produced primarily by NK cells and T-lymphocytes, that interact with macrophages and orchestrates leukocyte attraction [129]. IL-1β, TNF-α and IFN-γ all possess the ability to interact with osteoblasts and other bone cells. Osteoblasts themselves can produce IL-1β and TNF-α and receptors for all three cytokines can be found on osteoblasts and osteoclasts [121, 177].

3.1.3 Prostaglandins and Nitric Oxide

Prostaglandins, particularly PGE_2, play a significant role in modulating the inflammatory response, leading to symptoms such as pain, swelling and fever [178]. Evidence exists showing that prostaglandins play a role in bone remodelling; but during the inflammatory response expression and action of PGE_2 is very much altered

[149]. Prostaglandins are biologically active lipids, derived from arachidonic acid by the action of cyclooxygenase enzymes 1 and 2 (COX-1 and COX-2), producing an unstable immediate form, PGH_2. PGH_2 is converted to PGE_2 by PGE synthase (PGES). Likewise, PGD_2 is converted by PGD synthase. The two isoforms of the COX enzymes (COX-1 and COX-2) have distinct roles within the body. COX-1 is expressed constitutively in most tissues and has a role in prostacyclin production, which in turn is associated with vascular homeostasis [179]. COX-2 is an inducible enzyme involved in inflammation; normally undetectable, but can be generated in response to proinflammatory cytokine signalling, particularly IL-1β and TNF-α, leading to the generation of increased amounts of PGE_2 [180].

NO is a signalling molecule involved in a variety of physiological processes including vasodilation, neurotransmission and inflammation. The action of NO is determined by the site of synthesis, concentration and the environment of release [180]. NO is biosynthesised by the nitric oxide synthase (NOS) enzymes. The NOS enzymes function by oxidising the guanidine group of L-arginine, in a process that involves the oxidation of NADPH (nicotinamide adenine dinucleotide phosphate) and the reduction of molecular oxygen, resulting in the formation of L-citrulline and the NO molecule [181]. There are three isoforms of the NOS enzyme. Neuronal nitric oxide synthase (nNOS) and endothelial nitric oxide synthase (eNOS) are constitutively expressed in neural tissue and endothelial tissue respectively. The third isoform, inducible NOS (iNOS), is expressed in response to infection, inflammation or trauma. iNOS can lead to sustained generation of high levels of NO by osteoblasts, predominantly through proinflammatory cytokine signalling [175, 182, 183].

3.1.4 Investigation of the effects of proinflammatory cytokines

Whereas, the effects of proinflammatory cytokines have been comprehensively investigated on primary osteoblasts and osteoblast cell lines, little or no work has been performed on ESC-derived osteogenic cells. At the time of this study, there were no published comparative studies on ESC-derived and primary osteoblast response. The impact of these studies could have importance in production of a potential cell therapy for bone disease. The effect of creating a product under favourable conditions, that supports cell growth and maintenance of viability, and subsequently subjecting it to a damaged/diseased environment, could have a significant effect on the success or failure of the final therapy.

In this chapter, initial steps were taken towards discovering the effect that a proinflammatory environment had on the response of ESC-derived osteogenic cells. This response was compared to that of primary calvarial cells, a cell population containing mainly osteoblasts. Significant differences in the responses of the two cell types to exposure to the proinflammatory cytokines IL-1β, TNF-α and IFN-γ are described. Changes in combinations of cytokines and cytokine concentration were investigated and response in terms of viability, NO production, PGE_2 production and inducible enzyme expression, was assessed.

3.2 Experimental Design

For more detailed methods describing primary calvarial cell extraction and culture, mESC culture, EB formation, osteogenic differentiation and assay protocols see Chapter 2: Materials and Methods.

3.2.1 Response of Osteogenic Cells to Proinflammatory Cytokines

This group of experiments aimed to investigate the biochemical responses of primary calvarial cells and osteo-mESCs to proinflammatory cytokines. A schematic overview of experiments described in sections 3.2.1.ii, 3.2.1.iii and 3.2.1.iv can be found in figure 3.1.

3.2.1.i Dose response effect of individual cytokines on cell viability

Primary calvarial cells were seeded at a density of 10,600 cells/cm^2 in 96-well plates. EBs were formed from mESCs, dissociated and plated at the same density in gelatin-coated 96-well plates. Medium on both cell types was substituted with osteogenic medium (50 mM BGP, 50 µg/mL ascorbate 2-phosphate) the following day. This corresponds to day 0 of the experiment. From day 0, the cells were stimulated with the addition to the culture medium of: IL-1β at 0.1 ng/mL, 1 ng/mL and 10 ng/mL; TNF-α at 1 ng/mL, 10 ng/mL and 100 ng/mL; IFN-γ at 10 ng/mL, 100 ng/mL and 100 ng/mL, alongside an osteogenic control group containing no cytokines. To monitor

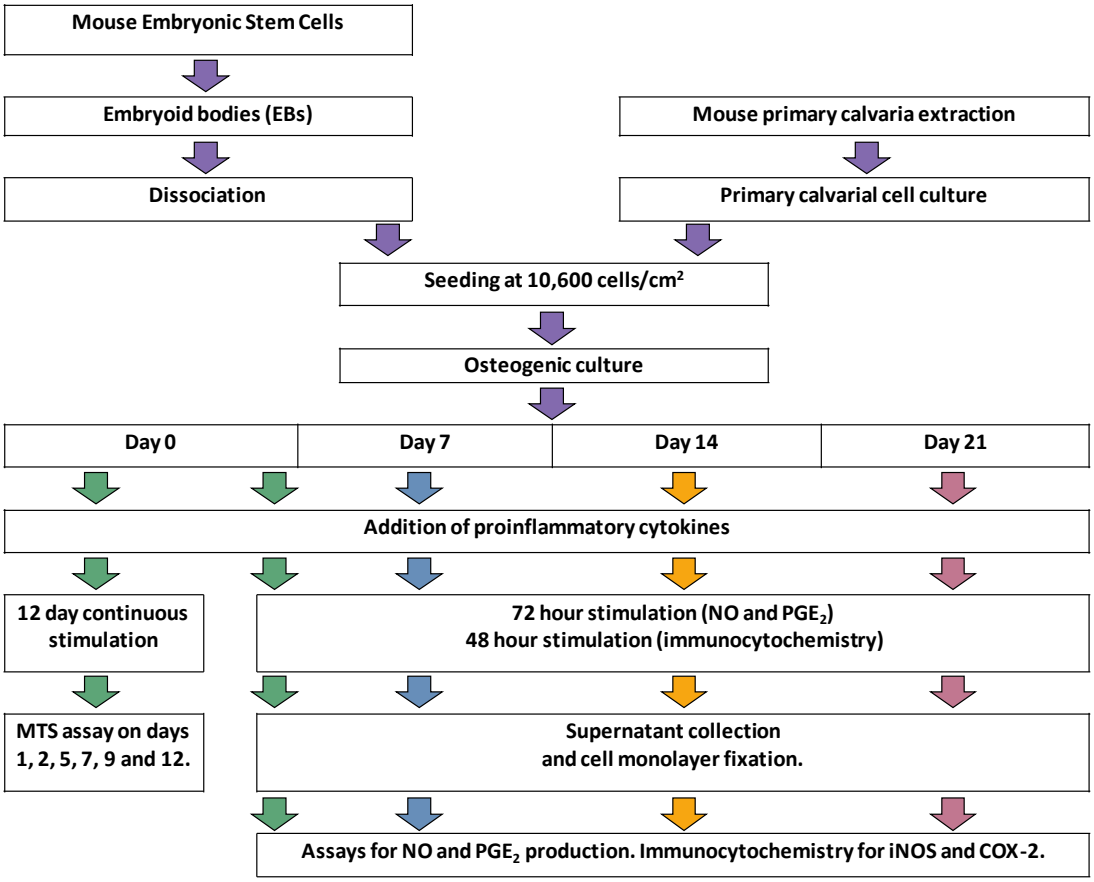

Figure 3.1: Schematic overview of experiments investigating response of osteogenic cells to proinflammatory cytokines. Schematic shows simplified experimental design for section 3.2.1, investigating response of primary calvarial cells and osteo-mESCs to IL-1β, TNF-α and IFN-γ, in terms of cell viability, NO production and inducible enzyme expression.

proliferation and change in cell viability over time, MTS assays were performed on days 2, 7 and 14. Each timepoint was represented by a separate 96-well plate.

3.2.1.ii Effect of combinations of proinflammatory cytokines on viability of osteogenic cells

Initially the setup to this experiment was identical to the dose response described above. From day 0 of osteogenic culture, the primary calvarial cells and osteo-mESCs were stimulated with various combinations of IL-1β (1 ng/mL), TNF-α (10 ng/mL) and IFN-γ (100 ng/mL) in the culture medium, alongside an osteogenic control group containing no cytokines. Cytokine groups included: IL-1β, TNF-α and IFN-γ alone; and combinations of IL-1β and TNF-α; IL-1β and IFN-γ; TNF-α and IFN-γ; and finally, IL-1β, TNF-α and IFN-γ. To monitor proliferation and change in cell viability over time, MTS assays were performed on days 1, 2, 5, 7, 9 and 12. Each timepoint was represented by a separate 96-well plate.

3.2.1.iii Nitric oxide and PGE_2 production in response to proinflammatory cytokines

Primary calvarial cells and dissociated EBs were plated in 96-well plates, as above. Cells were switched to osteogenic medium the following day (day 0). Different combinations of IL-1β (1 ng/mL), TNF-α (10 ng/mL) and IFN-γ (100 ng/mL) were added to the media at day 0, day 7, day 14 and day 21 of osteogenic culture.

Cytokine groups can be seen above, in section 3.2.1.1. Cytokines were applied for 72 hours at each of these timepoints before cell culture medium was collected for testing, and cell monolayers fixed in 10% (*w/v*) formalin. Supernatants were assessed for nitrite concentration via the Griess assay and PGE_2 concentration via EIA. DNA quantification by Hoechst assay was performed on the fixed cell monolayers; this was utilised to correct the nitrite and PGE_2 data for cell number.

3.2.1.iv Expression of inducible enzymes in response to proinflammatory cytokines

3.2.1.iv.a Immunocytochemistry

Expression of the inducible enzymes iNOS, COX-2 and PGES, at various timepoints of osteogenic differentiation was investigated by immunocytochemistry. Primary calvarial cells and osteo-mESCs were plated in 12-well plates and cultured in osteogenic medium from day 0. Proinflammatory cytokine stimulation (IL-1β (1 ng/mL), TNF-α (10 ng/mL) and IFN-γ (100 ng/mL), in combination) for 48 hours was performed at day 0, 7, 14 and 21 of osteogenic culture. Subsequently, cells were fixed in a 4% (*w/v*) solution of PFA and immunocytochemistry for iNOS, COX-2 and PGES performed using fluorescently-labelled secondary antibodies. Details of antibodies can be found in Chapter 2: Materials and Methods, Table 2.1 and Table 2.2. Control staining using primary antibody only and secondary antibody only was performed. Images were processed to remove background staining based on secondary antibody only controls.

3.2.1.iv.b RT-qPCR for iNOS expression

Primary calvarial cells and osteo-mESCs were differentiated in osteogenic culture medium in 6-well plates. Proinflammatory cytokine stimulation (IL-1β (1 ng/mL), TNF-α (10 ng/mL) and IFN-γ (100 ng/mL)) was performed at day 0 and day 21 of osteogenic culture for 48 hours. Subsequently, RNA samples were collected and RNA extracted. Reverse transcription of 500 ng RNA was performed and real-time qPCR completed for the iNOS gene. All values were normalised to the *Rpl32* ribosomal protein gene. For details of RT-qPCR methods and primers see Chapter 2: Materials and Methods.

3.2.2 Effect of Proinflammatory Cytokine Concentration

3.2.2.i Effect of decreasing proinflammatory cytokine concentration on cell response

The effect of lowering the concentration of the three cytokines, in combination, was investigated via a dose response experiment. Primary calvarial cells and osteo-mESCs were plated in 96-well plates and the next day culture medium replaced with osteogenic. IL-1β, TNF-α and IFN-γ in combination, at a ratio of 1:10:100, were added to the cell culture medium from day 0 of osteogenic culture; concentrations can be seen in table 3.1. MTS assays were performed on day 3, 10, 17 and 24 of continued cytokine application. To examine effect on cell response, proinflammatory cytokines at stated doses were added on day 7, 14 and 21 for 72 hours, supernatant collected and tested for nitrite concentration via the Griess assay.

Table 3.1: Cytokine concentrations utilised in dose response.

Dose	IL-1β (ng/mL)	TNF-α (ng/mL)	IFN-γ (ng/mL)
A	0.03125	0.3125	3.125
B	0.0625	0.625	6.25
C	0.125	1.25	12.5
D	0.25	2.5	25
E	0.5	5	50
F	1	10	100

3.2.2.ii Effect of increasing proinflammatory cytokine concentration on cell response

To investigate the effect of increasing the concentration of proinflammatory cytokines, from the "standard" used in previous experiments, primary calvarial cells and dissociated EBs were seeded in 12-well plates and cultured in osteogenic medium from day 0. Cells were stimulated with "standard" concentration proinflammatory cytokines in combination (IL-1β (1 ng/mL), TNF-α (10 ng/mL) and IFN-γ (100 ng/mL)) and 10x concentration (IL-1β (10 ng/mL), TNF-α (100 ng/mL) and IFN-γ (1000 ng/mL)), alongside an unstimulated osteogenic medium control. Cytokines were added to media at timepoints day 0 and day 21, applied for 72 hours, before supernatants collected and tested for nitrite and PGE_2 production.

3.2.3 Effect of mESC conditioned medium on primary calvarial cell response to proinflammatory cytokines.

The hypothesis that the mESCs may have an anti-inflammatory effect was investigated using mESC-conditioned medium (CM) on primary calvarial cells. Undifferentiated mESCs (on feeder layers) and early differentiation osteo-mESCs (day 0) were cultured for 72 hours with and without proinflammatory cytokines (IL-1β (1 ng/mL), TNF-α (10 ng/mL) and IFN-γ (100 ng/mL). The conditioned culture medium was collected after this period and passed through 0.2 µm filters to remove any cell debris. Primary calvarial cells were cultured in osteogenic medium until day 14. At this point culture medium was replaced with CM collected from the undifferentiated and differentiated mESCs. In some cases, proinflammatory cytokines were added. Control medium groups with and without proinflammatory cytokines were included. Viability of the primary calvarial cells was assessed by MTS assays on days 3, 7 and 10 after CM application. On these days, the supernatant was collected and tested for nitrite concentration via the Griess assay. Schematics showing the process of CM collection and application to the primary calvarial cells can be found in figure 3.2.

(A) Collection of conditioned medium from mESCs

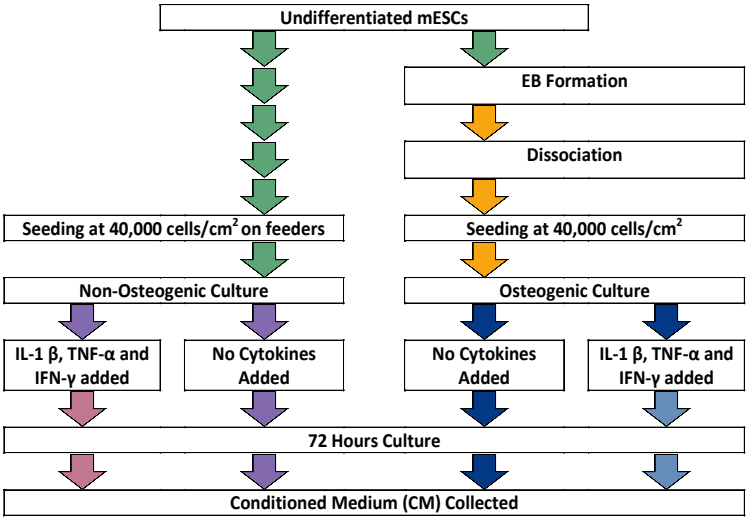

(B) Application of conditioned medium to primary calvarial cells

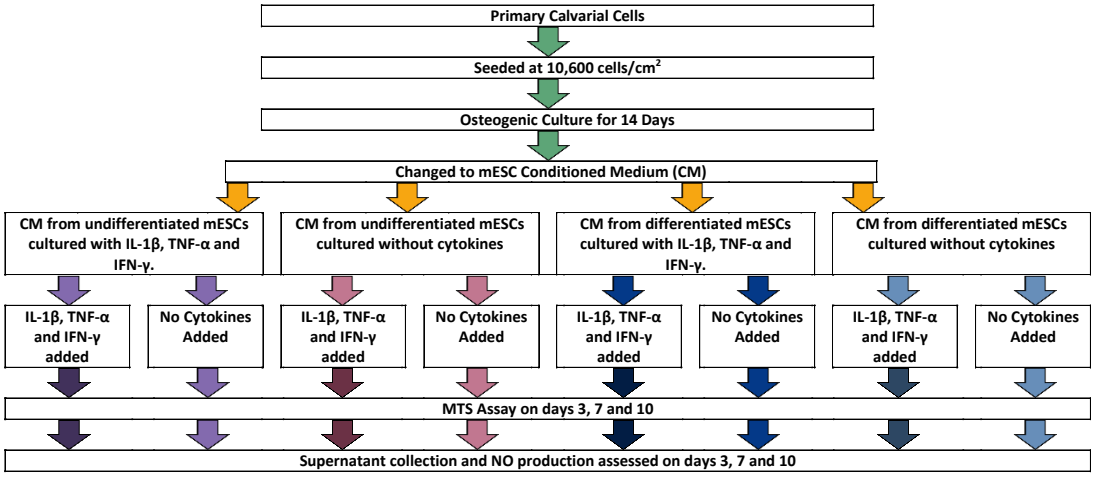

Figure 3.2: Schematic showing experimental design for the investigation of mESC conditioned medium on primary calvarial cell response to proinflammatory cytokines. (A) Schematic showing the process of conditioning the medium with undifferentiated and differentiated mESC. (B) Schematic showing the process of primary calvarial cell culture and application of the conditioned medium.

3.3 Results

3.3.1 Response of Osteogenic Cells to Proinflammatory Cytokines

3.3.1.i Dose response effect of individual cytokines on cell viability

Initial studies investigated the effect of different doses of IL-1β (0.1, 1 and 10 ng/mL), TNF-α (1, 10 and 100 ng/mL) and IFN-γ (10, 100 and 1000 ng/mL) on the cell viability of primary calvarial cells and osteo-mESCs, over a 14 day period. Results showed that all three cytokines had a negative effect on the viability of primary calvarial cells at 14 days, regardless of concentration (figure 3.3). Initially, at day 2, the cytokines had a positive effect on the cell viability of primary calvarial cells. The effects of IL-1β and TNF-α were more prominent at the highest dose (10 ng/mL and 100 ng/mL respectively), but the effects of IFN-γ appeared the same regardless of the dose. No significant effect on osteo-mESC viability, positive or negative, was seen with treatment by any cytokine at any dose (figure 3.4). From this point forward, it was decided to use the cytokines at concentrations of 1 ng/mL IL-1β, 10 ng/mL TNF-α and 100 ng/mL IFN-γ, also supported by available literature [127, 163, 183-187].

3.3.1.ii Effect of proinflammatory cytokines on cell viability

Primary calvarial cells and osteo-mESCs were cultured with different combinations of proinflammatory cytokines added to the culture medium, for up to 12 days, to establish effects on viability over time. Results showed that proinflammatory cytokines

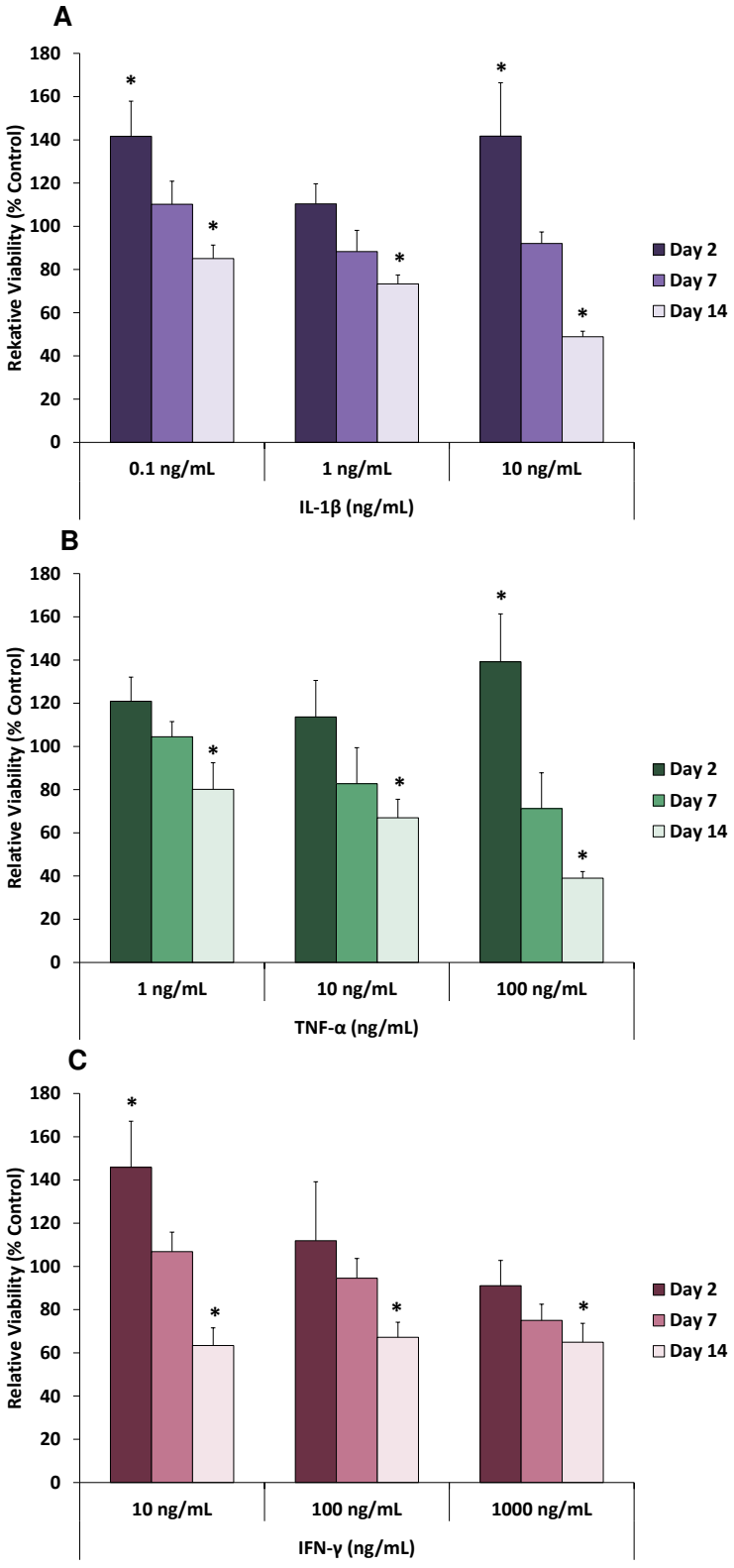

Figure 3.3: Dose response effect of IL-1β, TNF-α and IFN-γ on the viability of primary calvarial cells. Primary calvarial cells were treated with (A) IL-1β, (B) TNF-α and (C) IFN-γ, at different doses, over a 14 day period. Viability of cells at day 2, 7 and 14 was measured by MTS assay. Data shown as percentage of control reading for that day. Values represented by mean±SD (n=6). Statistical significance against control *p≤0.01.

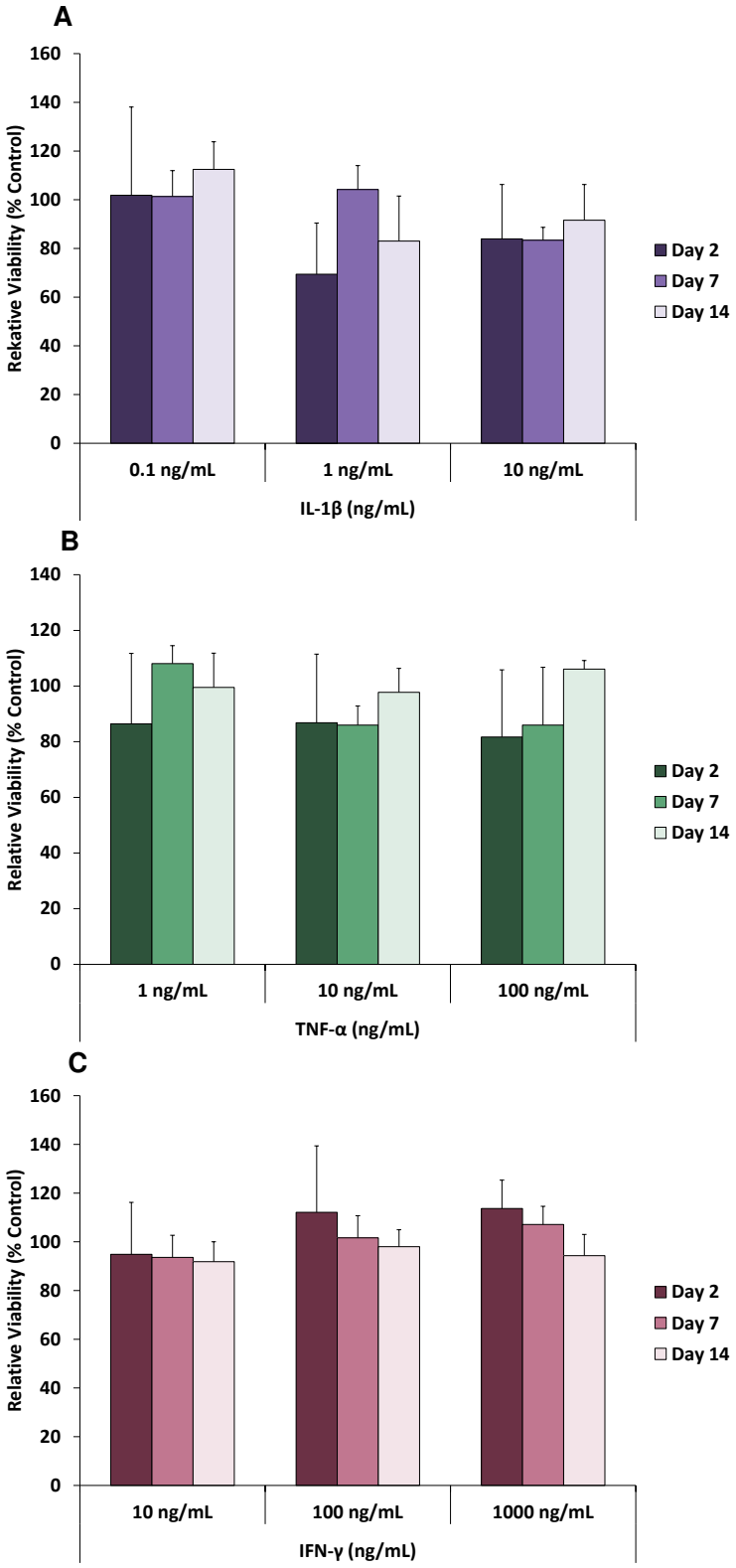

Figure 3.4: Dose response effect of IL-1β, TNF-α and IFN-γ on the viability of osteo-mESCs. Osteo-mESCs were treated with (A) IL-1β, (B) TNF-α and (C) IFN-γ, at different doses, over a 14 day period. Viability of cells at day 2, 7 and 14 was measured by MTS assay. Data shown as percentage of control reading for that day. Values represented by mean±SD (n=6).

had a negative effect on primary calvarial cell viability, which was not seen in the osteo-mESC cultures (figure 3.5). In primary calvarial cultures, combinations containing IL-1β initially had a stimulatory effect on cell proliferation, with increased cell numbers on day 2, when compared to control. By day 12, cell viability had dropped significantly in all cultures that contained a combination of more than one cytokine. Combining all three cytokines had a marked negative effect on primary calvarial cell viability; cell numbers began to fall at day 5, and continued until day 12, when viability compared to control, was less than 40%.

No significant effects on viability, positive or negative, were seen in the osteo-mESC cultures, with IL-β, TNF-α or IFN-γ in any combination (figure 3.5B).

3.3.1.iii NO and PGE_2 production in response to proinflammatory cytokines

The biochemical response of the cells to the presence of proinflammatory cytokines was investigated by monitoring production of NO, estimated as nitrite, and PGE_2 production, found within the cell culture medium. Nitrite (figure 3.6) and PGE_2 (figure 3.7) were measured after 72 hours proinflammatory cytokine stimulation, at different timepoints of culture, to determine change in response due to osteogenic differentiation.

Results for culture medium collected after proinflammatory cytokine treatment on day 0 and day 7 of osteogenic culture showed the primary calvarial cells produced significantly more nitrite than the control, in groups stimulated with IL-1β alone and IL-1β in combination with TNF-α and IFN-γ (figure 3.6A and B). This occurred particularly in cultures with all three cytokines present in combination. This trend was

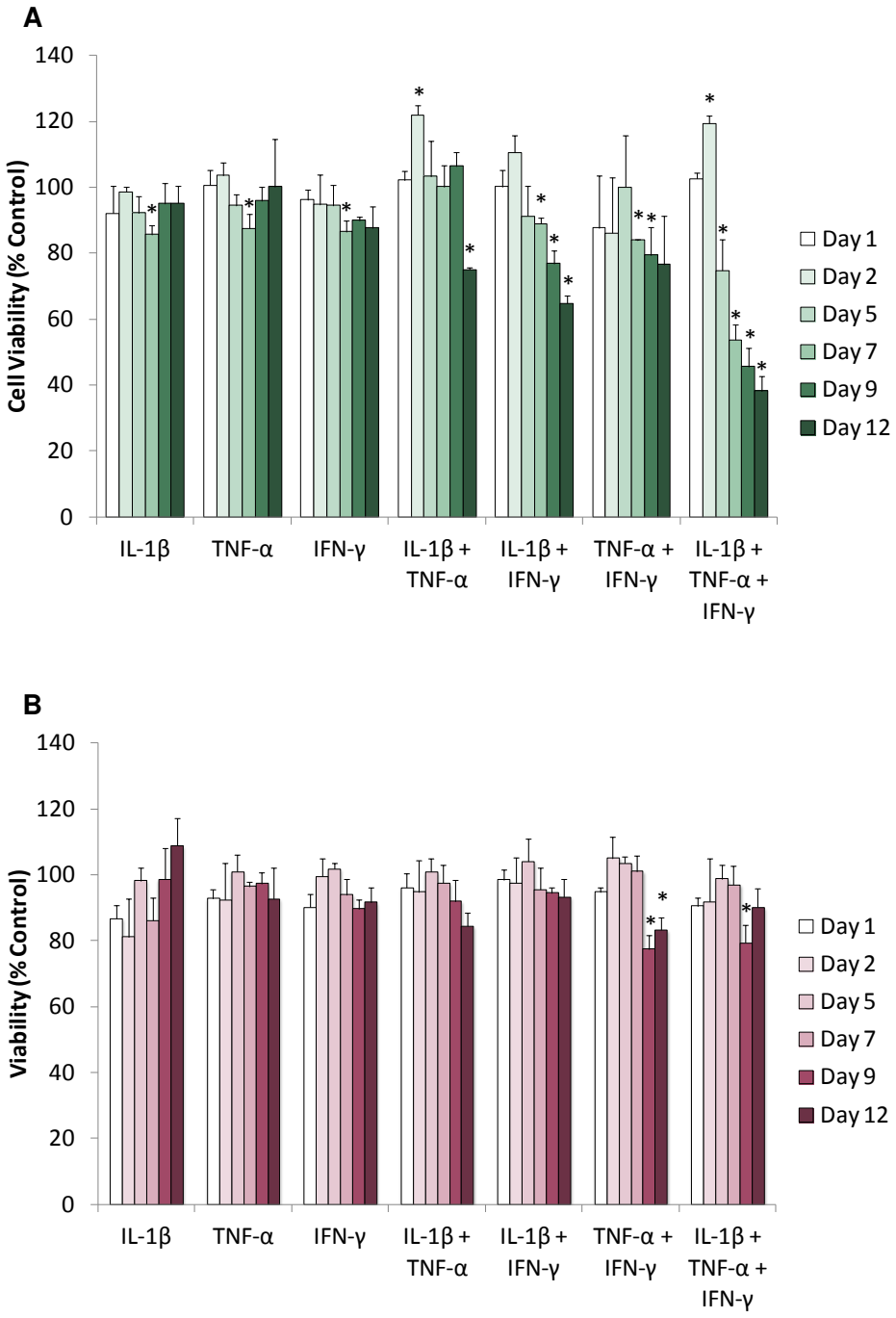

Figure 3.5: Effect of combinations of proinflammatory cytokines on cell proliferation and viability. (A) Primary calvarial cells and (B) osteo-mESCs were treated with different combinations of proinflammatory cytokines over a 12-day time period. Viability of cells at certain time-points was measured using the MTS assay. Data is shown as a percentage of control reading for that day. Experiment was repeated in triplicate each with n=6. Values are represented as mean±SEM of the three experiments. Statistical significance against control *p≤0.01.

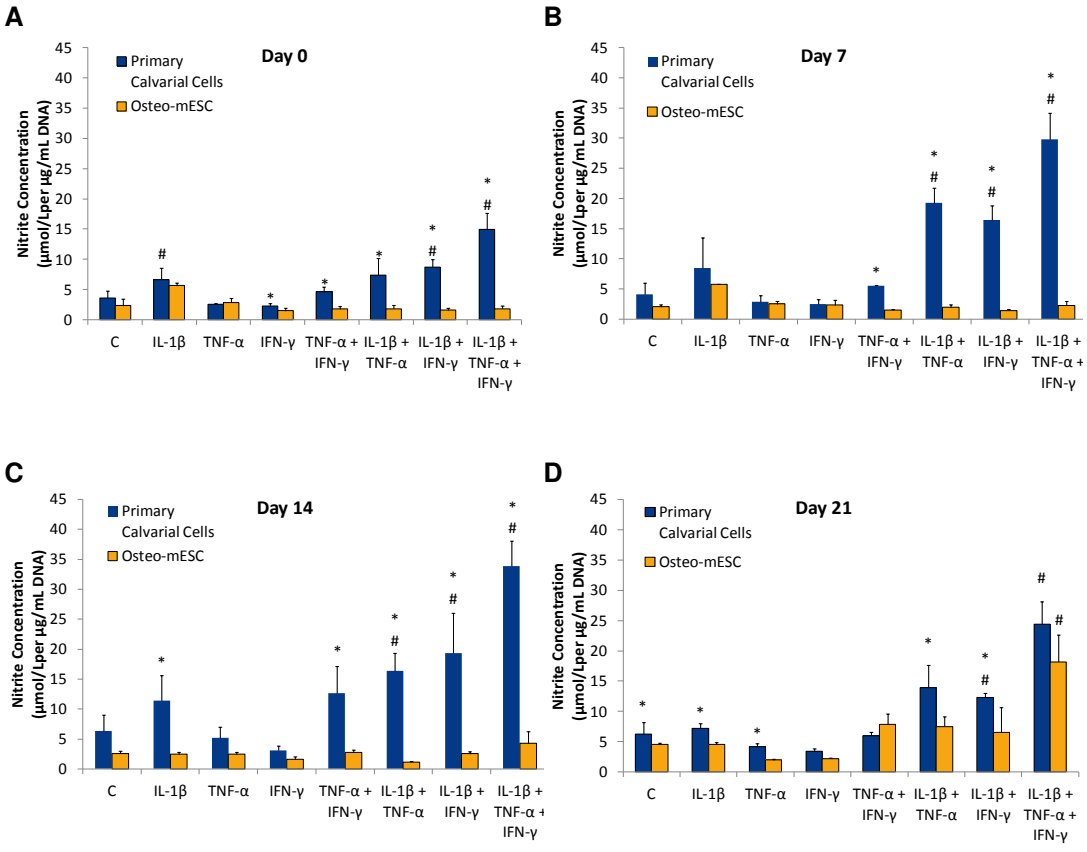

Figure 3.6: Effect of proinflammatory cytokines on NO production. Primary calvarial cells and osteo-mESCs were treated with different combinations of proinflammatory cytokines at (A) day 0, (B) day 7, (C) day 14 and (D) day 21 of osteogenic culture. Proinflammatory cytokine stimulation continued for 72 hours before supernatant collection and experiment end. Nitrite concentration in supernatant determined by Griess assay. Nitrite concentrations corrected for cell number using Hoechst DNA assay values. Values are represented as mean±SEM, experiment repeated in triplicate each with n=6. Statistical significance of primary calvarial response compared to osteo-mESC (*p≤0.01), statistical significance of response compared to control of same cell type (# p≤0.01).

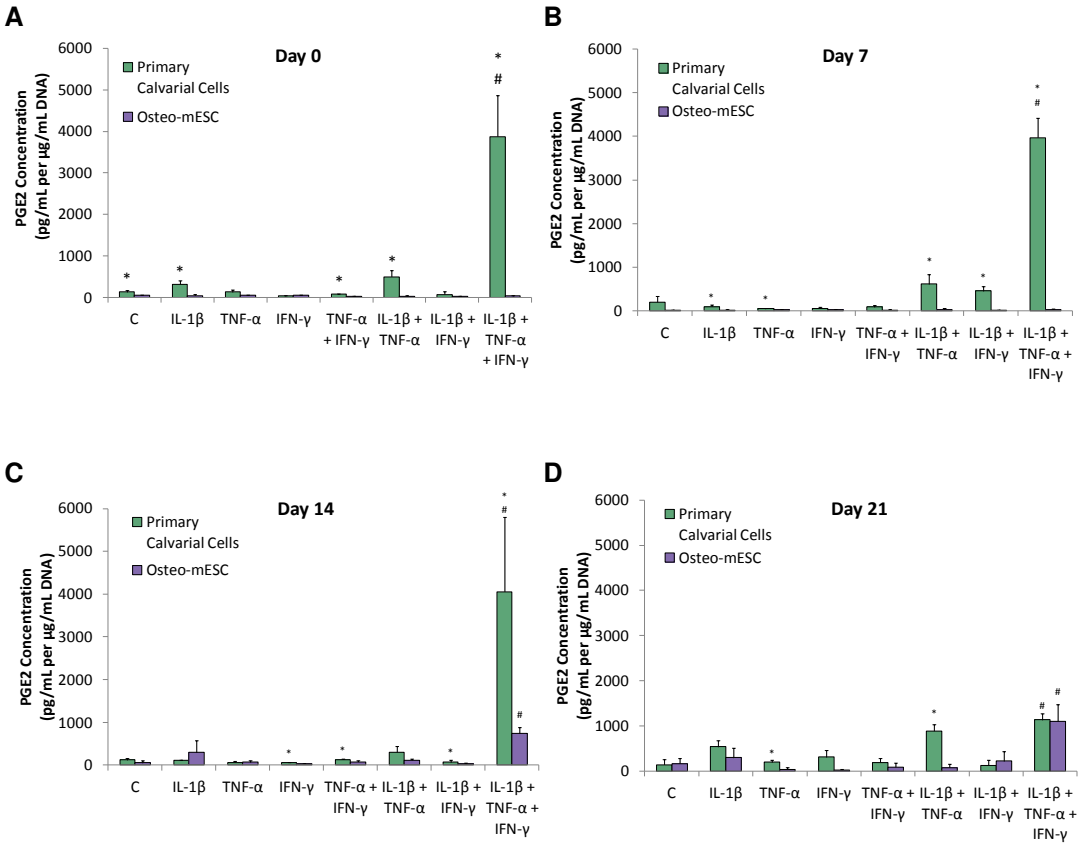

Figure 3.7: Effect of proinflammatory cytokines on PGE_2 production. Primary calvarial cells and osteo-mESCs were treated with different combinations of proinflammatory cytokines at (A) day 0, (B) day 7, (C) day 14 and (D) day 21 of osteogenic culture. Proinflammatory cytokine stimulation continued for 72 hours before supernatant collection and experiment end. PGE_2 concentration in supernatant determined by EIA. PGE_2 concentrations corrected for cell number using Hoechst DNA assay values. Values are represented as mean±SEM, experiment repeated in triplicate each with n=3. Statistical significance of primary calvarial response compared to osteo-mESC (*p≤0.01), statistical significance of response compared to control of same cell type (# p≤0.01).

also reflected in PGE_2 production (figure 3.7A and B), with maximum PGE_2 occurring at day 7. The day 0 and day 7 osteo-mESCs showed no significant nitrite or PGE_2 production in any group in response to proinflammatory cytokines, when compared to the control and compared to primary calvarial cells.

Treatment of the cells on day 14 showed little variation in the nitrite production trend (figure 3.6C). Primary calvarial cells exhibited increased nitrite production in groups treated with a combination of proinflammatory cytokines, reaching a maximum on day 14. The osteo-mESCs showed no significant nitrite production in any group. However, with PGE_2 production on day 14 (figure 3.7C), the osteo-mESCs show significantly increased levels in the group stimulated with IL-1β, TNF-α and IFN-γ, when compared to the control. This is still of a lower level than the primary calvarial cells.

Proinflammatory cytokine stimulation at day 21, showed increased response from the osteo-mESCs in terms of nitrite (figure 3.6D) and PGE_2 (figure 3.7D). Significant nitrite and PGE_2 production was seen in the group treated with all three cytokines; there was little difference between this and the levels in the primary calvarial cell group.

The response of both the primary calvarial cells and osteo-mESCs was most pronounced when IL-1β, TNF-α and IFN-γ were present in combination. From this point forward, it was decided to use the three cytokines in combination for all experiments, to ensure the optimal signalling effect was achieved.

3.3.1.iv Expression of inducible enzymes in response to proinflammatory cytokines

To visualise the response of cells to proinflammatory cytokines and examine the production of enzymes responsible for NO and PGE_2, immunocytochemistry of iNOS, COX-2 and PGES was performed. Staining was carried out on both primary calvarial cells and osteo-mESCs, allowing exploration into patterns of protein expression and changes with stage of osteogenic differentiation. Cytokines were added to the medium on day 0, 7, 14 and 21, for 48 hours, before cell monolayers were fixed. Expression of iNOS, the enzyme leading to the production of NO during inflammation, can be seen in figure 3.8 (primary calvarial cells) and figure 3.9 (osteo-mESCs). In primary calvarial cells, there is no staining in cultures treated with control medium but at each of the osteogenic differentiation timepoints, there is a marked increase in the level of staining when proinflammatory cytokines are present in the medium. Staining mostly occurs in the cell cytoplasm, but does not appear in all cells, indicating a heterogeneous cell response. In osteo-mESC cultures, no staining of iNOS is seen in day 0 or day 7 groups in control medium or proinflammatory cytokine medium. On day 14, iNOS staining begins to appear in small amounts in cells treated with cytokines and by day 21, iNOS staining is more evident, reflecting the trend seen with the nitrite results. Once again, it appears to be being expressed by some cells but not across the entire cell culture.

There is some staining in the osteo-mESC control medium cells on day 14 and 21, but it is much weaker compared to that seen with proinflammatory cytokine treatment at day 21.

COX-2 expression can be seen in the primary calvarial cells in figure 3.10 and the osteo-mESCs in figure 3.11. In primary calvarial cell cultures, COX-2 is seen in large

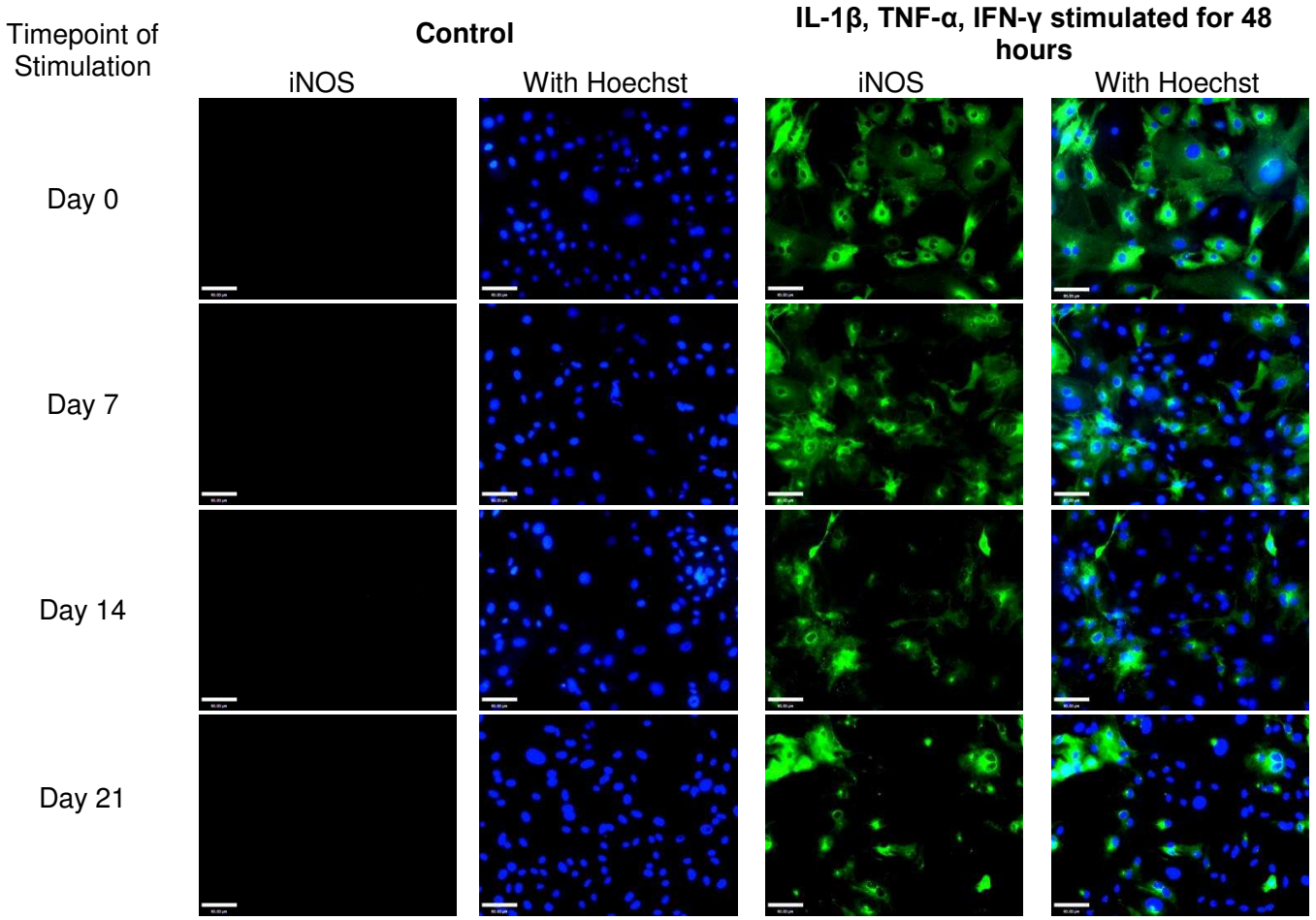

Figure 3.8: iNOS immunostaining in primary calvarial cells stimulated with proinflammatory cytokines. Cells were stimulated with IL-1β, TNFα and IFN-γ for 48 hours at either day 0, day 7, day 14 or day 21 of osteogenic culture before fixation. iNOS expression in both proinflammatory cytokine stimulated and control cultures was assessed by immunocytochemistry. Representative images shown. Scale bar = 90 µm.

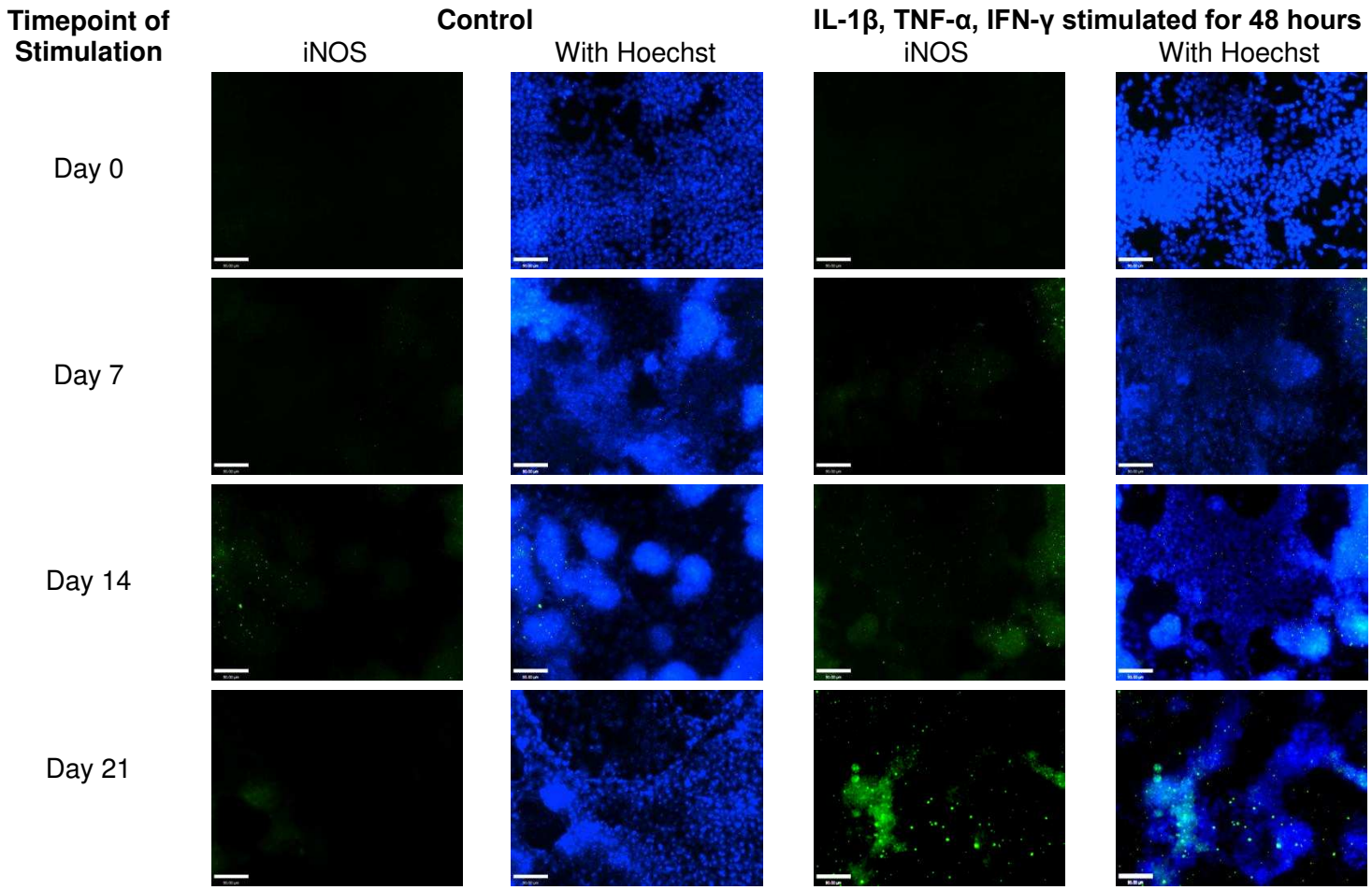

Figure 3.9: iNOS immunostaining in osteo-mESCs stimulated with proinflammatory cytokines. Cells were stimulated with IL-1β, TNFα and IFN-γ for 48 hours at either day 0, day 7, day 14 or day 21 of osteogenic culture before fixation. iNOS expression in both proinflammatory cytokine stimulated and control cultures was assessed by immunocytochemistry. Representative images shown. Scale bars=90 μm.

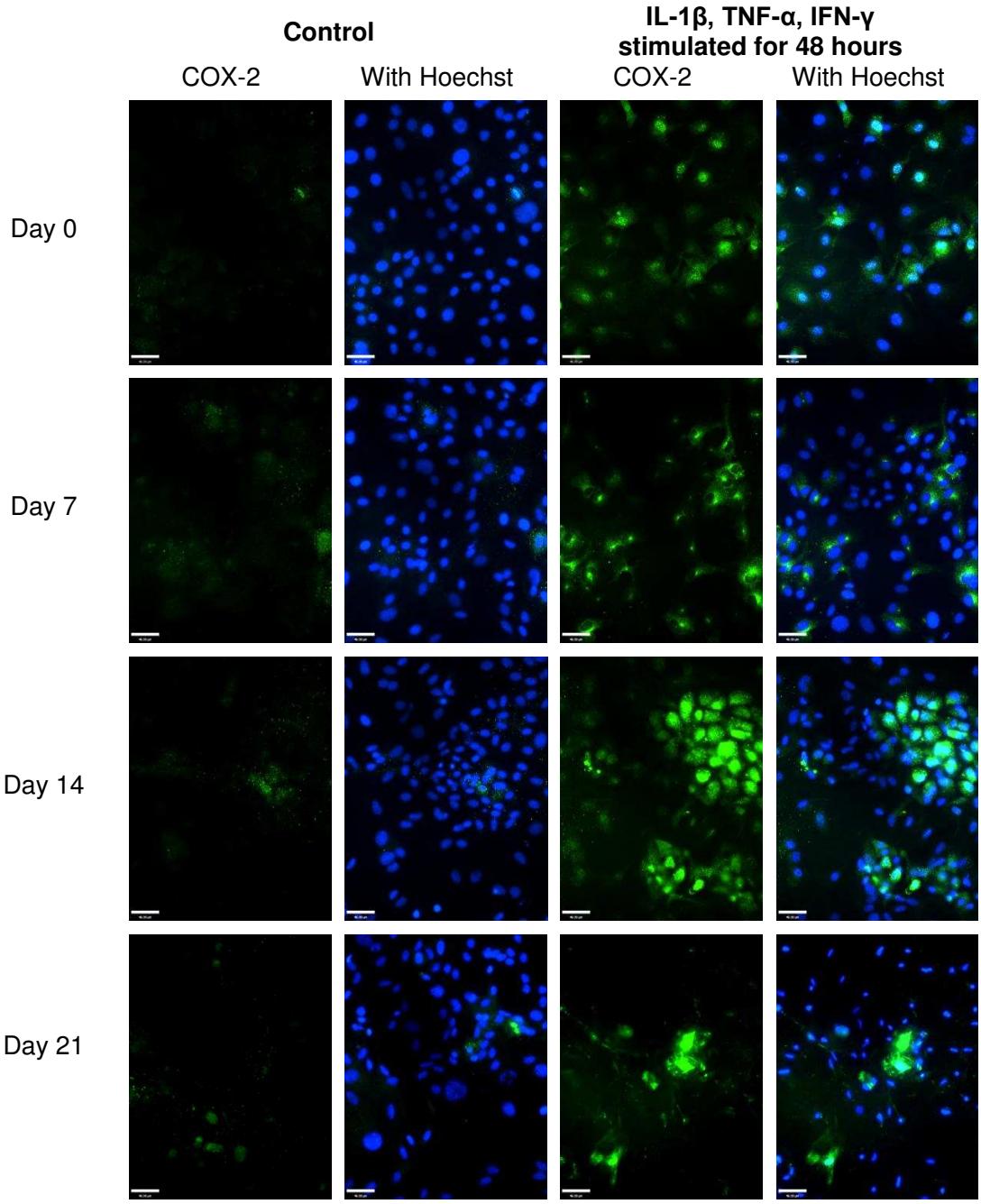

Figure 3.10: COX-2 immunostaining in primary calvarial cells stimulated with proinflammatory cytokines. Cells were stimulated with IL-1β, TNFα and IFN-γ for 48 hours at either day 0, day 7, day 14 or day 21 of osteogenic culture before fixation. COX-2 expression in both proinflammatory cytokine stimulated and control cultures was assessed by immunocytochemistry. Representative images shown.Scale bars=46 μm.

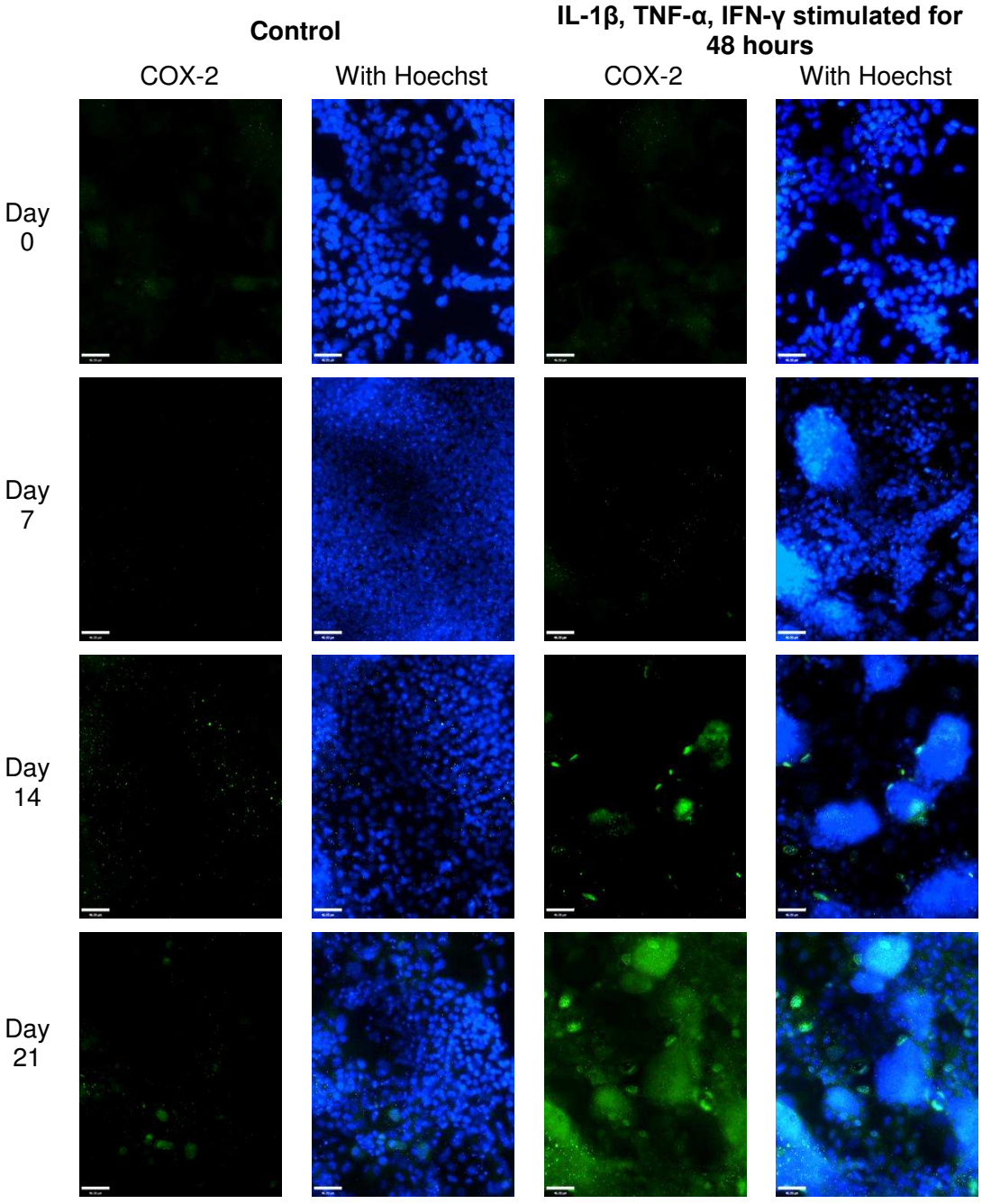

Figure 3.11: COX-2 immunostaining in osteo-mESCs stimulated with proinflammatory cytokines. Cells were stimulated with IL-1β, TNFα and IFN-γ for 48 hours at either day 0, day 7, day 14 or day 21 of osteogenic culture before fixation. COX-2 expression in both proinflammatory cytokine stimulated and control cultures was assessed by immunocytochemistry. Representative images shown. Scale bars=46 μm.

amounts in proinflammatory cytokine treated cultures, throughout all differentiation timepoints. Unlike iNOS, it can also be seen to a small degree in cultures treated with control medium only. COX-2 appears to be less widely expressed in primary calvarial cultures than iNOS, and at day 14 and 21 is seen predominantly in bone nodule-like configurations. Most staining is seen at day 14 and is consistent with PGE_2 production results. In osteo-mESC cultures, staining of COX-2 is not seen in proinflammatory cytokine treated cells until day 14. By day 21, more staining is seen. Weak staining is seen in cells cultured in control medium on day 14 and 21. Overall, expression of the inducible enzymes reflects and helps support data obtained on NO and PGE_2 production. Staining of PGES, found in Appendix V (figures AV.1 and AV.2), correlates with iNOS and COX-2 results.

Real-time qPCR results for the iNOS gene support the immunocytochemistry (figure 3.12). Increased levels of expression are only seen in primary calvarial cells when treated with proinflammatory cytokines at day 0 and day 21. All expression values for untreated primary calvarial cells and osteo-mESCs are low.

3.3.2 Effect of Proinflammatory Cytokine Concentration

3.3.2.i The effect of decreasing proinflammatory cytokine concentration on cell response

Investigation of the response of cells to decreasing cytokine concentrations was performed in terms of viability and nitrite production. The ratio of IL-1β to TNF-α to IFN-γ (1:10:100) in the medium was maintained; but concentration overall was

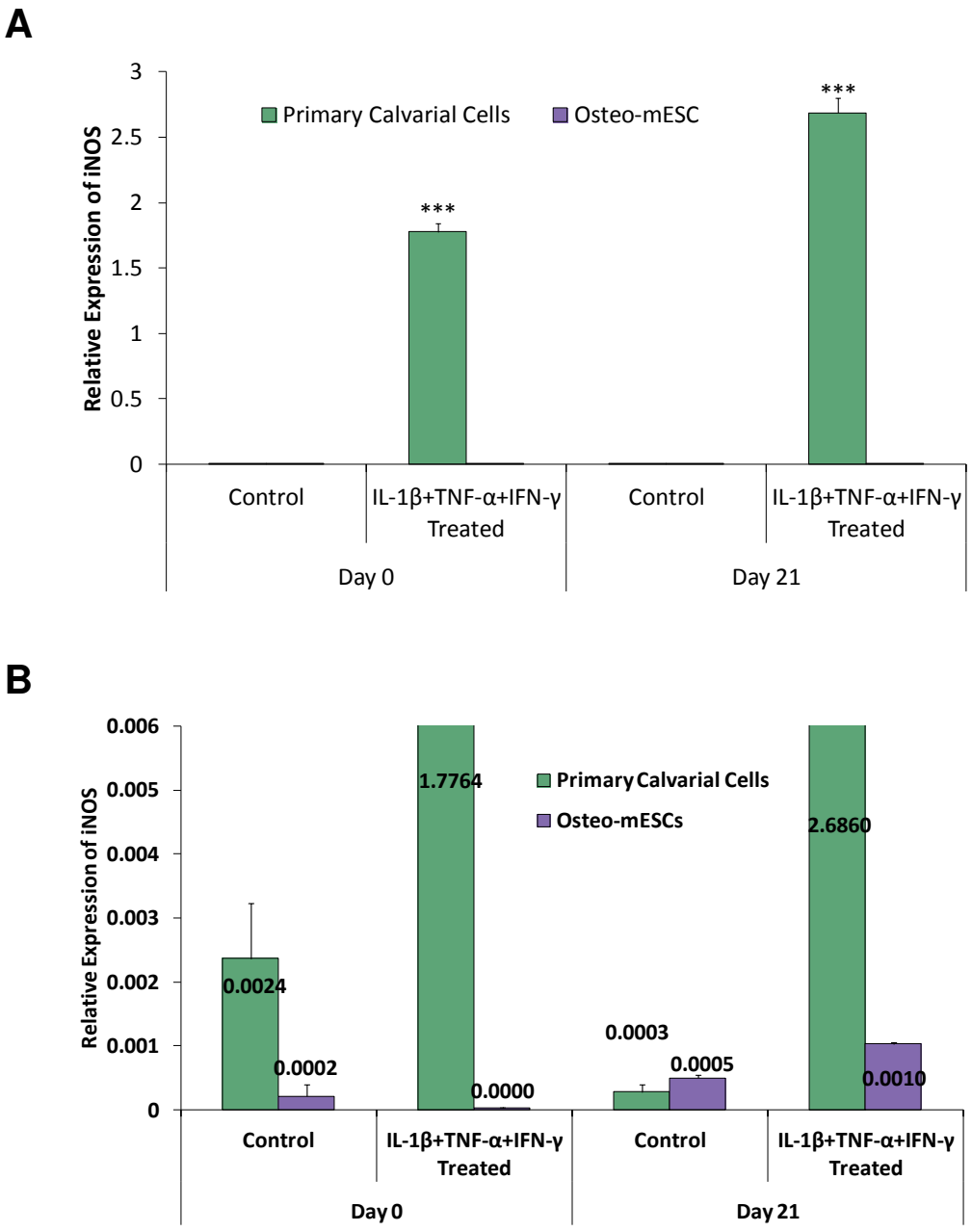

Figure 3.12: RT-qPCR of iNOS expression in proinflammatory cytokine treated cells. Primary calvarial cells and osteo-mESCs were treated with media containing IL-1β, TNF-α and IFN-γ for 48 hours at day 0 and day 21 of osteogenic culture. Real-time qPCR was performed for the iNOS gene. (A) All data (B) magnified data, showing data at the lower end of expression, with data value shown. Expression of each target gene normalised to *Rpl32*. Data shown is mean±SD of 3 independent experiments (n=3). Statistical significance of expression vs. control (*** p≤0.0001).

decreased by serial dilution. For each dilution, cell viability was monitored across days 3, 10, 17 and 24 (figure 3.13). In primary calvarial cell cultures, at the highest concentration of proinflammatory cytokines (Dose F - 1 ng/mL IL-1β, 10 ng/mL TNF-α and 100 ng/mL IFN-γ), a reduction in cell viability began at day 3 and cell numbers continued to fall throughout the remaining time. This also occurred in the lower concentrations (dose E, D, C, and B). There was no significant effect on primary calvarial cell viability with the lowest dose (A - 0.03125 ng/mL IL-1β, 0.3125ng/mL TNF-α and 3.125 ng/mL IFN-γ), but cell proliferation did not correspond with the control group. In contrast, in the osteo-mESC cultures (figure 3.13B) there was little effect of proinflammatory cytokines on cell viability, at any concentration, whether inhibitory or stimulatory.

Alongside effect on cell viability, nitrite production was also studied. Proinflammatory cytokine concentrations were as before, but doses of cytokines were applied at day 7, day 14 and day 21 for 72 hours, before medium supernatant samples were taken and tested for nitrite concentration (figure 3.14). At the lowest dose of cytokines (dose A), no significant nitrite production was seen across any timepoint in the primary calvarial cells or at day 21 in the next highest dose (dose B). Nitrite concentration in the medium reached a plateau from dose D upwards (0.25 ng/mL IL-1β, 2.5ng/mL TNF-α and 2.5 ng/mL IFN-γ). In primary calvarial cells, across all doses, nitrite production peaked at day 14.

The osteo-mESCs showed no significant nitrite production at any proinflammatory cytokine dose, except day 21 of osteogenic culture at the highest dose (Dose F).

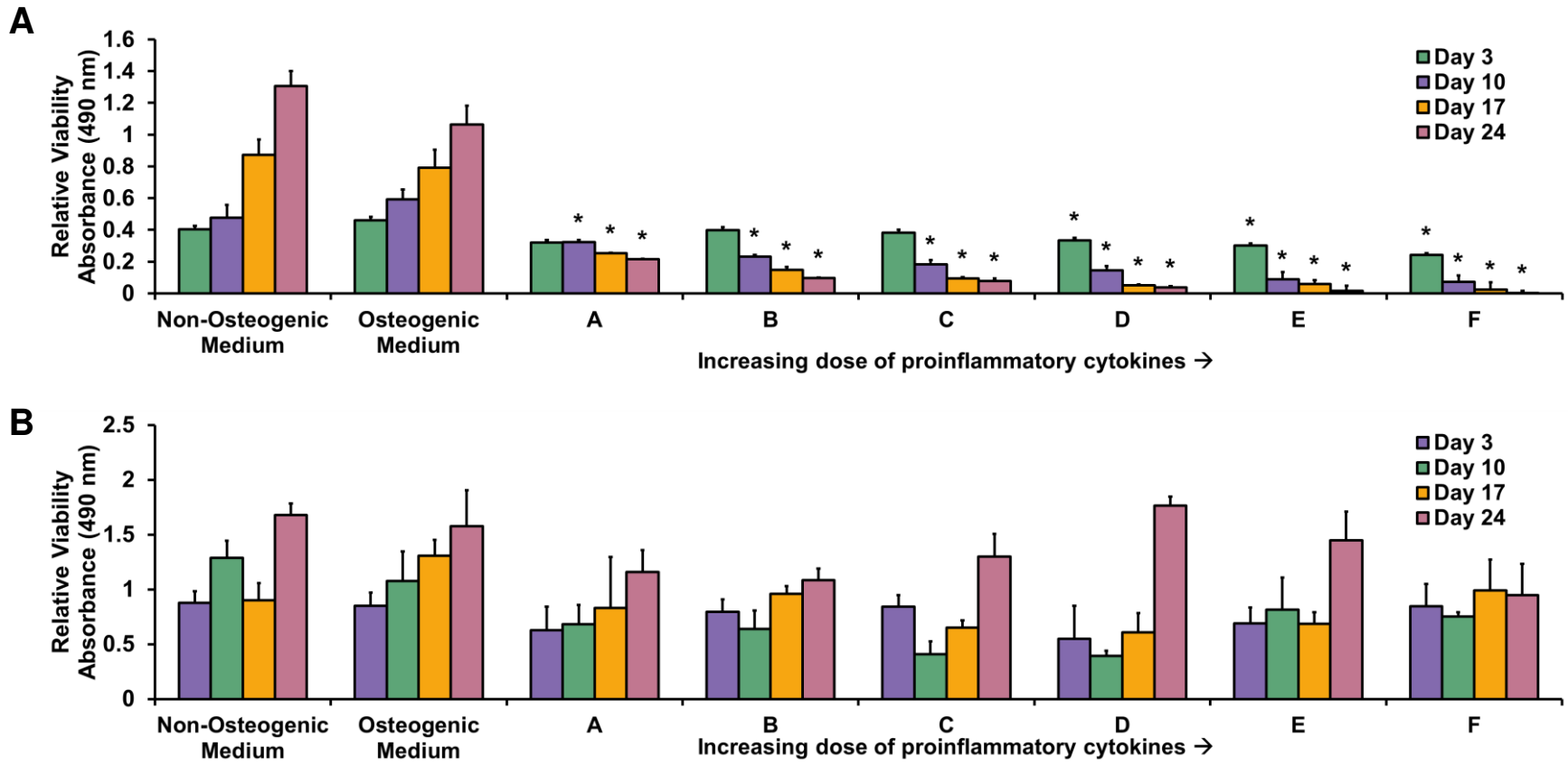

Figure 3.13: Dose response effect of proinflammatory cytokines on cell proliferation and viability. (A) Primary calvarial cells and (B) osteo-mESCs were treated with increasing concentrations of a combination of IL-1β, TNF-α and IFN-γ over a 24-day time period. Cytokine doses: A (Il-1β 0.03125 ng/mL, TNF-α 0.3125 ng/mL, IFN-γ 3.125 ng/mL); B (Il-1β 0.0625 ng/mL, TNF-α 0.625 ng/mL, IFN-γ 6.35 ng/mL); C (Il-1β 0.125 ng/mL, TNF-α 1.25 ng/mL, IFN-γ 12.5 ng/mL); D (Il-1β 0.25 ng/mL, TNF-α 2.5 ng/mL, IFN-γ 25 ng/mL); E (Il-1β 0.5 ng/mL, TNF-α 5 ng/mL, IFN-γ 50 ng/mL); F (Il-1β 1 ng/mL, TNF-α 10 ng/mL, IFN-γ 100 ng/mL). Viability of cells at certain time points was measured using the MTS assay. Data is shown as optical absorbance proportional to cell viability. Values are represented as mean±SD (n=6). Statistical significance against control (*p≤0.05).

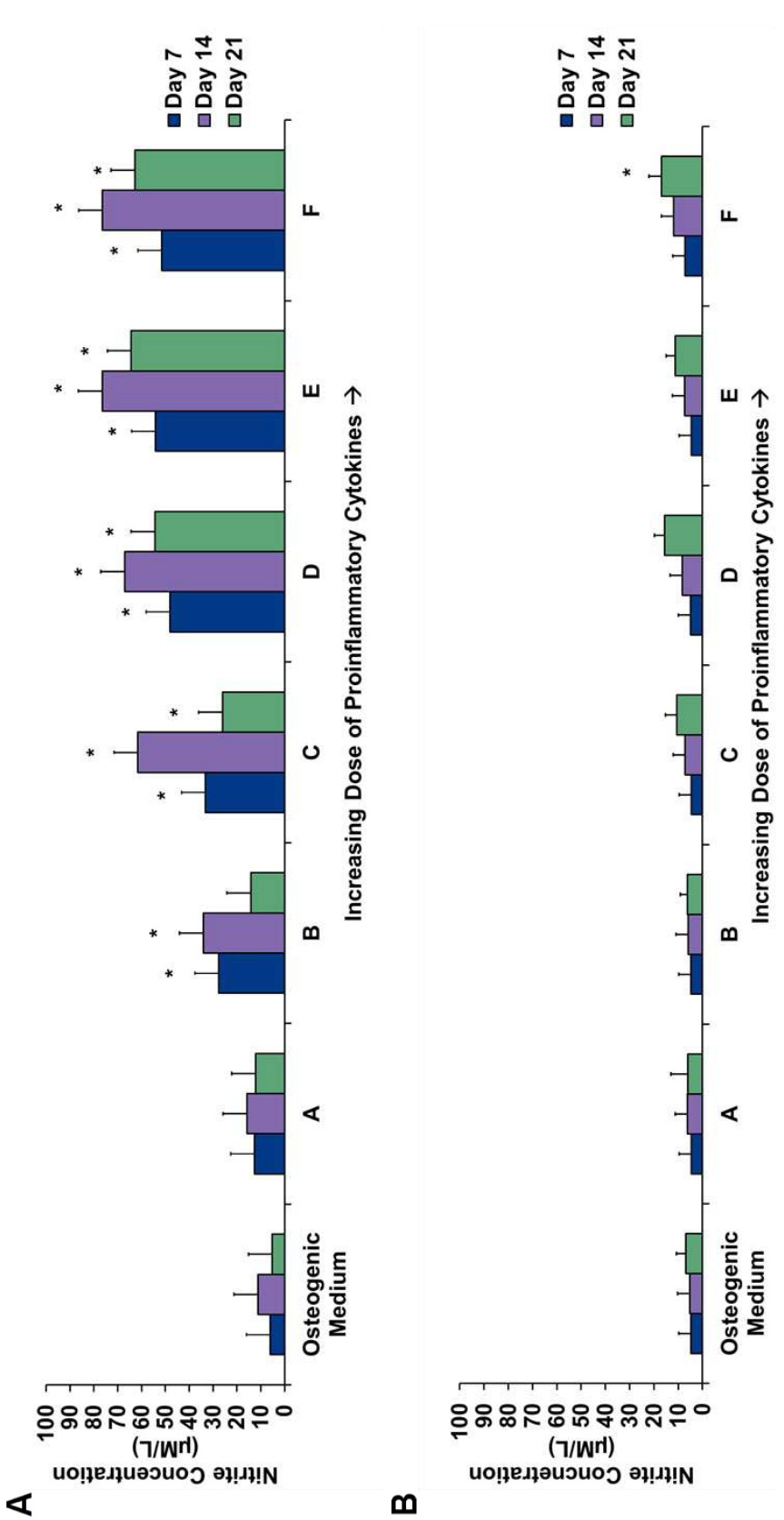

Figure 3.14: Dose response effect of proinflammatory cytokines on nitric oxide production. (A) Primary calvarial cells and (B) osteo-mESCs were treated with increasing concentrations of a combination of IL-1β, TNF-α and IFN-γ at time points of day 7, day 14 and day 21 of osteogenic culture. Proinflammatory cytokine stimulation continued for 3 days before supernatants were collected and experiment ended. Cytokine doses: A (Il-1β 0.03125 ng/mL, TNF-α 0.3125 ng/mL, IFN-γ 3.125 ng/mL); B (Il-1β 0.0625 ng/mL, TNF-α 0.625 ng/mL, IFN-γ 6.35 ng/mL); C (Il-1β 0.125 ng/mL, TNF-α 1.25 ng/mL, IFN-γ 12.5 ng/mL); D (Il-1β 0.25 ng/mL, TNF-α 2.5 ng/mL, IFN-γ 25 ng/mL); E (Il-1β 0.5 ng/mL, TNF-α 5 ng/mL, IFN-γ 50 ng/mL); F (Il-1β 1 ng/mL, TNF-α 10 ng/mL, IFN-γ 100 ng/mL). Nitrite concentration within the supernatant was measured using the Griess assay. Values are represented as mean±SD (n=6). Statistical significance against control (*p=0.05).

3.3.2.ii Effects of increasing proinflammatory cytokine concentration on cell response

Increasing the dose of proinflammatory cytokines from the standard 1 ng/mL IL-1β, 10 ng/mL TNF-α and 100 ng/mL IFN-γ, was also investigated in terms of both nitrite (figure 3.15) and PGE_2 (figure 3.16). In both cases, primary calvarial cells and osteo-mESCs were stimulated with no cytokines (control medium), medium containing standard concentration cytokines and medium containing 10x the standard concentration. Proinflammatory cytokine stimulation was performed for 72 hours at day 0 and day 21 of osteogenic culture, to investigate effect of cell differentiation. For both nitrite and PGE_2 production, increasing the dose by 10 times had no effect on final concentration indicating that a plateau of response had been reached. Results mirrored those that had been seen previously; on days 0 and 21 of osteogenic culture, nitrite and PGE_2 were produced in significant quantities by primary calvarial cells in response to proinflammatory signals. This did not occur in the osteo-mESCs. By day 21, the osteo-mESCs were producing significant levels of both nitrite and PGE_2 in response to the cytokines, at similar levels as the primary calvarial cells.

3.3.3 Effect of mESC conditioned medium on the response of primary calvarial cells to proinflammatory cytokines.

To investigate whether mESCs were releasing soluble anti-inflammatory factors into culture medium, CM from both undifferentiated and early differentiation mESCs was collected, both with stimulation by proinflammatory cytokines and without. CM was then used as culture medium on primary calvarial cell cultures with and without

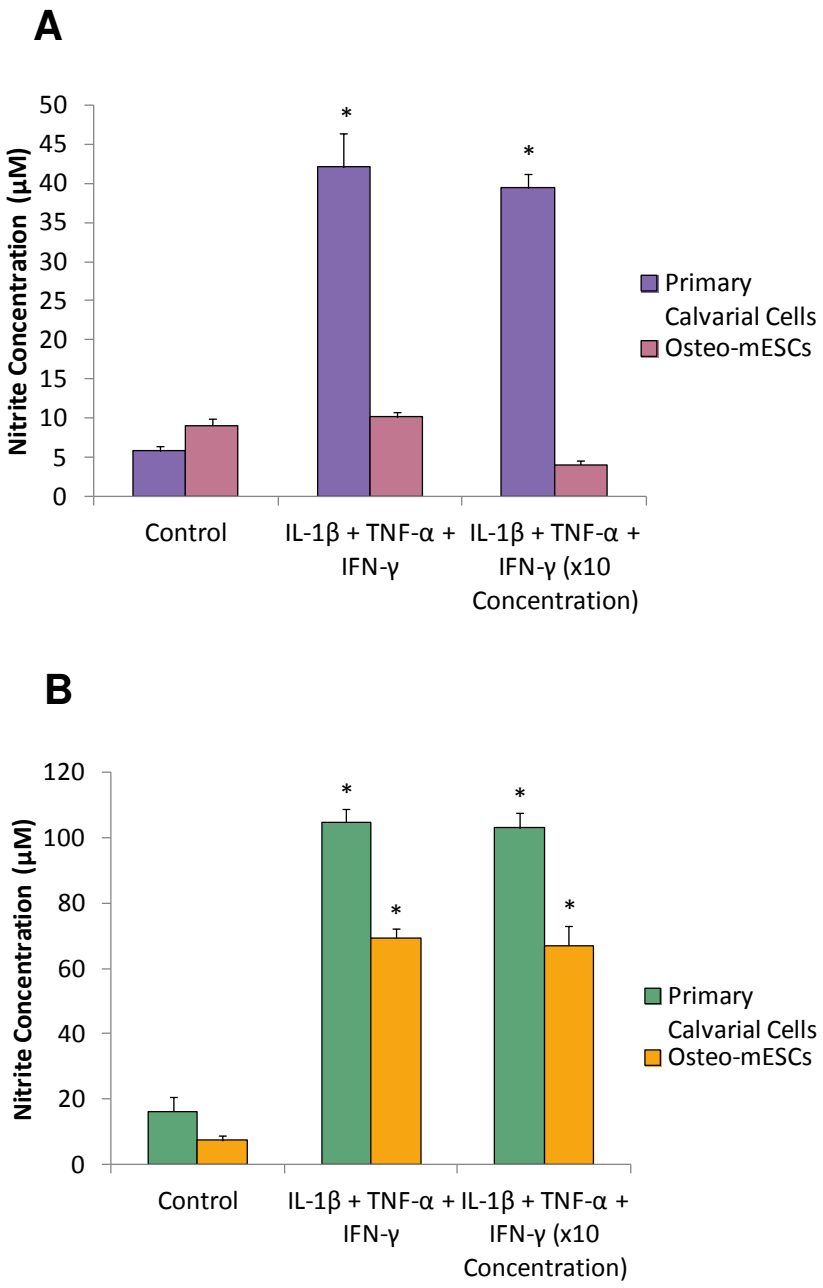

Figure 3.15: Effect of increased proinflammatory cytokine concentration on nitric oxide production. Primary calvarial cells and osteo-mESCs were treated with control media; media containing 1 ng/mL IL-1β, 10 ng/mL TNF-α and 100 ng/mL IFN-γ and media containing 10 times the concentration of all three cytokines. Proinflammatory cytokine stimulation occurred for 72 hours at (A) day 0 of osteogenic culture and (B) day 21 of osteogenic culture. Values are represented as mean±SD, n=6. Statistical significance of response compared to cell-specific control (*p<0.01)

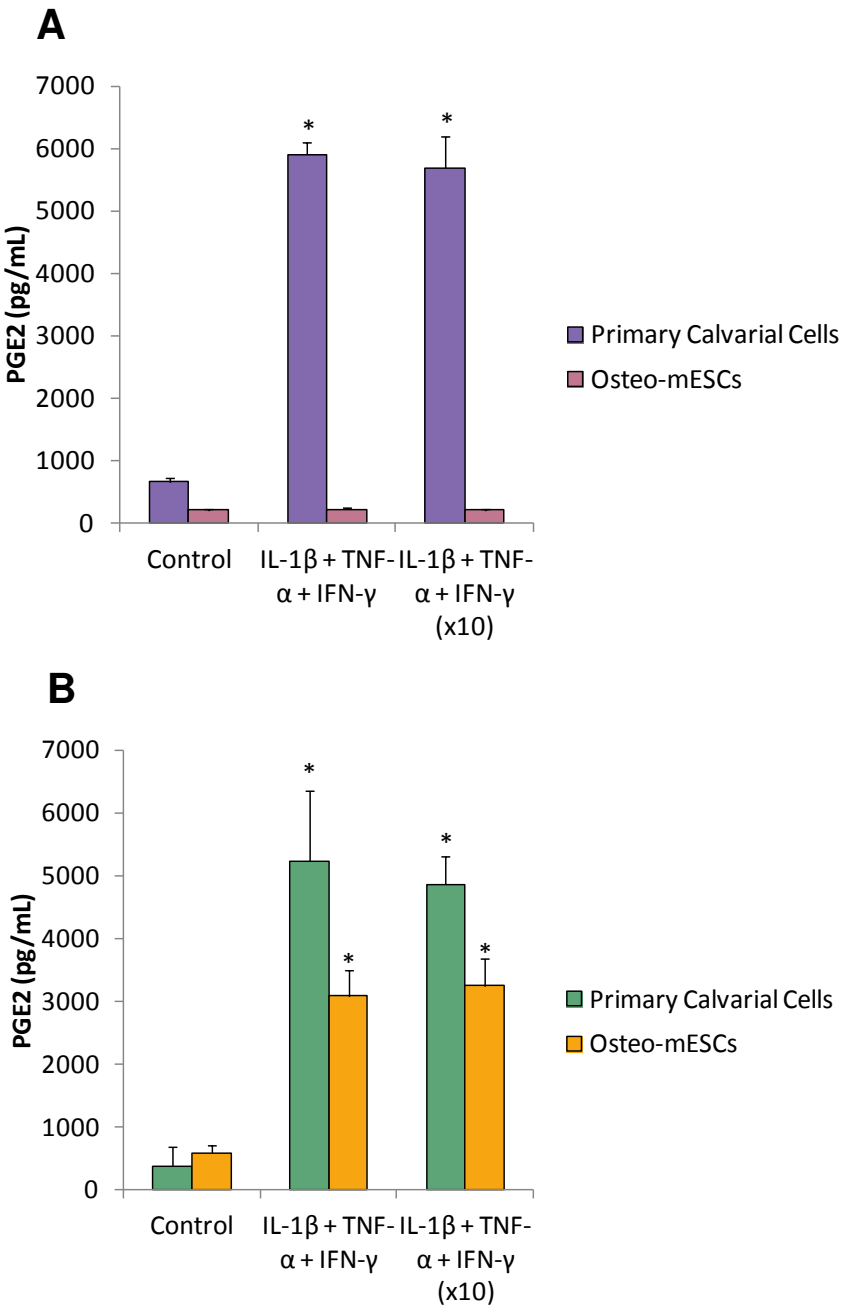

Figure 3.16: Effect of increased proinflammatory cytokine concentration on PGE_2 production. Primary calvarial cells and osteo-mESCs were treated with control media; media containing 1 ng/mL IL-1β, 10 ng/mL TNF-α and 100 ng/mL IFN-γ and media containing 10 times the concentration of all three cytokines. Proinflammatory cytokine stimulation occurred for 72 hours at (A) day 0 of osteogenic culture and (B) day 21 of osteogenic culture. Values are represented as mean±SD, n=4. Statistical significance of response compared to cell-specific control (*$p<0.01$).

proinflammatory cytokines. Cell viability (figure 3.17) and nitrite production (figure. 3.18), over 10 days, was considered. Figure 3.17 shows cell viability results for day 10. Results for MTS assays performed on day 3 and day 7 can be found in Appendix VI (figure AVI.1). Response to CM was compared to that of osteogenic medium (OM) with and without proinflammatory cytokines. Cytokines in OM initially had a negative effect on cell viability as cell numbers by day 10 had fallen to 40% of OM control. The CM from undifferentiated mESCs inhibited this reduction in cell viability, regardless of whether mESC medium had been treated with cytokines (figure 3.17A). Although, at day 10 there was still some difference between the CM and the OM control. The CM from early-differentiation mESCs had a slightly different effect. When the differentiated mESCs had not been cultured with proinflammatory cytokines, the CM alone had a negative effect on primary cell viability when compared to the OM control (figure 3.17B). This detrimental effect on the cells was negated when proinflammatory cytokines were added to the CM. In contrast, the CM from differentiated mESCs cultured with proinflammatory cytokines did not have a negative effect on cell viability, and inhibited the primary calvarial cell death that occurred via the proinflammatory cytokines.

Results showing levels of nitrite production by the primary calvarial cells were clearer (figure 3.18). This graph shows the cumulative nitrite concentration in the culture medium, over 10 days, with values taken from assays performed on day 3, day 7 and day 10. Individual results for these timepoints can be found in Appendix VI (figure AVI.1C). Cells produced nitrite in response to IL-1β, TNF-α and IFN-γ in OM medium. Results show nitrite values from control medium (no added cytokines in primary calvarial cell culture) subtracted from the proinflammatory cytokine treated-value. CM from undifferentiated and differentiated mESCs inhibited cytokine-induced nitrite production, regardless of whether the mESCs had been treated with cytokines. CM

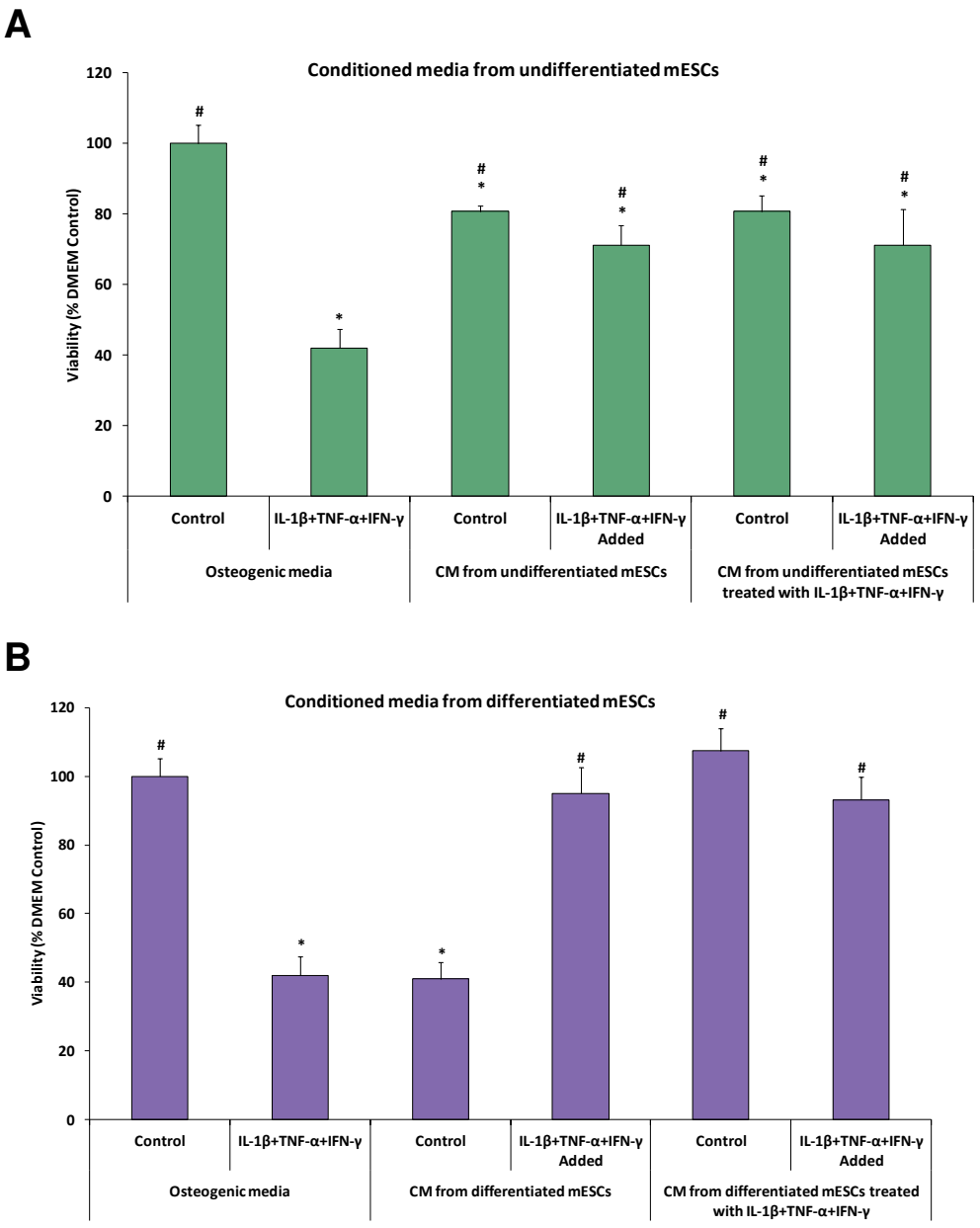

Figure 3.17: Effect of mESC conditioned medium (CM) on viability of cells treated with proinflammatory cytokines. Medium was conditioned by (A) undifferentiated and (B) differentiated mESCs for 10 days, with and without IL-1β (1ng/mL), TNF-α (10 ng/mL) and IFN-γ (100 ng/mL). Primary calvarial cells were cultured for 14 days before conditioned medium applied and subsequent proinflammatory cytokine stimulation for some groups. Cell viability determined by MTS assay and data shown as a percentage of DMEM control reading. Values are represented as mean±SD n=6 (experiment performed in triplicate, representative experiment shown). Statistical significance of response compared to DMEM control (*p≤0.01), statistical significance of response compared DMEM with IL-1β, TNF-α and IFN-γ (# p≤0.01).

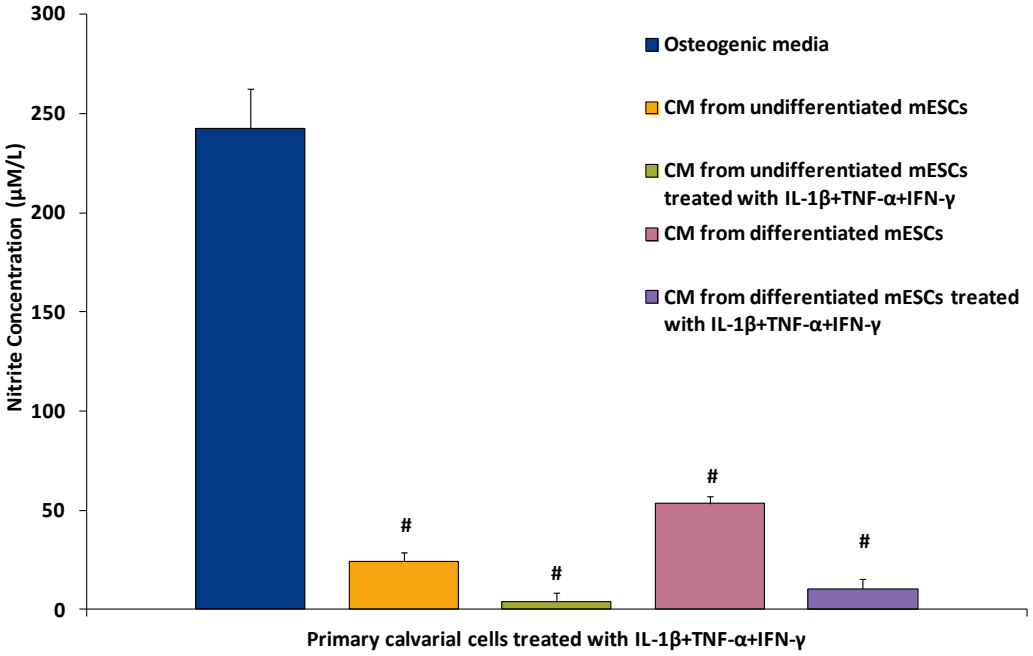

Figure 3.18: Effect of mESC conditioned medium on nitric oxide production of cells treated with proinflammatory cytokines. Medium was conditioned by undifferentiated and differentiated mESCs for 3 days, with or without IL-1β (1ng/mL), TNF-α (10 ng/mL) and IFN-γ (100 ng/mL). Primary calvarial cells were cultured for 14 days before conditioned medium applied and subsequent proinflammatory cytokine stimulation for some groups. Nitrite production measured at day 10. All groups supplemented with IL-1β, TNF-α and IFN-γ when added to primary calvarial cells. Control (no proinflammatory cytokines) readings subtracted from treated groups. Values shown as mean±SD, n=6, representative of 3 independent experiments. Statistical significance vs. OM with IL-1β, TNF-α and IFN-γ (# p≤0.01).

from differentiated mESCs with no proinflammatory cytokines treatment was the least effective of the groups.

3.4 Discussion

The aims of this chapter were to investigate the effect that a proinflammatory environment has on the responses of osteogenically differentiated mESCs, and compare them to the responses of the more well-described primary calvarial cells. Within the study, the primary calvarial cells were used as a “benchmark” for response to proinflammatory cytokines. Cells responded to IL-1β, TNF-α and IFN-γ in the medium, by showing reductions in cell viability, producing significantly increased amounts of NO and PGE_2, with associated increased expression of iNOS and COX-2. An elevated level of NO, associated with iNOS, contributes to localised cell and tissue damage, and can be involved in bone resorption and inhibition of bone formation [163, 166, 175, 183, 184]. PGE_2, produced through the COX-2 pathway, is induced in osteoblasts by the presence of proinflammatory cytokines, is a potent stimulator of bone resorption and can inhibit osteoblast growth and proliferation [176, 188, 189]. Levels of NO and PGE_2 production, along with the expression of iNOS, COX-2 and PGES help explain the marked fall in viability of the primary calvarial cells with prolonged exposure to proinflammatory cytokines. Conversely, the apparent lack of response and possible deficiency of these signalling molecules and enzymes in early differentiation osteo-mESC cultures may explain the stability of these cells in terms of viability.

Many authors have published work demonstrating the similarity of ESC-derived osteogenic cells to that of osteoblasts using established differentiation protocols. Protein expression, gene expression and mineral deposition have shown to be similar [60, 61, 164, 190, 191]. The efficacy of these differentiation protocols has been called into question. However, detailed comparative studies have been minimal [192, 193]. In this work, it was shown that although there are phenotypic similarities between the

cell types, there are distinct differences in biochemistry, as suggested by different responses to cytokines.

The two cells types in this investigation cannot be described as directly comparable, as the osteo-mESCs have been shown to be a heterogenous population of cells (see chapter 4). Levels of osteogenic differentiation between the two cell types is not comparable as the osteo-mESCs start considerably further behind in the developmental continuum. However, *in vitro* the two cells types do both form mineralised nodules at 21 days (see figure 4.2), and literature states that at this point the ESCs have differentiated to osteoblast-like cells [60, 61, 164, 190, 191]. Thus, this was considered to be the final timepoint, and a comparison of *in vitro* osteogenic differentiation and the effects of proinflammatory cytokines is discussed further in chapter 4. Although the cells are not directly comparable, it is clear that as a whole population, early differentiation osteo-mESCs do not respond to the presence of the proinflammatory cytokines by producing nitric oxide, PGE_2 and the associated enzymes iNOS, COX-2 and PGES. At this stage, the mechanisms contributing to these differences have not been determined, but it can be hypothesised that receptor and signal transduction pathways may be less developed or active in mESC-derived osteoblasts. Currently, there is very little available literature demonstrating the expression of receptors for these cytokines by mESCs and whether, if present, the receptors are functionally active. ESCs and early ES-derived vascular cells have been shown to have a low level of TNF-receptors and it has been reported that Nuclear Factor-κB (NF-κB), a transcriptional regulator that plays a key role in immunity and inflammation, has relatively low expression in undifferentiated ES cells but activity increases during differentiation [194, 195]. Expression of TLRs, another group of receptors associated with the immune and inflammatory response, have been shown to be significantly downregulated on hESCs [196]. This lack of evidence

of proinflammatory cytokine receptors expressed by osteo-mESCs would be an interesting point to address in future work, and if they are not expressed, at which point of differentiation this occurs.

Further evidence for differences in the biochemistry of these cells is supported by the finding that conditioned culture medium from both undifferentiated and differentiated mESCs can inhibit or reduce the effects of proinflammatory cytokines, on primary calvarial cells. ESCs have previously been shown to suppress proinflammatory cytokine production by T-cells, and to have immunosuppressive tendencies [197-200]. The work in this study may link into previous descriptions of ESCs as immunoprivileged [201, 202]. The very low levels of response to IL-1β, TNF-α and IFN-γ of the osteo-mESCs during early differentiation and the increasing response over the 21 days, reflects results that show the immunoprivileged state of ESCs diminishes as levels of differentiation increase [155, 156, 203]. The immune response and inflammation are innately linked through the cells and molecules involved, and proinflammatory cytokines, such as IFN-γ, have a large role in the expression of MHC antigens that lead to immune rejection [204, 205].

If elucidated, the diminished response of the osteo-mESCs to cytokines, particularly in the early stages of differentiation, may show some application in regenerative medicine and wound healing, although much more investigation would need be performed. Another type of stem cell, the mesenchymal stem cell has had impact, as MSCs have been shown to be attracted to the wound microenvironment; homing to the site of injured tissue, evading the immune system and promoting wound healing [206-209]. MSCs have shown potential to treat inflammatory immune-mediated diseases such as GVHD and Crohn's disease, by the release of anti-inflammatory factors such as IL-1ra and TGF-β [151, 210, 211]. MSCs derived from human ESCs have been shown to suppress the proliferation of lymphocytes and resist the cytotoxic

effects of NK cells in vitro, and have anti-inflammatory effects in vivo [198-200]. If osteogenic-cells derived from ESCs could offer these same advantages, they could be a candidate for cell therapies. ESCs offer more versatility than MSCs and have an excellent proliferative potential. If differentiation protocols could be improved and validated, so the threat of tumourigenicity is reduced, the risk of immune rejection and damage by inflammation may be moderated if using embryonic-derived cells as a therapy.

In cell therapies, it has previously been suggested that stem cells may play roles in: homing to injured areas; acting in an anti-inflammatory manner; using paracrine factors to support cell survival, and differentiating to functional cells [198, 212, 213]. In this study, it has been demonstrated that in early differentiation, osteogenic ESCs can survive an inflammatory environment, without the biochemical response that primary cells produce. The survival of these cells may lead to increased proliferation of host cells or inhibition of inflammation, whilst differentiation into functional tissue. The findings in this study help to support the promise that osteogenically differentiated ESCs have in understanding, and in the longer term, treating inflammatory bone disease.

Chapter 4:
Effect of Proinflammatory Cytokines on Osteogenic Differentiation of mESCs and Primary Calvarial Cells

4.1 Introduction

4.1.1 Overview

Current understanding of the effects of diseased environments on stem cell behaviour is limited, and interaction of bone cells within the inflammatory microenvironment is poorly understood. The effect that inflammation has on osteogenic differentiation is an important factor when considering any cell type as a therapy or model for bone disease. The previous chapter discussed the biochemical response of ESCs to proinflammatory signalling; in this chapter, the aim was to investigate the effects on osteogenic differentiation of the cells and the subsequent formation of *in vitro* bone nodules.

4.1.2 *In Vitro* Osteogenic Differentiation

In the body, bone development is highly regulated and the resulting structure is organised and hierarchically ordered [214]. *In vivo* bone development progresses through distinct development stages that follow commitment of MSCs to the

osteoblast lineage, proliferation of osteoprogenitors and maturity of the differentiated osteoblast, leading to the formation of mineralised ECM [68].

In vitro differentiation of primary osteoblasts and osteoblast cell lines results in the formation of mineralised bone nodules, when cultured in the presence of BGP and ascorbate [162, 215]. The ECM deposited by osteoblasts *in vitro* has been shown to include collagen-I (col-I), fibronectin, OCN and OPN, and staining for these proteins is often strongest around the mineralised nodules [216-219]. *In vitro*, there is a clear progression of osteogenic differentiation, with distinct stages. Osteoprogenitors can differentiate into mature osteoblasts only if they undergo growth arrest and begin to establish a collagenous ECM. Therefore, after first seeding, cells undergo a proliferation phase within the first 1-7 days, subsequently genes associated with cell proliferation, such as *c-Fos* and *c-Myc*, fall in expression level as a collagen matrix is synthesised and deposited [220, 221]. Sequential expression of differentiation related proteins then occurs, first with ALP, followed by BSP, OPN and finally, OCN [218, 221-224].

Both mouse and human ESCs have also been shown to differentiate osteogenically *in vitro,* exhibiting molecular and structural features resembling bone tissue, by formation of mineralised bone nodule structures [60, 190, 225, 226]. The majority of osteogenic differentiation protocols induce cell differentiation by including factors in the culture medium, such as BGP, ascorbate, dexamethasone, simvastatin, retinoic acid, vitamin D_3 and BMPs [30, 65, 227-232]. Bone nodules have been shown to stain positive for the presence of calcium and phosphate by alizarin red and von Kossa staining, respectively. The expression of bone matrix proteins, such as col-I and OCN, in ESC cultures has also been shown [30, 60, 225, 233].

4.1.3 Proinflammatory Cytokines and Osteogenic Differentiation

As discussed in Chapter 1, the cytokines IL-1β, TNF-α and IFN-γ play roles in bone regulation and are critical mediators of inflammation. The effect of these cytokines, particularly in combination, on the osteogenic differentiation of ESCs, has been minimally investigated. The effects on bone cells are well described and are summarised in chapter 1, table 1.2. The acute inflammatory process plays a critical role in fracture healing with proinflammatory signalling occurring for short time periods and ending within days, and IL-1 and TNF have both been shown to be expressed transiently at sites of bone formation [234, 235]. With this in mind during this study, the effects of short bursts of proinflammatory cytokine signalling on osteogenic differentiation of the primary calvarial cells and the osteo-mESCs were investigated. The consequences of this short burst of cytokine stimulation, in terms of bone nodule formation, mineral deposition and ECM production were examined, looking at the time-point of osteogenic differentiation of the cells that cytokine stimulation occurs.

4.1.4 Cell-Sorting for Osteogenic Populations

In both extracted primary bone cell populations and osteogenically-differentiated ESCs there is some level of heterogeneity within the cultured cell population. Cell sorting techniques can be used to select for certain cell populations based on marker expression. Common cell sorting techniques include centrifuge sorting, fluorescence activated cell sorting (FACS) and MACS. There is currently no commonly used marker of the early osteoblast. Although, Stro-1 and ALP have previously been used to generate osteoblast populations from bone marrow and bone tissue extracts [236-

240], they were unsuitable for this investigation. Stro-1 may only be expressed on human cells and ES cells can constitutively express high levels of ALP [241, 242]. Cad-11 has previously been used to purify ES cells, and is a good candidate in this case [243]. Cad-11 is a cell adhesion molecule strongly associated with bone formation and osteogenic differentiation [244, 245]. In this study, MACS was used to separate a population of osteoprogenitors from the osteogenically differentiated ESC population, using the cad-11 marker. The cad-11 cell sorting allowed the investigation of the response of the sorted cell populations to proinflammatory cytokine signalling, allowing comparison with the responses of the unsorted osteo-mESCs, described in the previous chapter.

4.2 Experimental Design

For more detailed methods describing primary calvarial cell extraction and culture, mESC culture, EB formation, osteogenic differentiation and assay protocols see Chapter 2: Materials and Methods.

As discussed in the introduction to this chapter (section 4.1.2) *in vitro* osteogenic differentiation follows a clear progression, with distinct stages [162, 215-224]. To reflect this progression, assay timepoints were chosen to reflect the points at which literature describes certain differentatiation markers to be expressed. For example, ALP is considered to be an early osteogenic marker and expression peaks between day 12 and 14; thus, the ALP assay was performed on day 14. Col-I is the first ECM protein to be produced and can be found from approximately day 14 onwards. Cad-11 is expressed from at least day 16. These were stained for on the same samples at day 21, as this allowed for col-I accumulation to be assessed alongside a cellular marker. Total time for bone nodule formation during *in vitro* osteogenic differentiation is 21 to 28 days, thus alizarin red staining for calcium deposition, and OCN and OPN protein staining was performed at 21 and 28 days respectively. This day 28 timepoint was chosen because OCN is the ultimate osteogenic ECM protein to be produced, and is often not found until the later stages of differentiation.

4.2.1 Osteogenic differentiation of primary calvarial cells and osteo-mESCs

Osteogenic differentiation of the primary calvarial cells and the osteo-mESCs was compared using a range of techniques and markers. Mineralisation potential was

assessed by alizarin red staining of the cells, after 21-days growth in osteogenic medium (50 mM BGP, 50 µg/mL ascorbate 2-phosphate, 10 µM dexamethasone) or non-osteogenic medium. Formation of bone nodules was also assessed by immunocytochemical staining for col-I and cad-11 after 21 days osteogenic culture. OCN and OPN double-staining in osteogenic and non-osteogenic medium, after 28 days, was investigated. Details of antibodies can be found in Chapter 2: Materials and Methods, table 2.1 and table 2.2.

Levels of osteogenic markers (*Runx2, Col1a1, Opn)* after osteogenic culture were assessed by RT-qPCR. RNA was extracted after 18 days culture, reverse transcription of 400 ng RNA performed and real-time expression analysis carried out. Expression of each target gene was normalised to the *Rpl32* ribosomal protein gene. Details of RT-qPCR protocol and primer sequences can be found in Chapter 2: Materials and Methods.

4.2.2 Effect of proinflammatory cytokines on osteogenic differentiation of osteo-mESCs and primary calvarial cells.

This group of experiments aimed to investigate the effect of short term stimulation with proinflammatory cytokines on the osteogenic differentiation of primary calvarial cells and osteo-mESCs. A schematic overview of experiments described in sections 4.2.2.i, 4.2.2.ii and 4.2.2.iii can be found in figure 4.1.

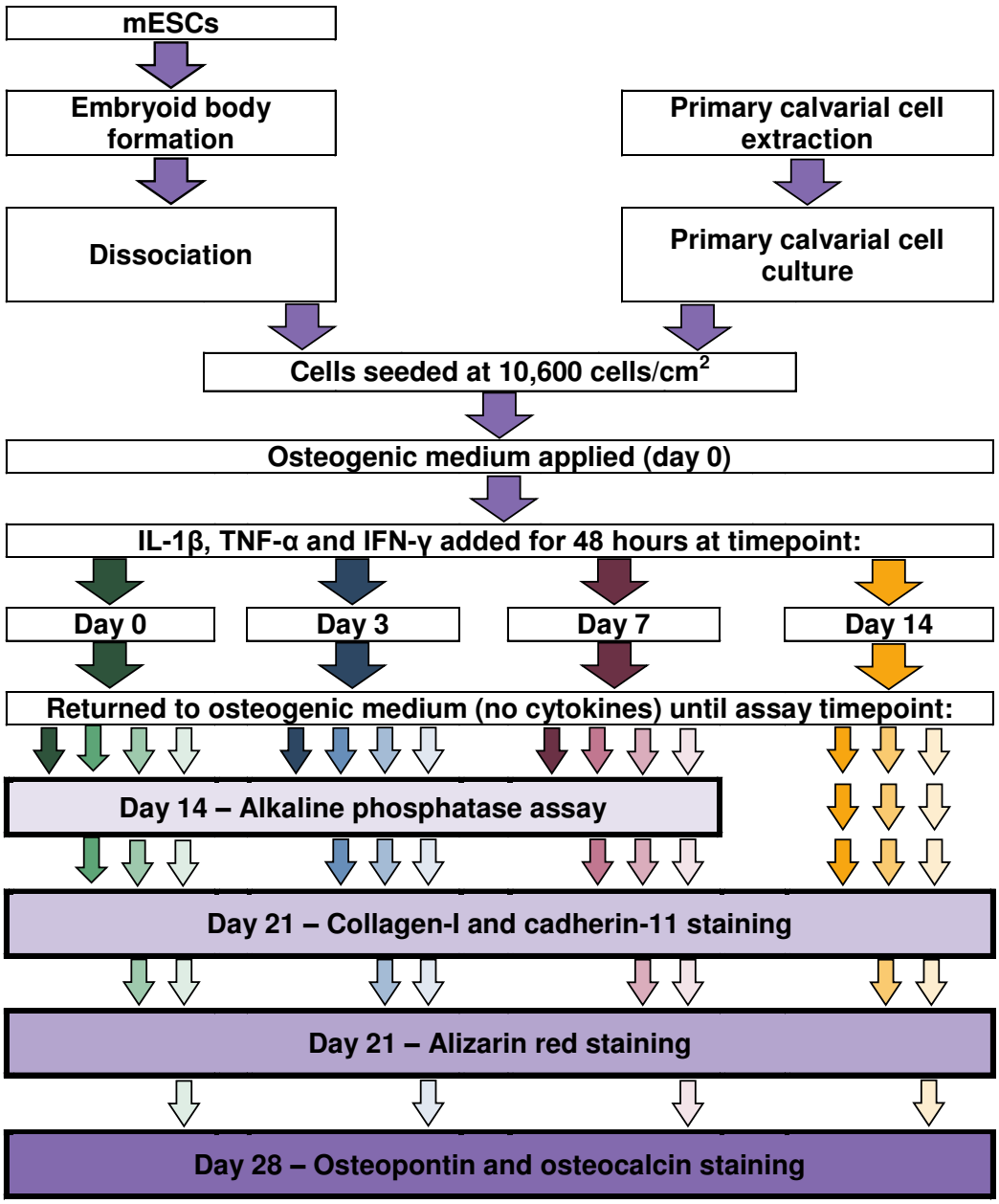

Figure 4.1: Schematic overview of experiments investigating the response of osteogenic cells to proinflammatory cytokines. Schematic shows simplified experimental design for section 4.2.2, investigating the effect of "short bursts" of IL-1β, TNF-α and IFN-γ exposure, at different timepoints of osteogenic differentiation of osteo-mESCs and primary calvarial cells.

4.2.2.i Effect of proinflammatory cytokines on mineralisation potential of primary calvarial cells and osteo-mESCs

Primary calvarial cells and osteo-mESCs were plated in 6-well plates. Cells were cultured in osteogenic medium (50 mM BGP, 50 µg/mL ascorbate 2-phosphate, and 10 µM dexamethasone) for 21 days. At timepoints day 0, 3, 7 and 14 of osteogenic culture, IL-1β (1ng/mL), TNF-α (10 ng/mL) and IFN-γ (100 ng/mL) were added to medium for 48 hours. Each timepoint was represented by a separate plate. After cytokine treatment, cells were changed back to non-cytokine osteogenic medium and cultured until day 28. Due to the anti-inflammatory effects of dexamethasone, during proinflammatory cytokine treatment and 24 hours after, cells were cultured in osteogenic medium without dexamethasone. Controls were treated identically. After 28 days, cells were fixed in 10% (*w/v*) formalin and stained for calcium deposition with 2% (*w/v*) alizarin red S. Cultures were imaged using a stereo dissection microscope for macro-well images and an inverted light microscope with Hoffman contrast for higher magnification images. Percentage area stained by alizarin red in macro-well images was quantified using image J software.

4.2.2.ii Effect of proinflammatory cytokines on alkaline phosphatase activity of osteogenic cells

Experiments were performed as above, (mineralisation experiment), with the exceptions that 12-well plates were used and the endpoint was day 14. Timepoints of cytokine treatment were day 0, 3 and 7 for 48 hours and subsequently cells were changed back to control osteogenic medium. ALP activity was assessed at day 14 using the pNPP assay, and values were corrected for cell number using fluorescent Hoechst readings.

4.2.2.iii Effect of proinflammatory cytokines on expression of osteogenic proteins

Experiments were performed identically to the mineralisation potential experiment with the same timepoints and endpoint at day 28, when cell were fixed in 4% (*w/v*) PFA. Immunofluorescence was performed, with double staining for OPN and OCN, and col-I and cad-11. Antibody details and the immunocytochemistry protocol can be found in Materials and Methods, tables 2.1 and 2.2. Nuclear counterstaining with Hoechst 33258 was performed. Imaging was carried out with an inverted fluorescence microscope and image processing was completed to remove non-specific background using Volocity software.

4.2.3 Cadherin-11 sorting of osteo-mESCs

MACS was used to sort for preosteoblasts within the osteo-mESC cultures using the cad-11 cell surface marker. Osteo-mESCs were cultured on gelatin-coated T75 cm^2 flasks in osteogenic medium (50 mM BGP, 50 µg/mL ascorbate 2-phosphate and 10 µM dexamethasone) for 16 days. At this point, cells were detached and MACS separation performed for cad-11 positive cells. Description of MACS separation procedure can be found in Chapter 2: Materials and Methods, along with details of antibodies used (tables 2.1 and 2.2)

4.2.3.i Osteogenic potential of cadherin-11 sorted osteo-mESCs

Cad-11 positive and negative cells were plated separately at a density of 200,000 cells/well in gelatin-coated 6-well plates. Cells were cultured in osteogenic medium

with 10 µM dexamethasone for a further 21 days. Subsequently, half the plates were fixed with 4% (*w/v*) PFA and immunocytochemistry performed for OCN, OPN and Col-I. The remaining plates were fixed in 10% (*w/v*) formalin and stained for calcium deposition with alizarin red S.

4.2.3.ii Response of cadherin-11 sorted mESCs to proinflammatory cytokines

Cad-11 positive and negative osteo-mESCs were plated separately in gelatin-coated 6-well plates at a 200,000 cells/well. Cells were cultured in osteogenic medium. At day 7 and day 14 after MACS sorting, cells were treated with IL-1β (1ng/mL), TNF-α (10 ng/mL) and IFN-γ (100 ng/mL). At this point, dexamethasone was removed from the medium in both treated and control. After 48 hours cytokine treatment, medium samples were collected and cell monolayers fixed in 4% (*w/v*) PFA. Samples were tested for nitrite and PGE_2 concentration. Cell monolayers were stained via immunocytochemistry for the presence of iNOS.

4.3 Results

4.3.1 Osteogenic differentiation of primary calvarial cells and osteo-mESCs

*In vitro o*steogenic differentiation of mESCs was compared to the differentiation of mouse primary calvarial cells. After 21 days in osteogenic medium, both cell types showed formation of specific areas of mineralizing matrix or nodules, as suggested by alizarin red staining (figure 4.2A). Under magnification, these nodules appeared to have similar structure in both osteo-mESC and primary cultures. Subjective observation showed nodules were more abundant in osteo-mESC cultures. Alizarin red staining was not seen in non-osteogenic culture medium controls.

The formation of nodules was further assessed by immunocytochemistry, revealing similar localised expression of col-I and cad-11, within nodules formed by both cell types (figure 4.2B). Figure 4.2D shows localised expression of ECM proteins OPN and OCN by both cell types in nodular areas. In non-osteogenic medium, the expression of OPN and OCN was minimal.

Figure 4.2C shows real-time PCR analysis of expression of *Runx2, Col1a1* and *Opn* at day 18 of osteogenic culture. There are significant differences in the level of expression of all three genes in the osteo-mESCs when compared to the primary calvarial cells, with expression levels of all genes lower in the osteo-mESCs.

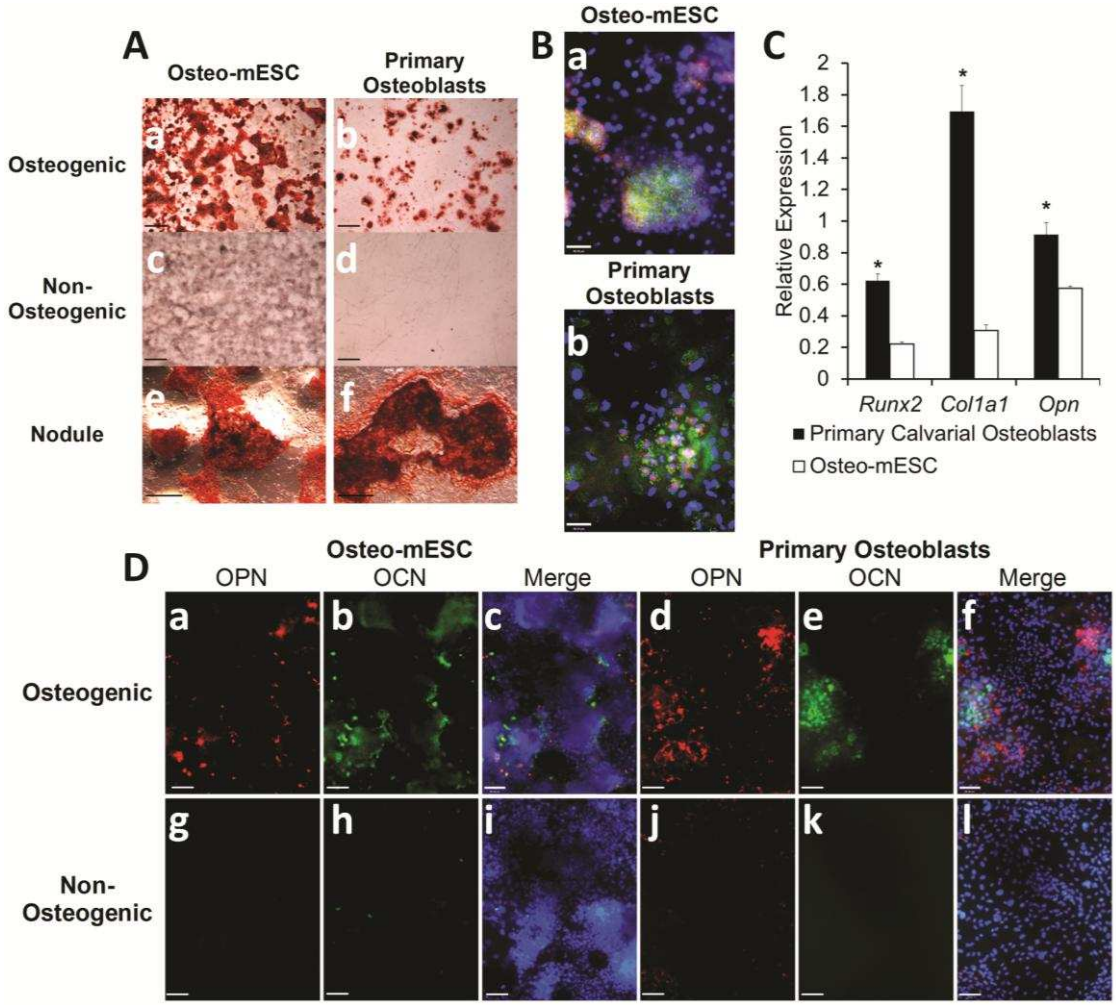

Figure 4.2: Osteogenic differentiation of osteo-mESCs and mouse primary calvarial cells. (A) Representative images of alizarin red staining of bone nodules in osteogenic and non-osteogenic medium at 21 days culture (scale bar = 2 mm), high magnification image of osteo-mESC and primary calvarial cell bone nodules in osteogenic medium (scale bar = 20 µm). (B) Representative images showing expression of collagen-1 (green), cadherin-11 (red) and nuclei (blue) in bone nodules formed by osteo-mESCs and primary calvarial cells (scale bar = 48 µm). (C) RT-qPCR analysis performed on primary calvarial cells and osteo-mESCs at day 18 of culture for osteogenic markers *Runx2, Col1a1* and *Opn.* Expression of each target gene normalised to *Rpl32*. Data shown is mean±SD of 3 independent experiments (n=3). *Statistical significance of primary calvarial cells vs. osteo-mESCs, p≤0.05. (D) Representative images showing expression of osteopontin (red) and osteocalcin (green) in osteogenic and non-osteogenic cultures of osteo-mESCs and primary calvarial cells. Merge image shows OPN and OCN with Hoechst nuclear staining (scale bar = 90 µm).

4.3.2 The effect of proinflammatory cytokines on mineralisation potential of primary calvarial cells and osteo-mESCs

Cells were treated with proinflammatory cytokines at day 0, 3, 7 and 14 of osteogenic culture for 48 hours. Subsequently medium was changed back to osteogenic medium without cytokines, and culture continued until day 28, at which point alizarin red staining was performed. The effect this short exposure to cytokines had on primary calvarial cultures can be seen in figure 4.3 and osteo-mESC cultures in figure 4.4. Quantification of staining using image analysis can be found in figure 4.5. Short timecourses of cytokine treatment at all timepoints had significant effects on the eventual mineralisation of the primary calvarial cells. Treatment for 48 hours on day 0, 3 and 7 showed almost no alizarin red staining, suggesting no calcium deposition, on day 28, although there did appear to be some nodule formation. Treatment on day 14 had less effect than other timepoints, but calcium deposition was very much reduced, with around 5% staining compared to control. Hoffman contrast images show the reduced deposition of calcium.

The osteo-mESCs were less noticeably affected by the cytokine treatment. Treatment on day 0 or 3 showed very little effect on alizarin red staining compared to control. Treatment on day 7, showed increased levels of staining across the well. Cytokine stimulation on day 14 showed the inverse to the primary calvarial cells, with staining levels decreased to around 50% of the control and staining appearing to be less concentrated. The non-osteogenic medium controls in both cell cultures (not pictured) showed minimal staining.

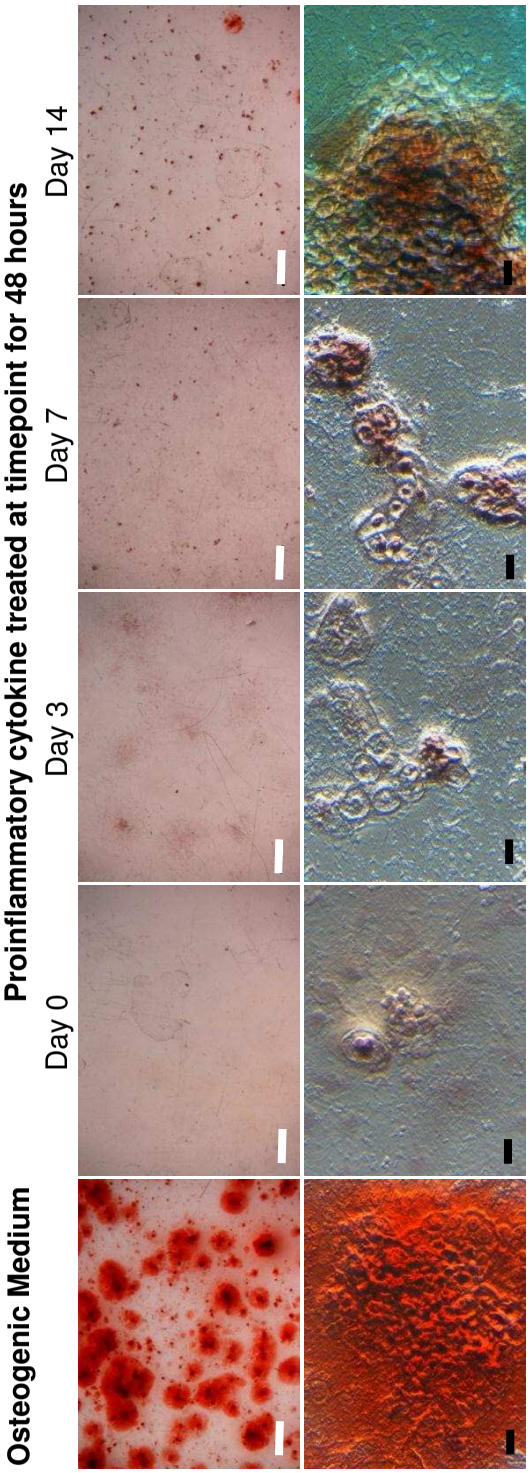

Figure 4.3: Effect of proinflammatory cytokines on calcium deposition of primary calvarial cells. Cells were stimulated with IL-1β, TNFα and IFN-γ for 48 hours at either day 0, day 3, day 7 or day 14 of osteogenic culture. Subsequently, culture media was returned to control osteogenic media until day 28 and calcium deposition was stained with alizarin red S. Representative images shown. Scale bars: Bone nodules=2 mm, Hoffman Contrast = 100 µm.

Figure 4.4: Effect of proinflammatory cytokines on calcium deposition of osteo-mESCs. Cells were stimulated with IL-1β, TNFα and IFN-γ for 48 hours at either day 0, day 3, day 7 or day 14 of osteogenic culture. Subsequently, culture media was returned to control osteogenic media until day 28 and calcium deposition was stained with alizarin red S. Representative images shown. Scale bars: Bone nodules=2 mm, Hoffman Contrast = 100 µm.

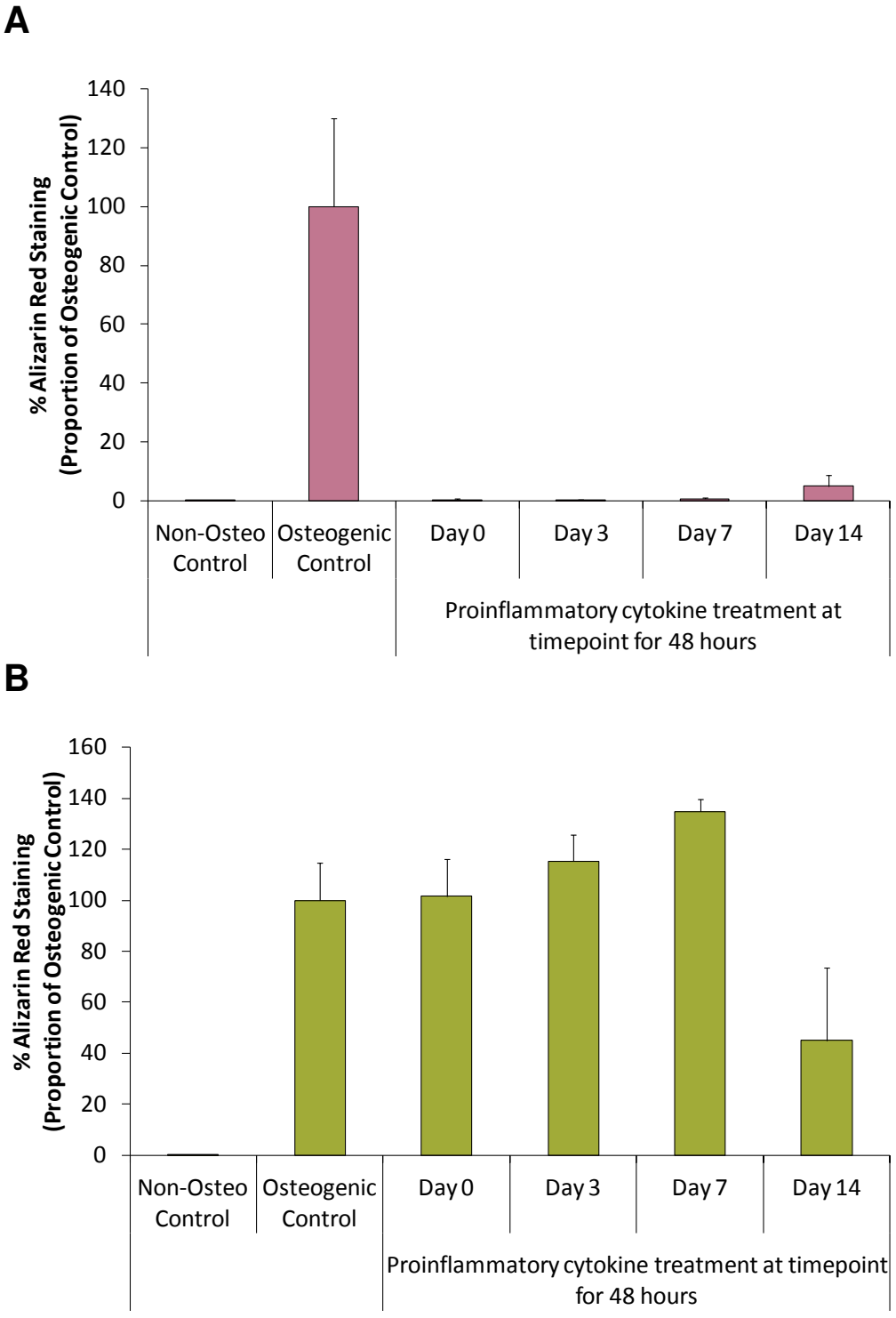

Figure 4.5: Quantification of effect of proinflammatory cytokines on calcium deposition. Percentage alizarin red staining was quantified for (A) Primary calvarial cells and (B) osteo-mESCs. Cells were treated with medium containing 1 ng/mL IL-1β, 10 ng/mL TNF-α and 100 ng/mL IFN-γ for 48 hours at day 0, 3 and 7 of osteogenic culture. Subsequently, culture medium was returned to control osteogenic medium and experiment was ended on day 28. Values are corrected to proportion of osteogenic control. Mean±SD (n=6).

4.3.3 The effect of proinflammatory cytokines on the alkaline phosphatase activity of osteogenic cells

Primary calvarial cells and osteo-mESCs were treated with proinflammatory cytokines at day 0, 3 and 7 of osteogenic culture for 48 hours. Medium was subsequently changed back to osteogenic medium and culture continued until day 14; at which point an ALP activity assay was performed. Figure 4.6 shows the effect that this acute proinflammatory cytokine treatment has on (A) primary calvarial cells and (B) osteo-mESCs. Treatment of the primary calvarial cells for 48 hours at all 3 timepoints had a significant negative effect on the eventual ALP activity, with treatment on day 0 having the largest effect. In osteo-mESC cultures, a significant effect was seen only with treatment on day 3 and this showed an increase in eventual ALP activity.

4.3.4 The effect of proinflammatory cytokines on the expression of osteogenic proteins in primary calvarial and osteo-mESC cultures

Production of ECM proteins associated with osteogenic differentiation was assessed by immunocytochemistry for OCN, OPN, col-I and cad-11. Double staining for OPN and OCN was performed to assess localised expression on the same sample. Figure 4.7 shows primary calvarial cells and figure 4.8 shows osteo-mESCs. Cell cultures were treated with short exposure to proinflammatory cytokines for 48 hours at either day 0, 3, 7 or 14. Cell culture medium was then changed back to osteogenic and continued until day 28 to investigate eventual effect on matrix deposition.

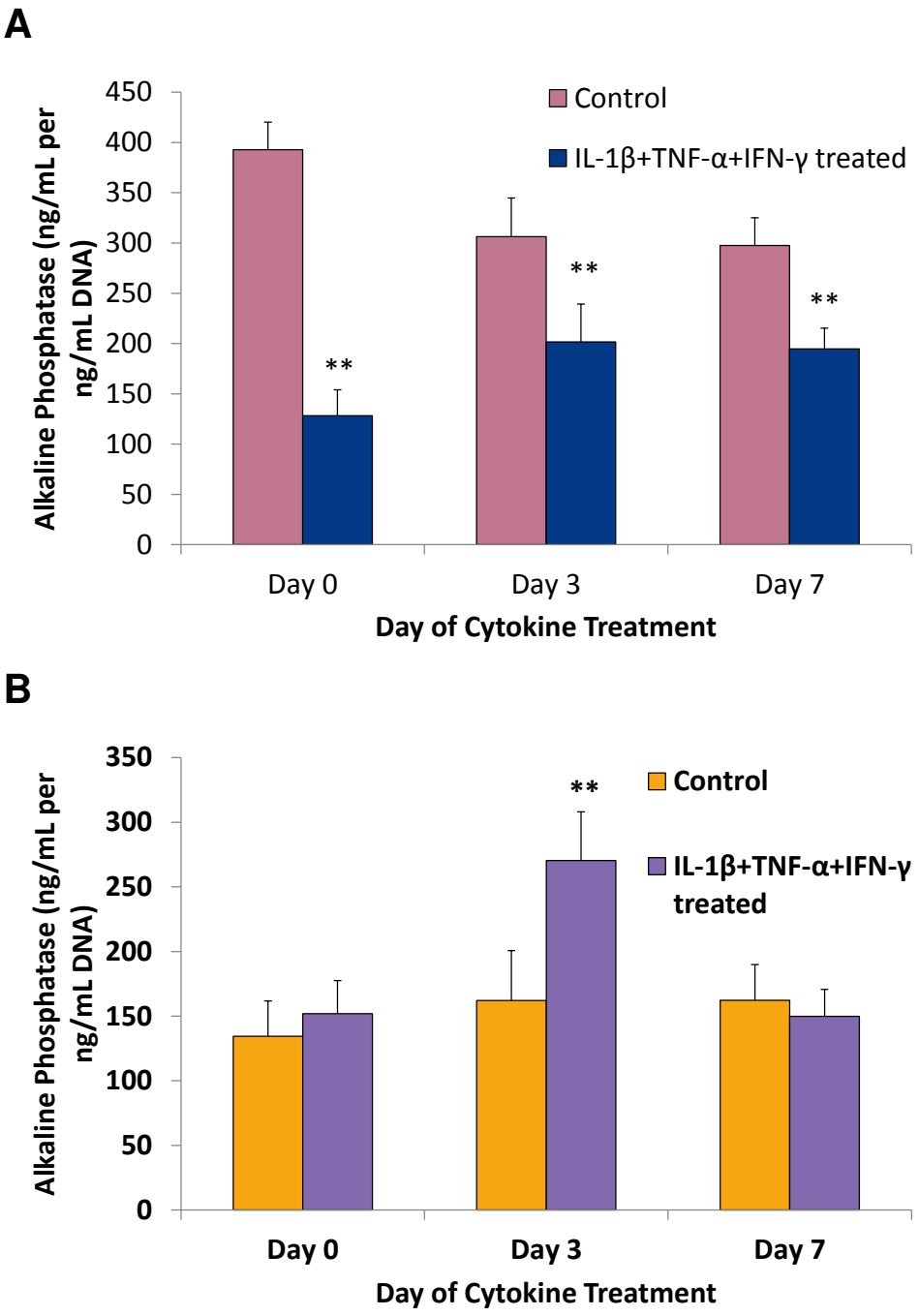

Figure 4.6: Effect of proinflammatory cytokines on alkaline phosphatase activity. (A) Primary calvarial cells and (B) osteo-mESCs were treated with medium containing 1 ng/mL IL-1β, 10 ng/mL TNF-α and 100 ng/mL IFN-γ for 48 hours at day 0, 3 and 7 of osteogenic culture. Culture medium was returned to control osteogenic medium and experiment was ended on day 14. Alkaline phosphatase activity was assessed via pNPP assay and values corrected for DNA concentration. Values are represented as mean±SD, n=6, experiment repeated 3 times. **statistical significance of response to cytokines compared to control ($p<0.01$).

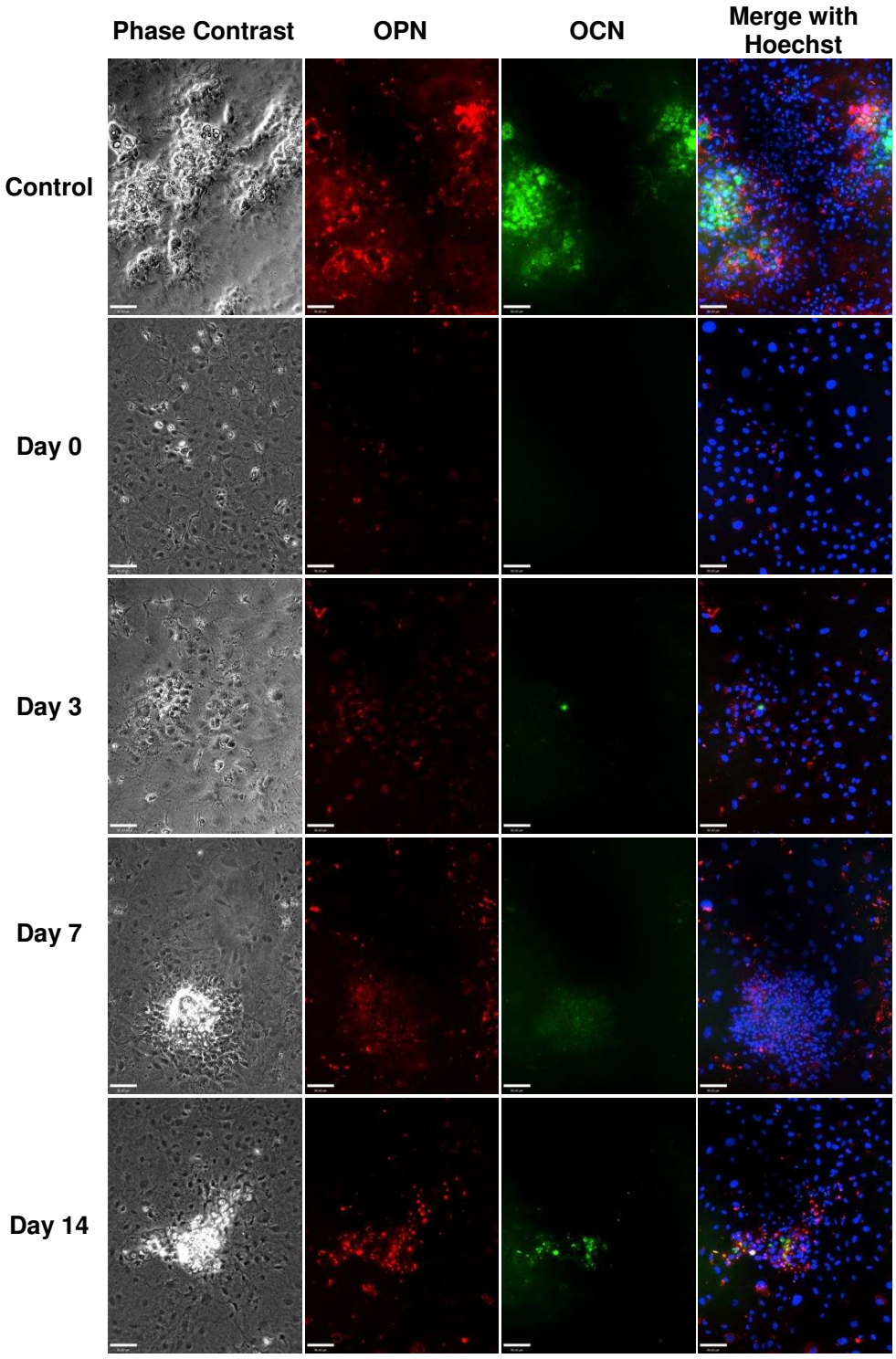

Figure 4.7: Expression of osteopontin and osteocalcin in primary calvarial cells stimulated with proinflammatory cytokines. Cells were stimulated with IL-1β, TNFα and IFN-γ for 48 hours at either day 0, day 3, day 7 or day 14 of osteogenic culture. Culture medium was returned to control osteogenic medium and OPN (red) and OCN (green) expression assessed by immunocytochemistry on day 28. Representative images shown. Scale bar=90 µm.

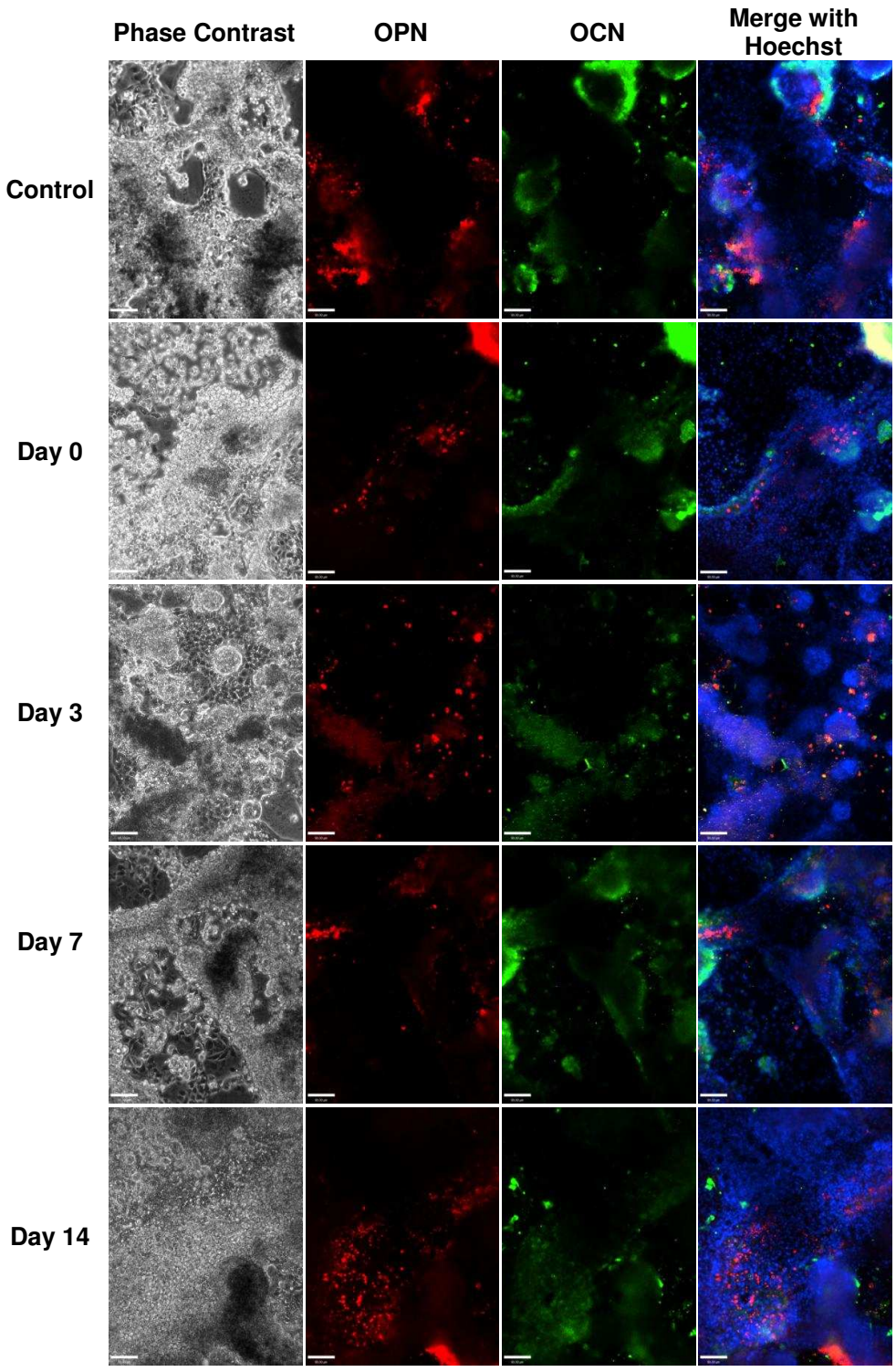

Figure 4.8: Expression of osteopontin and osteocalcin in osteo-mESCs stimulated with proinflammatory cytokines. Cells were stimulated with IL-1β, TNFα and IFN-γ for 48 hours at either day 0, day 3, day 7 or day 14 of osteogenic culture. Culture medium was returned to control osteogenic medium and OPN (red) and OCN (green) expression assessed by immunocytochemistry on day 28. Representative images shown. Scale bar=90 µm.

In primary calvarial cell cultures in control osteogenic medium, OCN and OPN were co-localised around bone nodule areas, with OCN deposited in the centre of the nodule and OPN more dispersed. When primary calvarial cells were treated with cytokines on day 0, there was no eventual bone nodule formation or deposition of OPN and OCN on day 28. A similar result occurred with treatment on day 3, although there was a little more evidence of bone nodule formation, as seen in the phase contrast image. Proinflammatory cytokine treatment for 48 hours on day 7 appeared to allow limited eventual nodule formation and there was marked reduction in staining for OPN and OCN. With treatment at day 14, nodules had formed and there was evidence of both OCN and OPN staining.

Figure 4.8 shows staining of OCN and OPN in osteo-mESCs. Phase contrast images showed the cultures are densely packed and contained a heterogeneous population of cells. In control osteogenic medium, after 28 days, the osteo-mESCs showed co-localised staining for OCN and OPN in what appear to be nodular areas. Across the cytokine treatment timepoints, there were very few obvious differences in staining between groups, and nodules appeared to form regardless of proinflammatory cytokine treatment.

Staining for cad-11 and col-I in primary calvarial cultures can be seen in figure 4.9. In osteogenic medium controls, col-I can be found in and around the bone nodules and is localised in areas where there is a high level of cad-11. As with OCN and OPN staining, proinflammatory cytokine treatment on day 0, led to zero nodule formation, a large amount of cell death and no col-I or cad-11 staining. When treated on day 3, cells survived until day 28 and there was some evidence of nodule formation with a few involving cad-11 positive cells. Very little col-I was seen. Treatment on day 7 allowed nodule formation involving cad-11 cells and some col-I deposition. Cytokine treatment on day 14 had a reduced effect on col-I staining.

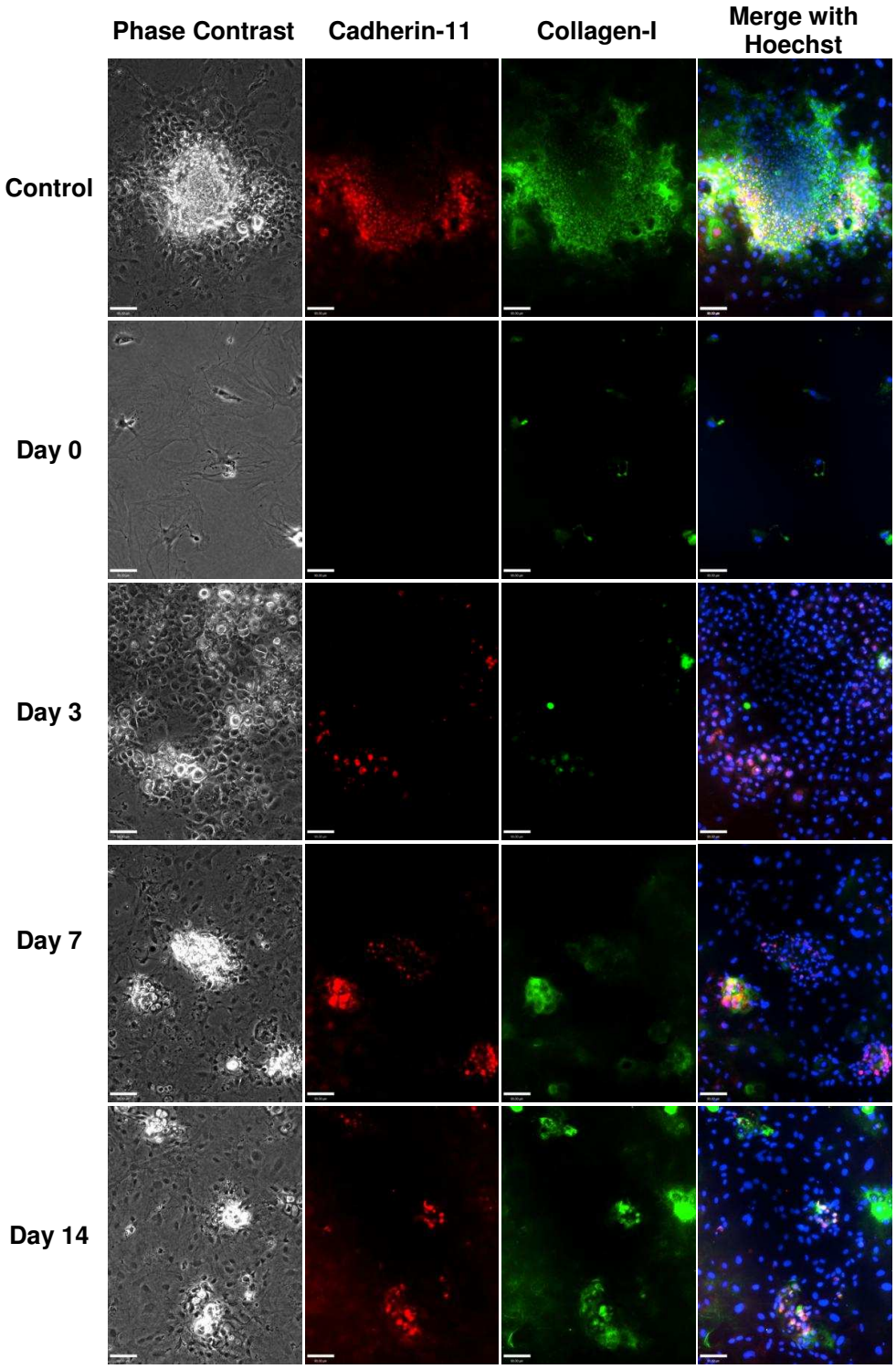

Figure 4.9: Expression of cadherin-11 and collagen-I in primary calvarial cells stimulated with proinflammatory cytokines. Cells were stimulated with IL-1β, TNFα and IFN-γ for 48 hours at either day 0, day 3, day 7 or day 14 of osteogenic culture. Culture medium was returned to control osteogenic medium and cadherin-11 (red) and collagen-I (green) expression assessed by immunocytochemistry on day 28. Representative images shown. Scale bar=90 µm.

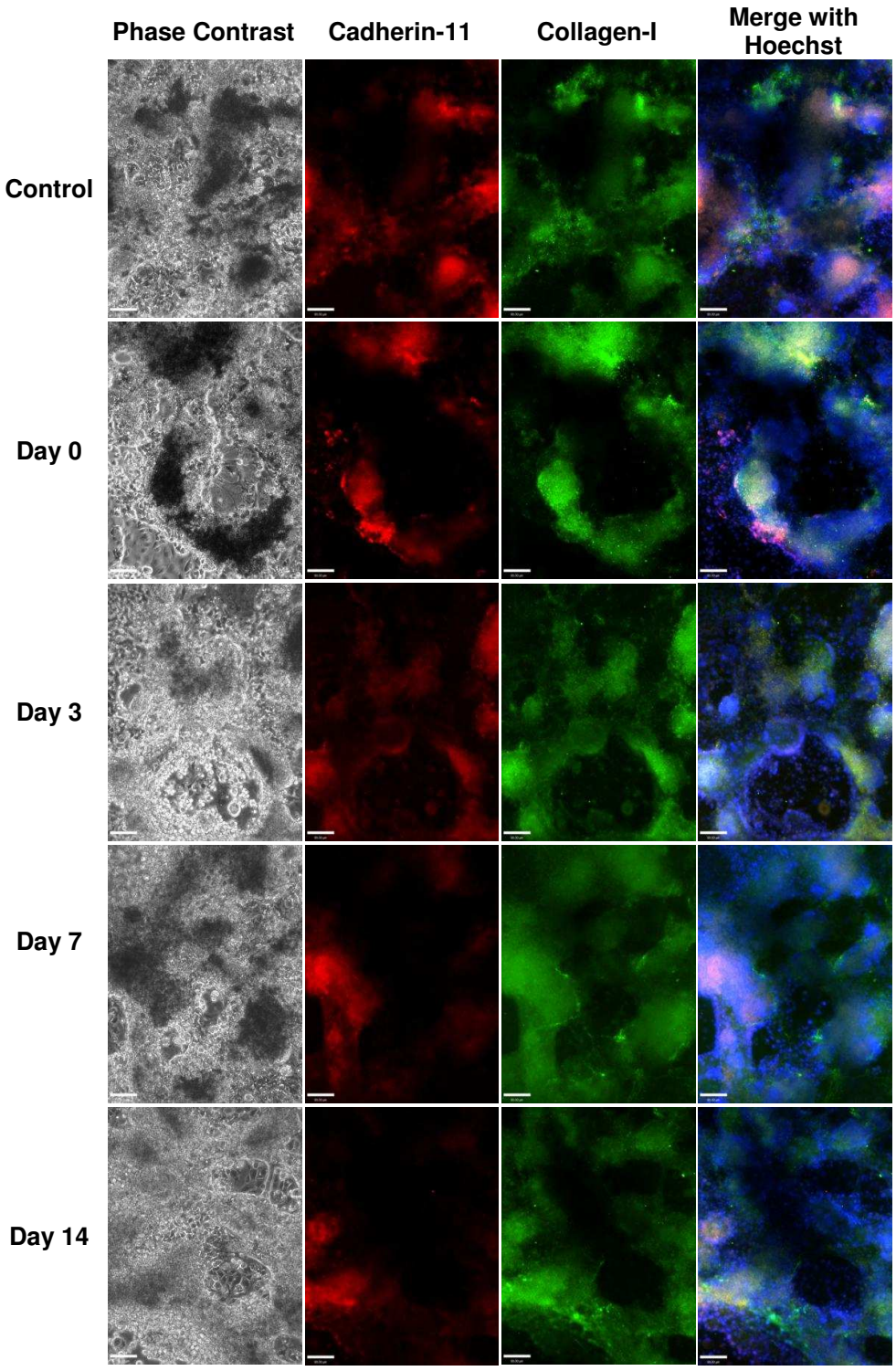

Figure 4.10: Expression of cadherin-11 and collagen-I in osteo-mESCs stimulated with proinflammatory cytokines. Cells were stimulated with IL-1β, TNFα and IFN-γ for 48 hours at either day 0, day 3, day 7 or day 14 of osteogenic culture. Culture medium was returned to control osteogenic medium and cad-11 (red) and col-I (green) expression assessed by immunocytochemistry on day 28. Representative images shown. Scale bar=90 µm.

Figure 4.10 shows cad-11 and col-I expression in osteo-mESC cultures. Col-I staining was widely dispersed across the cultures, but appeared most strong in areas of cad-11 staining. There was no obvious negative effect of proinflammatory cytokine treatment on levels of cad-11 or col-I staining. There may have been an enhanced effect on col-I staining with treatment on day 7, but this was difficult to quantify.

4.3.5 Cadherin-11 sorting of osteo-mESCs

In order to reduce heterogeneity within the differentiated osteo-mESCs and to investigate levels of osteogenesis, cell sorting for preosteoblasts was attempted. After 16 days osteogenic culture, osteo-mESCs were sorted via MACS for the presence of cad-11. Figure 4.11 shows box-plots illustrating data distribution of cell sorting. The average percentage of cad-11 positive cells was 21.2% and numbers were comparable between cell sorting experiments. Figure 4.12 shows phase contrast images of cad-11 positive and negative cell populations. Before cell sorting, the osteo-mESCs were a densely packed heterogeneous cell population. After cell sorting, cell morphology differences can be seen between cad-11 positive and negative cells. By day 7, the cad-11 positive cells displayed a morphology more similar to that of primary calvarial cells and by day 21, formed what appeared to be bone nodules. The cad-11 negative cells showed a mix of distinct cell morphologies and over time developed more heterogeneity across the cell population.

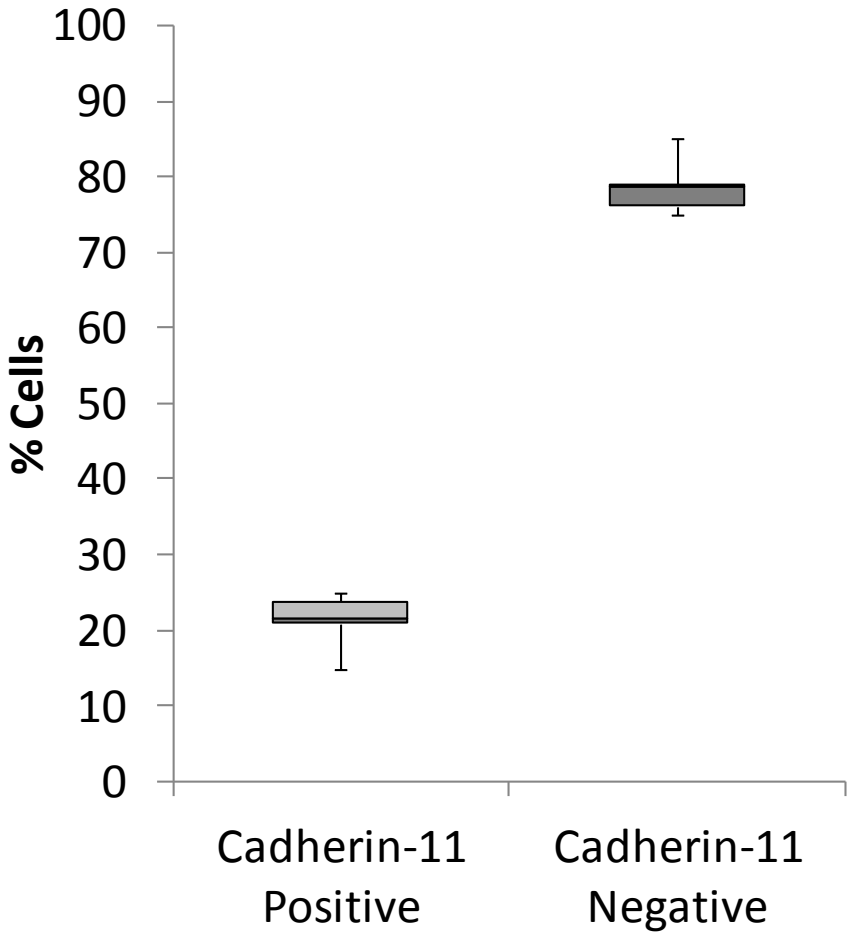

Figure 4.11: MACS sorting for cadherin-11. Box-plots showing data distribution of percentage of cadherin-11 positive and negative cells (n=6).

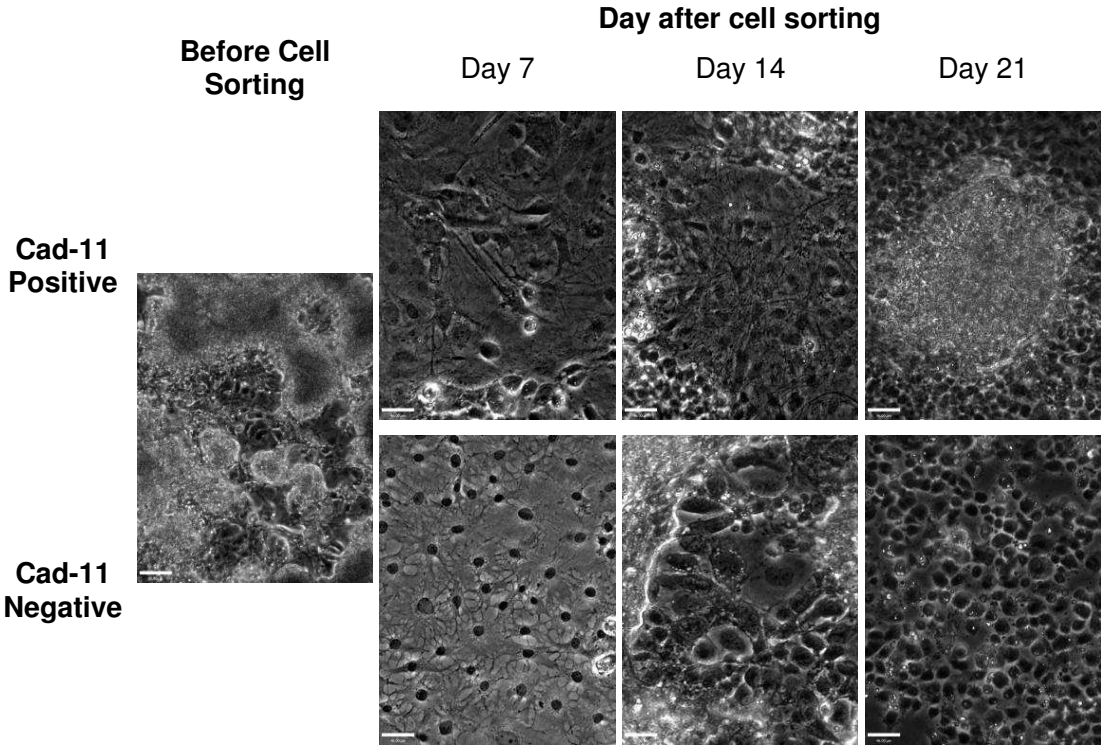

Figure 4.12: Representative phase contrast images of osteo-mESCs before and after MACS sorting for cadherin-11. Scale bar=46 µm.

4.3.5.i Osteogenic potential of cadherin-11 sorted osteo-mESCs

Immunostaining for OCN and OPN after cell sorting can be seen in figure 4.13. In cad-11 positive osteo-mESCs, bone nodule-like structures were seen within the cultures. Within these nodules, OCN staining was seen around the edge and OPN distributed in the nodule centre. In cad-11 negative osteo-mESCs, there was weak staining for OCN, but no OPN was seen. No nodule-like structures were observed. Figure 4.14 shows col-I staining in cad-11 positive and negative osteo-mESCs. In the cad-11 positive cultures, there was a substantial amount of staining in a web-like mesh around the cells. Col-I is present in the cad-11 negative cultures but staining was globular and less defined, and was sparse across the culture.

Matrix mineralisation by the cad-11 positive and negative osteo-mESCs was investigated by alizarin red staining for calcium deposits. Figure 4.15A shows macro-well staining of calcium deposition and figure 4.15B shows quantification of the alizarin red images. Nodule formation with calcium deposition was seen at much higher levels in the cad-11 positive cells than negative. Calcium deposition had begun by day 7, but nodule number continued to increase and staining became denser over the 21-day period. Very little staining was seen in the cad-11 negative cells. By day 21, there was some staining for calcium, but this did not appear to be in nodules, when compared to the cad-11 positive cells. Figure 4.16 shows higher magnification images of the calcium deposition staining, with Hoffman contrast, and fluorescent images of the alizarin red stain. These images show that the cad-11 positive cells form discrete nodules within the cultures with distinct areas of calcium deposition. The cad-11 negative cells showed areas of alizarin red staining, but calcium deposition was less dense and nodules were difficult to discern.

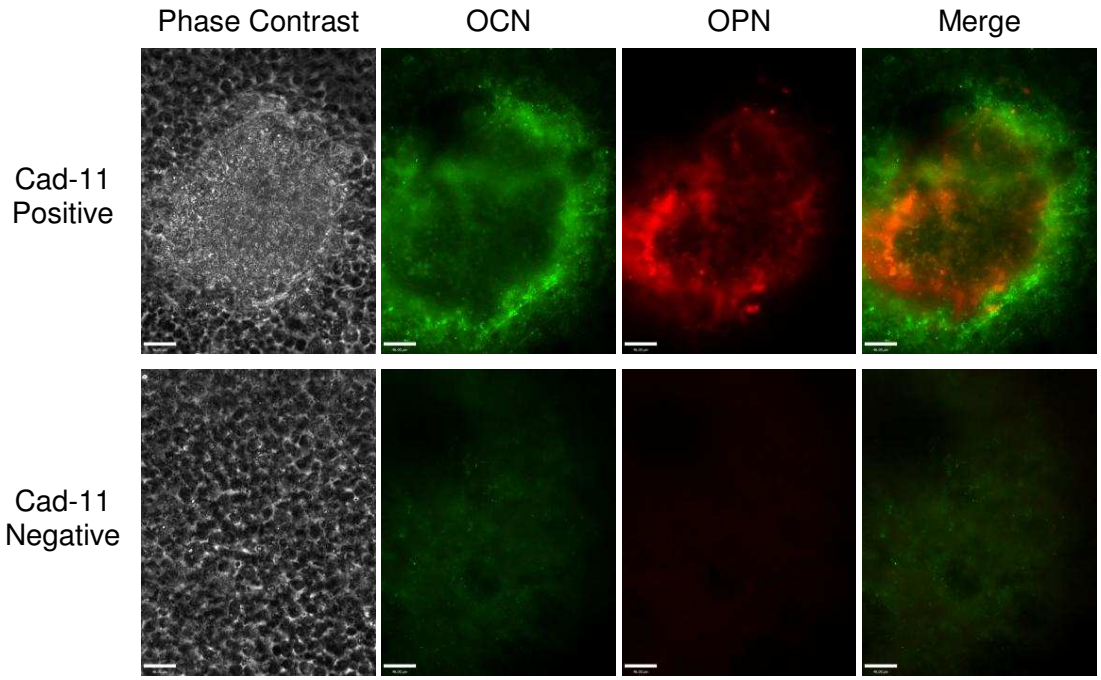

Figure 4.13: Osteocalcin and osteopontin expression in cadherin-11 sorted cells. Cells were sorted for cadherin-11 via MACS and cultured in osteogenic medium for 21 days. Representative images show immunocytochemistry of OCN (green) and OPN (red). Scale bars=46 µm.

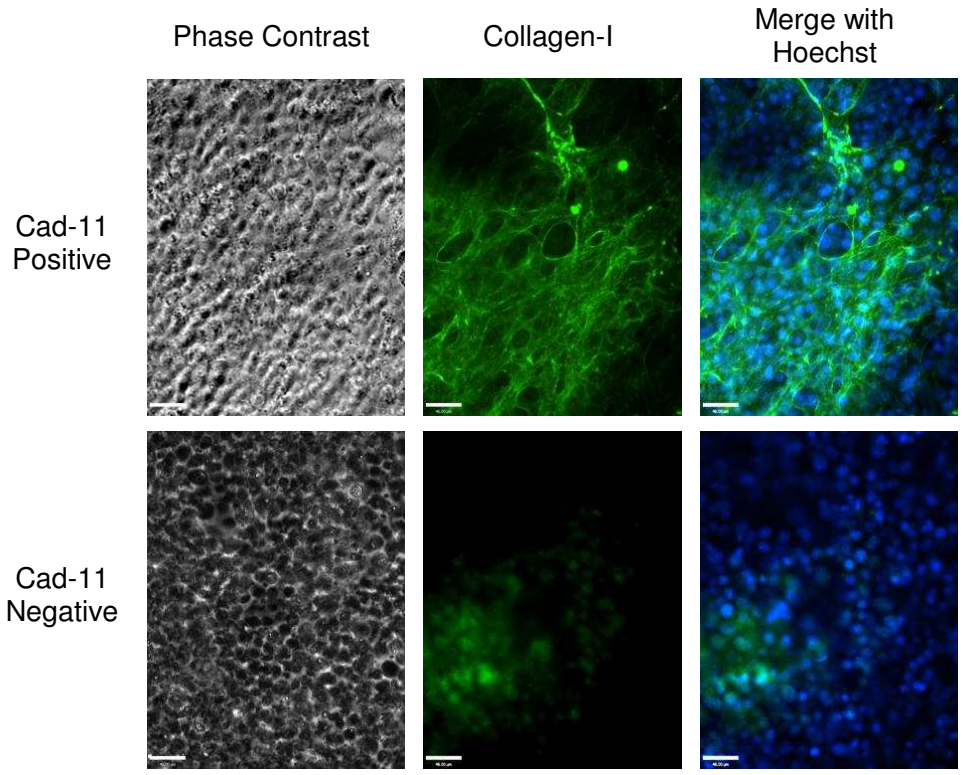

Figure 4.14: Collagen-I expression in cadherin-11 sorted cells. Cells were sorted for cad-11 via MACS and cultured in osteogenic media for 21 days. Representative images show immunocytochemistry of Col-I expression. Scale bars=46 µm.

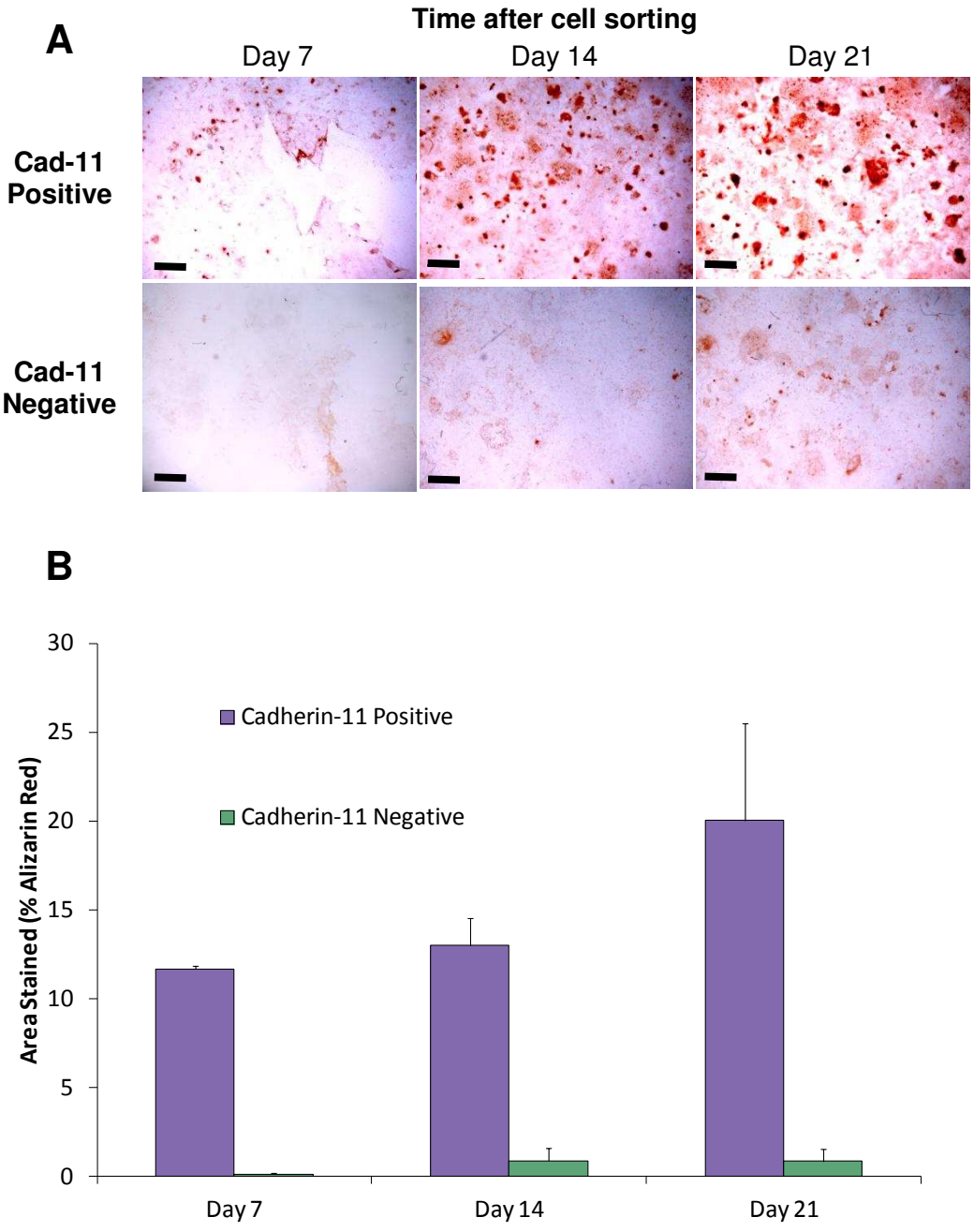

Figure 4.15: Calcium deposition by cadherin-11 sorted osteo-mESCs. (A) Representative images of alizarin red staining of casherin-11 sorted osteo-mESCs. Cells were sorted via MACS and subsequently cultured in osteogenic media for up to 21 days. Cells were fixed in 10% formalin at timepoints and stained with alizarin red S. Scale bar=2 mm (B) Images were quantified using imageJ software to show percentage area stained. Values represent mean±SD (n=6).

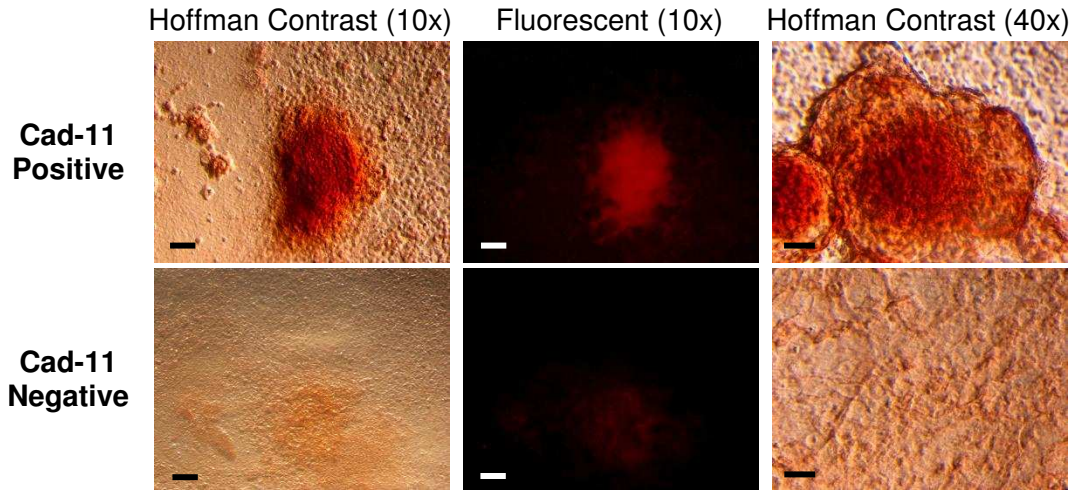

Figure 4.16: Bone nodule formation of cadherin-11 sorted osteo-mESCs. Cells were sorted via MACS and subsequently cultured in osteogenic media for up to 21 days. Cells were fixed in 10% formalin at timepoints and stained with alizarin red S. Fluorescent images of alizarin red S taken under TRITC filter. Representative images shown. Scale bar: (10x)=100 µm, (40x)=40 µm.

4.3.5.ii Response of cadherin-11 sorted osteo-mESCs to proinflammatory cytokines

The response of the cad-11 sorted osteo-mESCs to the presence of IL-1β, TNF-α and IFN-γ in the culture medium was investigated, to examine differences to previous data of non-sorted cells. Cytokines were added to the medium for 48 hours, at either 7 or 14 days after cell sorting. At these points, medium samples were collected, and cell monolayers fixed.

Figure 4.17 shows nitrite concentrations at (A) day 7 and (B) day 14. Higher production of NO occurred in response to proinflammatory cytokines, compared to control medium, in both cad-11 positive and negative cells, at both timepoints. However, on day 7 and day 14, NO was produced in significantly higher amounts by the cad-11 positive cells when compared to the cad-11 negative cells. Total concentration of nitrite in the medium was comparatively higher when cells were stimulated on day 7 than day 14.

Figure 4.18 shows PGE_2 concentrations in medium at (A) day 7 and (B) day 14. As with nitrite, significant amounts of PGE_2 were produced by both cad-11 positive and negative cells, at both timepoints, in response to the presence of proinflammatory cytokines. Conversely, to the nitrite results, PGE_2 production in cytokine medium at day 7 was higher in cad-11 negative cultures than cad-11 positive, but this was also true of cad-11 negative cells in control medium. By day 14, levels of PGE_2 produced by both positive and negative cells had fallen dramatically, compared to day 7. At day 14, production in cad-11 positive cells was higher than that of cad-11 negative.

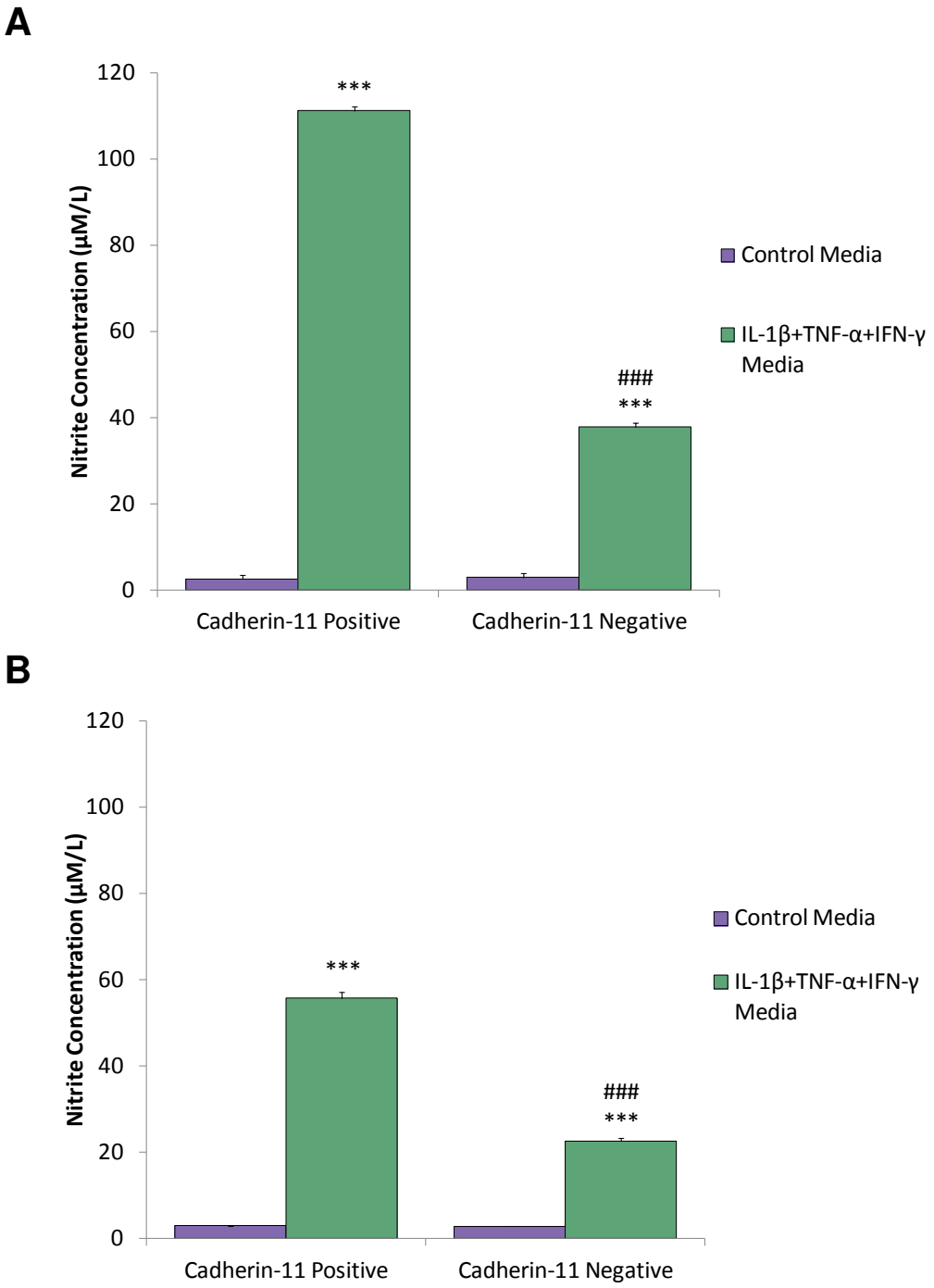

Figure 4.17: Nitric oxide response of cadherin-11 sorted osteo-mESCs to proinflammatory cytokines. Osteo-mESCs were sorted for cad-11 expression via MACS. Sorted cells were treated with IL-1β, TNF-α and IFN-γ at (A) day 7 and (B) day 14 after sorting. Nitrite concentration was measured in medium 48 hours after cytokine treatment. Values are represented as mean±SEM, n=9, ***Statistical significance of cytokine treated versus control ($p \leq 0.001$) ###Statistical significance of cad-11 negative versus cad-11 positive ($p \leq 0.001$).

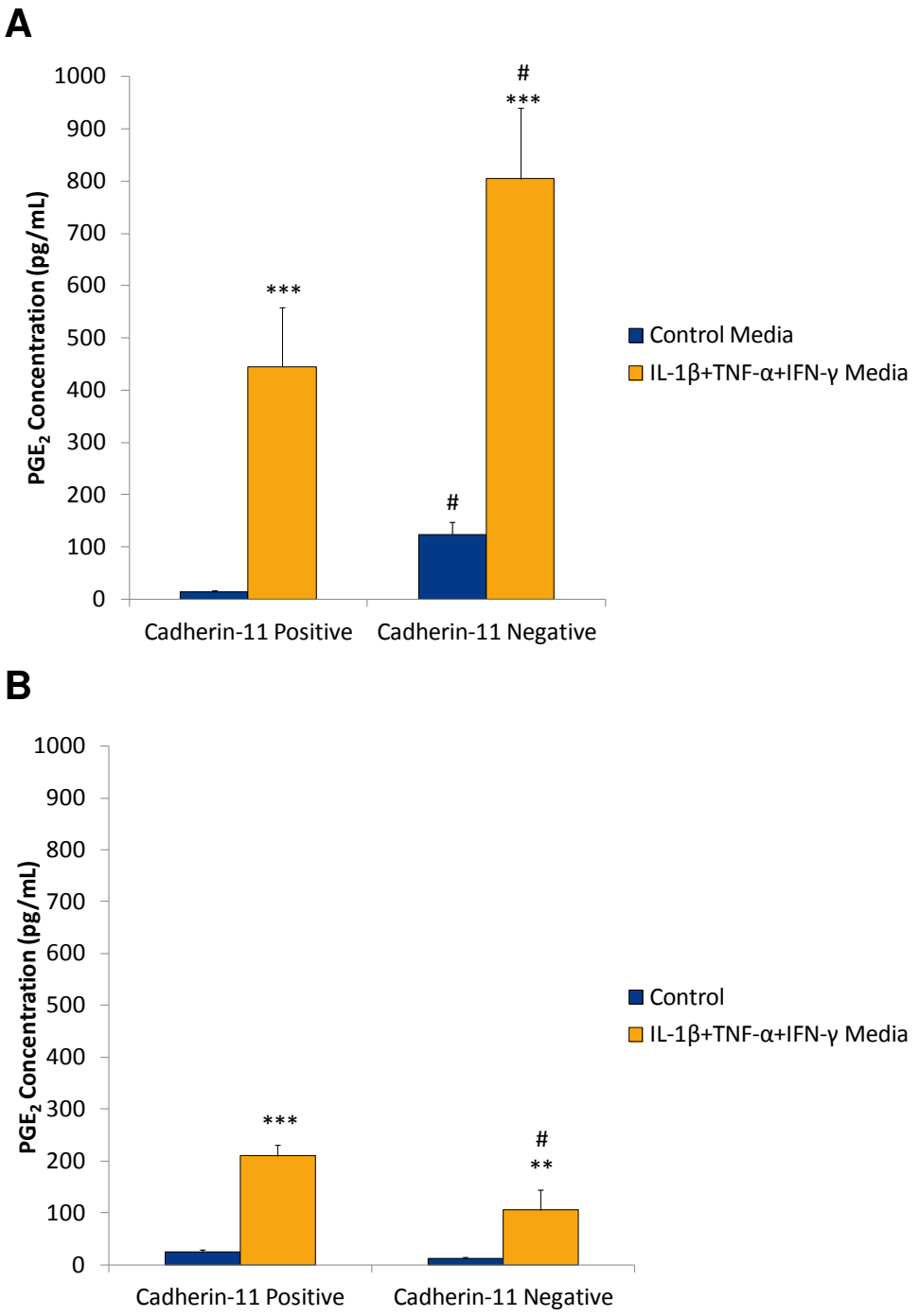

Figure 4.18: PGE_2 response of cadherin-11 sorted osteo-mESCs to proinflammatory cytokines. Osteo-mESCs were sorted for cad-11 expression via MACS. Sorted cells were treated with IL-1β, TNF-α and IFN-γ at (A) day 7 and (B) day 14 after sorting. PGE_2 concentration was measured in medium 48 hours after cytokine treatment. Values are represented as mean±SEM, n=9. Statistical significance of cytokine treated versus control ***(p≤0.001)**(p≤0.01). Statistical significance of cad-11 negative versus cad-11 positive #(p≤0.5).

Figure 4.19 shows expression of the iNOS enzyme by the sorted cells, in response to proinflammatory cytokines. Results are largely comparative with those of NO production shown in figure 4.16. Staining of iNOS was seen only in cad-11 positive cells that had been stimulated with proinflammatory cytokines, not control cultures. More staining was seen on day 7 than day 14, but both cultures showed staining reminiscent of cytokine-induced iNOS production in the primary calvarial cells (see figure 3.8). Staining in cad-11 negative cultures appeared only in cells cultured with cytokines. iNOS was staining was marked in some cells, but was not present throughout the culture. This occurred on both day 7 and day 14.

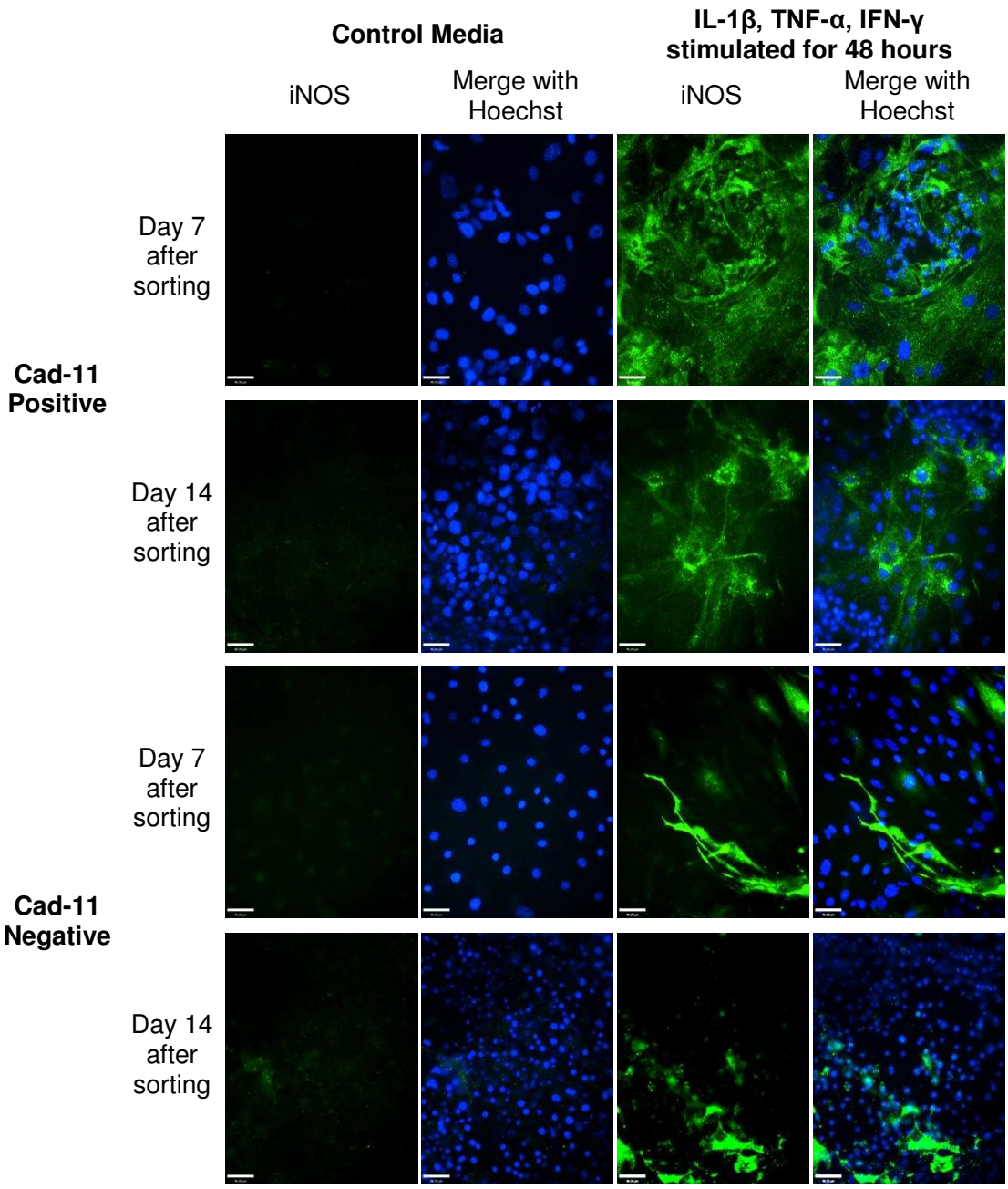

Figure 4.19: iNOS expression in cadherin-11 sorted osteo-mESCs stimulated with proinflammatory cytokines. Cells were stimulated with IL-1β, TNFα and IFN-γ for 48 hours, at day 7 or day 14 after cell sorting. iNOS expression in both proinflammatory cytokine stimulated and control cultures were assessed at this time by immunocytochemistry. Representative images shown. Scale bars=46 μm.

4.4 Discussion

The aim of this chapter was to investigate the effects that 'short bursts' or exposure periods of proinflammatory cytokine stimulation may have on the eventual osteogenic differentiation of both osteo-mESCs and primary calvarial cells. Osteogenic differentiation of the mESCs was also further investigated by cell sorting for putative osteoprogenitors with the cad-11 marker.

In vitro osteogenic differentiation of primary osteoblasts and osteogenically differentiated ESCs have both been well described, but there have been few comparative studies. In this investigation, both cell types showed expression of markers indicative of osteogenic differentiation and formed nodules comprising mineralizing matrix, as has been previously described [60, 162, 246]. Both cell types expressed proteins associated with osteoblast differentiation such as OPN, OCN and col-I, particularly in areas with cellular nodules. Nodules like these are believed to show features of embryonic woven bone in their biochemical and morphological characteristics [247, 248]. Expression of the cell-to-cell adhesion molecule cad-11, found in high levels on osteoblasts, and important in the formation of mesenchymal tissues in embryo development, was seen in both cell types [249, 250]. Morphology of the osteogenic embryonic stem cell cultures showed a more heterogeneous population than that of the primary calvarial cells and within nodules there were a larger number of nuclei.

Many authors have published work showing the similarity of ESC-derived osteogenic cells to that of osteoblasts, in terms of protein expression, gene expression, mineral deposition and in vivo models, using established osteogenic differentiation protocols [60, 61, 164, 190, 191]. The efficacy of these protocols has been called into question

and detailed comparative studies have been minimal [61, 192, 193]. In the previous chapter, distinct differences in the biochemical response of the two cell types to cytokines were demonstrated, despite the phenotypic similarities shown by expression of osteogenic markers, in this chapter. This suggests that more in depth studies showing possible differences in osteogenic differentiation of ESCs compared to primary osteoblasts are required. In 2009, Gentleman et al. used a materials science approach to compare mineralised nodules of neonatal mouse osteoblasts, bone marrow derived-MSCs and mESCs. They concluded that the bone nodules formed by mESCs showed distinct differences to those of the osteoblasts and MSCs in terms of formation time, production of the collagen-II intermediary stage and Raman spectra of mineral structure. The mESCs showed a less complex structure that showed a higher level of crystallinity [192]. Differences in the levels of gene expression between the two cell types were found in this study, with the osteo-mESCs expressing lower levels of *Runx2, Col1a1* and *Opn.* This may be because the osteo-mESCs were at a different stage of differentiation to the primary cells or be because within the cultures there is a heterogeneous population of cells that dilute the osteogenic cell population.

The cytokines used throughout these studies have well known effects as signalling molecules and mediators of the inflammatory response. The role of these cytokines in bone regeneration and fracture healing is less well established. In this study, cells were exposed to ‘short bursts’ of IL-1β, TNF-α and IFN-γ treatment. Any effects on eventual osteogenic differentiation, depending on the timepoint of cell culture were then assessed. Throughout the studies, the primary calvarial cells showed large responses to the transient exposure of proinflammatory cytokines, which had knock-on effects on the final differentiation state. When treated on day 0 or day 3, the cells tended to survive the 48 hours in the presence of the cytokines but then viability

would begin to drop. Cells did survive for the full differentiation protocol but subjective observation showed final cell number was significantly reduced. This had the effect that bone nodules did not form and matrix was not deposited. The effect was more noticeable on day 0 than day 3. IL-1β, TNF-α and IFN-γ have previously been shown to cause apoptosis of osteoblasts, particularly when applied in combination [183, 184, 251], this may have caused many of the eventual effects seen on cell differentiation. Overall, in this study, cytokine treatment of primary calvarial cells caused decreased calcium deposition, ALP activity and inhibited matrix formation (OCN, OPN and col-I). The effects of the cytokines seemed to decrease at later stages of differentiation, but could still be seen with cytokine treatment at day 14, the latest timepoint performed.

Many previous reports have focused on the effects of individual cytokines on osteoblast differentiation; but when used in combination, more similarly to the *in vivo* environment, effects are often synergistic and can be enhanced [252, 253]. Individually, in terms of osteoblast function, IL-1β and TNF-α have very similar actions: inhibition of bone nodule formation, decreased ALP activity, inhibition of OCN production and inhibition of col-I deposition, both in mouse and human osteoblasts [110, 114, 174, 254-256]. Many of these effects are partially mediated by NO, prostaglandins and the COX-2 pathways, which were shown in the previous chapter to be stimulated by the presence of proinflammatory cytokines [173, 186]. IL-1 and TNF can initially act as mitogens, causing increased proliferation of osteoblasts and increased DNA synthesis; slowing rates of differentiation [112, 173]. The effect of the treatment of osteoblasts with IFN-γ are slightly different. IFN-γ has been shown to cause inhibition of osteoblast proliferation and increased ALP activity, however OCN synthesis and col-I deposition are still inhibited [86, 121, 122]. There is also evidence that IFN-γ may inhibit some of the bone resorption caused by IL-1 [177, 257]. The results produced in this investigation substantiate previous results and show that

there is an enhanced inhibitory effect by the proinflammatory cytokines when used in combination, with the effects of IL-1 most prominent, even though the duration of cytokine treatment was short.

In this study, the mESCs showed a very different response to the presence of proinflammatory cytokines when compared to the primary calvarial cells, and the importance of timepoint of cytokine signal appeared to be of greater significance. The results also mirrored those seen in the previous chapter, with very little visible response from the osteo-mESCs when treated with cytokines in the early stages of differentiation. The largest effects in the study were seen on calcium deposition of the osteo-mESCs. Final levels of calcium deposition were not affected when cells were treated at the early timepoints of day 0 or day 3, but when treated at day 7, levels of matrix calcium appeared to increase and when treated on day 14, the inverse occurred, with levels of calcium staining falling. ALP activity was enhanced only when cytokine treatment occurred on day 3. The immunocytochemistry showed very few differences in osteogenic matrix deposition in response to cytokines, although there may have been enhanced matrix formation with treatment on day 7, which would correlate with enhanced calcium deposition. In order to show more definitively whether the cytokines were having an effect on the osteogenic differentiation of the mESCs, more in-depth studies would need to be performed looking at quantitative gene expression or protein expression, and possibly with more timepoints or longer exposure to the cytokines. Cytokine signalling had a dramatic effect on the primary calvarial cells and has been shown to have a large effect on bone development, thus, it would be reasonable to assume that there would eventually be an effect on osteogenic differentiation of mESCs. For the moment, these results show that in the early stages of differentiation, when no cell sorting has been performed, there is very

little effect of short burst proinflammatory cytokine signalling on the osteogenic differentiation of mESCs.

There has been very little study of the effects of cytokines on osteogenic differentiation of ES cells; more has been performed investigating the effect on MSCs. Proinflammatory cytokines have been shown to both inhibit and enhance osteogenic differentiation of MSCs. Overall, Runx2 and collagen expression appears to be inhibited, but ALP and mineralisation has been described as both enhanced and repressed [187, 258-260]. I believe that the discrepancy in *in vitro* results can be attributed to varying doses of the cytokine, different stage of differentiation at treatment time and varying length of cytokine exposure. These studies were performed with only one cytokine and previous studies show that the use of cytokines in combination is more realistic and may give differing results. The overwhelming conclusion is that considerably more study can be performed looking at the effect of proinflammatory cytokines on stem cell differentiation, as there is a wealth of knowledge to be gathered.

Due to how little is known about the efficacy of the current osteogenic differentiation protocols for ES cells, and the apparent heterogeneous cell populations that were seen in the early differentiation work, it was decided to perform cell sorting for a more osteogenic population within the mESCs. There is no definitive, well-characterised marker of the early osteoblast and most often, panels of markers are used to determine whether osteogenic differentiation has occurred. Osteogenesis of ES cells often requires first inducing ES-derived MSCs, sometimes using cell-sorting techniques [191, 261]. The intention in this study was to avoid the need to perform this step and harvest directly a population of osteogenic cells from the mESC cultures. MACS was chosen as the method of choice for cell sorting, due to ease of use, but this required the identification of a cell surface marker associated with

osteoblasts. Cad-11 has previously been used to purify ES cells, and appeared to be a good candidate in this case [243]. Previous immunostaining of the osteo-mESCs had shown that the protein was being expressed by day 18, but it was decided to take the timepoint of sorting back to day 16, to attempt to purify early differentiation osteogenic cells. In the cell sorting experiments a cad-11 positive ratio of about 21% was acheived, which was considerably less than had been previously described [243]. It is also worth noting that during MACS, there was a substantial reduction in the number of cells by the end of the process, and after seeding, many of the cells did not attach to the plate. This may have skewed the data somewhat, and in future, it would be advantageous to optimise this process further to attempt to achieve higher numbers of cad-11 positive cells.

The MACS data demonstrates the potential of using cad-11 to purify an osteogenic cell population from mESCs. The cad-11 positive cells differentiated to osteoblasts as intimated by cell morphology, compared to primary calvarial cells, formation of bone nodules and expression of osteogenic markers OCN, OPN and col-I. When comparing results to the previous results from unsorted osteo-mESCs, nodules were more defined, with distinct ECM deposition, particularly with col-I. The cad-11 negative population showed a more heterogeneous population of cells, and minimal bone nodule formation and staining for osteogenic ECM proteins. The success of the cad-11 sorting may indicate that if performed on human cells, a STRO-1/ALP/cad-11 sorting procedure would yield a highly purified population of osteoblasts. However, it may be that these markers target a similar population of cells and increasing the complexity of the sorting procedure would not improve the purity of cell yield. An advantage of using cad-11 as a marker, as opposed to STRO-1, is the level of characterisation the cell surface marker has received [244, 250, 262, 263].

To expand the cell-sorting investigation, it was decided to study the effect that the proinflammatory cytokines would have on the response of the cad-11 positive and negative fractions. Both cad-11 positive and negative cells responded to the presence of the cytokines by producing NO and PGE_2, similarly to the previous results of the primary calvarial cells. These results appear to be very different to the early response of the unsorted osteo-mESCs, but by day 7 after cell sorting, the cells would have been under osteogenic differentiation for 23 days, and it was shown previously that the unsorted cells begin to respond by this point. It is clear that NO response to cytokines is higher in the cad-11 positive fraction than cad-11 negative cells. However, there was no statistical difference in PGE_2 response at 7 days after sorting, between cad-11 positive and negative cells, and only a slight difference at 14 days. It is also interesting to note that at 14 days after cell sorting, levels of both NO and PGE_2 production were lower than at 7 days. This decrease in production with progressive differentiation also occurred with the primary calvarial cells (see chapter 3). Staining of iNOS expression in the cad-11 positive and negative fractions allowed better visualisation of the response of the cells to the cytokines. In positive cultures, iNOS expression appeared to occur across the entire cell population, particularly at day 7. Whereas, in negative cultures iNOS was only expressed in certain cells of the population, adding weight to the belief that this is still a highly heterogeneous environment. Many cell types, such as fibroblasts and epithelial cells [264-266], respond to the presence of these cytokines with the production of NO and PGE_2, and it may be that the cad-11 negative mESCs had differentiated to cells other than the osteoblast, despite being cultured in osteogenic medium. These results taken together support the belief that in sorting for cad-11, a population of cells that reacts more similarly to the early osteoblast has been purified. The cad-11 adhesion molecule has previously been associated with inflammation, particularly in the synovium, and may play an important part in inflammatory arthritis [267, 268]. So it

may be that in sorting for this protein, a population of cells was unearthed that was more likely to react to the presence of the cytokines, and therefore selecting a cad-11 positive population of cells is no optimal when thinking about differentiation of ES cells for therapeutic purposes.

Chapter 5:
Control of Inflammation: An *in vitro* osteoblast inflammation model and manufacture and testing of anti-inflammatory releasing scaffolds

5.1 Introduction

5.1.1 Overview

In the case of non-union fractures, large bone-defects or diseases such as RA or OP, the environment of implantation for tissue engineered therapy will likely be one of inflammation and imbalanced bone healing. There are many drugs available, of different mechanisms of action, which can be used to modulate and control this inflammatory environment. In this chapter, the effect of these anti-inflammatory drugs on a calvarial osteoblast inflammation model is studied. This is then extended into the investigation of release of anti-inflammatory drugs from porous scaffolds, and the effect of this release on the calvarial osteoblast inflammation model.

5.1.2 Bone and fracture healing

Bone is a highly vascularised and dynamic tissue that provides structural support and protection to the soft tissue of the body [66]. Under normal circumstances, bone has

significant capacity for repair and regeneration and is one of the few tissues that can heal without a scar [269]. Fundamentally, fracture healing consists of three stages: inflammation, repair and remodelling. The initial inflammatory phase plays a critical role in healing and many of the processes that occur at this stage may determine the outcome of bone repair. Fracture healing involves several cytokines and growth factors, including those previously discussed. Within 24 hours of bone injury, neutrophils and macrophages will have migrated into the wound site and levels of TNF-α, IL-1α, IL-1β and IL-6 will reach their peak [270]. These cytokines, alongside TGF-β and proteins of the BMP family, lead to recruitment of more inflammatory cells, promotion of angiogenesis and mesenchymal stem cell differentiation [271]. This acute inflammatory phase usually lasts for one week, after which inflammatory mediators return to baseline levels [272-274]. During the remodelling phase of fracture healing, the expression levels of cytokines such as IL-1, TNF-α and IL-6 rise once more, but do not reach the levels of the acute inflammatory response. Due to the complexity of events during the fracture healing process, there can occasionally be clinical instances where inflammation fails to resolve the problem, such as inflammatory diseases, severe body reactions and non-union fractures [275]. These instances provide targets for tissue engineering and regenerative medicine strategies.

5.1.3 Non-union fractures and bone defects

For a fracture to be defined as non-union there is required to have been a period of at least 9 months after injury, without fracture healing, during which time multiple therapies will have been attempted. Systemic factors that can lead to non-healing of fractures include: malnutrition and vitamin deficiency, particularly vitamin B6; diabetes

with sensory neuropathy; smoking and nicotine usage; osteoporosis, and the use of NSAIDs. Local factors within the bone such as infection, lack of vascularisation, biomechanical instability, poor bone contact (large defects or bone displacement) and complications after surgery, can also lead to non-unions [276]. The current "gold-standard" treatment for non-union fractures and defects is autologous bone grafts; however, such grafts are limited due to availability and can have disadvantages such as donor site morbidity, additional surgery and chronic pain for the patient [277].

5.1.4 Bone substitutes and inflammation

Many tissue engineering and regenerative medicine strategies have been devised for the treatment of non-union fractures and bone defects, predominantly involving the production of bone substitutes. These "bone substitutes" needs to provide biophysical stability, support cell growth and aid bone regeneration. Both biological and synthetic materials for bone repair have been reported, such as collagen [278], demineralised bone matrix (DBM) [279], porous metals [280], glass ceramics [281], calcium phosphates [282] and synthetic polymers [283]. All these materials have advantages and disadvantages. A disadvantage of any tissue-engineered therapy is inflammation, adverse tissue response and foreign body reaction, caused upon implantation and degradation [284, 285]. Adapting a bone tissue engineering scaffold to release anti-inflammatory mediators may enhance the properties of the therapy and improve success rates upon implantation [286].

5.1.5 Anti-inflammatory drug release

A critical advantage of local delivery of anti-inflammatory drugs via scaffolds, rather than systemic delivery, is the ability to bypass some of the side effects that can occur with drug treatment. Anti-inflammatory drugs that have been used in bone disease include steroids (glucocorticoids), non-steroidal anti-inflammatory drugs (NSAIDs), bisphosphonates and disease modifying anti-rheumatic drugs (DMARDs).

5.1.5.i Glucocorticoids

Glucocorticoids such as dexamethasone or prednisolone are often used to treat chronic inflammation, such as that found in RA. Glucocorticoids bind to glucocorticoid receptors (GR) that can be found on virtually all cell types. The act of binding to this receptor can inhibit proinflammatory response through synthesis of anti-inflammatory proteins and repression of the NF-κB and AP-1 proinflammatory transcription factors, amongst others [287]. Glucocorticoids have wide-ranging effects and can have many side effects, including delayed fracture healing [288]. Other side-effects due to systemic treatment include hyperglycaemia (steroid diabetes), increased skin atrophy, muscle atrophy, eye problems such as glaucoma and cataracts, effects on the cardiovascular system such as hypertension, and effects on the gastrointestinal system [289]. Due to these properties and side effects, tissue engineering studies have focused on strategies to avoid systemic treatment and enable direct delivery of the drug to the point of inflammation, via release from polymeric scaffolds [290, 291].

5.1.5.ii NSAIDs

The term NSAID encompasses a wide variety of drugs, ranging from over-the-counter medications such as ibuprofen, diclofenac and aspirin, to prescription only drugs like celecoxib. NSAIDs are frequently used as pain relievers due to good analgesic qualities and lesser side-effects than opioids. NSAIDs target the COX enzymes that lead to prostaglandin production. The majority of NSAIDs block both COX-1 and COX-2 activity, but more recently, drugs have been developed that target COX-2 specifically. There are four different mechanisms to NSAIDs inhibition of COX activity: aspirin covalently modifies a residue in the active site and irreversibly inactivates the enzyme; ibuprofen and diclofenac compete reversibly for the substrate binding site; indomethacin forms a salt bridge between a carboxylate and an arginine amino acid; and lastly some drugs can preferentially bind to COX-2 rather than COX-1 [292]. Common side-effects of taking NSAIDs include gastrointestinal ulceration and bleeding, hepato-renal dysfunction and skin reactions [293]. NSAIDs of all types have been reported to have both detrimental effects and no effect on bone healing in humans, and results from animal models are equally divided [294-297]. The COX enzymes, particularly COX-2, have been shown to play a role in bone regeneration and fracture healing, thus it would be reasonable to assume there may be some knock-on effect of COX inhibition on fracture healing [298, 299].

Release of various NSAIDs, to aid in tissue engineering strategies has been shown by a variety of groups. Diclofenac has been released from PLGA particles [300], piroxicam and diclofenac from supercritical fluid emulsion PLGA particles [301] and ibuprofen from PLGA electrospun fibres [302] and polyurethane foam[303] .

5.1.5.iii DMARDs and Cytokine-Specific Antagonists

Due to the negative effects of non-specific glucocorticoids, chronic inflammation is increasingly being treated using medications that specifically target proinflammatory cytokines. Cytokine specific inhibitors, particularly those that block TNF, are particularly effective in treating RA. These include the decoy receptor construct etanercept (Enbrel; Pfizer), which binds to free TNF, reducing the amount present in inflammation, and monoclonal antibodies such as infliximab (Remicade; Janssen Biotech) and adalimumab (Humira; Abbott) that attach to TNF-α and stop receptor binding. Other agents block interleukin activity in inflammation, such as tocilizumab (Actemra; Roche), an IL-6 receptor antibody and anakinra (Kineret; Amgen), a recombinant IL-1ra protein [145]. Side effects of some of these drugs are yet to be elucidated, but can include problems such as increased risk of serious infections, B-cell depletion and gastrointestinal problems [304]. Little work has been performed studying the release of these drugs from tissue engineering scaffolds, but one example is the release of IL1-ra from PLGA microspheres for the purpose of treating metastatic cancers [305].

5.1.6 *In vivo* and *in vitro* models for evaluating anti-inflammatory tissue engineering strategies

Current validation methods for testing the properties and effectiveness of anti-inflammatory drugs released as part of tissue engineering studies are predominantly *in vivo* animal models such as subcutaneous-suture-induced inflammation, induced mono-articular arthritis, wound models, carrageenan-oedema and air pouch models [136, 290, 291]. *In vitro* models include the use of tissue slices, including those of rat

mandible [306-308]. In this chapter, a simple *in vitro* calvarial osteoblast inflammation model is used, developed based on observations and techniques investigated in previous chapters. This model is then been used to evaluate anti-inflammatory drug release from a scaffold intended for bone repair. The *in vitro* model is not intended to replace animal models, but offers a simple initial step to gather information about levels of effectiveness of drug release from scaffolds.

5.2 Experimental Design

For more detailed methods describing primary calvarial cell extraction and culture and manufacture of PLGA/PEG scaffolds and assay protocols see Chapter 2.

5.2.1 *In vitro* calvarial osteoblast inflammation model

A simple *in vitro* calvarial osteoblast inflammation model was developed based on results from previous chapters. Primary calvarial cells were chosen due to their significant response to the presence of proinflammatory cytokines. Cells were cultured in monolayer, in well-plates for 14 days in osteogenic medium (50 mM BGP and 50 μg/mL ascorbate 2-phosphate). The timepoint of 14 days was chosen as during this time the cells will produce osteogenic matrix and a high level of response to IL-1β, TNF-α and IFN-γ can be induced, in terms of nitrite and PGE_2 (see figures 3.6 and 3.7). The concentration of cytokines added to the medium was generally 0.25 ng/mL IL-1β, 2.5 ng/mL TNF-α and 25 ng/mL IFN-γ, unless otherwise stated. Concentrations were based on the dose response work performed (figure 3.13 and 3.14). Cell response was monitored via viability measurements (MTS, LDH and live/dead™) and NO and PGE_2 production.

5.2.2 Validation of the *in vitro* calvarial osteoblast inflammation model using anti-inflammatory agents

The anti-inflammatory drugs dexamethasone, diclofenac sodium, ibuprofen, prednisolone and piroxicam, and the recombinant protein IL-1ra, were tested for their

effect on the calvarial osteoblast inflammation model. Drugs were first dissolved in DMSO to improve solubility and DMSO concentration was accounted for non-drug controls. Response in both osteogenic control medium and osteogenic medium containing IL-1β, TNF-α and IFN-γ was studied. Primary calvarial cells were seeded in 96-well plates and cultured in osteogenic medium for 14 days, before being supplemented with the anti-inflammatory mediators and proinflammatory cytokines. Cell response was investigated after 3 days of drug presence, by MTS assay, nitrite accumulation in media and PGE_2 production.

5.2.3 Long-term effect of diclofenac sodium on the *in* vitro calvarial osteoblast inflammation model

Diclofenac sodium was chosen as the anti-inflammatory drug to take into further, more in-depth studies, looking at longer-term cell viability and response, and effect on osteogenic differentiation. Diclofenac sodium was chosen for several reasons: NSAIDs show appealing properties as an anti-inflammatory in bone treatment; diclofenac has good solubility in water and stability over time; successful results in both PGE_2 and nitrite inhibition in initial testing; and finally, more available literature describing release of diclofenac via various techniques [300, 309, 310]

5.2.3.i Effect of diclofenac sodium on long-term cell viability

Primary calvarial cells were cultured in 96-well plates in osteogenic medium, for 14 days. Medium was subsequently changed to four groups: osteogenic control medium, medium with 100 μM diclofenac sodium, medium with proinflammatory cytokines and

medium with proinflammatory cytokines and 100 µM diclofenac sodium. MTS assays to assess cell viability were performed, on separate plates, on days 1, 3, 5, 7, 14 and 21.

5.2.3.ii Effect of diclofenac sodium on nitric oxide and PGE_2 production

Primary calvarial cells were plated as for the viability experiment above, and investigation performed with identical medium groups. Medium collections were carried out on days 0, 2, 6, 9, 13, 16, 20 and 27. Nitrite concentration within the medium was tested at all timepoints, via the Griess assay. Collected supernatants for days 0-6, 7-3, 14-20 and 21-27, were combined and PGE_2 concentration tested by EIA.

5.2.3.iii Effect of diclofenac sodium on osteogenic differentiation of primary calvarial cells

Primary calvarial cells were cultured in 6-well plates for 14 days in osteogenic medium, before supplementation with 100 µM diclofenac sodium and/or IL-1β, TNF-α and IFN-γ. Cells were then cultured for a further 7 days in this medium. Immunocytochemistry was performed for expression of OCN with OPN and col-I with cad-11. Antibody details found in tables 2.1 and 2.2. Hoechst 33258 nuclear counterstaining was performed and staining imaged using fluorescent microscopy.

Note: Some of the data collection in this experiment was performed with assistance from Mr Thomas Heathman, as part of an EPSRC Doctoral Training Centre in Regenerative Medicine mini-project.

5.2.4 Release of diclofenac sodium from PLGA/PEG scaffolds intended for bone repair

5.2.4.i PLGA/PEG scaffolds

PLGA/PEG scaffolds were manufactured in moulds producing cylindrical scaffolds of 12 mm length and 6 mm diameter. Scaffolds were sintered at 37°C for 3 hours before being used experimentally. SEM imaging of PLGA/PEG was kindly performed by Dr Cheryl Rahman, School of Pharmacy, University of Nottingham. In all experiments, scaffolds with different initial drug loading were produced in triplicate batches.

5.2.4.ii Measurement of drug release from PLGA/PEG scaffolds.

PLGA/PEG scaffolds were produced containing diclofenac sodium at concentrations of 1000, 800, 650, 450 and 300 µg/scaffold. Control scaffolds containing no diclofenac sodium were also manufactured. Scaffolds were placed into bijoux in 1.5 mL PBS or 1.5 mL phenol red-free αMEM, containing pen-strep. Release experiments are often performed into PBS, but as the scaffolds would later be used in a cell study in medium, phenol red-free αMEM (with 1% (*v/v*) pen-strep) was utilised. To determine drug concentrations released, medium was completely removed from the scaffolds and replaced with fresh PBS or αMEM. Concentration of diclofenac sodium within the release sample was measured by UV spectrophotometry at a wavelength of 276 nm. Concentration of drug was calculated using a standard curve. All scaffolds were produced in triplicate and each release sample was measured in triplicate. Initial

drug release was measured after 3 hours, daily for 4 days, then at certain timepoints until scaffolds had degraded or experiment end.

Note: Some of the data collection in this experiment was performed with assistance from Mr Thomas Heathman and Mr Arif Abed, as part of EPSRC Doctoral Training Centre in Regenerative Medicine mini-projects.

5.2.4.iii Use of calvarial osteoblast inflammation model to assess diclofenac sodium release from PLGA/PEG scaffolds

To assess success of release of diclofenac sodium, the *in vitro* osteoblast inflammation model was utilised. Plates (24-well) were seeded with primary calvarial cells and cultured in osteogenic medium for 14 days. After this time, medium was removed and scaffolds placed into transwells above the cell monolayer (see figure 5.1). Scaffolds with initial loading 0, 300, 650 and 1000 µg of diclofenac sodium were studied. Medium (2 mL to cover scaffold) was then replaced with either control osteogenic medium or osteogenic medium containing proinflammatory cytokines. Initial cytokine concentration was 1 ng/mL IL-1β, 10 ng/mL TNF-α and 100 ng/mL IFN-γ. All medium was collected after 24 hours (day 1) and replaced with control or cytokine medium containing 0.25 ng/mL IL-1β, 2.5 ng/mL TNF-α and 25 ng/mL IFN-γ. This medium was collected after 24 hours on scaffold and cells (day 2) and replaced with medium containing 0.0625 ng/mL IL-1β, 0.65 ng/mL TNF-α and 6.25 ng/mL IFN-γ. This medium was left for a further 5 days (day 7) until final collection. Experiments ended on day 7 and a Live/Dead assay performed on the cell monolayers.

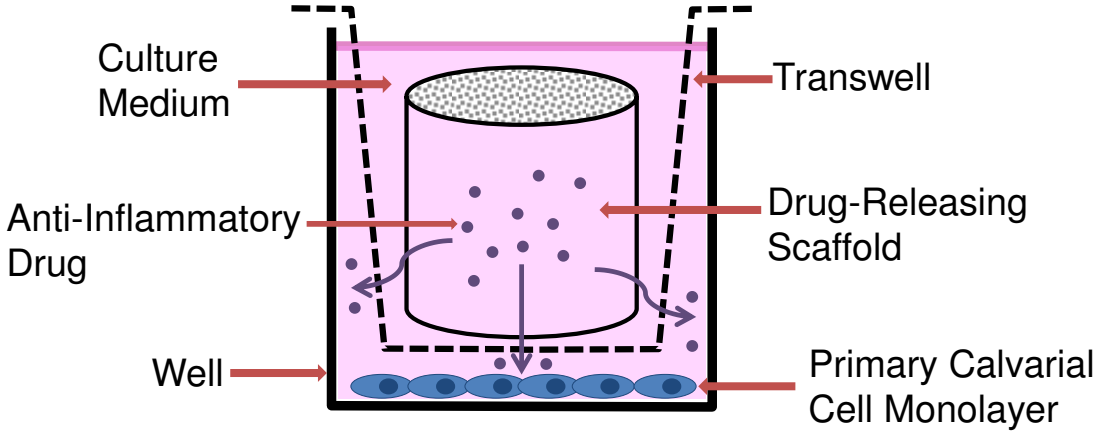

Figure 5.1: Diclofenac sodium release from PLGA/PEG scaffolds experimental set-up. Scaffolds were placed into permeable transwells within a 24-well plate seeded with primary calvarial cells in osteogenic medium. Anti-inflammatory drug was then released into the culture medium.

Media samples from day 1, day 2 and day 7 were tested for nitrite, PGE_2 and LDH concentration, to determine effectiveness of released drug. These initial studies concentrate on the first 7 days of release, corresponding to the occurrence of acute inflammation upon scaffold implantation. Concentration of released diclofenac sodium was determined using collected medium samples and UV spectrophotometry.

Note: Some of the data collection in this experiment was performed with assistance from Miss Emily Britchford, as part of an EPSRC Doctoral Training Centre in Regenerative Medicine mini-project.

5.3 Results

5.3.1 Validation of calvarial osteoblast inflammation model using anti-inflammatory agents

Basic validation of the primary calvarial cell inflammation model was carried out using a range of anti-inflammatory mediators. The effect of dexamethasone, diclofenac sodium and IL-1ra on cell viability was investigated, in medium with and without proinflammatory cytokines, over a range of drug concentrations. The ability of the drugs at different concentrations to inhibit cytokine-induced production of NO and PGE_2 was also assessed.

5.3.1.i Dexamethasone

Validation results for the corticosteroid dexamethasone can be seen in figure 5.2. For cell viability (figure 5.2A), all values have been corrected to percentage of osteogenic control. The proinflammatory cytokine control shows a reduced cell viability of approximately 30%, and had the most noteworthy effect across all groups. At concentrations of over 500 µM, dexamethasone had a significant negative effect on cell viability, regardless of the presence of proinflammatory cytokines. At concentrations of 500 µM and under, dexamethasone significantly prevented the fall in viability caused by the effects of the cytokines. The ability of dexamethasone to inhibit NO production induced by IL-1β, TNF-α and IFN-γ can be seen in figure 5.1B. At all concentrations of dexamethasone, from 100 µM upwards, the levels of proinflammatory cytokine-induced nitrite were significantly reduced, with the most

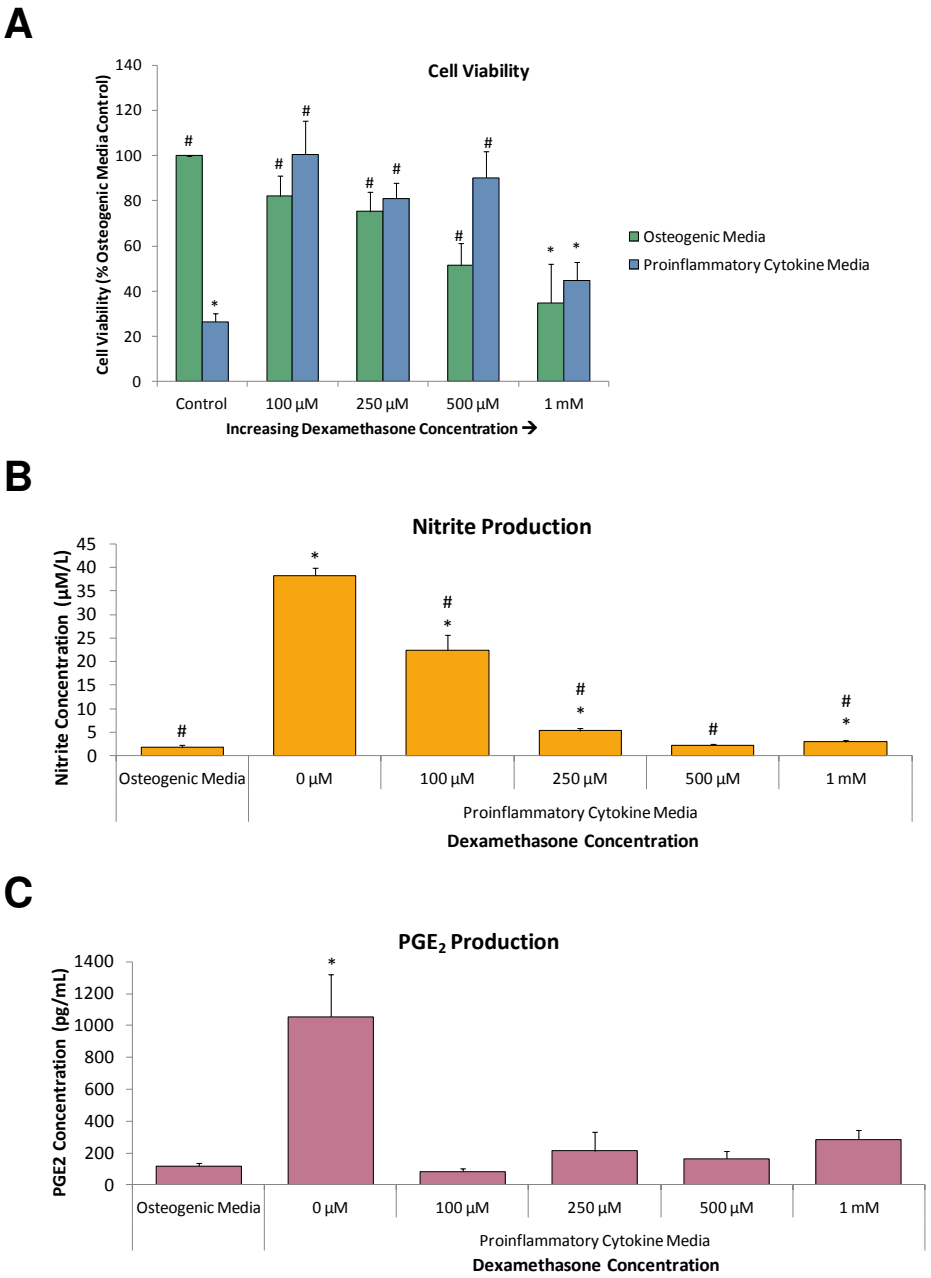

Figure 5.2: Anti-inflammatory effect of dexamethasone. Primary calvarial cells were cultured for 10 days in osteogenic media and subsequently supplemented with dexamethasone and proinflammatory cytokines. (A) Cell viability, determined by MTS assay, after 3 days in either basal osteogenic or proinflammatory cytokine media, with dexamethasone at increasing concentrations. Values are represented as mean±SD, n=6. (B) Nitrite concentration in media after 3 days proinflammatory cytokine and dexamethasone treatment. Values are represented as mean±SD, n=6. (C) PGE_2 concentration in media after 3 days proinflammatory cytokine and dexamethasone treatment. Values are represented as mean±SD, n=4. For all results: #Statistical significance vs. proinflammatory cytokine control (0 µM dexamethasone) ($p \leq 0.05$), *Statistical significance vs. osteogenic media ($p \leq 0.05$).

notable effect at 500 µM. Dexamethasone inhibition of cytokine-induced PGE_2 production (figure 5.2C) also occurred across all concentrations.

5.3.1.ii Diclofenac Sodium

The results of the effect of diclofenac sodium on the inflammation model can be seen in figure 5.3. At concentrations of 500 µM and over, diclofenac had an inhibitory effect on cell viability, with a viability of 30% at 1 mM drug concentration. At a concentration of 250 µM, diclofenac prevented the drop in cell viability caused by the cytokine medium, but at 100 µM, the concentration of drug was not sufficiently high enough to prevent the actions of the cytokines. Proinflammatory cytokine induced nitrite (figure 5.3B) was inhibited at concentrations of 250 µM and upwards, although at 1 mM this may be related to the drop in cell viability. PGE_2 production was inhibited by the diclofenac sodium at all concentrations (figure 5.3C).

5.3.1.iii IL-1ra

The presence of IL-1ra in osteogenic medium had no negative effect on cell viability at any concentration (figure 5.4A). At the highest concentration of 1000 ng/mL, IL-1ra prevented the fall in cell viability caused by the actions of the cytokine medium. At 500 ng/mL there was some preventative effect but not statistically significant. Below 500 ng/mL, the presence of IL-1ra did not significantly affect viability. Likewise, IL-1ra only inhibited nitrite production at concentrations of 500 ng/mL and above (figure 5.4B), although PGE_2 was inhibited at concentrations of 100 ng/mL upwards (figure 5.4C).

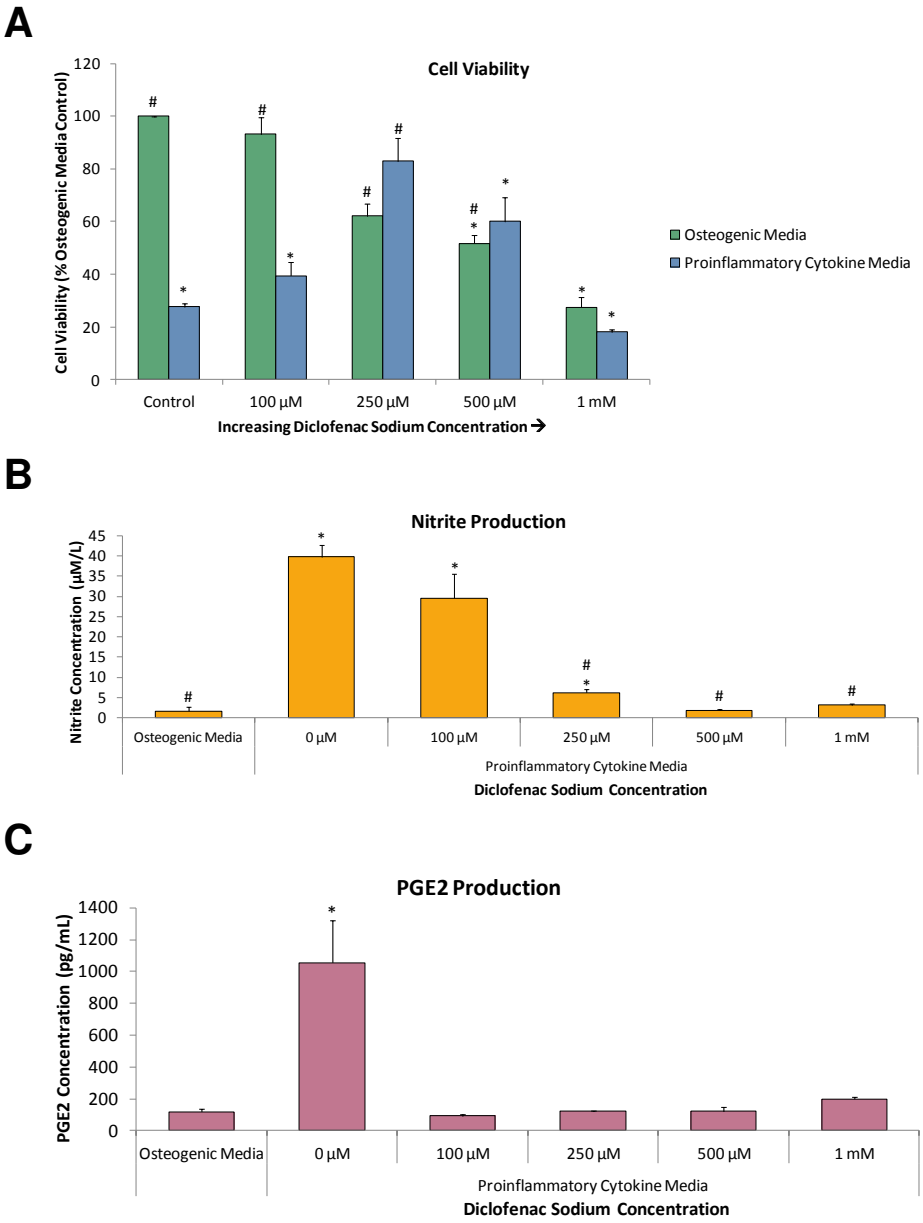

Figure 5.3: Anti-inflammatory effect of diclofenac sodium. Primary calvarial cells were cultured for 10 days in osteogenic media and subsequently supplemented with diclofenac sodium and proinflammatory cytokines. (A) Cell viability, determined by MTS assay, after 3 days in either basal osteogenic or proinflammatory cytokine media, with diclofenac sodium at increasing concentrations. Values are represented as mean±SD, n=6. (B) Nitrite concentration in media after 3 days proinflammatory cytokine and diclofenac sodium treatment. Values are represented as mean±SD, n=6. (C) PGE_2 concentration in media after 3 days proinflammatory cytokine and diclofenac sodium treatment. Values are represented as mean±SD, n=4. For all results: #Statistical significance vs. proinflammatory cytokine control (0 µM diclofenac sodium) ($p \leq 0.05$), *Statistical significance vs. osteogenic media ($p \leq 0.05$).

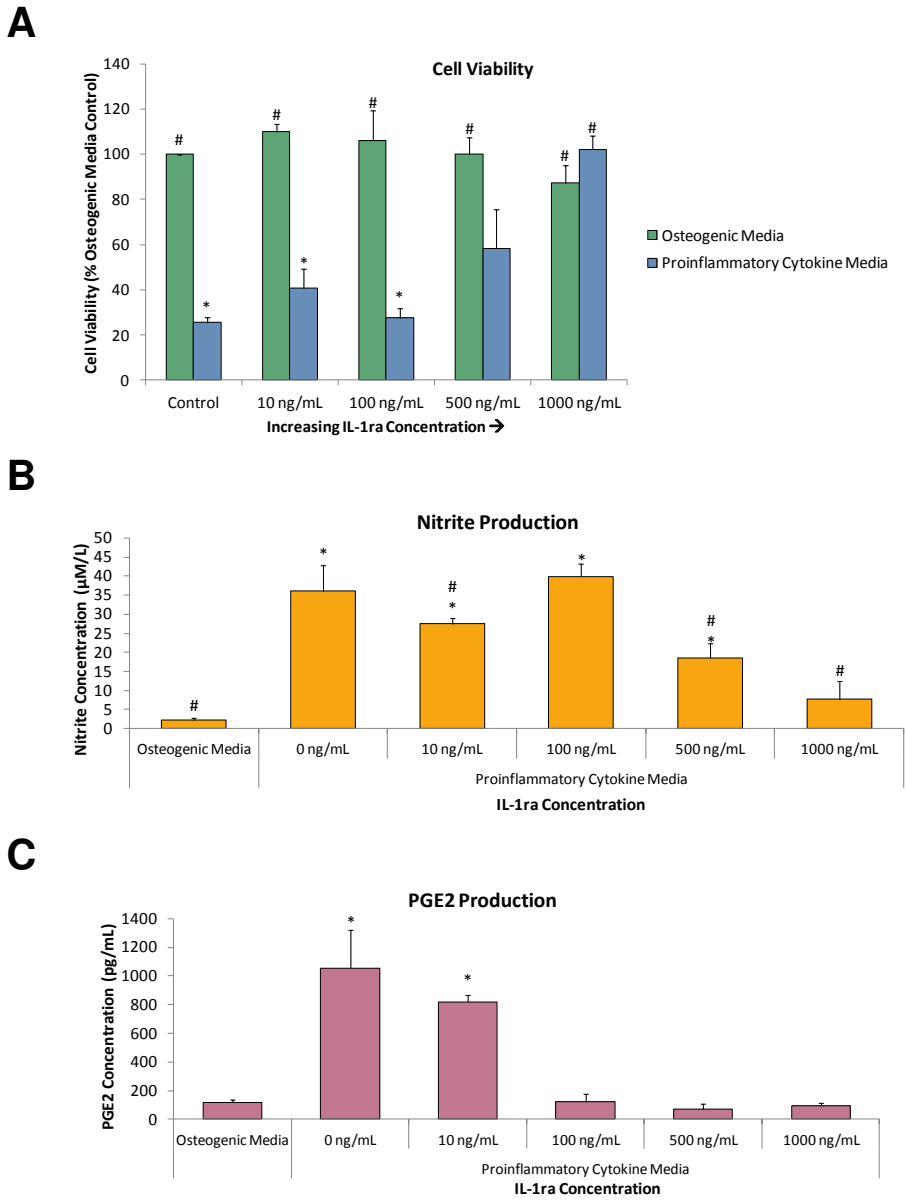

Figure 5.4: Anti-inflammatory effect of IL-1ra. Primary calvarial cells were cultured for 10 days in osteogenic media and subsequently supplemented with IL-1ra and proinflammatory cytokines. (A) Cell viability, determined by MTS assay, after 3 days in either basal osteogenic or proinflammatory cytokine media, with IL-1ra at increasing concentrations. Values are represented as mean±SD, n=6. (B) Nitrite concentration in media after 3 days proinflammatory cytokine and IL-ra treatment. Values are represented as mean±SD, n=6. (C) PGE_2 concentration in media after 3 days proinflammatory cytokine and IL-1ra treatment. Values are represented as mean±SD, n=4. For all results: #Statistical significance vs. proinflammatory cytokine control (0 ng/mL IL-1ra) ($p \leq 0.05$), *Statistical significance vs. osteogenic media ($p \leq 0.05$).

Results for prednisolone, ibuprofen and piroxicam can be found in Appendix VII, and follow the same trends as the drugs described above. Taken together, all results validate that the simple bone inflammation model can give valuable information on the effects of anti-inflammatory drugs.

5.3.2 Long-term effect of diclofenac sodium on the *in vitro* osteoblast inflammation model

Diclofenac sodium was chosen as the anti-inflammatory drug to take forward into more in-depth studies of the bone inflammation model, for reason discussed in the experimental design section. Predominantly, diclofenac was chosen due to good performance in initial testing and desirable solubility properties, allowing the removal of DMSO from drug preparation steps. Duration of studies was increased, looking at cell viability and inhibition of nitrite and PGE_2 production. The effect that the presence of diclofenac sodium had on osteogenic matrix deposition was also studied.

5.3.2.i Effect of diclofenac sodium on 21-day cell viability

Primary calvarial cells were cultured in osteogenic medium for 14 days before cytokines and diclofenac sodium added. Cell viability was monitored for the following 21 days and values converted to a proportion of the osteogenic control reading for that day (figure 5.5). IL-1β, TNF-α and IFN-γ caused the most noteworthy drop in viability over the 21 day period, to 32%. The presence of 100 μM diclofenac sodium caused a slight drop in viability over the 21 days, showing a slight toxicity to the cells.

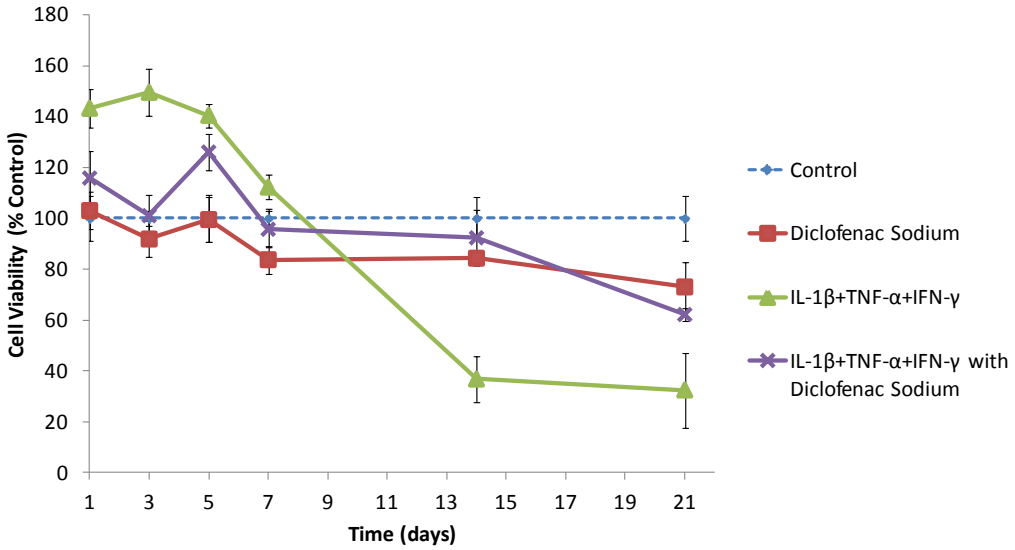

Figure 5.5: Long-term effect of diclofenac sodium on viability of primary calvarial cells in proinflammatory cytokine media. Primary calvarial cells were cultured in osteogenic media for 14 days before investigation began. Proinflammatory cytokines were applied throughout the 21 day period. Diclofenac sodium was added to media at a concentration of 100 µM. Cell viability at timepoints was measured by MTS assay and absorbance values converted to percentage control. Values are represented as mean±SD, n=6. Experiment was repeated in triplicate (representative experiment shown).

With diclofenac sodium present alongside the cytokines, the fall in viability was less severe than cytokines alone, with a viability of 92% at day 14 and 62% at day 21.

5.3.2.ii Effect of diclofenac sodium on proinflammatory cytokine-induced nitric oxide and PGE_2 production

The long-term effect of diclofenac sodium on NO (as nitrite) and PGE_2 production in the bone inflammation model was investigated. Figure 5.6 and 5.7 show cumulative production of nitrite and PGE_2 respectively, by the primary calvarial cells over a 27-day period. Across all timepoints, the presence of IL-1β, TNF-α and IFN-γ, caused significantly increased nitrite and PGE_2 production, compared to control osteogenic medium and 100 μM diclofenac sodium alone. Nitrite accumulation in groups treated with both cytokines and diclofenac sodium was significantly lower across all timepoints than those with cytokines alone. However, nitrite levels in this group remained significantly higher than the controls. Diclofenac sodium was more effective in inhibiting PGE_2 production; accumulated PGE_2 concentration in the group treated with cytokines and diclofenac was very similar to controls across all timepoints. Diclofenac sodium was shown to maintain effectiveness as an anti-inflammatory in this model across a 27-day time period.

5.3.2.iii Effect of diclofenac sodium on osteogenic differentiation of primary calvarial osteoblasts

Figure 5.8 shows primary calvarial cell staining for OPN and OCN, and the effect of 7 days treatment of 100 μM diclofenac sodium and/or IL-1β, TNF-α and IFN-γ. Nuclear staining with Hoechst has also been performed to show cell distribution/localisation.

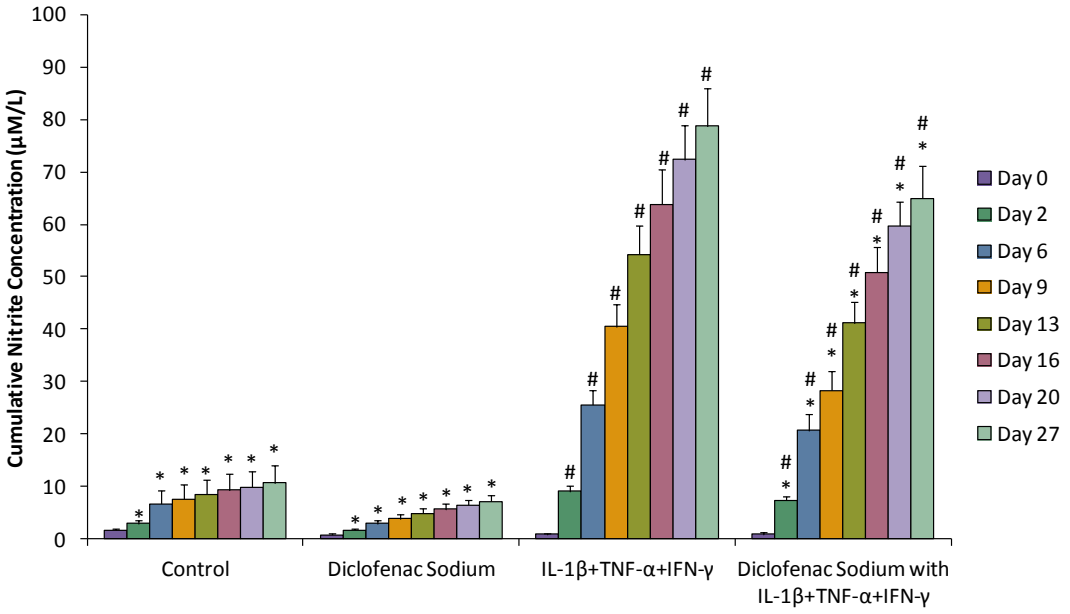

Figure 5.6: Long-term effect of diclofenac sodium on cumulative nitrite production by primary calvarial cells in proinflammatory cytokine media. Primary calvarial cells were grown in osteogenic media for 14 days before investigation began. Proinflammatory cytokines were applied throughout the 27 day period. Diclofenac sodium was added to media at a concentration of 100 µM. Nitrite concentration in culture medium at timepoints was measured by Griess assay. Values are represented as cumulative mean±cumulative SD, n=6. Experiment was repeated in triplicate (representative experiment shown). *Statistical significance vs. IL-β+TNF-α+IFN-γ ($p \leq 0.01$), #Statistical significance vs. control ($p \leq 0.01$).

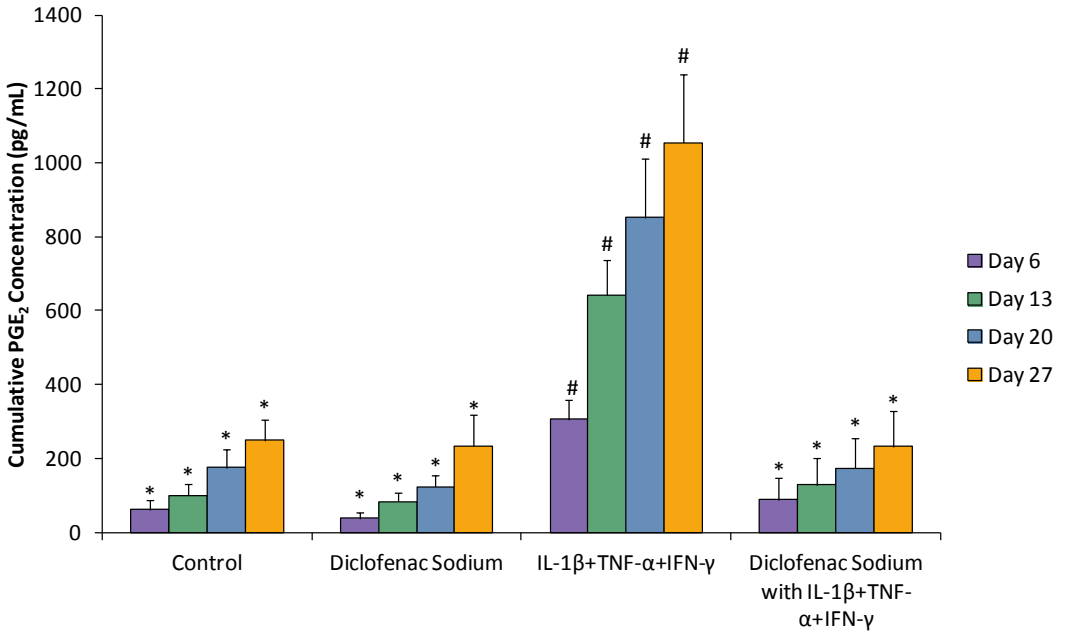

Figure 5.7: Long-term effect of diclofenac sodium on cumulative cytokine-induced PGE_2 production by primary calvarial cells. Primary calvarial cells were grown in osteogenic media for 14 days before investigation began. Proinflammatory cytokines were applied throughout the 27 day period. Diclofenac sodium was added to media at a concentration of 100 µM. Combined PGE_2 concentration in media at timepoints was measured by enzyme-linked immunoassay. Values are represented as cumulative mean±cumulative SD, n=6. Experiment was repeated in triplicate (representative experiment shown). *Statistical significance vs. IL-β+TNF-α+IFN-γ ($p \leq 0.01$), #Statistical significance vs. control ($p \leq 0.01$).

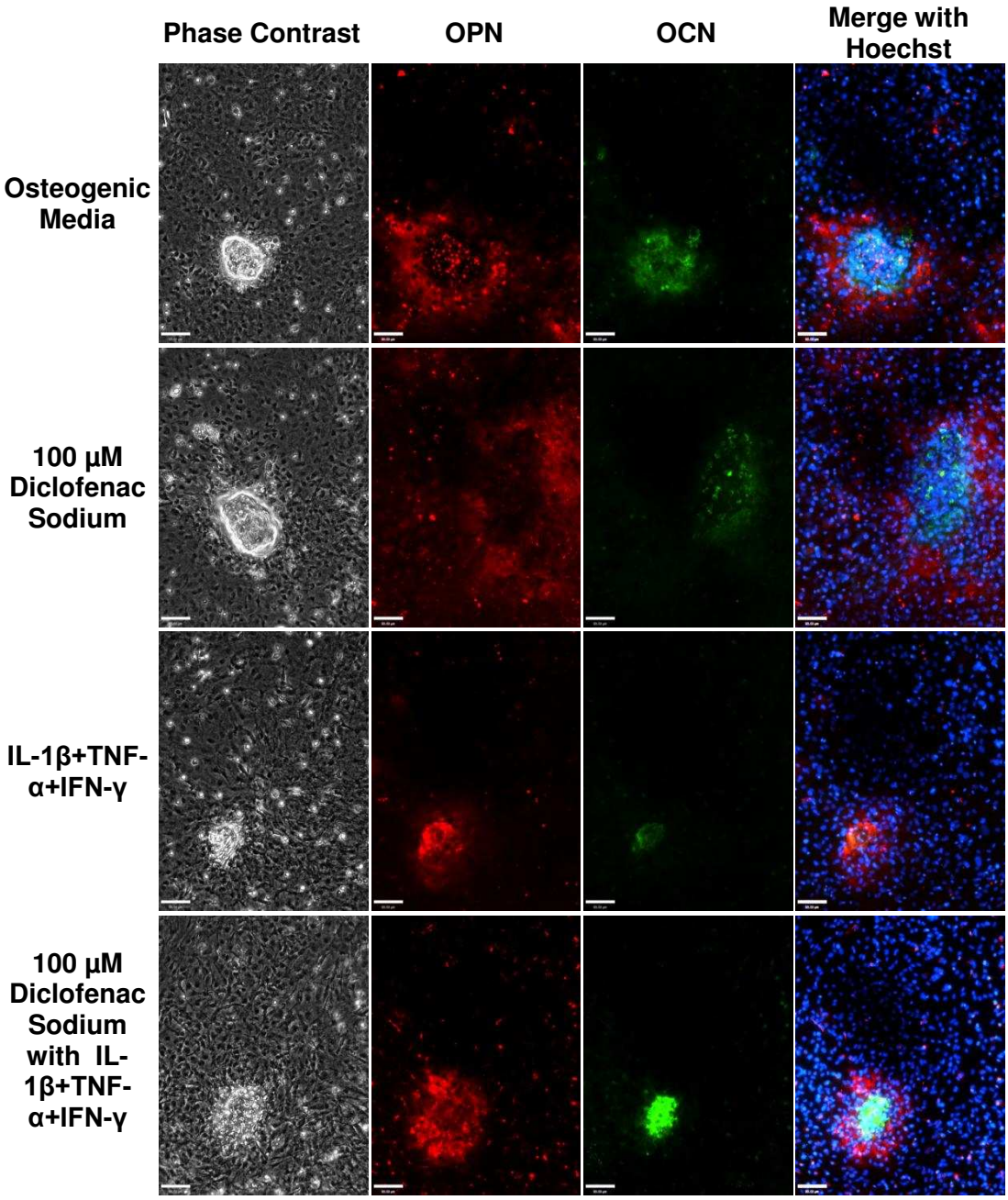

Figure 5.8: Expression of osteopontin and osteocalcin in primary calvarial cells stimulated with proinflammatory cytokines and diclofenac sodium. Primary calvarial cells were cultured in osteogenic media for 14 days, then for 7 days in osteogenic media containing 100 µM diclofenac sodium and/or IL-1β, TNF-α and IFN-γ. Representative images of osteopontin (red) and osteocalcin (green) expression assessed by immunocytochemistry on day 21. Scale bar=90 µm.

Compared to osteogenic medium alone, treatment with proinflammatory cytokines produced smaller and less abundant nodules with dense OPN staining and little OCN. Hoechst staining showed that there were fewer cells within nodules relative to osteogenic controls. In diclofenac sodium treated cells, OPN staining was more dispersed and OCN staining concentrated within the nodules. In proinflammatory cytokine with diclofenac groups, the nodules were of a similar size and cell density to the controls.

Figure 5.9 shows col-I and cad-11 staining of primary calvarial cells after exposure to proinflammatory cytokines and diclofenac sodium. In all groups, marked col-I staining was seen in cad-11 positive regions. Once again, the cytokine treated group produced smaller bone nodules with more disperse staining for col-I than osteogenic control groups. Cells treated with diclofenac sodium showed col-I and cad-11 staining that was similar to that of the osteogenic control. When diclofenac sodium was present alongside the cytokines, some effects of the proinflammatory cytokines were apparent, with col-I staining similar to that of cytokine treatment alone with col-I less concentrated around nodules than the control. However, cad-11 appeared to have a stronger staining than that of the cytokine only group, more similar to the staining of the control medium group.

5.3.3 Diclofenac sodium release from PLGA/PEG scaffolds

The effect of releasing diclofenac sodium from PLGA/PEG scaffolds was investigated. Release rates were monitored and PLGA/PEG scaffolds releasing diclofenac sodium were tested using the *in vitro* osteoblast inflammation model.

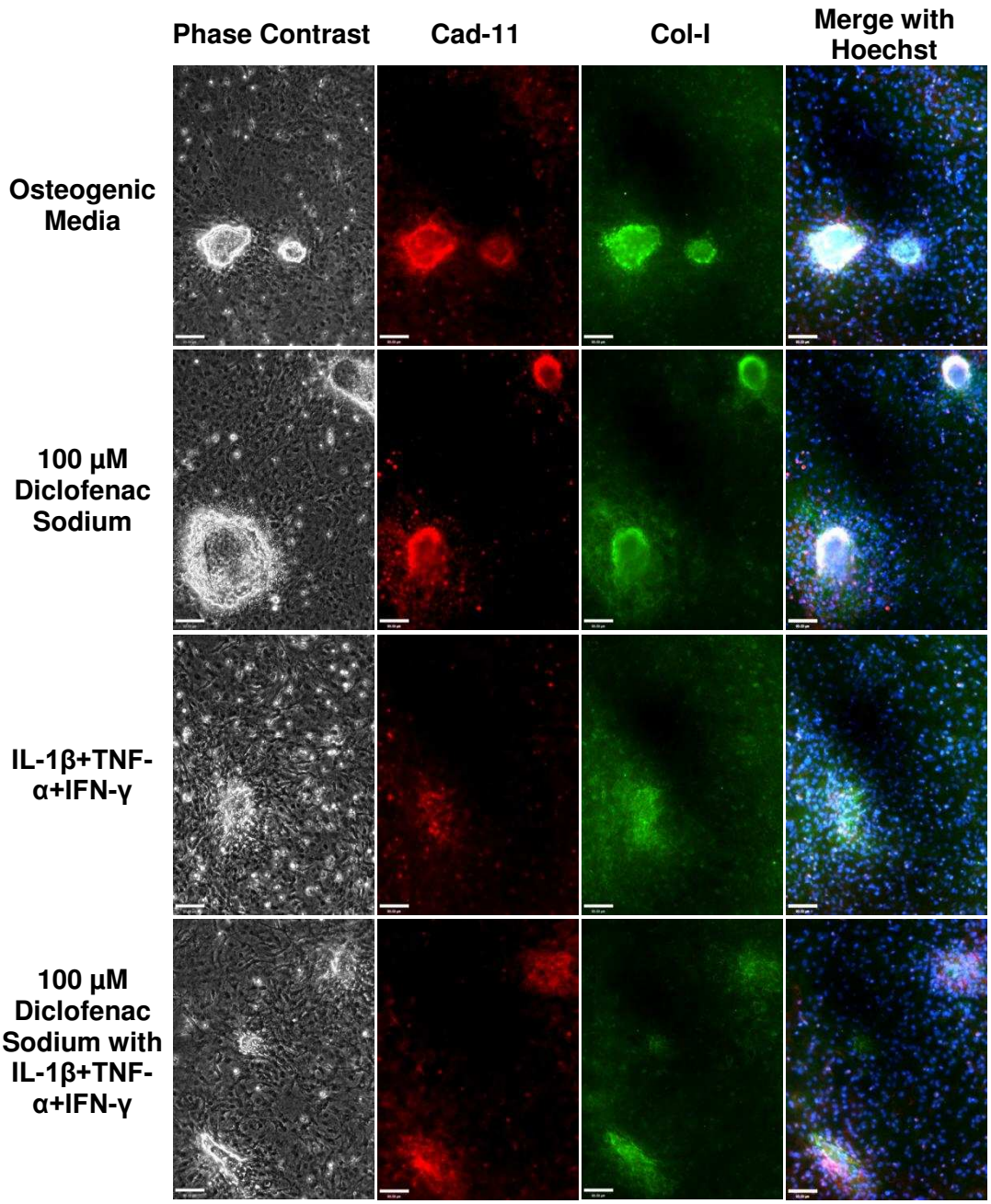

Figure 5.9: Expression of cadherin-11 and collagen-1 in primary calvarial cells stimulated with proinflammatory cytokines and diclofenac sodium. Primary calvarial cells were cultured in osteogenic media for 14 days, then for 7 days in osteogenic media containing 100 µM diclofenac sodium and/or IL-1β, TNF-α and IFN-γ. Representative images of cadherin-11 (red) and collagen-I (green) expression assessed by immunocytochemistry on day 21. Scale bar=90 µm.

5.3.3.i PLGA/PEG scaffolds.

Figure 5.10 shows the formed PLGA/PEG scaffolds and the microstructure of the scaffolds. PLGA/PEG microparticles were mixed with PBS/drug solution to form a paste and were packed into PTFE moulds, producing cylindrical scaffolds of 12 mm length and 6 mm diameter after sintering. The scaffolds have a porous microstructure (figure 5.10B), with pores formed by particles bridging when sintered. The formed scaffolds showed swelling after being placed in PBS or medium to release and after 5 weeks showed little degradation (figure 5.10B). Eventual degradation took about 9 weeks.

5.3.3.ii *In vitro* release of diclofenac sodium from PLGA/PEG scaffolds.

5.3.3.ii.a Effect of initial loading mass of drug

The release of diclofenac sodium from the PLGA/PEG scaffolds over time was assessed by UV spectrophotometry and converted to mass via a standard curve. The cumulative mass release of the scaffolds can be seen in figure 5.11, and this mass converted to percentage of initial loading in figure 5.12. These profiles show release into phenol-red free αMEM. Scaffolds were loaded with concentrations of diclofenac ranging from 300 µg/scaffold to 1000 µg/scaffold, to determine effect of initial drug loading on release profile. All scaffolds showed a similar release profile, regardless of initial loading. Scaffolds showed an initial drug burst release of 55-62%. This burst is due to immediate release of the drug adsorbed to the scaffold surface, when the scaffold is placed in liquid after sintering. After this burst, drug release slows, with approximately another 20% release after day 1 and another 3% on day 2. After day 4,

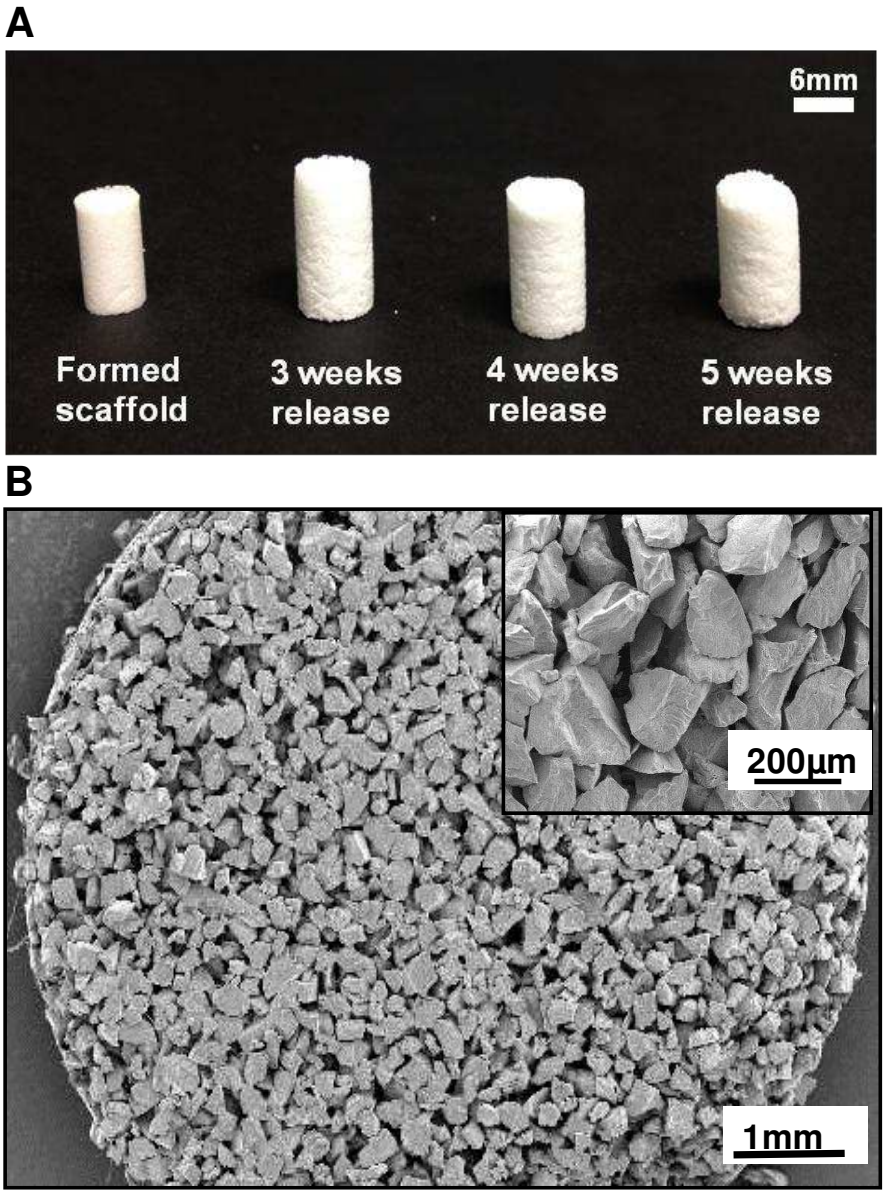

Figure 5.10: PLGA/PEG scaffolds. Temperature-sensitive and biodegradable poly(lactic-co-glycolic acid) (PLGA) and poly(ethylene glycol) (PEG) microparticle scaffold. (A) Formed and sintered scaffolds showing swelling and degradation over a 5 week period (B) SEM image showing the porosity of the scaffold and microstructure of the scaffold (inset, image courtesy of Cheryl Rahman).

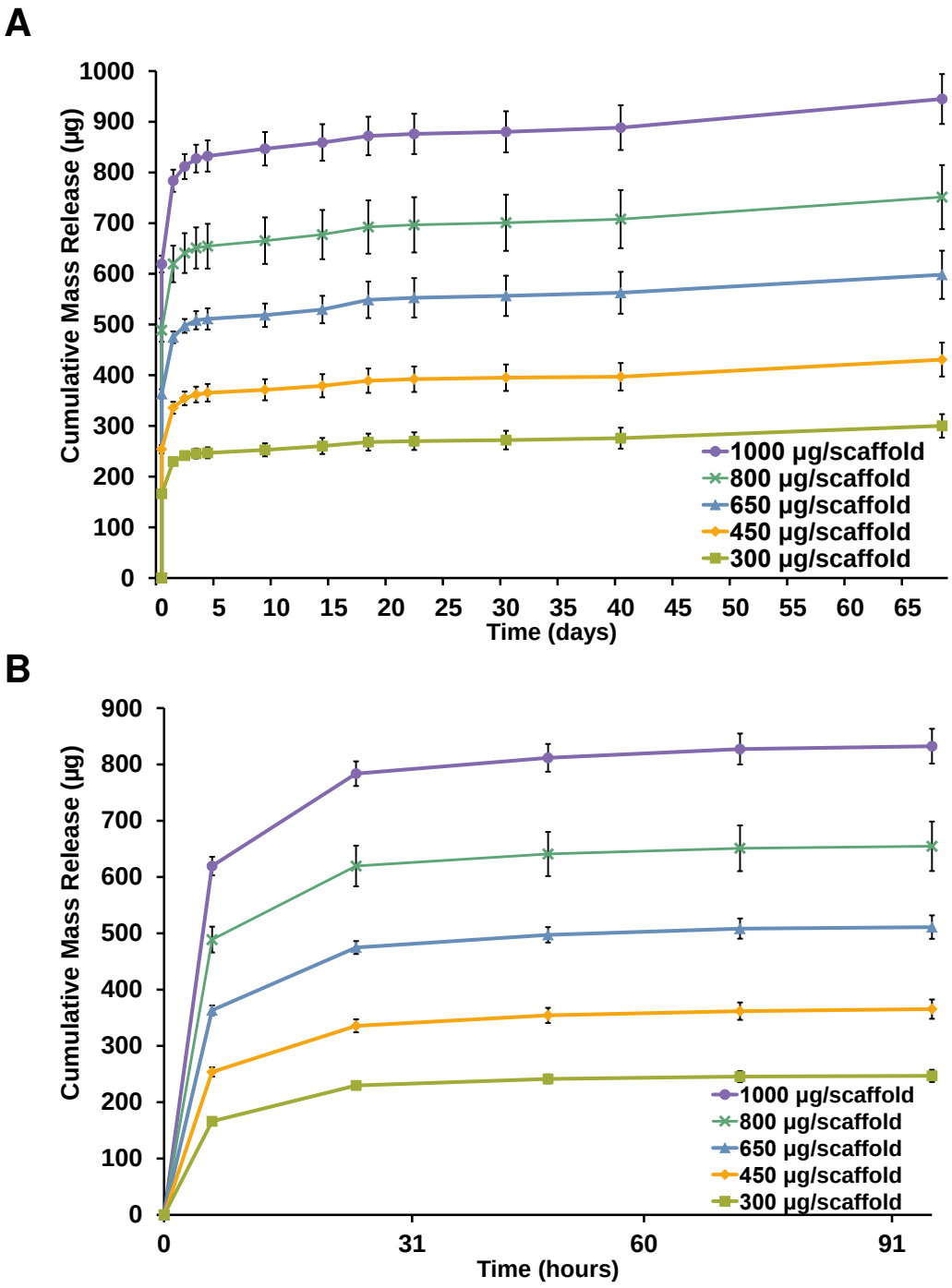

Figure 5.11: Cumulative mass release of diclofenac sodium from PLGA/PEG scaffolds. PLGA/PEG scaffolds were loaded with various initial concentrations of diclofenac sodium. (A) Mass of drug released over the full 68 day time course. (B) Mass released over first 4 days. Mass of drug released at each timepoint was assessed by UV spectrophotometry and expressed cumulatively over time. Values represented by mean of triplicate scaffold release, each measured in triplicate (n=9). Error represented by cumulative standard deviation.

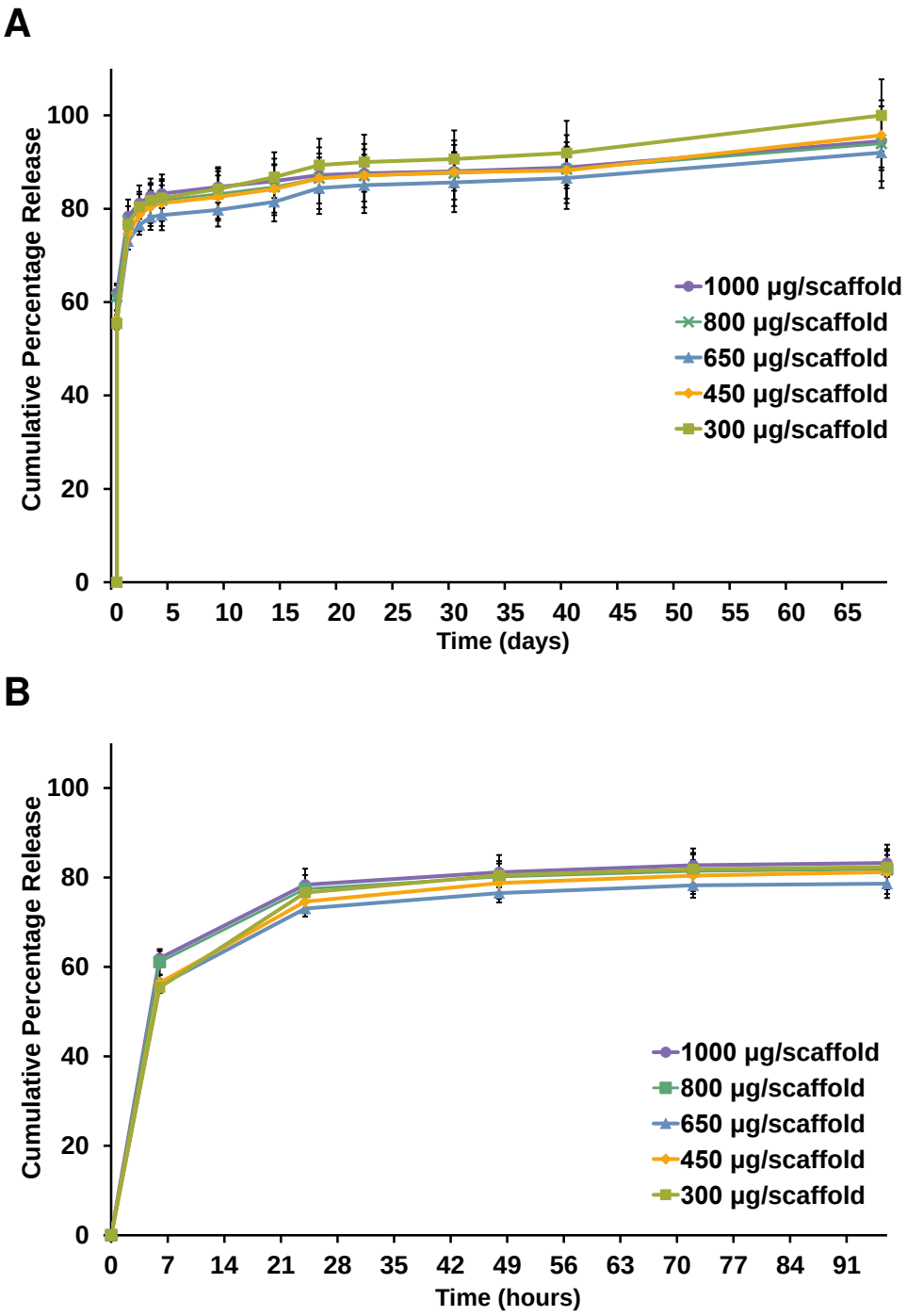

Figure 5.12: Cumulative percentage release of diclofenac sodium from PLGA/PEG scaffolds. PLGA/PEG scaffolds were loaded with various initial concentrations of diclofenac sodium. (A) Percentage of drug released over 68 day time course. (B) Percentage of drug released over first 4 days. Mass of drug released at each timepoint was assessed by UV spectrophotometry and expressed as a percentage of initial loading. Values represented by mean of triplicate scaffold release, each measured in triplicate (n=9). Error represented by cumulative standard deviation.

release reached a steady state of around 0.2% per day. From day 42, this rate increased slightly to about 0.3% per day as the scaffolds degraded. By day 68, the scaffolds had degraded and total percentage release for each scaffold was nearing 100%, with error.

5.3.3.ii.a Consistency of Drug Release

To assess consistency of release between scaffold batches, three different batches of 650 µg scaffolds were manufactured on different days. Diclofenac sodium release into PBS was measured at certain timepoints (figure 5.13). The three batches showed consistent release profiles, but differed in the mass of the initial burst. After the burst, the mass release was very similar, with batch #1 and batch #3, showing almost identical curves.

5.3.3.ii.b Release into cell culture medium containing FBS

Lastly, release of diclofenac sodium into full medium (phenol red free αMEM, 10% FBS, pen-strep and L-Glutamine), from the transwell system, was investigated to ensure that release into the *in vitro* bone model would be consistent with the release curves shown previously. Figure 5.14 shows percentage release from a 650 µg diclofenac sodium loaded scaffold. The release profile is very similar to those shown previously, with a high burst and a steady, slow release from day 4. There is a larger amount of error in these results, due to high background readings from protein in the medium, when performing UV spectrophotometry.

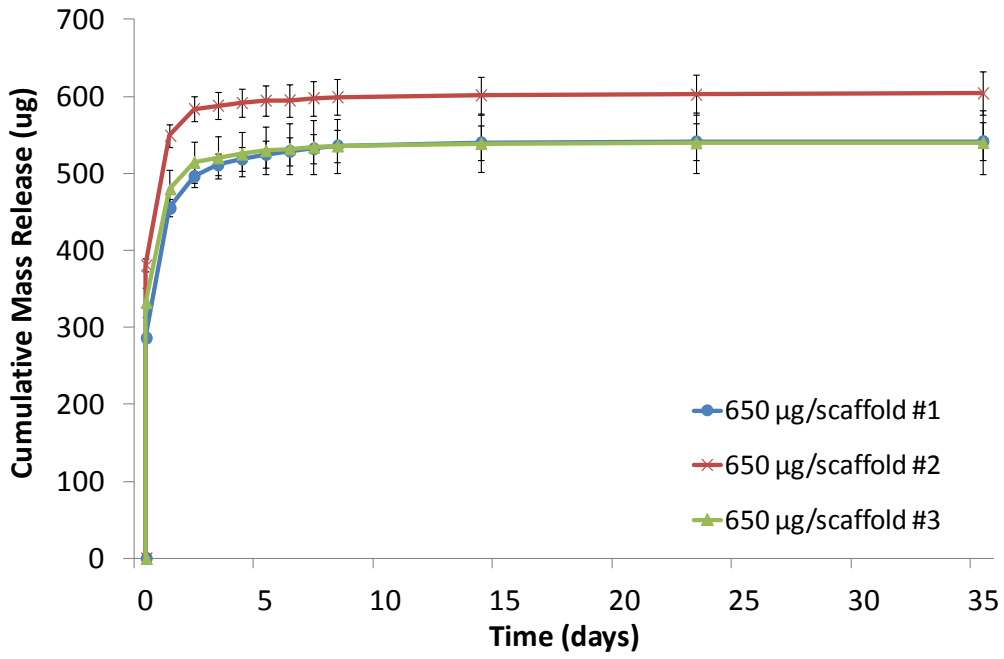

Figure 5.13: Consistency of mass release of diclofenac sodium from scaffold batches. Three different batches of PLGA/PEG scaffolds were manufactured loaded with 650 µg diclofenac sodium. Mass of drug released at each timepoint was assessed by UV spectrophotometry and expressed cumulatively over time. Values represented by mean of triplicate scaffold release, each measured in triplicate (n=9). Error represented by cumulative standard deviation.

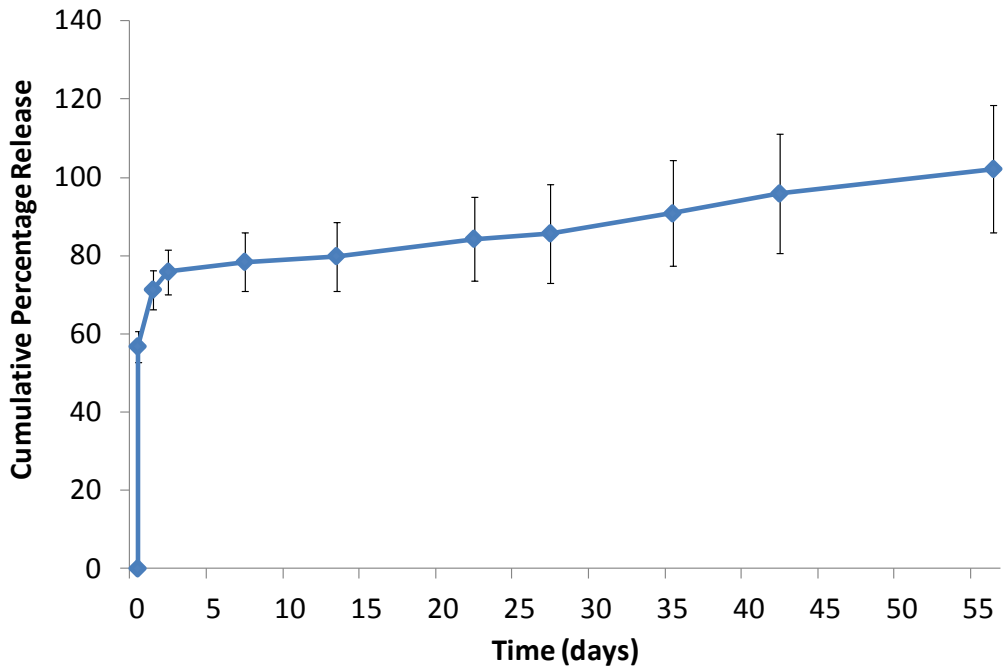

Figure 5.14: *In vitro* percentage release of diclofenac sodium from transwell model into full media. PLGA/PEG scaffolds were manufactured loaded with 650 µg diclofenac sodium. Scaffolds were placed into transwells and drug release overtime into full osteogenic media monitored. Mass of drug released at each timepoint was assessed by UV spectrophotometry and expressed cumulatively. Values represented by mean of triplicate scaffold release, each measured in triplicate (n=9). Error represented by cumulative standard deviation.

5.3.3.iii Diclofenac sodium release from PLGA/PEG scaffolds into *in vitro* osteoblast inflammation model.

Primary calvarial cell response to the release of diclofenac sodium from PLGA/PEG scaffolds, in both osteogenic and proinflammatory cytokine medium was investigated. Levels of nitrite, and PGE_2 in media samples were measured, to assess the effectiveness of the released drug. LDH levels were measured to indicate the cytotoxicity of the drug and proinflammatory cytokines. Live/dead images were taken on day 7, to show final levels of cell viability.

5.3.3.iii.a Final viability of primary calvarial cells after diclofenac sodium release

Live/dead images were taken of primary calvarial cell monolayer at day 7 and can be seen in figure 5.15. Images were quantified to compare different groups and the results can be seen in figure 5.16. Images show that in osteogenic medium with no scaffold, there are very few dead cells and those are most likely caught in the matrix of the living cells. The same is true of the 0 µg and 300 µg loaded scaffolds. There are an increased number of dead cells caused by the 650 µg loaded scaffold, but this is not a statistically significant result. Raising the loading to 1000 µg causes a very large increase in the number of dead cells and lowers the percentage viability to below 20%, indicating the concentration of diclofenac released in the burst is toxic to the cell monolayer. In proinflammatory cytokine medium, cells with no scaffold and 0 µg scaffolds, suffered from a large fall in viability, to around 33% and 23% respectively. Release of diclofenac from the 300 µg and 650 µg scaffolds improved

Figure 5.15: Live/Dead™ images of cell monolayers after diclofenac sodium release from PLGA/PEG scaffolds. Diclofenac sodium was released into medium of primary calvarial cells from PLGA/PEG scaffolds placed in transwells. Medium on cells was either control osteogenic medium, or osteogenic medium containing IL-1β, TNF-α and IFN-γ. After 7 days release, scaffolds were removed and Live/Dead images of cell monolayers taken. Representative images of live staining merged with dead staining shown. Scale bar=46 µm.

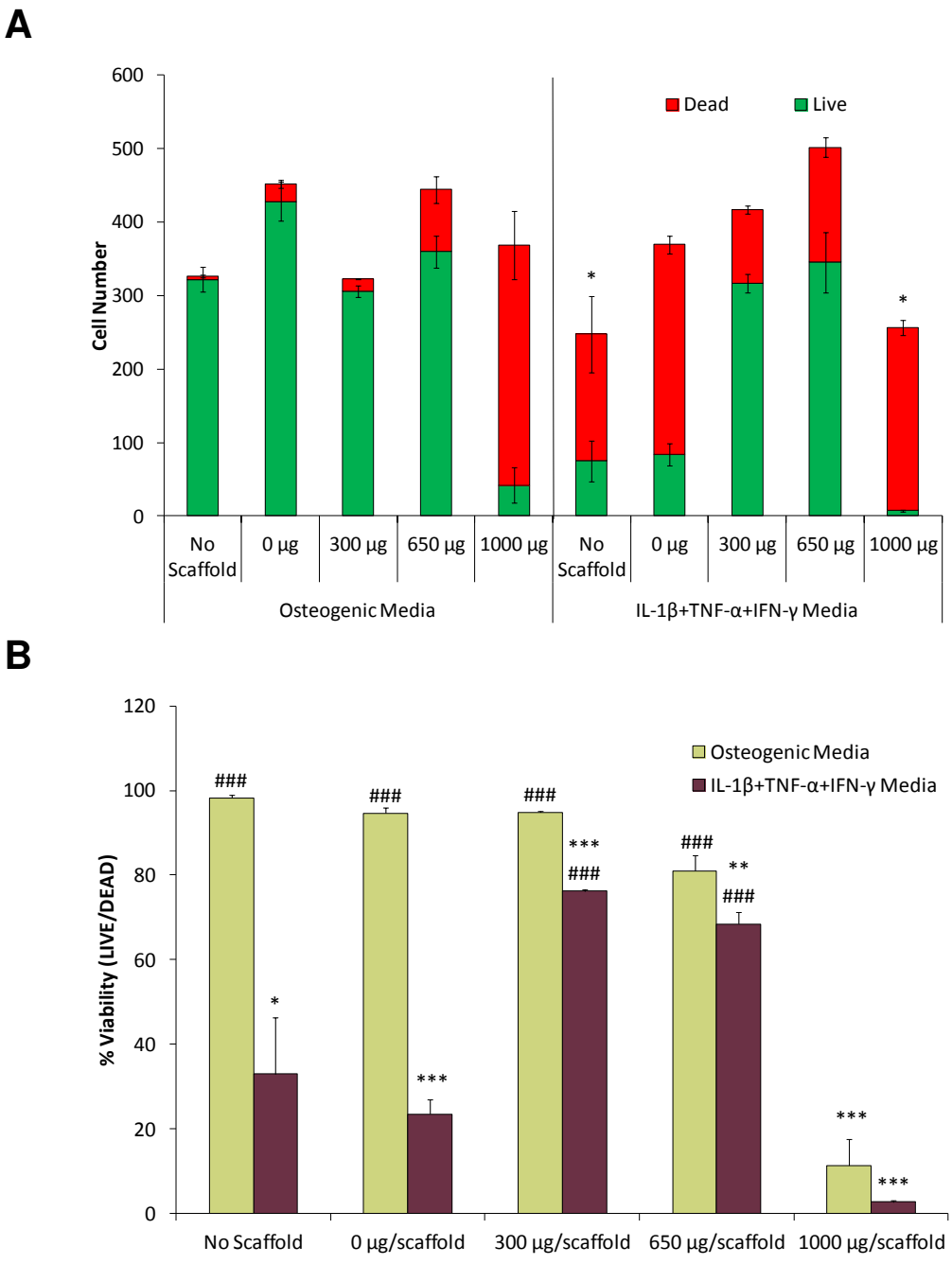

Figure 5.16: Live/Dead™ image quantification of cell monolayers after diclofenac sodium relase from PLGA/PEG scaffolds. Diclofenac sodium was released into medium of primary calvarial cells, from PLGA/PEG scaffolds placed in transwells. Medium on cells was either control osteogenic media, or osteogenic media containing IL-1β, TNFα and IFN-γ. After 7 days release, scaffolds were removed and Live/Dead™ images of cell monolayers taken. (A) Image quantification performed to determine number of live and dead cells *Statistical significance of total cell number vs. total cell number in 0 µg/scaffold in OM ($p \leq 0.01$). (B) Percentage of live cells in each group (n=9). Statistical significance vs. 0 µg/scaffold in OM (*$p \leq 0.01$, **$p \leq 0.001$, ***$p \leq 0.0001$). Statistical significance vs. 0 µg/scaffold in cytokine medium (### $p \leq 0.0001$).

viability in cytokine medium 76% and 68% correspondingly, demonstrating that the diclofenac inhibited the effects of the cytokines. The 1000 µg loaded scaffold in cytokine medium showed an enhanced negative effect with significantly less total cells and a cell viability of 3%.

5.3.3.iii.b Effect of diclofenac sodium-releasing PLGA/PEG scaffolds on LDH production in the osteoblast inflammation model

Release of LDH (cytotoxicity marker) over the 7 day diclofenac sodium release can be seen in figure 5.17. In control osteogenic medium, cytotoxicity levels are low and the presence of the scaffold causes no additional release of LDH into the medium. In medium containing IL-1β, TNF-α and IFN-γ, there is increased levels of cytotoxicity in the "no scaffold" group on day 1, compared to the 0 µg scaffolds, in both osteogenic and cytokine medium. Increased cytotoxicity is also seen in the medium of the 650 µg and 1000 µg scaffold on day 1 and day 2. LDH levels reach a peak on day 2 in the 1000 µg scaffold and by day 7, levels are low, presumably because there has been maximum cell death previously. All scaffold groups except for 1000 µg show significantly increased LDH between days 3 to 7 in cytokine medium, compared to the 0 µg scaffold in control medium. Taken cumulatively over the 7 days (figure 5.17B), the 1000 µg/scaffold shows almost 100% cytotoxicity, most likely due to the diclofenac sodium rather than the proinflammatory cytokines. The 650 µg scaffold shows significantly more cumulative cytotoxicity than the 0 µg scaffold, but the 300 µg does not.

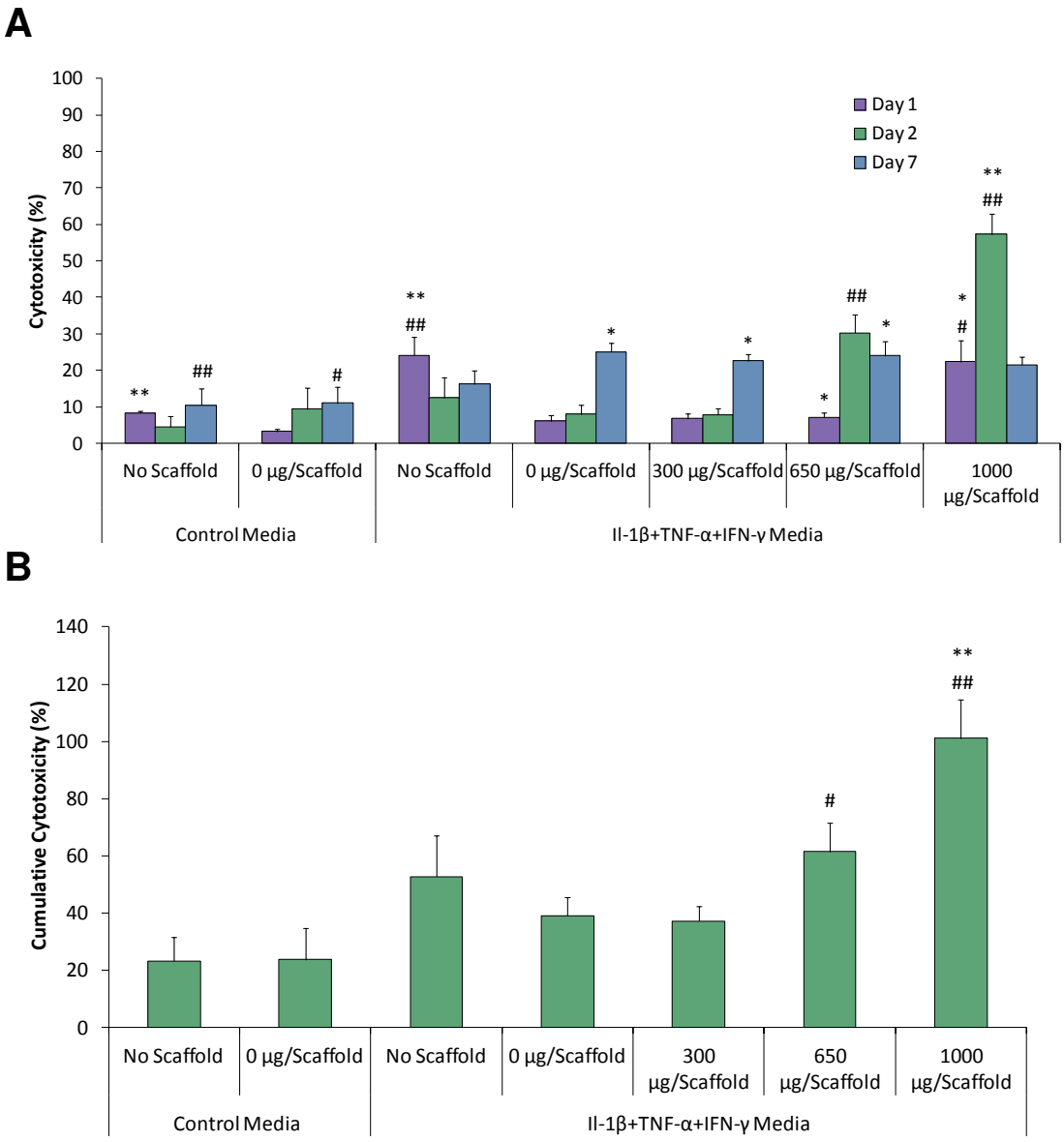

Figure 5.17: Effect of diclofenac sodium releasing PLGA/PEG scaffolds on cytotoxicity, in the *in vitro* calvarial osteoblast inflammation model. LDH in the media was measured on day 1, 2 and 7, after the scaffold placed in the transwell. (A) Cytotoxicity levels each day. (B) Cumulative cytotoxicity over 7 days. Values represented as mean±SEM (3 separate experiments, each with n=3). #Statistical significance vs. 0 µg/scaffold in cytokine media, (#p≤0.01, ##p≤0.001). *Statistical significance vs. 0 µg/scaffold in control media, (*p≤0.01, ** p≤0.001).

5.3.3.iii.c Effect of diclofenac sodium-releasing PLGA/PEG scaffolds on nitric oxide production in the osteoblast inflammation model

Levels of nitrite in the medium were measured after day 1, day 2 and at day 7, to estimate NO production, and can be seen in figure 5.18. In the "no scaffold" and 0 µg scaffold groups in control medium, there was minimal NO production, across all timepoints. When proinflammatory cytokines were present in the medium, "no scaffold" and with 0 µg scaffold showed significantly increased nitrite, across all timepoints, correlating with previous work. The 300 µg diclofenac releasing scaffolds showed significant inhibition of NO production on day 1, but day 2 and day 7 levels were significantly increased, compared to control. The 650 µg scaffolds showed inhibition of NO production across all timepoints, although by day 7, concentrations were also increased to significantly higher than control. Scaffolds releasing 1000 µg diclofenac, showed low nitrite production across all timepoints, but when relating back to Live/Dead and LDH results, low nitrite levels from day 2 onwards can be correlated with very low cell viability. Cumulative nitrite production across the 7 days (figure 5.18B) shows that the 300 µg scaffold did not significantly inhibit cytokine-induced NO production, although it does appear that levels were reduced. At 650 µg diclofenac sodium release, inhibition was more successful. The 1000 µg scaffolds appear to inhibit proinflammatory cytokine induced NO production but as mentioned previously, this may also be due to low cell number.

5.3.3.iii.d Effect of diclofenac sodium-releasing PLGA/PEG scaffolds on PGE_2 production in the calvarial osteoblast inflammation model

Concentration of PGE_2 in the medium, across the 7 days diclofenac sodium release was measured on day 1, day 2 and day 7 and can be seen in figure 5.19. PGE_2

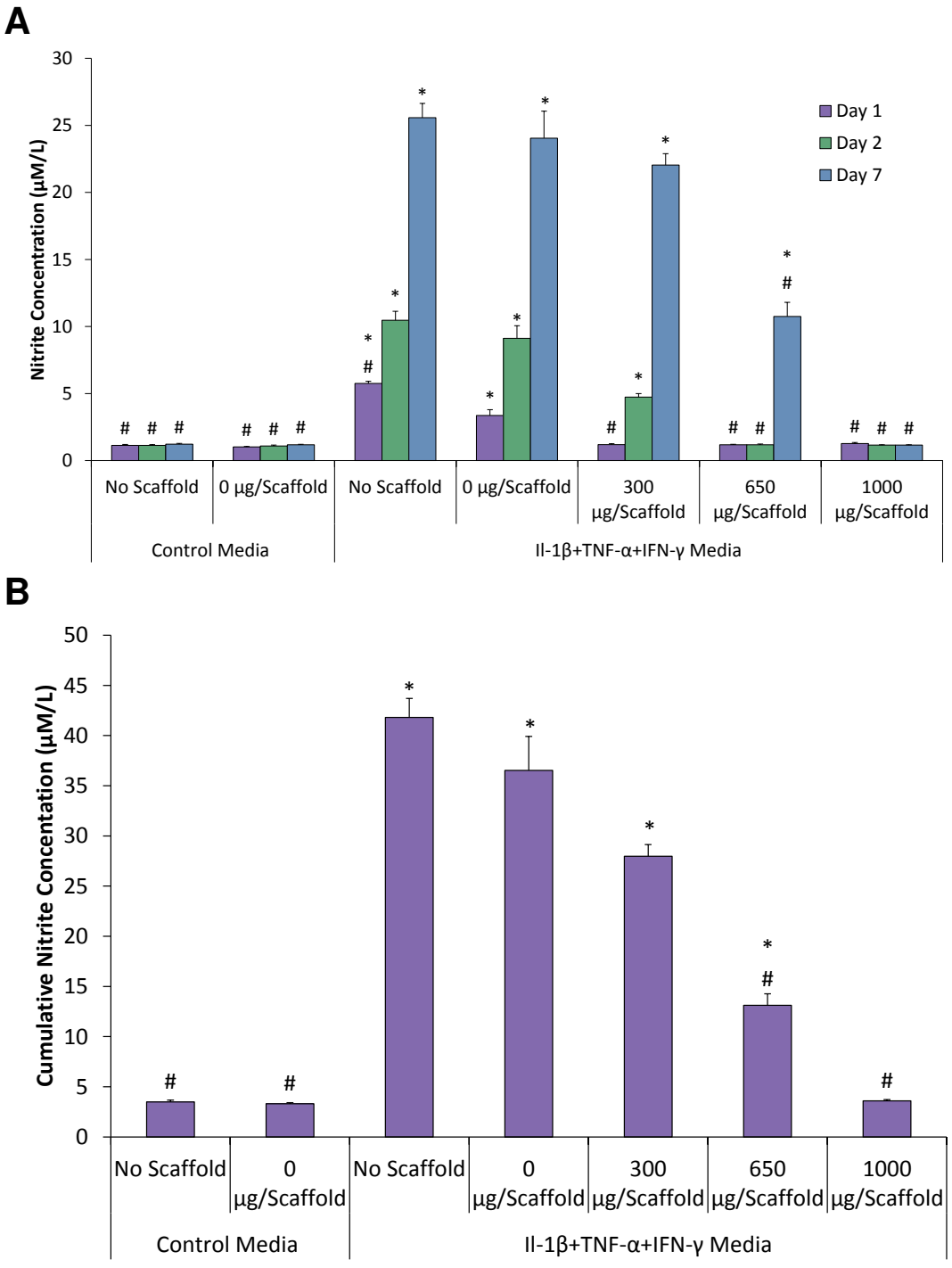

Figure 5.18: Effect of diclofenac sodium releasing PLGA/PEG scaffolds on nitrite production in the calvarial osteoblast inflammation model. Nitrite accumulation in the medium was measured on day 1, 2 and 7, after scaffold placed in transwell. (A) Concentration of nitrite at each timepoint. (B) Cumulative nitrite concentration over 7 days. Values represented as mean±SEM (3 separate experiments, each with n=3). Statistical significance vs. 0 µg/scaffold in cytokine media, (#p≤0.0001). *Statistical significance vs. 0 µg/scaffold in control media, (*p≤0.0001).

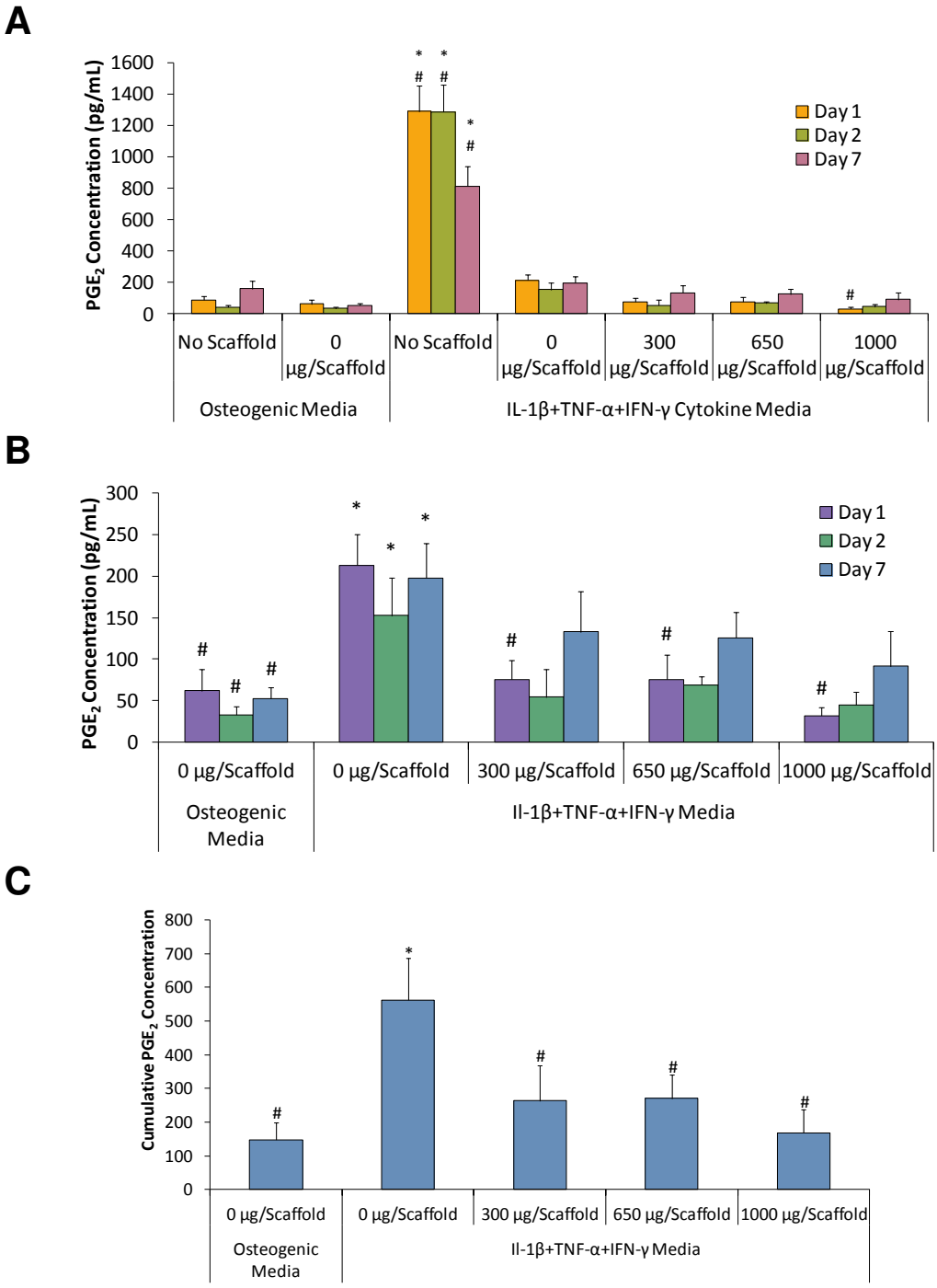

Figure 5.19: Effect of diclofenac sodium releasing PLGA/PEG scaffolds on PGE_2 production in the *in vitro* calvarial osteoblast inflammation model. PGE_2 accumulation in the media was measured on day 1, 2 and 7, after scaffold placed in transwell. (A) Concentration of PGE_2 each day, including "no scaffold" experimental groups. (B) Comparison of concentration of PGE_2 each day, excluding "no scaffold" experimental groups. (C) Cumulative PGE_2 concentration over 7 days, excluding "no scaffold" groups. Values represented as mean±SEM (3 separate experiments, each with n=3). # Statistical significance vs. 0 µg/scaffold in cytokine media, p≤0.01. *Statistical significance vs. 0 µg/scaffold in control media, p≤0.01.

concentration across all groups, at all timepoints can be seen in figure 5.19A. When all groups are shown on the same graph, the “no scaffold” experimental group in cytokine medium shows a very large amount of PGE_2 production, skewing the data. It should be expected that similar levels of PGE_2 are produced by cells with 0 µg scaffolds but this is not seen when assaying the medium. I believe that some of the PGE_2 released by the cells is adsorbing to the scaffold, and not remaining soluble in the medium, causing a large amount of variation in the results.

To get a more valuable understanding of how the scaffolds are affecting PGE_2 response, results excluding the “no scaffold” controls can be found in figure 5.19B. This figure shows that at all timepoints, the 0 µg scaffold showed increased PGE_2 production in proinflammatory cytokine medium compared to control osteogenic medium. Significant inhibition of PGE_2 was then seen at day 1 by the 300 µg, 650 µg and 1000 µg diclofenac-releasing scaffolds, and was reduced across these groups on day 2 and day 7, compared to 0 µg scaffolds in cytokine medium. Cumulative PGE_2 concentration (figure 5.18C) in the medium until day 7 showed that all diclofenac sodium loaded scaffolds, showed significant inhibition of PGE_2 production, in proinflammatory cytokine medium.

5.3.3.iii.e Concentration of diclofenac sodium released from PLGA/PEG scaffolds

Average mass of diclofenac released at each timepoint was calculated from UV spectrophotometry data (figure 5.20). Data approximately followed that of previous release curves. The largest release occurred over the first 24 hours (day 1) and ranged from 60-70%, total loading. This drug would then be removed during medium collection and over the next 24 hours, 12-15% total loaded drug would be released

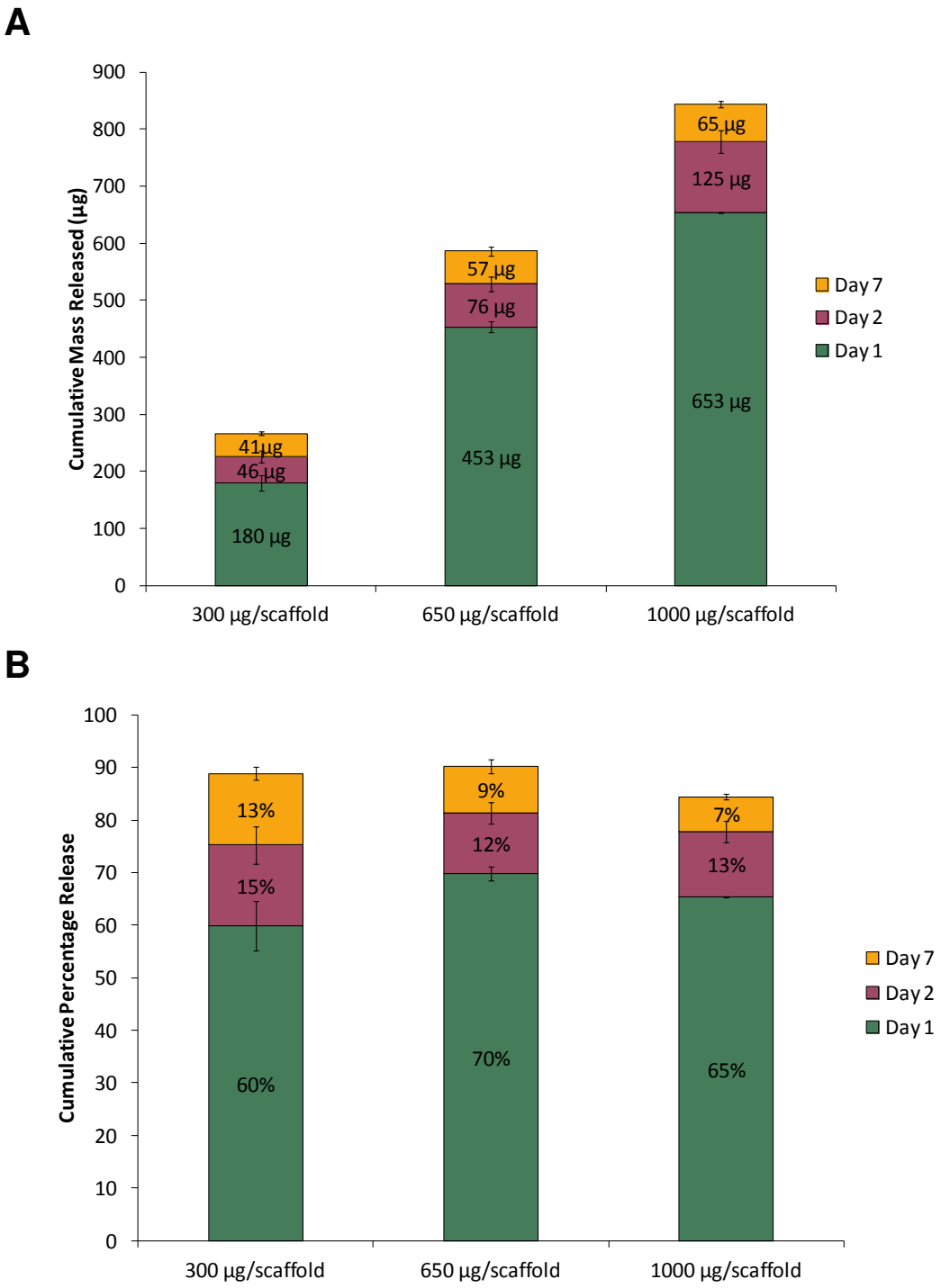

Figure 5.20: Diclofenac sodium release from PLGA/PEG scaffolds onto bone inflammation model. (A) Average mass of diclofenac sodium released by each timepoint, from 300, 650 and 1000 µg loaded scaffolds. (B) Average percentage diclofenac sodium released by each timepoint. Values represented by mean±SEM of each timepoint (n=9, 3 separate experiments).

into the model, before being removed. Over the next 5 days until day 7, approximately another 7-13% diclofenac would be released, until experiment end.

5.4 Discussion

Studies performed in this chapter show further validation of the inflammatory calvarial osteoblast model, investigation of the effects of anti-inflammatory drugs on primary calvarial cells, and examined the use of PLGA/PEG scaffolds as a release vehicle for diclofenac sodium. Early work performed using anti-inflammatory drug inhibition of NO and PGE_2, enabled simple validation of the calvarial osteoblast inflammatory model. Cell response to the drugs mirrored what was expected and remained consistent with literature. The glucocorticoids, dexamethasone and prednisolone, inhibited both NO and PGE_2 production. Glucocorticoids are very potent anti-inflammatories and work via many different mechanisms. Glucocorticoids, including dexamethasone and prednisolone destabilize the mRNA of COX-2 by inhibiting the MAPK p38 [311-314]. Whilst affecting PGE_2 production, dexamethasone also works to inhibit transcriptional activity leading to the production of iNOS, leading to decreased NO production. Destabilisation of the iNOS mRNA occurs, reducing the half-life by 50% [311, 315]. Although glucocorticoids have powerful anti-inflammatory and immunomodulatory effects, prolonged systemic treatment can adversely affect fracture healing, cause osteoporosis and increase the risk of fracture [316]. Steroid treatment can cause *in vivo* apoptosis of osteoblasts and osteocytes, and inhibit osteoblastogenesis, eventually leading to a decreased BMD [317, 318]. Due to these unfavourable side effects, it was decided not to pursue the use of dexamethasone in the scaffold release experiments, at this time. Used more predominantly as a treatment for RA and serious autoimmune conditions, the powerful anti-inflammatory effects would require more control over the method of release, to prevent the overwhelming side effects. An alternative reason for not pursuing the use of dexamethasone in this system is crossover in the use of the drug as an osteogenic

agent during *in vitro* culture. There is a discrepancy between the actions of dexamethasone to enhance *in vitro* osteogenesis of MSCs and ESCs [60, 319], and the negative effects during *in vivo* bone healing [316, 320]. As this study describes a very simple *in vitro* model, it was thought that this inconsistency in properties might add an extra level of complexity to the experiment.

Diclofenac sodium, ibuprofen and piroxicam were all very effective at inhibiting PGE_2 production and all did so at the lowest concentration. The ability of NSAIDs to inhibit the COX-2 pathway, and therefore PGE_2 production, has been discussed at length in the literature [292, 321]. The ability of NSAIDs to inhibit NO production is not so well known, but did occur to a certain degree with ibuprofen and with diclofenac, in longer-term studies and when released from the PLGA/PEG scaffolds. Aspirin, indomethacin and ibuprofen have all been shown to inhibit iNOS activity and NO production in macrophages stimulated with LPS and IFN-γ [322, 323]. This process does not cause complete inhibition of cytokine-induced NO production, and unlike glucocorticoid action, is not caused by inhibition of iNOS mRNA [324]. The diclofenac sodium results in this study show partial inhibition of NO production, in agreement with this statement. Interactions have previously been shown to exist between the COX and NOS pathways in a number of cells including osteoblasts [325-328]; however the inhibitory effects of NSAIDs on NO production have been shown to be both COX-dependent and COX-independent [323, 327].

The use of IL-1ra as an anti-inflammatory treatment for RA is in relative infancy. The current therapy is a non-glycosylated form of the IL-1ra protein; drug name anakinra and marketed under the name Kineret by Amgen. In this study, recombinant mouse non-glycosylated IL-1ra was used to simulate the drug. The protein performed very well in viability tests and showed no toxicity to the cell model at any concentration. Tests for the anti-inflammatory properties were less conclusive. Effective inhibition of

both NO and PGE_2 production only occurred at the highest concentration of 1000 ng/mL. Concentrations used were based on available literature and due to the expense of using recombinant proteins, it was not possible to try IL-1ra at higher concentrations [210, 329]. In clinical studies, anakinra showed moderate but statistically significant therapeutic efficacy in RA [330]. Further indirect head-to-head comparisons of anakinra vs. other biological DMARDs have suggested that it is less efficacious in treating RA than anti-TNF therapies [331, 332]. Considering this, it may have been of more interest to investigate the effect of an anti-TNF therapy on the inflammation model.

The initial screening of several types of anti-inflammatory mediator allowed selection of drugs to take forward for further screening of the inflammation model. Diclofenac sodium was chosen for several reasons: NSAIDs show appealing properties as an anti-inflammatory in bone treatment; good solubility in water and stability over time; successful results in both PGE_2 and nitrite inhibition in initial testing; and finally, more literature available describing release of diclofenac via various techniques [300, 309, 310]. Initial studies had been carried out for 3 days only; it was now necessary to look at the response of the cells to longer-term exposure to drug and cytokines. At this point, a concentration of 100 µM diclofenac sodium was chosen for *in vitro* studies, as cell viability at this concentration was not affected in the short term, cytokine-induced PGE_2 production was completely inhibited and there was some inhibition of NO. Over 21 days, results followed those of the short-term studies; the diclofenac had limited effect on cell viability and worked to inhibit the effects of the cytokines. The cell viability measurements were important, as anti-inflammatory drugs have previously been shown to induce apoptosis and arrest the cell cycle [333, 334]. This can be seen to a degree with the diclofenac sodium but only at the very highest concentrations. However, when used at therapeutic concentrations (100 µM), NSAIDs such as

diclofenac, have been shown to have no toxic effects on osteoblast viability and results in this study support this [335]. Over time, PGE_2 was blocked effectively and although cytokine-induced NO levels remained higher than controls, there was inhibition compared to cytokine only. These results gave some indication of how diclofenac may act upon release from scaffolds, and the concentrations that would be required. An initial release of around 100 µM would not affect cell viability drastically but was probably the minimum concentration required for effective blocking of inflammatory signals. This would be the equivalent of around 30 µg/mL mass release.

Short investigations were carried out studying the effect of diclofenac sodium on the formation of bone nodules and deposition of osteogenic matrix, building on work discussed in chapter 4. The effect of NSAIDs on bone formation and healing is one of contention, with some studies showing that *in vivo* treatment with drugs such as diclofenac, do not affect fracture healing [336-338]. Conversely, the majority of studies suggest that NSAIDs delay the fracture healing process [339-342]. NSAID treatment of *in vitro cell* cultures has revealed no significant effect on osteogenic differentiation of MSCs or osteoblasts [334, 335, 343]. In this investigation, the presence of diclofenac appeared to have a minor effect on the deposition of OPN and OCN, but not col-I. Cad-11 was present in the nodules, indicating the presence of osteoblasts. Results with cytokines in the culture medium supported the work of the previous chapter, with smaller nodules formed and less deposition of osteogenic ECM proteins, particularly OCN. Diclofenac prevented some of the effects of the cytokines, but was not completely effective, suggesting that although anti-inflammatory drugs inhibit responses in terms of NO and PGE_2, it may be more difficult to maintain the correct balance for osteogenic differentiation *in vivo.*

With knowledge of the effect of diclofenac on the bone inflammation model more secure, the development of a tissue engineered release system could progress. The

Tissue Engineering group at Nottingham has a base of knowledge using the PLGA/PEG system, and properties and suitability for bone tissue engineering have already been well-established [169-171]. The PLGA/PEG scaffold system has been shown to be effective in the release of chemotherapy drugs for the treatment of brain cancer after surgical resection, and BMP-2 for bone repair [170, 344]. The inclusion of anti-inflammatory drug release would enable enhancement of the properties of the PLGA/PEG scaffolds in bone repair, rather than only exploiting the scaffold as a drug delivery vehicle. The scaffolds are prepared from PLGA/PEG particles that form a paste when mixed with a carrier solution, this carrier solution can contain the drug of choice, which is then incorporated into the scaffold when the paste hardens at 37°C. One current limitation of this system is the solubility of the drug in the carrier. A solvent can be used, but at too high a concentration, this starts to affect the polymer particles and the drug release. The drug in the carrier adsorbs to the surface of the particles and becomes physically entrapped within the pores of the scaffold. Drug release from these scaffolds is uncontrolled and occurs via diffusion through the pores; release can depend upon drug properties and interaction between the drug and the polymer. In the case of diclofenac, release consisted of a very large burst within the first few hours, due to drug molecules loose within scaffold, immediately releasing into the medium. In some cases, this would have be considered an undesirable effect, but in the case of in vivo inflammation this burst release of anti-inflammatory correlates well with an influx of proinflammatory cytokines to the area upon implantation of the scaffold (see figure 5.21). After the burst, release slowed rapidly. Day 1 to day 4, drug release can be explained by diffusion of the drug through water-filled pores. From day 4, release slowed substantially, but followed an almost first-order release profile, as the remaining drug found a way through the scaffold, diffusing into the medium.

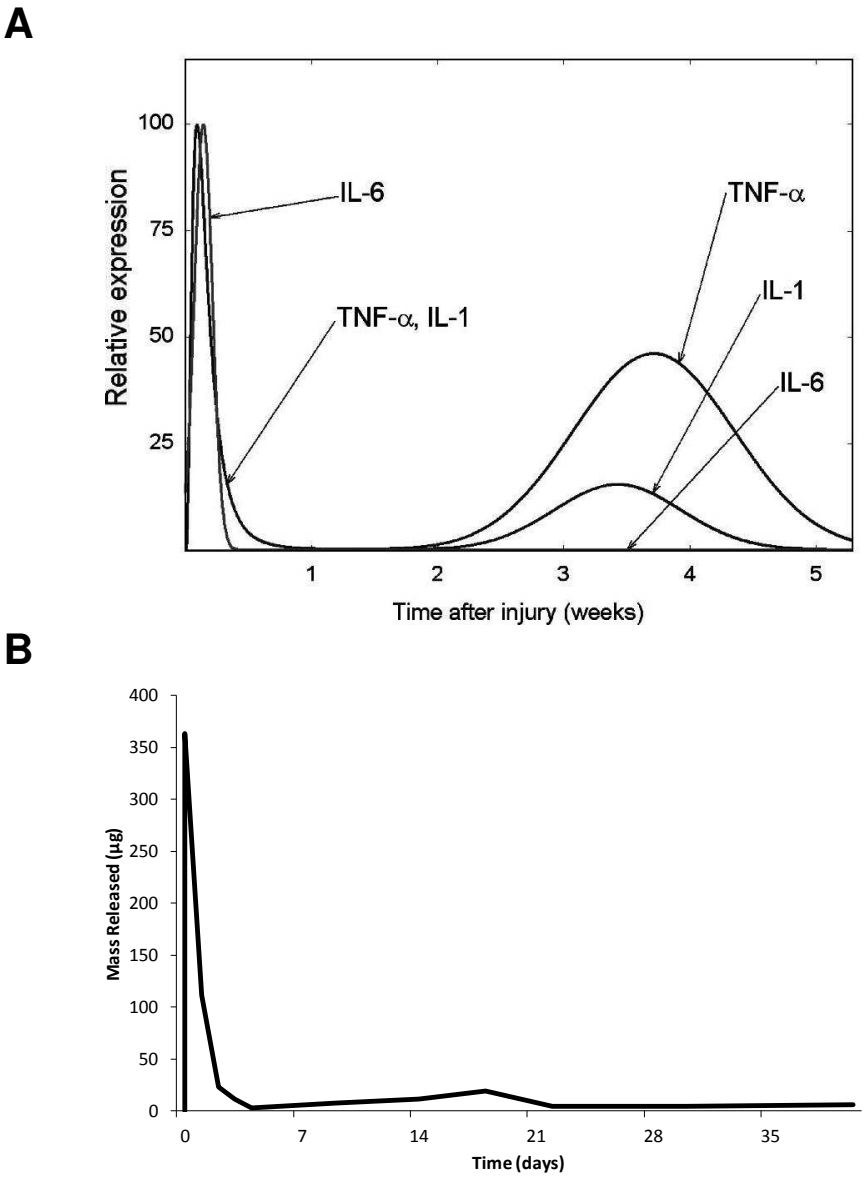

Figure 5.21: Comparison of non-cumulative mass release of drug from PLGA/PEG scaffold with *in vivo* proinflammatory cytokine expression. (A) Temporal expression of proinflammatory signals after bone injury/scaffold implantation (schematic adapted from Mountziaris and Mikos [271]) (B) Average non-cumulative mass released from 650 µg diclofenac sodium loaded PLGA/PEG scaffolds over time.

Initial loading of the drug had very little effect on the percentage release profile, and consistency of release between batches of scaffolds correlated well, only differing in initial burst release. The composition of the carrier into which the drug was released did not affect the release profile, but as more components were introduced into the medium, background readings increased, creating more error in the spectrophotometry. The length of time over which the majority of the diclofenac was released was about 6 days. This is in keeping with other tissue engineered anti-inflammatory release strategies that have shown 3-6 days [300-302]. Longer more controlled release could be achieved by using other scaffolds, such as PLGA microspheres [345, 346]. This system could be adapted to change release profile by incorporating the drug into the melt-blend of the PLGA/PEG when producing the particles. Drug diffusion out of the scaffold would then become more difficult as the drug has to travel through the particles themselves.

Diclofenac sodium release onto the cell inflammation model was performed from transwells. This allowed the cell monolayer to be kept separate from the scaffold, in order to maintain simplicity and not to introduce an extra level of complexity with migration of cells onto the scaffold or biomechanical effects of scaffold surface. The transwell system allowed drug release into the cell culture medium, which could freely diffuse through the pores of the membrane to the cell monolayer. The system had disadvantages; the scaffold swelled as water was imbibed and it became constrained by the edges of the transwell, possibly affecting release. Nevertheless, as experiments were kept to a maximum of 7 days, this effect had little time to come into consequence. The medium level had to be kept above the scaffold to ensure drug release; consequently, the final concentration of drug was diluted slightly. These disadvantages aside, the simple system worked successfully to demonstrate that diclofenac sodium release was effective as an anti-inflammatory mediator.

Cell viability in the model, was used as an indicator of effective concentration of drug. A balance between the mass of drug released to achieve an effective anti-inflammatory dose with the maintenance of cell viability had to be attained. The highest scaffold loading of 1000 µg/scaffold showed almost complete cell death by day 7 of release, and LDH results suggested that the majority of this had occurred by day 2. Most probably, this was a property of the large burst release. This large cell death rendered results of PGE_2 and nitrite obsolete, as low values only indicated low cell numbers. There was more success with scaffolds loaded with 300 µg or 650 µg drug. Results indicate that an initial loading between the two would give optimum results for cell viability and inhibition of inflammatory markers.

The *in vivo* environment is vastly different to the one created in this study, but it was attempted to reflect it by starting with a large concentration of proinflammatory cytokines that then decreased from day 1, and was low up until day 7. Medium was replaced a certain to timepoints to prevent accumulation of the drug in the system having too much effect on cell viability. An issue that emerged as the system developed was adsorption of PGE_2 and medium proteins, such as the proinflammatory cytokines, to the PLGA/PEG scaffold. This was reflected most obviously in results for PGE_2, but could also be seen in nitrite and LDH readings, resulting in lower values when scaffolds were present. This issue would continue into be an issue that would carry over to *in vivo* work, with the presence of a scaffold affecting the natural environment of wound healing. Protein adsorption can illicit the immune responses and affect cellular processes [347, 348]. Much work has been performed using surface modification to reduce this property [349, 350]. Overall, the model performed well in showing that the drug was effective after release.

Chapter 6:
Discussion

The overall aim of this study was to consider bone tissue engineering strategies in the context of inflammation; looking at both the effect and control of inflammatory signalling. Often, the potential effects of introducing bone regeneration strategies into environments of disease and damage are overlooked, despite the fact that many of the signalling pathways in inflammation have effects on bone development and healing.

The first objective of this investigation was to develop an *in vitro* simulation of the inflammatory environment, which could be used throughout the study. Proinflammatory cytokines such as IL-1β, TNF-α and IFN-γ have been used extensively to represent inflammatory signals in *in vitro* osteoblast and MSC cultures, and effects of these cytokines have been discussed throughout the preceding chapters [259, 351-353]. In many of these reported studies, only one cytokine is used to stimulate the cells, rather than the combination of cytokines that was used in the majority of these experiments. In developing the *in vitro* inflammatory environment, the greatest response of the primary calvarial cells, in terms of NO and PGE_2, was seen when the three cytokines were present in combination in the medium. This did not elicit a response from the early differentiation osteo-mESCs, even when concentration was increased to 10 times what is normally described in the literature. For this reason, it was decided to consistently use the three cytokines in combination, to be sure of a high level of response from the primary calvarial cells that could be easily compared to that of the osteo-mESCs. Using more than one cytokine also

simulated an environment more similar to that of *in vivo* inflammation, although a very simplified one, without the cells of the immune system and of increased cytokine concentrations.

The novelty of this work lay in the investigation of the response of osteo-mESCs to proinflammatory cytokines. To give the results context, they were compared to the responses of the primary calvarial cells. The primary cells consistently produced NO and PGE_2, in response to the inflammatory signalling, regardless of stage of osteogenic differentiation. There was also an effect on osteogenic matrix production and bone nodule formation in response to short bursts of cytokine stimulation, at all stages of osteogenic culture. The interesting results lay with the osteo-mESCs that did not produce NO or PGE_2 in response to the cytokines, until the very latest stages of osteogenesis. Unfortunately, it was not possible to fully elucidate the mechanisms accountable for this lack of response during the course of this investigation. It may be postulated that it is cytokine-receptor or inflammatory pathway related. Interestingly, the mESCs did show signs of anti-inflammatory properties, with mESC CM showing inhibition of the cytokine-induced effects on the primary calvarial cells. Along with work describing the possible immunotolerance of ESCs, these results may help promote the potential that ESC-derived cells have in regenerative strategies, and in possible modulation of the immune and inflammatory response [354, 355].

Another objective of the study was to examine the osteogenic differentiation of the mESCs, comparing it to differentiation of the primary cells. The protocol used for osteogenic differentiation was a standard protocol featuring BGP, ascorbate and dexamethasone, which has been described many times throughout the literature [30, 60, 61]. The only consideration faced was the use of dexamethasone, as it also has a function as a potent anti-inflammatory; a property shown to great effect in chapter 5, inhibiting the effects of the cytokine signalling on the calvarial osteoblast inflammation

model. This predicament was overcome by removing the dexamethasone when cytokines were present in the cell culture medium, and for at least 24 hours after, for any residual signalling effects to occur. In hindsight, it may have been less problematic to use a different molecule for the osteogenic induction, such as simvastatin, which has been shown to induce osteogenic differentiation of mESCs [228]. ESCs have also been shown to produce bone nodules in the presence of just BGP and ascorbate, without an osteoinductive molecule such as dexamethasone, and this was the case for this investigation in experiments that required continuous culture with proinflammatory cytokines [60].

In comparing the differentiation of the two cell types, some major differences were seen. Alizarin red staining showed very different configurations of the stained bone nodules within the cultures. Subjective observation indicated that there were far more nodules in osteo-mESC cultures. There have been differences shown in the speed of nodule formation, and composition and configuration of mineralised matrix produced by osteo-mESCs, compared with MSCs and primary osteoblasts [61, 192]. Perhaps with further investigation, the results in this study would have reached the same conclusion.

In support of the osteogenic differentiation of mESCs, this study showed col-I, OCN and OPN deposited in the matrix and the presence of cad-11 positive cells. None of this was seen within the control cells cultured in non-osteogenic medium. This indicates that there is osteoinduction occurring within the mESC cultures, but results do not compare to that of primary cells, possibly due to the dilution of the ESC-derived osteogenic population, with other cell types. Heterogeneity within ESC cultures has been reported as an issue when considering production of cell therapies; particularly the danger of contamination with undifferentiated ESCs, which could go on to form teratomas [356-358]. Therefore, an ESC therapy will require a pure

population of the cell of interest. The most likely way to achieve this is by using cell-sorting techniques such as FACS or MACS. In this investigation, MACS proved successful in selecting a population of cells, positive for the marker cad-11. This population then went on to show osteogenic differentiation that was more similar to that of the primary calvarial cells, than the unsorted osteo-mESCs. The disadvantage of this sorting procedure, was the low yield of cells that showed positive for cad-11 and the amount of cells lost in the MACS process. As this experiment was an initial trial, to determine whether the MACS process and the cad-11 marker were suitable, the results were in fact very promising. If continuing with this line of investigation, it would be of interest to fully optimise the process, identifying the ideal stage of osteogenic culture to perform the sorting procedure on the mESCs. The inclusion of alternative markers and improvement of the experimental process, so cell loss was minimised, would also be advantageous. It may have been interesting to perform the MACS selection process on the primary calvarial cells, as these also show a heterogeneous population in culture.

In chapter 5, the focus of the study was adjusted from effect of inflammation, to possible methods of control of inflammation. There are currently many drugs and therapies available to help control the symptoms of inflammatory bone disease. Tissue engineering and regenerative medicine offer the opportunity to address the imbalance in bone healing and inflammation, that can be the cause of the disease or non-healing. In this study, a method of drug release was shown from a polymeric scaffold that had already been designed for the purposes of bone regeneration. This system was very simple but showed itself to be effective in initial *in vitro* studies, involving the calvarial osteoblast inflammation model. I believe that one of the key factors in creating a regenerative therapy for bone that will modulate inflammation, lies in creating a balance between allowing enough of the natural healing

inflammation process, but not permitting it to overwhelm the regenerative capacity of the therapy or upset the balance of bone healing. This will require careful thought about the type of incorporated anti-inflammatory drug, the method and concentration of release and knowledge of the mechanisms of inflammation within the ailment. To extend the work performed in this study, it would have been interesting to use the inflammation model to test other mechanisms of drug release, such as polymeric microparticles that offer more control over the release rate [27]. These microparticles could then have been incorporated into the PLGA/PEG system. This would also allow the investigation into other drug types, as with this system, drug solubility is not such as issue. It may also be more realistic to the *in vivo* environment to move to a 3D model of inflammation, and culture the cells upon the scaffold, where drug and cytokine interactions will be altered from the 2D environment.

This investigation has opened up many future avenues of research following both engineering and biological paths. There is a wealth of knowledge that could be gained by further investigating the ESC response to inflammatory signalling. The work performed in this study used mouse cells and the most obvious step is to transfer to a human cell model, which would be more applicable to human disease. There could be much potential in looking at cytokine receptor expression on the cells and exploration of the changes that occur during ESC differentiation, that eventually lead to a cytokine-induced cell response. Alternative techniques could be used to look further into gene and protein expression during osteogenic differentiation of the cells, and the possible effects of the inflammatory cytokines.

I think it is important to continue to examine the efficacy of osteogenic differentiation protocols, to ensure confidence that the cells being produced are of an osteoblastic lineage. There is also much scope for the development of efficient cell sorting protocols for ESCs, which lead to purified populations of ESC-derived osteogenic

cells. From a tissue engineering perspective, improved knowledge of bone inflammation and disease, and cell response to these environments, could lead to improved therapeutic results when using tissue engineered strategies. Overall, it is very important that researchers consider the disease environment when designing a regenerative strategy and aim to redress the balance of inflammation that prevents natural healing .

Chapter 7:
References

1. Nerem RM. Cellular engineering. *Ann Biomed Eng.* 1991;**19**:529-545.
2. Langer R, Vacanti JP. Tissue Engineering. *Science.* 1993;**260**:920-926.
3. Vacanti CA. History of tissue engineering and a glimpse into its future. *Tissue engineering.* 2006;**12**:1137-1142.
4. Mason C, Dunnill P. A brief definition of regenerative medicine. *Regenerative medicine.* 2008;**3**:1-5.
5. Mason C, Brindley DA, Culme-Seymour EJ, Davie NL. Cell therapy industry: billion dollar global business with unlimited potential. *Regenerative medicine.* 2011;**6**:265-272.
6. Till JE, McCulloch EA. Direct measurement of radiation sensitivity of normal mouse bone marrow cells. *Radiat Res.* 1961;**14**:213-222.
7. Evans MJ, Kaufman MH. Establishment in culture of pluripotential cells from mouse embryos. *Nature.* 1981;**292**:154-156.
8. Martin GR. Isolation of a pluripotent cell line from early mouse embryos cultured in medium conditioned by teratocarcinoma stem cells. *Proc Natl Acad Sci USA.* 1981;**78**:7634-7638.
9. Niwa H. Mouse ES cell culture system as a model of development. *Dev Growth Differ.* 2010;**52**:275-283.
10. Thomson JA, Itskovitz-Eldor J, Shapiro SS, Waknitz MA, Swiergiel JJ, Marshall VS, Jones JM. Embryonic stem cell lines derived from human blastocysts. *Science.* 1998;**282**:1145-1147.
11. Takahashi K, Yamanaka S. Induction of pluripotent stem cells from mouse embryonic and adult fibroblast cultures by defined factors. *Cell.* 2006;**126**:663-676.
12. Brindley David A, Davie Natasha L, Sahlman William A, Bonfiglio Gregory A, Culme-Seymour Emily J, Reeve Brock C, Mason C. Promising Growth and Investment in the Cell Therapy Industry during the First Quarter of 2012. *Cell Stem Cell.* 2012;**10**:492-496.
13. Mason C, Manzotti E. Regenerative medicine cell therapies: numbers of units manufactured and patients treated between 1988 and 2010. *Regenerative medicine.* 2010;**5**:307-313.
14. FDA. Approved Cellular and and Gene Therapy Products. Available at: http://www.fda.gov/BiologicsBloodVaccines/CellularGeneTherapyProducts/ApprovedProducts/default.htm. Accessed 15th September, 2012.
15. Dimitriou R, Jones E, McGonagle D, Giannoudis PV. Bone regeneration: current concepts and future directions. *BMC Med.* 2011;**9**:66.
16. Berner A, Reichert JC, Muller MB, et al. Treatment of long bone defects and non-unions: from research to clinical practice. *Cell Tissue Res.* 2012;**347**:501-519.
17. Salgado AJ, Coutinho OP, Reis RL. Bone tissue engineering: State of the art and future trends. *Macromol Biosci.* 2004;**4**:743-765.
18. Waese EYL, Kandel RR, Stanford WL. Application of stem cells in bone repair. *Skeletal Radiol.* 2008;**37**:601-608.

19. Rose F, Oreffo ROC. Bone tissue engineering: Hope vs hype. *Biochem Biophys Res Commun.* 2002;**292**:1-7.
20. Rosen V. Harnessing the parathyroid hormone, Wnt, and bone morphogenetic protein signaling cascades for successful bone tissue engineering. *Tissue Eng Part B Rev.* 2011;**17**:475-479.
21. FDA. InFUSE Bone Graft/LT-CAGE Lumbar Tapered Fusion Device P000058. Available at: http://www.fda.gov/MedicalDevices/ProductsandMedicalProcedures/DeviceApprovalsandClearances/Recently-ApprovedDevices/ucm083423.htm. Accessed 15th September, 2012.
22. FDA. OP-1 - H010002. Available at: http://www.fda.gov/MedicalDevices/ProductsandMedicalProcedures/DeviceApprovalsandClearances/Recently-ApprovedDevices/ucm085026.htm. Accessed 15th September, 2012.
23. Olympus. Olympus Corporation Milestones. Available at: http://www.olympusamerica.com/corporate/corp_milestones.asp. Accessed 15th September, 2012.
24. Carragee EJ, Hurwitz EL, Weiner BK. A critical review of recombinant human bone morphogenetic protein-2 trials in spinal surgery: emerging safety concerns and lessons learned. *Spine J.* 2011;**11**:471-491.
25. Bessa PC, Casal M, Reis RL. Bone morphogenetic proteins in tissue engineering: the road from laboratory to clinic, part II (BMP delivery). *J Tissue Eng Regen Med.* 2008;**2**:81-96.
26. Wang H, Boerman OC, Sariibrahimoglu K, Li Y, Jansen JA, Leeuwenburgh SC. Comparison of micro- vs. nanostructured colloidal gelatin gels for sustained delivery of osteogenic proteins: Bone morphogenetic protein-2 and alkaline phosphatase. *Biomaterials.* 2012.
27. Kirby GTS, White LJ, Rahman CV, Cox HC, Qutachi O, Rose FRAJ, Hutmacher DW, Shakesheff KM, Woodruff MA. PLGA-Based Microparticles for the Sustained Release of BMP-2. *Polymers.* 2011;**3**:571-586.
28. Bruder SP, Kurth AA, Shea M, Hayes WC, Jaiswal N, Kadiyala S. Bone regeneration by implantation of purified, culture-expanded human mesenchymal stem cells. *J Orthop Res.* 1998;**16**:155-162.
29. Horwitz EM, Prockop DJ, Fitzpatrick LA, et al. Transplantability and therapeutic effects of bone marrow-derived mesenchymal cells in children with osteogenesis imperfecta. *Nat Med.* 1999;**5**:309-313.
30. Bielby RC, Boccaccini AR, Polak JM, Buttery LDK. In vitro differentiation and in vivo mineralization of osteogenic cells derived from human embryonic stem cells. *Tissue engineering.* 2004;**10**:1518-1525.
31. Kim S, Kim S-S, Lee S-H, Eun Ahn S, Gwak S-J, Song J-H, Kim B-S, Chung H-M. In vivo bone formation from human embryonic stem cell-derived osteogenic cells in poly(d,l-lactic-co-glycolic acid)/hydroxyapatite composite scaffolds. *Biomaterials.* 2008;**29**:1043-1053.
32. Klimanskaya I, Chung Y, Becker S, Lu S-J, Lanza R. Human embryonic stem cell lines derived from single blastomeres. *Nature.* 2006;**444**:481-485.
33. Pekkanen-Mattila M, Pelto-Huikko M, Kujala V, Suuronen R, Skottman H, Aalto-Setälä K, Kerkelä E. Spatial and temporal expression pattern of germ layer markers during human embryonic stem cell differentiation in embryoid bodies. *Histochem Cell Biol.* 2010;**133**:595-606.
34. Wobus AM, Kaomei G, Shan J, et al. Retinoic acid accelerates embryonic stem cell-derived cardiac differentiation and enhances development of ventricular cardiomyocytes. *J Mol Cell Cardiol.* 1997;**29**:1525-1539.

35. Wiles MV, Keller G. Multiple hematopoietic lineages develop from embryonic stem (ES) cells in culture. *Development.* 1991;**111**:259-267.
36. Bain G, Kitchens D, Yao M, Huettner JE, Gottlieb DI. Embryonic stem cells express neuronal properties in vitro. *Dev Biol.* 1995;**168**:342-357.
37. Rohwedel J, Maltsev V, Bober E, Arnold HH, Hescheler J, Wobus AM. Muscle cell differentiation of embryonic stem cells reflects myogenesis in vivo: developmentally regulated expression of myogenic determination genes and functional expression of ionic currents. *Dev Biol.* 1994;**164**:87-101.
38. Kramer J, Hegert C, Guan K, Wobus AM, Muller PK, Rohwedel J. Embryonic stem cell-derived chondrogenic differentiation in vitro: activation by BMP-2 and BMP-4. *Mech Dev.* 2000;**92**:193-205.
39. Lumelsky N, Blondel O, Laeng P, Velasco I, Ravin R, McKay R. Differentiation of embryonic stem cells to insulin-secreting structures similar to pancreatic islets. *Science.* 2001;**292**:1389-1394.
40. Williams RL, Hilton DJ, Pease S, et al. Myeloid-leukemia inhibitory factor maintains the developmental potential of embryonic stem cells. *Nature.* 1988;**336**:684-687.
41. Xu C, Inokuma MS, Denham J, Golds K, Kundu P, Gold JD, Carpenter MK. Feeder-free growth of undifferentiated human embryonic stem cells. *Nat Biotechnol.* 2001;**19**:971-974.
42. Scholer HR, Ruppert S, Suzuki N, Chowdhury K, Gruss P. New type of POU domain in germ line-specific protein Oct-4. *Nature.* 1990;**344**:435-439.
43. Yuan H, Corbi N, Basilico C, Dailey L. Developmental-specific activity of the FGF-4 enhancer requires the synergistic action of Sox2 and Oct-3. *Genes Dev.* 1995;**9**:2635-2645.
44. Rogers MB, Hosler BA, Gudas LJ. Specific expression of a retinoic acid-regulated, zinc-finger gene, Rex-1, in preimplantation embryos, trophoblast and spermatocytes. *Development.* 1991;**113**:815-824.
45. Ginis I, Luo Y, Miura T, et al. Differences between human and mouse embryonic stem cells. *Dev Biol.* 2004;**269**:360-380.
46. Odorico JS, Kaufman DS, Thomson JA. Multilineage differentiation from human embryonic stem cell lines. *Stem cells.* 2001;**19**:193-204.
47. Schwartz SD, Hubschman JP, Heilwell G, et al. Embryonic stem cell trials for macular degeneration: a preliminary report. *Lancet.* 2012;**379**:713-720.
48. US N. Sub-retinal transplantation of hESC derived RPE(MA09-hRPE) Cells in Patients with Stargardt's Macular Dystrophy. Available at: http://clinicaltrials.gov/ct2/show/NCT01345006?term=NCT01345006&rank=1. Accessed 16th September, 2012.
49. Wilson A, Trumpp A. Bone-marrow haematopoietic-stem-cell niches. *Nat Rev Immunol.* 2006;**6**:93-106.
50. Shum L, Coleman CM, Hatakeyama Y, Tuan RS. Morphogenesis and dysmorphogenesis of the appendicular skeleton. *Birth Defects Res C Embryo Today.* 2003;**69**:102-122.
51. Krampera M, Pizzolo G, Aprili G, Franchini M. Mesenchymal stem cells for bone, cartilage, tendon and skeletal muscle repair. *Bone.* 2006;**39**:678-683.
52. Friedenstein AJ, Chailakhjan RK, Lalykina KS. The development of fibroblast colonies in monolayer cultures of guinea-pig bone marrow and spleen cells. *Cell Tissue Kinet.* 1970;**3**:393-403.
53. Pittenger MF, Mackay AM, Beck SC, et al. Multilineage potential of adult human mesenchymal stem cells. *Science.* 1999;**284**:143-147.
54. Dominici M, Le Blanc K, Mueller I, et al. Minimal criteria for defining multipotent mesenchymal stromal cells. The International Society for Cellular Therapy position statement. *Cytotherapy.* 2006;**8**:315-317.

55. Si YL, Zhao YL, Hao HJ, Fu XB, Han WD. MSCs: Biological characteristics, clinical applications and their outstanding concerns. *Ageing Res Rev.* 2011;**10**:93-103.
56. Gurdon JB, Melton DA. Nuclear Reprogramming in Cells. *Science.* 2008;**322**:1811-1815.
57. Yu JY, Vodyanik MA, Smuga-Otto K, et al. Induced pluripotent stem cell lines derived from human somatic cells. *Science.* 2007;**318**:1917-1920.
58. Hussein SM, Nagy AA. Progress made in the reprogramming field: new factors, new strategies and a new outlook. *Curr Opin Genet Dev.* 2012.
59. Li F, Bronson S, Niyibizi C. Derivation of murine induced pluripotent stem cells (iPS) and assessment of their differentiation toward osteogenic lineage. *J Cell Biochem.* 2010;**109**:643-652.
60. Buttery LDK, Bourne S, Xynos JD, Wood H, Hughes FJ, Hughes SPF, Episkopou V, Polak JM. Differentiation of osteoblasts and in vitro bone formation from murine embryonic stem cells. *Tissue engineering.* 2001;**7**:89-99.
61. Shimko DA, Burks CA, Dee KC, Nauman EA. Comparison of in vitro mineralization by murine embryonic and adult stem cells cultured in an osteogenic medium. *Tissue engineering.* 2004;**10**:1386-1398.
62. Hwang YS, Kang YY, Mantalaris A. Directing embryonic stem cell differentiation into osteogenic/chondrogenic lineage in vitro. *Biotechnol Bioeng.* 2007;**12**:15-21.
63. Ezekiel UR, Muthuchamy M, Ryerse JS, Heuertz RM. Single embryoid body formation in a multi-well plate. *Electron J Biotechnol.* 2007;**10**.
64. Kurosawa H, Imamura T, Koike M, Sasaki K, Amano Y. A simple method for forming embryoid body from mouse embryonic stem cells. *J Biosci Bioeng.* 2003;**96**:409-411.
65. Duplomb L, Dagouassat M, Jourdon P, Heymann D. Differentiation of osteoblasts from mouse embryonic stem cells without generation of embryoid body. *In Vitro Cell Dev Biol Anim.* 2007;**43**:21-24.
66. Price JS, Oyajobi BO, Russell RGG. The Cell Biology of Bone Growth. *Eur J Clin Nutri.* 1994;**48**:S131-S131.
67. Marieb EB. Human Anatomy and Physiology. San Franscisco: Pearson Benjamin Cummings; 2003.
68. Owen M. The origin of bone cells. *Int Rev Cytol.* 1970;**28**:213-238.
69. Ducy P, Zhang R, Geoffroy V, Ridall AL, Karsenty G. Osf2/Cbfa1: a transcriptional activator of osteoblast differentiation. *Cell.* 1997;**89**:747-754.
70. Komori T, Yagi H, Nomura S, et al. Targeted disruption of Cbfa1 results in a complete lack of bone formation owing to maturational arrest of osteoblasts. *Cell.* 1997;**89**:755-764.
71. Hughes FJ, Turner W, Belibasakis G, Martuscelli G. Effects of growth factors and cytokines on osteoblast differentiation. *Periodontology 2000.* 2006;**41**:48-72.
72. Hong JH, Hwang ES, McManus MT, et al. TAZ, a transcriptional modulator of mesenchymal stem cell differentiation. *Science.* 2005;**309**:1074-1078.
73. Ryoo HM, Hoffmann HM, Beumer T, Frenkel B, Towler DA, Stein GS, Stein JL, van Wijnen AJ, Lian JB. Stage-specific expression of Dlx-5 during osteoblast differentiation: involvement in regulation of osteocalcin gene expression. *Mol Endocrinol.* 1997;**11**:1681-1694.
74. Owen TA, Bortell R, Yocum SA, et al. Coordinate occupancy of AP-1 sites in the vitamin D-responsive and CCAAT box elements by Fos-Jun in the osteocalcin gene: model for phenotype suppression of transcription. *Proc Natl Acad Sci U S A.* 1990;**87**:9990-9994.

75. Nakashima K, Zhou X, Kunkel G, Zhang Z, Deng JM, Behringer RR, de Crombrugghe B. The novel zinc finger-containing transcription factor osterix is required for osteoblast differentiation and bone formation. *Cell.* 2002;**108**:17-29.
76. Beresford JN. Osteogenic stem-cells and the stromal system of bone and marrow. *Clin Orthop Relat Res.* 1989:270-280.
77. Manolagas SC. Birth and death of bone cells: basic regulatory mechanisms and implications for the pathogenesis and treatment of osteoporosis. *Endocr Rev.* 2000;**21**:115-137.
78. Skerry TM, Bitensky L, Chayen J, Lanyon LE. Early strain-related changes in enzyme activity in osteocytes following bone loading in vivo. *J Bone Miner Res.* 1989;**4**:783-788.
79. MacDonald BR, Takahashi N, McManus LM, Holahan J, Mundy GR, Roodman GD. Formation of multinucleated cells that respond to osteotropic hormones in long term human bone marrow cultures. *Endocrinology.* 1987;**120**:2326-2333.
80. Baron R. Molecular mechanisms of bone resorption by the osteoclast. *Anatom Rec.* 1989;**224**:317-324.
81. Hilborn J, Bjursten LM. A new and evolving paradigm for biocompatibility. *J Tissue Eng Regen Med.* 2007;**1**:110-119.
82. Martin RB. The importance of mechanical loading in bone biology and medicine. *J Musculoskelet Neuronal Interact.* 2007;**7**:48-53.
83. Spencer GJ, Genever PG. Long-term potentiation in bone--a role for glutamate in strain-induced cellular memory? *BMC Cell Biol.* 2003;**4**:9.
84. Szczesniak AM, Gilbert RW, Mukhida M, Anderson GI. Mechanical loading modulates glutamate receptor subunit expression in bone. *Bone.* 2005;**37**:63-73.
85. Rubin J, Rubin C, Jacobs CR. Molecular pathways mediating mechanical signaling in bone. *Gene.* 2006;**367**:1-16.
86. Goldring MB, Goldring SR. Skeletal tissue response to cytokines. *Clin Orthop Relat Res.* 1990:245-278.
87. Canalis E. Effect of insulin-like growth factor-1 on DNA and protein synthesis in cultured rat calvaria. *J Clin Invest.* 1980;**66**:709-719.
88. Celil AB, Campbell PG. BMP-2 and insulin-like growth factor-I mediate Osterix (Osx) expression in human mesenchymal stem cells via the MAPK and protein kinase D signaling pathways. *J Biol Chem.* 2005;**280**:31353-31359.
89. Bonewald LF, Mundy GR. Role of transforming growth factor-beta in bone remodelling. *Clin Orthop Relat Res.* 1990:261-276.
90. Chenu C, Pfeilschifter J, Mundy GR, Roodman GD. Transforming growth factor-beta inhibits formation of osteoclast-like cells in log-term human marrow cultures. *Proc Natl Acad Sci U S A.* 1988;**85**:5683-5687.
91. Alliston T, Choy L, Ducy P, Karsenty G, Derynck R. TGF-beta-induced repression of CBFA1 by Smad3 decreases cbfa1 and osteocalcin expression and inhibits osteoblast differentiation. *EMBO J.* 2001;**20**:2254-2272.
92. Maeda S, Hayashi M, Komiya S, Imamura T, Miyazono K. Endogenous TGF-beta signaling suppresses maturation of osteoblastic mesenchymal cells. *EMBO J.* 2004;**23**:552-563.
93. Robey PG, Young MF, Flanders KC, Roche NS, Kondaiah P, Reddi AH, Termine JD, Sporn MB, Roberts AB. Osteoblasts synthesize and respond to transforming growth factor-type beta (TGF-beta) in vitro. *J Cell Biol.* 1987;**105**:457-463.
94. Niswander L, Martin GR. FGF-4 and BMP-2 have opposite effects on limb growth. *Nature.* 1993;**361**:68-71.

95. Canalis E, Raisz LG. Effect of fibroblast growth factor on cultured fetal rat calvaria. *Metabolism.* 1980;**29**:108-114.
96. Hurley MM, Abreu C, Harrison JR, Lichtler AC, Raisz LG, Kream BE. Basic fibroblast growth factor inhibits type I collagen gene expression in osteoblastic MC3T3-E1 cells. *J Biol Chem.* 1993;**268**:5588-5593.
97. Mansukhani A, Bellosta P, Sahni M, Basilico C. Signaling by fibroblast growth factors (FGF) and fibroblast growth factor receptor 2 (FGFR2)-activating mutations blocks mineralization and induces apoptosis in osteoblasts. *J Cell Biol.* 2000;**149**:1297-1308.
98. Rydziel S, Durant D, Canalis E. Platelet-derived growth factor induces collagenase 3 transcription in osteoblasts through the activator protein 1 complex. *J Cell Physiol.* 2000;**184**:326-333.
99. Graves DT, Valentin-Opran A, Delgado R, Valente AJ, Mundy G, Piche J. The potential role of platelet-derived growth factor as an autocrine or paracrine factor for human bone cells. *Connect Tissue Res.* 1989;**23**:209-218.
100. Wang EA, Rosen V, Dalessandro JS, et al. Recombinant human bone morphogenetic protein induces bone-formation. *Proc Natl Acad Sci U S A.* 1990;**87**:2220-2224.
101. Hughes FJ, Collyer J, Stanfield M, Goodman SA. The effects of bone morphogenetic protein-2, -4, and -6 on differentiation of rat osteoblast cells in vitro. *Endocrinology.* 1995;**136**:2671-2677.
102. Urist MR, Strates BS. Bone morphogenetic protein. *J Dent Res.* 1971;**50**:1392-1406.
103. Zhou S. TGF-beta regulates beta-catenin signaling and osteoblast differentiation in human mesenchymal stem cells. *J Cell Biochem.* 2011;**112**:1651-1660.
104. McCarthy TL, Centrella M. Novel links among Wnt and TGF-beta signaling and Runx2. *Mol Endocrinol.* 2010;**24**:587-597.
105. Tang N, Song WX, Luo J, et al. BMP-9-induced osteogenic differentiation of mesenchymal progenitors requires functional canonical Wnt/beta-catenin signalling. *J Cell Mol Med.* 2009;**13**:2448-2464.
106. Kamiya N, Kobayashi T, Mochida Y, Yu PB, Yamauchi M, Kronenberg HM, Mishina Y. Wnt inhibitors Dkk1 and Sost are downstream targets of BMP signaling through the type IA receptor (BMPRIA) in osteoblasts. *J Bone Miner Res.* 2010;**25**:200-210.
107. Gaur T, Lengner CJ, Hovhannisyan H, et al. Canonical WNT signaling promotes osteogenesis by directly stimulating Runx2 gene expression. *J Biol Chem.* 2005;**280**:33132-33140.
108. Rawadi G, Vayssiere B, Dunn F, Baron R, Roman-Roman S. BMP-2 controls alkaline phosphatase expression and osteoblast mineralization by a Wnt autocrine loop. *J Bone Miner Res.* 2003;**18**:1842-1853.
109. Winkler DG, Sutherland MS, Ojala E, Turcott E, Geoghegan JC, Shpektor D, Skonier JE, Yu C, Latham JA. Sclerostin inhibition of Wnt-3a-induced C3H10T1/2 cell differentiation is indirect and mediated by bone morphogenetic proteins. *J Biol Chem.* 2005;**280**:2498-2502.
110. Gowen M, Wood DD, Ihrie EJ, McGuire MKB, Russell RGG. An interleukin-1 like factor stimulates bone resorption in vitro. *Nature.* 1983;**306**:378-380.
111. Hanazawa S, Ohmori Y, Amano S, Hirose K, Miyoshi T, Kumegawa M, Kitano S. Human purified interleukin-1 inhibits DNA synthesis and cell growth of osteoblastic cell line (MC3T3-E1), but enhances alkaline phosphatase activity in the cells. *FEBS Lett.* 1986;**203**:279-284.
112. Ohmori Y, Hanazawa S, Amano S, Hirose K, Kumegawa M, Kitano S. Effects of recombinant human interleukin-1 alpha and interleukin-1 beta on cell

growth and alakline phosphatase of the mouse osteoblastic cell line MC3T3-E1. *Biochimica et biophysica acta.* 1988;**970**:22-30.
113. Canalis E. Interleukin-1 has independent effects on deoxyribonucleic acid and collagen synthesis in cultures of rat calvariae. *Endocrinology.* 1986;**118**:74-81.
114. Ellies LG, Aubin JE. Temporal sequence of interleukin-1 alpha-mediated stimulation and inhibition of bone formation by isolated fetal rat calvaria cells in vitro. *Cytokine.* 1990;**2**:430-437.
115. Stashenko P, Dewhirst FE, Rooney ML, Desjardins LA, Heeley JD. Interleukin-1 beta is a potent inhibitor of bone formation in vitro. *J Bone Miner Res.* 1987;**2**:559-565.
116. Rickard DJ, Gowen M, MacDonald BR. Proliferative responses to estradiol, IL-1 alpha and TGF beta by cells expressing alkaline phosphatase in human osteoblast-like cell cultures. *Calcif Tissue Int.* 1993;**52**:227-233.
117. Littlewood AJ, Aarden LA, Evans DB, Russell RGG, Gowen M. Human osteoblast-like cells do not respond to interleukin-6. *J Bone Miner Res.* 1991;**6**:141-148.
118. Hughes FJ, Howells GL. Interleukin-6 inhibits bone formation in vitro. *Bone Miner.* 1993;**21**:21-28.
119. Yeh LC, Zavala MC, Lee JC. Osteogenic protein-1 and interleukin-6 with its soluble receptor synergistically stimulate rat osteoblastic cell differentiation. *J Cell Physiol.* 2002;**190**:322-331.
120. Bertolini DR, Nedwin GE, Bringman TS, Smith DD, Mundy GR. Stimulation of bone resorption and inhibition of bone formation in vitro by human tumour necrosis factors. *Nature.* 1986;**319**:516-518.
121. Gowen M, MacDonald BR, Russell RG. Actions of recombinant human gamma-interferon and tumor necrosis factor alpha on the proliferation and osteoblastic characteristics of human trabecular bone cells in vitro. *Arthritis Rheum.* 1988;**31**:1500-1507.
122. Smith DD, Gowen M, Mundy GR. Effects of interferon-gamma and other cytokines on collagen synthesis in fetal rat bone cultures. *Endocrinology.* 1987;**120**:2494-2499.
123. Takayanagi H, Sato K, Takaoka A, Taniguchi T. Interplay between interferon and other cytokine systems in bone metabolism. *Immunol Rev.* 2005;**208**:181-193.
124. Marsh JL, Slongo TF, Agel J, et al. Fracture and dislocation classification compendium-2007 - Orthopaedic Trauma Association classification, database and outcomes committee. *J Orthop Trauma.* 2007;**21**:S1-S133.
125. Lien E, Ingalls RR. Toll-like receptors. *Crit Care Med.* 2002;**30**:S1-11.
126. Oppenheim J, Feldmann M, Durum SK. Cytokine Reference: A compendium of cytokines and other mediators of host defence. London: London; San Diego: Academic Press; 2001.
127. Park YG, Kim KW, Song KH, Lee JM, Hong JJ, Moon SK, Kim CH. Combinatory responses of proinflamamtory cytokines on nitric oxide-mediated function in mouse calvarial osteoblasts. *Cell Bio Int.* 2009;**33**:92-99.
128. Hughes FJ, Buttery LD, Hukkanen MV, O'Donnell a, Maclouf J, Polak JM. Cytokine-induced prostaglandin E2 synthesis and cyclooxygenase-2 activity are regulated both by a nitric oxide-dependent and -independent mechanism in rat osteoblasts in vitro. *J Biol Chem.* 1999;**274**:1776-1782.
129. Schroder K, Hertzog PJ, Ravasi T, Hume DA. Interferon-gamma: an overview of signals, mechanisms and functions. *J Leukoc Biol.* 2004;**75**:163-189.
130. Kaley G, Weiner R. Prostaglandin E1: A potential mediator of the inflammatory reponse. *Ann N Y Acad Sci.* 1971;**180**:338-350.

131. Willoughby DA. Effects of prostaglandins PGF2a and PGE1 on vascular permeability. *J Pathol Bacteriol.* 1968;**96**:381-387.
132. Brocklehurst WE. Role of kinins and prostaglandins in inflammation. *Proc R Soc Med.* 1971;**64**:4-6.
133. Majno G, Palade GE. Studies on inflammation. 1. The effect of histamine and serotonin on vascular permeability: an electron microscopic study. *J Biophys Biochem Cytol.* 1961;**11**:571-605.
134. Frank MM, Fries LF. The role of complement in inflammation and phagocytosis. *Immunol Today.* 1991;**12**:322-326.
135. Coleman JW. Nitric oxide in immunity and inflammation. *Int Immunopharmacol.* 2001;**1**:1397-1406.
136. Willoughby D, Winyard PG. Inflammation Protocols. Totowa, NJ: Humana Press; 2003.
137. Ryan GB, Majno G. Acute inflammation. A review. *Am J Pathol.* 1977;**86**:183-276.
138. Feghali CA, Wright TM. Cytokines in acute and chronic inflammation. *Front Biosci.* 1997;**2**:d12-26.
139. Ali T, Lam D, Bronze MS, Humphrey MB. Osteoporosis in inflammatory bowel disease. *Am J Med.* 2009;**122**:599-604.
140. Shead EF, Haworth CS, Barker H, Bilton D, Compston JE. Osteoclast function, bone turnover and inflammatory cytokines during infective exacerbations of cystic fibrosis. *J Cyst Fibros.* 2010;**9**:93-98.
141. Yoshihara A, Seida Y, Hanada N, Miyazaki H. A longitudinal study of the relationship between periodontal disease and bone mineral density in community-dwelling older adults. *J Clin Periodontol.* 2004;**31**:680-684.
142. Niederberger E, Geisslinger G. The IKK-NF-kappaB pathway: a source for novel molecular drug targets in pain therapy? *FASEB journal : official publication of the Federation of American Societies for Experimental Biology.* 2008;**22**:3432-3442.
143. Schett G, Zwerina J, Firestein G. The p38 mitogen-activated protein kinase (MAPK) pathway in rheumatoid arthritis. *Annals of the rheumatic diseases.* 2008;**67**:909-916.
144. Thalhamer T, McGrath MA, Harnett MM. MAPKs and their relevance to arthritis and inflammation. *Rheumatology (Oxford, England).* 2008;**47**:409-414.
145. Redlich K, Smolen JS. Inflammatory bone loss: pathogenesis and therapeutic intervention. *Nature reviews. Drug discovery.* 2012;**11**:234-250.
146. Malemud CJ, Miller AH. Pro-inflammatory cytokine-induced SAPK/MAPK and JAK/STAT in rheumatoid arthritis and the new anti-depression drugs. *Expert opinion on therapeutic targets.* 2008;**12**:171-183.
147. Gallo J, Raska M, Mrazek F, Petrek M. Bone remodeling, particle disease and individual susceptibility to periprosthetic osteolysis. *Physiological research / Academia Scientiarum Bohemoslovaca.* 2008;**57**:339-349.
148. Skerry TM. The effects of the inflammatory response on bone growth. *Eur J Clin Nutr.* 1994;**48**:S190-S198.
149. Hopkins SJ. Cytokines and eicosanoids in rheumatic diseases. *Annals of the rheumatic diseases.* 1990;**49**:207-210.
150. Singer NG, Caplan AI. Mesenchymal stem cells: mechanisms of inflammation. *Annu Rev Pathol.* 2011;**6**:457-478.
151. Di Nicola M, Carlo-Stella C, Magni M, Milanesi M, Longoni PD, Matteucci P, Grisanti S, Gianni AM. Human bone marrow stromal cells suppress T-lymphocyte proliferation induced by cellular or nonspecific mitogenic stimuli. *Blood.* 2002;**99**:3838-3843.

152. Krampera M, Glennie S, Dyson J, Scott D, Laylor R, Simpson E, Dazzi F. Bone marrow mesenchymal stem cells inhibit the response of naive and memory antigen-specific T cells to their cognate peptide. *Blood.* 2003;**101**:3722-3729.
153. Aggarwal S, Pittenger MF. Human mesenchymal stem cells modulate allogeneic immune cell responses. *Cell.* 2005;**105**:1815-1822.
154. Drukker M, Katz G, Urbach A, Schuldiner M, Markel G, Itskovitz-Eldor J, Reubinoff B, Mandelboim O, Benvenisty N. Characterization of the expression of MHC proteins in human embryonic stem cells. *Proc Natl Acad Sci U S A.* 2002;**99**:9864-9869.
155. Draper JS, Pigott C, Thomson JA, Andrews PW. Surface antigens of human embryonic stem cells: changes upon differentiation in culture. *J Anat.* 2002;**200**:249-258.
156. Drukker M, Katchman H, Katz G, Friedman SET, Shezen E, Hornstein E, Mandelboim O, Reisner Y, Benvenisty N. Human embryonic stem cells and their differentiated derivatives are less susceptible to immune rejection than adult cells. *Stem Cells.* 2006;**24**:221-229.
157. Redd MJ, Cooper L, Wood W, Stramer B, Martin P. Wound healing and inflammation: embryos reveal the way to perfect repair. *Philos Trans R Soc Lond B Biol Sci.* 2004;**359**:777-784.
158. Martin P, Souza DD, Martin J, et al. Wound Healing in the PU . 1 Null Mouse — Tissue Repair Is Not Dependent on Inflammatory Cells. *Curr Biol.* 2003;**13**:1122-1128.
159. Robertson E, Bradley A, Kuehn M, Evans M. Germ-line transmission of genes introduced into cultured pluripotential cells by retroviral vector. *Nature.* 1986;**323**:445-448.
160. Keller G, Kennedy M, Papayannopoulou T, Wiles MV. Hematopoietic commitment during embryonic stem cell differentiation in culture. *Mol Cell Biol.* 1993;**13**:473-486.
161. McMahon AP, Bradley A. The Wnt-1 (int-1) proto-oncogene is required for development of a large region of the mouse brain. *Cell.* 1990;**62**:1073-1085.
162. Ecarot-Charrier B, Glorieux FH, Vanderrest M, Pereira G. Osteoblasts isolated from mouse calvaria initiate matrix mineralization in culture. *J Cell Biol.* 1983;**96**:639-643.
163. Helfrich MH, Evans DE, Grabowski PS, Pollock JS, Ohshima H, Ralston SH. Expression of nitric oxide synthase isoforms in bone and bone cell cultures. *J Bone Miner Res.* 1997;**12**:1108-1115.
164. Hwang YS, Polak JM, Mantalaris A. In vitro direct osteogenesis of murine embryonic stem cells without embryoid body formation. *Stem cells and development.* 2008;**17**:963-970.
165. Peck WA, Birge SJ, Jr., Brandt J. Collagen synthesis by isolated bone cells: stimulation by ascorbic acid in vitro. *Biochimica et biophysica acta.* 1967;**142**:512-525.
166. Ralston SH, Ho LP, Helfrich MH, Grabowski PS, Johnston PW, Benjamin N. Nitric oxide: a cytokine-induced regulator of bone resorption. *J Bone Miner Res.* 1995;**10**:1040-1049.
167. Zhao S, Fernald RD. Comprehensive algorithm for quantitative real-time polymerase chain reaction. *J Comput Biol.* 2005;**12**:1047-1064.
168. Kabat EA, Furth J. A histochemical study of the distribution of alkaline phosphatase in various normal and neoplastic tissues. *Am J Pathol.* 1941;**17**:303-318 305.
169. Dhillon A, Schneider P, Kuhn G, et al. Analysis of sintered polymer scaffolds using concomitant synchrotron computed tomography and in situ mechanical

testing. *Journal of materials science. Materials in medicine.* 2011;**22**:2599-2605.
170. Rahman CV, Ben-David D, Dhillon A, Kuhn G, Gould TW, Muller R, Rose FR, Shakesheff KM, Livne E. Controlled release of BMP-2 from a sintered polymer scaffold enhances bone repair in a mouse calvarial defect model. *J Tissue Eng Regen Med.* 2012.
171. Rahman CV, Cox HC, Hamilton LG, Quirk RA, Rose F, Shakesheff KM. Injectable Scaffold for Bone Tissue Engineering Applications. *J Pharm Pharmacol.* 2010;**62**:1508-1509.
172. Rahman CV, Kuhn G, White LJ, et al. PLGA/PEG-hydrogel composite scaffolds with controllable mechanical properties. *J Biomed Mater Res B Appl Biomater.* 2013.
173. Hurley MM, Fall P, Harrison JR, Petersen DN, Kream BE, Raisz LG. Effects of transforming growth factor-alpha and interleukin-1 on DNA synthesis, collagen-synthesis, procollagen messenger RNA levels, and prostaglandin E2 production in cultured fetal rat calvaria. *J Bone Miner Res.* 1989;**4**:731-736.
174. Ikeda E, Kusaka M, Hakeda Y, Yokota K, Kumegawa M, Yamamoto S. Effect of interleukin-1 beta on osteoblastic clone MC3T3-E1 cells. *Calcif Tissue Int.* 1988;**43**:162-166.
175. Damoulis PD, Hauschka PV. Cytokines induce nitric oxide production in mouse osteoblasts. *Biochem Biophys Res Commun.* 1994;**201**:924-931.
176. Akatsu T, Takahashi N, Udagawa N, Imamura K, Yamaguchi a, Sato K, Nagata N, Suda T. Role of prostaglandins in interleukin-1-induced bone resorption in mice in vitro. *J Bone Miner Res.* 1991;**6**:183-189.
177. Gowen M, Mundy GR. Actions of recombinant interleukin 1, interleukin 2, and interferon-gamma on bone resorption in vitro. *Journal of immunology (Baltimore, Md. : 1950).* 1986;**136**:2478-2482.
178. Williams TJ. The role of prostaglandins in inflammation. *Ann R Coll Surg Engl.* 1978;**60**:198-201.
179. Bolego C, Buccellati C, Prada A, Gaion RM, Folco G, Sala A. Critical role of COX-1 in prostacyclin production by human endothelial cells under modification of hydroperoxide tone. *FASEB journal : official publication of the Federation of American Societies for Experimental Biology.* 2009;**23**:605-612.
180. Willoughby D, Tomlinson A, eds. Inducible Enzymes in the Inflammatory Response. 1st ed. Basel: Birkhauser Verlag 1999.
181. Ignarro LJ. Nitric oxide. A novel signal transduction mechanism for transcellular communication. *Hypertension.* 1990;**16**:477-483.
182. Gross SS, Wolin MS. Nitric oxide: pathophysiological mechanisms. *Annu Rev Physiol.* 1995;**57**:737-769.
183. Damoulis PD, Hauschka PV. Nitric oxide acts in conjunction with proinflammatory cytokines to promote cell death in osteoblasts. *J Bone Miner Res.* 1997;**12**:412-422.
184. Kuzushima M, Mogi M, Togari A. Cytokine-induced nitric-oxide-dependent apoptosis in mouse osteoblastic cells: Involvement of p38MAP kinase. *Arch Oral Biol.* 2006;**51**:1048-1053.
185. Abe T, Hikiji H, Shin WS, Koshikiya N, Shima S-i, Nakata J, Susami T, Takato T, Toyo-oka T. Targeting of iNOS with antisense DNA plasmid reduces cytokine-induced inhibition of osteoblastic activity. *American journal of physiology, endocrinology and metabolism.* 2003;**285**:E614-621.
186. Hikiji H, Shin WS, Koizumi T, Takato T, Susami T, Koizumi Y, Okai-Matsuo Y, Toyo-Oka T. Peroxynitrite production by TNF-alpha and IL-1beta: implication for suppression of osteoblastic differentiation. *Am J Physiol Endocrinol Metab.* 2000;**278**:E1031-1037.

187. Lacey DC, Simmons PJ, Graves SE, Hamilton JA. Proinflammatory cytokines inhibit osteogenic differentiation from stem cells: implications for bone repair during inflammation. *Osteoarthritis Cartilage.* 2009;**17**:735-742.
188. de Brum-Fernandes AJ, Laporte S, Heroux M, Lora M, Patry C, Menard HA, Dumais R, Leduc R. Expression of prostaglandin endoperoxide synthase-1 and prostaglandin endoperoxide synthase-2 in human osteoblasts. *Biochem Biophys Res Commun.* 1994;**198**:955-960.
189. Saito S, Ngan P, Rosol T, Saito M, Shimizu H, Shinjo N, Shanfeld J, Davidovitch Z. Involvement of PGE Synthesis in the Effect of Intermittent Pressure and Interleukin-1 on Bone Resorption. *J Dent Res.* 1991;**70**:27-33.
190. Arpornmaeklong P, Wang Z, Pressler MJ, Brown SE, Krebsbach PH. Expansion and Characterization of Human Embryonic Stem Cell-Derived Osteoblast-Like Cells. *Cell Reprogram.* 2010;**12**:377-389.
191. Harkness L, Mahmood A, Ditzel N, Abdallah BM, Nygaard JV, Kassem M. Selective isolation and differentiation of a stromal population of human embryonic stem cells with osteogenic potential. *Bone.* 2011;**48**:231-241.
192. Gentleman E, Swain RJ, Evans ND, et al. Comparative materials differences revealed in engineered bone as a function of cell-specific differentiation. *Nat Mater.* 2009;**8**:763-770.
193. Rashidi H, Strohbuecker S, Jackson L, Kalra S, Blake AJ, France L, Tufarelli C, Sottile V. Differences in the pattern and regulation of mineral deposition in human cell lines of osteogenic and non-osteogenic origin. *Cells Tissues Organs.* 2012;**195**:484-494.
194. Zampetaki A, Zeng LF, Xiao QZ, Margariti A, Hu YH, Xu QB. Lacking cytokine production in ES cells and ES-cell-derived vascular cells stimulated by TNF-alpha is rescued by HDAC inhibitor trichostatin A. *Am J Physiol Cell Physiol.* 2007;**293**:C1226-C1238.
195. Kim YE, Kang HB, Park JA, Nam KH, Kwon HJ, Lee Y. Upregulation of NF-kappaB upon differentiation of mouse embryonic stem cells. *BMB Rep.* 2008;**41**:705-709.
196. Foldes G, Liu A, Badiger R, et al. Innate immunity in human embryonic stem cells: comparison with adult human endothelial cells. *PLoS One.* 2010;**5**:e10501.
197. Han KH, Ro H, Hong JH, et al. Immunosuppressive mechanisms of embryonic stem cells and mesenchymal stem cells in alloimmune response. *Transpl Immunol.* 2011;**25**:7-15.
198. Tan Z, Su ZY, Wu RR, Gu B, Liu YK, Zhao XL, Zhang M. Immunomodulative effects of mesenchymal stem cells derived from human embryonic stem cells in vivo and in vitro. *J Zhejiang Univ Sci B.* 2011;**12**:18-27.
199. Trivedi P, Hematti P. Derivation and immunological characterization of mesenchymal stromal cells from human embryonic stem cells. *Exp Hematol.* 2008;**36**:350-359.
200. Yen BL, Chang CJ, Liu KJ, Chen YC, Hu HI, Bai CH, Yen ML. Brief report - Human embryonic stem cell-derived mesenchymal progenitors possess strong immunosuppressive effects toward natural killer cells as well as T lymphocytes. *Stem Cells.* 2009;**27**:451-456.
201. Ladhoff J, Bader M, Brosel S, Effenberger E, Westermann D, Volk HD, Seifert M. Low immunogenicity of endothelial derivatives from rat embryonic stem cell-like cells. *Cell research.* 2009;**19**:507-518.
202. Drukker M, Benvenisty N. The immunogenicity of human embryonic stem-derived cells. *Trends Biotechnol.* 2004;**22**.

203. Swijnenburg RJ, Tanaka M, Vogel H, et al. Embryonic stem cell immunogenicity increases upon differentiation after transplantation into ischemic myocardium. *Circulation.* 2005;**112**:I166-172.
204. Hidalgo LG, Halloran PF. Role of IFN-gamma in allograft rejection. *Crit Rev Immunol.* 2002;**22**:317-349.
205. Collins T, Korman AJ, Wake CT, et al. Immune interferon activates multiple class II major histocompatibility complex genes and the assocites invariant chain gene in human-endothelial cells and dermal fibroblasts. *Proc Natl Acad Sci U S A.* 1984;**81**:4917-4921.
206. Lee EY, Xia Y, Kim WS, Kim MH, Kim TH, Kim KJ, Park BS, Sung JH. Hypoxia-enhanced wound-healing function of adipose-derived stem cells: Increase in stem cell proliferation and up-regulation of VEGF and bFGF. *Wound Repair Regen.* 2009;**17**:540-547.
207. Chamberlain G, Fox J, Ashton B, Middleton J. Concise review: Mesenchymal stem cells: Their phenotype, differentiation capacity, immunological features, and potential for homing. *Stem Cells.* 2007;**25**:2739-2749.
208. Mansilla E, Marin GH, Sturla F, et al. Human mesenchymal stem cells are tolerized by mice and improve skin and spinal cord injuries. *Transplantation Proc.* 2005;**37**:292-294.
209. Liu H, Kemeny DM, Heng BC, Ouyang HW, Melendez AJ, Cao T. The immunogenicity and immunomodulatory function of osteogenic cells differentiated from mesenchymal stem cells. *Journal of immunology (Baltimore, Md. : 1950).* 2006;**176**:2864-2871.
210. Ortiz LA, Dutreil M, Fattman C, Pandey AC, Torres G, Go K, Phinney DG. Interleukin 1 receptor antagonist mediates the antiinflammatory and antifibrotic effect of mesenchymal stem cells during lung injury. *Proc Natl Acad Sci U S A.* 2007;**104**:11002-11007.
211. Sotiropoulou PA, Perez SA, Gritzapis AD, Baxevanis CN, Papamichail M. Interactions between human mesenchymal stem cells and natural killer cells. *Stem Cells.* 2006;**24**:74-85.
212. Mishra PK. Bone marrow-derived mesenchymal stem cells for treatment of heart failure: is it all paracrine actions and immunomodulation? *J Cardiovasc Med.* 2008;**9**:122-128.
213. Wang XJ, Li QP. The roles of mesenchymal stem cells (MSCs) therapy in ischemic heart diseases. *Biochem Biophys Res Commun.* 2007;**359**:189-193.
214. Tarnowski CP, Ignelzi MA, Morris MD. Mineralization of developing mouse calvaria as revealed by Raman microspectroscopy. *J Bone Miner Res.* 2002;**17**:1118-1126.
215. Hasegawa Y, Shimada K, Suzuki N, Takayama T, Kato T, Iizuka T, Sato S, Ito K. The in vitro osteogenetic characteristics of primary osteoblastic cells from a rabbit calvarium. *J Oral Sci.* 2008;**50**:427-434.
216. Evans ND, Gentleman E, Chen X, Roberts CJ, Polak JM, Stevens MM. Extracellular matrix-mediated osteogenic differentiation of murine embryonic stem cells. *Biomaterials.* 2010;**31**:3244-3252.
217. Moursi AM, Damsky CH, Lull J, Zimmerman D, Doty SB, Aota S, Globus RK. Fibronectin regulates calvarial osteoblast differentiation. *J Cell Sci.* 1996;**109 (Pt 6)**:1369-1380.
218. Nefussi JR, Brami G, Modrowski D, Oboeuf M, Forest N. Sequential expression of bone matrix proteins during rat calvaria osteoblast differentiation and bone nodule formation in vitro. *The journal of histochemistry and cytochemistry : official journal of the Histochemistry Society.* 1997;**45**:493-503.

219. de Oliveira PT, Zalzal SF, Irie K, Nanci A. Early expression of bone matrix proteins in osteogenic cell cultures. *The journal of histochemistry and cytochemistry : official journal of the Histochemistry Society.* 2003;**51**:633-641.
220. Franceschi RT. The developmental control of osteoblast-specific gene expression: role of specific transcription factors and the extracellular matrix environment. *Crit Rev Oral Biol Med.* 1999;**10**:40-57.
221. Quarles LD, Yohay DA, Lever LW, Caton R, Wenstrup RJ. Distinct proliferative and differentiated stages of murine MC3T3-E1 cells in culture: an in vitro model of osteoblast development. *J Bone Miner Res.* 1992;**7**:683-692.
222. Gerstenfeld LC, Chipman SD, Glowacki J, Lian JB. Expression of differentiated function by mineralizing cultures of chicken osteoblasts. *Dev Biol.* 1987;**122**:49-60.
223. Owen TA, Aronow M, Shalhoub V, et al. Progressive development of the rat osteoblast phenotype in vitro: reciprocal relationships in expression of genes associated with osteoblast proliferation and differentiation during formation of the bone extracellular matrix. *J Cell Physiol.* 1990;**143**:420-430.
224. Franceschi RT, Iyer BS. Relationship between collagen synthesis and expression of the osteoblast phenotype in MC3T3-E1 cells. *J Bone Miner Res.* 1992;**7**:235-246.
225. Woll NL, Heaney JD, Bronson SK. Osteogenic nodule formation from single embryonic stem cell-derived progenitors. *Stem cells and development.* 2006;**15**:865-879.
226. Sottile V, Thomson A, McWhir J. In vitro osteogenic differentiation of human ES cells. *Cloning Stem Cells.* 2003;**5**:149-155.
227. Woll NL, Bronson SK. Analysis of embryonic stem cell-derived osteogenic cultures. *Methods in molecular biology.* 2006;**330**:149-159.
228. Pagkalos J, Cha JM, Kang Y, Heliotis M, Tsiridis E, Mantalaris A. Simvastatin induces osteogenic differentiation of murine embryonic stem cells. *J Bone Miner Res.* 2010;**25**:2470-2478.
229. Kawaguchi J, Mee PJ, Smith AG. Osteogenic and chondrogenic differentiation of embryonic stem cells in response to specific growth factors. *Bone.* 2005;**36**:758-769.
230. Phillips BW, Belmonte N, Vernochet C, Ailhaud G, Dani C. Compactin enhances osteogenesis in murine embryonic stem cells. *Biochem Biophys Res Commun.* 2001;**284**:478-484.
231. zur Nieden NI, Kempka G, Ahr HJ. In vitro differentiation of embryonic stem cells into mineralized osteoblasts. *Differentiation.* 2003;**71**:18-27.
232. zur Nieden NI, Kempka G, Rancourt DE, Ahr HJ. Induction of chondro-, osteo- and adipogenesis in embryonic stem cells by bone morphogenetic protein-2: effect of cofactors on differentiating lineages. *BMC Dev Biol.* 2005;**5**:1.
233. Alfred R, Taiani JT, Krawetz RJ, Yamashita A, Rancourt DE, Kallos MS. Large-scale production of murine embryonic stem cell-derived osteoblasts and chondrocytes on microcarriers in serum-free media. *Biomaterials.* 2011;**32**:6006-6016.
234. Dodds RA, Merry K, Littlewood A, Gowen M. Expression of mRNA for IL1 beta, IL6 and TGF beta 1 in developing human bone and cartilage. *The journal of histochemistry and cytochemistry : official journal of the Histochemistry Society.* 1994;**42**:733-744.
235. Einhorn TA, Majeska RJ, Rush EB, Levine PM, Horowitz MC. The expression of cytokine activity by fracture callus. *J Bone Miner Res.* 1995;**10**:1272-1281.
236. Walsh S, Jefferiss C, Stewart K, Jordan GR, Screen J, Beresford JN. Expression of the developmental markers STRO-1 and alkaline phosphatase in cultures of human marrow stromal cells: regulation by fibroblast growth

factor (FGF)-2 and relationship to the expression of FGF receptors 1-4. *Bone.* 2000;**27**:185-195.
237. Herbertson A, Aubin JE. Cell sorting enriches osteogenic populations in rat bone marrow stromal cell cultures. *Bone.* 1997;**21**:491-500.
238. Purpura KA, Zandstra PW, Aubin JE. Fluorescence activated cell sorting reveals heterogeneous and cell non-autonomous osteoprogenitor differentiation in fetal rat calvaria cell populations. *J Cell Biochem.* 2003;**90**:109-120.
239. van den Dolder J, Jansen JA. Enrichment of osteogenic cell populations from rat bone marrow stroma. *Biomaterials.* 2007;**28**:249-255.
240. Tare RS, Mitchell PD, Kanczler J, Oreffo RO. Isolation, differentiation, and characterisation of skeletal stem cells from human bone marrow in vitro and in vivo. *Methods in molecular biology.* 2012;**816**:83-99.
241. Pera MF, Reubinoff B, Trounson A. Human embryonic stem cells. *J Cell Sci.* 2000;**113 (Pt 1)**:5-10.
242. Adewumi O, Aflatoonian B, Ahrlund-Richter L, et al. Characterization of human embryonic stem cell lines by the International Stem Cell Initiative. *Nat Biotechnol.* 2007;**25**:803-816.
243. Bourne S, Polak JM, Hughes SPF, Buttery LDK. Osteogenic differentiation of mouse embryonic stem cells: Differential gene expression analysis by cDNA microarray and purification of osteoblasts by cadherin-11 magnetically activated cell sorting. *Tissue engineering.* 2004;**10**:796-806.
244. Okazaki M, Takeshita S, Kawai S, Kikuno R, Tsujimura A, Kudo A, Amann E. Molecular cloning and characterization of OB-cadherin, a new member of cadherin family expressed in osteoblasts. *J Biol Chem.* 1994;**269**:12092-12098.
245. Kawaguchi J, Kii I, Sugiyama Y, Takeshita S, Kudo A. The transition of cadherin expression in osteoblast differentiation from mesenchymal cells: consistent expression of cadherin-11 in osteoblast lineage. *J Bone Miner Res.* 2001;**16**:260-269.
246. Bellows C, Aubin J, Heersche J, Antosz M. Mineralized bone nodules formed in vitro from enzymatically released rat calvaria cell populations. *Calcif Tissue Int.* 1986;**38**:143-154.
247. Bellows CG, Aubin JE. Determination of numbers of osteoprogenitors present in isolated fetal rat calvaria cells in vitro. *Dev Biol.* 1989;**133**:8-13.
248. Beresford JN, Graves SE, Smoothy CA. Formation of mineralized nodules by bone derived cells in vitro: a model of bone formation? *Am J Med Genet.* 1993;**45**:163-178.
249. Hoffmann I, Balling R. Cloning and expression analysis of a novel mesodermally expressed cadherin. *Dev Biol.* 1995;**169**:337-346.
250. Kimura Y, Matsunami H, Inoue T, Shimamura K, Uchida N, Ueno T, Miyazaki T, Takeichi M. Cadherin-11 expressed in association with mesenchymal morphogenesis in the head, somite, and limb bud of early mouse embryos. *Dev Biol.* 1995;**169**:347-358.
251. Tsuboi M, Kawakami A, Nakashima T, et al. Tumor necrosis factor-alpha and interleukin-1 beta increase the Fas-mediated apoptosis of human osteoblasts. *J Lab Clin Med.* 1999;**134**:222-231.
252. Kaur K, Hardy R, Ahasan MM, et al. Synergistic induction of local glucocorticoid generation by inflammatory cytokines and glucocorticoids: implications for inflammation associated bone loss. *Annals of the rheumatic diseases.* 2010;**69**:1185-1190.
253. Togari A, Arai M, Mogi M, Kondo A, Nagatsu T. Coexpression of GTP cyclohydrolase I and inducible nitric oxide synthase mRNAs in mouse

osteoblastic cells activated by proinflammatory cytokines. *FEBS Lett.* 1998;**428**:212-216.
254. Vermes C, Chandrasekaran R, Jacobs JJ, Galante JO, Roebuck KA, Glant TT. The effects of particulate wear debris, cytokines, and growth factors on the functions of MG-63 osteoblasts. *J Bone Joint Surg Am.* 2001;**83A**:201-211.
255. Pischon N, Darbois LM, Palamakumbura AH, Kessler E, Trackman PC. Regulation of collagen deposition and lysyl oxidase by tumor necrosis factor-alpha in osteoblasts. *J Biol Chem.* 2004;**279**:30060-30065.
256. Kuroki T, Shingu M, Koshihara Y, Nobunaga M. Effects of cytokines on alkaline phosphatase and osteocalcin production, calcification and calcium release by human osteoblastic cells. *Br J Rheumatol.* 1994;**33**:224-230.
257. Gowen M, Nedwin GE, Mundy GR. Preferential inhibition of cytokine-stimulated bone resorption by recombinant inteferon-gamma. *J Bone Miner Res.* 1986;**1**:469-474.
258. Ding J, Ghali O, Lencel P, Broux O, Chauveau C, Devedjian JC, Hardouin P, Magne D. TNF-alpha and IL-1beta inhibit RUNX2 and collagen expression but increase alkaline phosphatase activity and mineralization in human mesenchymal stem cells. *Life Sci.* 2009;**84**:499-504.
259. Hess K, Ushmorov A, Fiedler J, Brenner RE, Wirth T. TNFalpha promotes osteogenic differentiation of human mesenchymal stem cells by triggering the NF-kappaB signaling pathway. *Bone.* 2009;**45**:367-376.
260. Mountziaris PM, Tzouanas SN, Mikos AG. The interplay of bone-like extracellular matrix and TNF signalling on *in vitro* differentiation of mesenchymal stem cells. *Journal of biomedical materials research. Part A.* 2012;**100A**:1097-1106.
261. Arpornmaeklong P, Brown SE, Wang Z, Krebsbach PH. Phenotypic characterization, osteoblastic differentiation, and bone regeneration capacity of human embryonic stem cell-derived mesenchymal stem cells. *Stem cells and development.* 2009;**18**:955-968.
262. Cheng SL, Lecanda F, Davidson MK, Warlow PM, Zhang SF, Zhang L, Suzuki S, St John T, Civitelli R. Human osteoblasts express a repertoire of cadherins, which are critical for BMP-2-induced osteogenic differentiation. *J Bone Miner Res.* 1998;**13**:633-644.
263. Di Benedetto A, Watkins M, Grimston S, Salazar V, Donsante C, Mbalaviele G, Radice GL, Civitelli R. N-cadherin and cadherin 11 modulate postnatal bone growth and osteoblast differentiation by distinct mechanisms. *J Cell Sci.* 2010;**123**:2640-2648.
264. Willis RA, Nussler AK, Fries KM, Geller DA, Phipps RP. Induction of nitric oxide synthase in subsets of murine pulmonary fibroblasts: effect on fibroblast interleukin-6 production. *Clin Immunol Immunopathol.* 1994;**71**:231-239.
265. Robbins RA, Barnes PJ, Springall DR, Warren JB, Kwon OJ, Buttery LD, Wilson AJ, Geller DA, Polak JM. Expression of inducible nitric oxide in human lung epithelial cells. *Biochem Biophys Res Commun.* 1994;**203**:209-218.
266. Unemori EN, Ehsani N, Wang M, Lee S, McGuire J, Amento EP. Interleukin-1 and transforming growth factor-alpha: synergistic stimulation of metalloproteinases, PGE2, and proliferation in human fibroblasts. *Experimental cell research.* 1994;**210**:166-171.
267. Chang SK, Noss EH, Chen M, et al. Cadherin-11 regulates fibroblast inflammation. *Proc Natl Acad Sci U S A.* 2011;**108**:8402-8407.
268. Kiener HP, Karonitsch T. The synovium as a privileged site in rheumatoid arthritis: cadherin-11 as a dominant player in synovial pathology. *Best Pract Res Clin Rheumatol.* 2011;**25**:767-777.

269. McKibbin B. The biology of fracture healing in long bones. *J Bone Joint Surg Br.* 1978;**60-B**:150-162.
270. Schaffer M, Barbul A. Lymphocyte function in wound healing and following injury. *Br J Surg.* 1998;**85**:444-460.
271. Mountziaris PM, Mikos AG. Modulation of the inflammatory response for enhanced bone tissue regeneration. *Tissue Eng Part B Rev.* 2008;**14**:179-186.
272. Kon T, Cho TJ, Aizawa T, Yamazaki M, Nooh N, Graves D, Gerstenfeld LC, Einhorn TA. Expression of osteoprotegerin, receptor activator of NF-kappaB ligand (osteoprotegerin ligand) and related proinflammatory cytokines during fracture healing. *J Bone Miner Res.* 2001;**16**:1004-1014.
273. Cho TJ, Gerstenfeld LC, Einhorn TA. Differential temporal expression of members of the transforming growth factor beta superfamily during murine fracture healing. *J Bone Miner Res.* 2002;**17**:513-520.
274. Rundle CH, Wang H, Yu H, et al. Microarray analysis of gene expression during the inflammation and endochondral bone formation stages of rat femur fracture repair. *Bone.* 2006;**38**:521-529.
275. Kolar P, Schmidt-Bleek K, Schell H, Gaber T, Toben D, Schmidmaier G, Perka C, Buttgereit F, Duda GN. The early fracture hematoma and its potential role in fracture healing. *Tissue Eng Part B Rev.* 2010;**16**:427-434.
276. Perumal V, Roberts CS. (ii) Factors contributing to non-union of fractures. *Curr Orthop.* 2007;**21**:258-261.
277. Dimitriou R, Mataliotakis GI, Angoules AG, Kanakaris NK, Giannoudis PV. Complications following autologous bone graft harvesting from the iliac crest and using the RIA: a systematic review. *Injury.* 2011;**42 Suppl 2**:S3-15.
278. Ferreira AM, Gentile P, Chiono V, Ciardelli G. Collagen for bone tissue regeneration. *Acta biomaterialia.* 2012;**8**:3191-3200.
279. Wildemann B, Kadow-Romacker A, Haas NP, Schmidmaier G. Quantification of various growth factors in different demineralized bone matrix preparations. *Journal of biomedical materials research. Part A.* 2007;**81**:437-442.
280. Ryan G, Pandit A, Apatsidis DP. Fabrication methods of porous metals for use in orthopaedic applications. *Biomaterials.* 2006;**27**:2651-2670.
281. Ohtsuki C, Kamitakahara M, Miyazaki T. Bioactive ceramic-based materials with designed reactivity for bone tissue regeneration. *J R Soc Interface.* 2009;**6 Suppl 3**:S349-360.
282. Bohner M. Calcium orthophosphates in medicine: from ceramics to calcium phosphate cements. *Injury.* 2000;**31 Suppl 4**:37-47.
283. Sabir M, Xu X, Li L. A review on biodegradable polymeric materials for bone tissue engineering applications. *J Mater Sci.* 2009;**44**:5713-5724.
284. Corry D, Moran J. Assessment of acrylic bone cement as a local delivery vehicle for the application of non-steroidal anti-inflammatory drugs. *Biomaterials.* 1998;**19**:1295-1301.
285. Bostman O, Pihlajamaki H. Clinical biocompatibility of biodegradable orthopaedic implants for internal fixation: a review. *Biomaterials.* 2000;**21**:2615-2621.
286. Mourino V, Boccaccini AR. Bone tissue engineering therapeutics: controlled drug delivery in three-dimensional scaffolds. *J R Soc Interface.* 2010;**7**:209-227.
287. Smoak KA, Cidlowski JA. Mechanisms of glucocorticoid receptor signaling during inflammation. *Mech Ageing Dev.* 2004;**125**:697-706.
288. Aspenberg P. Drugs and fracture repair. *Acta Orthop.* 2005;**76**:741-748.
289. Schacke H, Docke WD, Asadullah K. Mechanisms involved in the side effects of glucocorticoids. *Pharmacol Ther.* 2002;**96**:23-43.

290. Khaled K, Sarhan HA, Ibrahim MA, Ali AH, Naguib YW. Prednisolone-Loaded PLGA Microspheres. In Vitro Characterization and In Vivo Application in Adjuvant-Induced Arthritis in Mice. *Aaps Pharmscitech.* 2010;**11**:859-869.
291. Hickey T, Kreutzer D, Burgess DJ, Moussy F. In vivo evaluation of a dexamethasone/PLGA microsphere system designed to suppress the inflammatory tissue response to implantable medical devices. *Journal of biomedical materials research. Part A.* 2002;**61**:180-187.
292. Vane JR, Botting RM. Mechanism of action of nonsteroidal anti-inflammatory drugs. *Am J Med.* 1998;**104**:2S-8S; discussion 21S-22S.
293. Rainsford KD. Profile and mechanisms of gastrointestinal and other side effects of nonsteroidal anti-inflammatory drugs (NSAIDs). *Am J Med.* 1999;**107**:27S-35S; discussion 35S-36S.
294. Kurmis AP, Kurmis TP, O'Brien JX, Dalen T. The effect of nonsteroidal anti-inflammatory drug administration on acute phase fracture-healing: a review. *J Bone Joint Surg Am.* 2012;**94**:815-823.
295. Cottrell J, O'Connor JP. Effect of Non-Steroidal Anti-Inflammatory Drugs on Bone Healing. *Pharmaceuticals.* 2010;**3**:1668-1693.
296. Pountos I, Georgouli T, Calori GM, Giannoudis PV. Do nonsteroidal anti-inflammatory drugs affect bone healing? A critical analysis. *ScientificWorldJournal.* 2012;**2012**:606404.
297. Barry S. Non-steroidal anti-inflammatory drugs inhibit bone healing: a review. *Vet Comp Orthop Traumatol.* 2010;**23**:385-392.
298. Simon AM, Manigrasso MB, O'Connor JP. Cyclo-oxygenase 2 function is essential for bone fracture healing. *J Bone Miner Res.* 2002;**17**:963-976.
299. Zhang X, Schwarz EM, Young DA, Puzas JE, Rosier RN, O'Keefe RJ. Cyclooxygenase-2 regulates mesenchymal cell differentiation into the osteoblast lineage and is critically involved in bone repair. *J Clin Invest.* 2002;**109**:1405-1415.
300. Tunçay M, Caliş S, Kaş HS, Ercan MT, Peksoy I, Hincal aa. Diclofenac sodium incorporated PLGA (50:50) microspheres: formulation considerations and in vitro/in vivo evaluation. *Int J Pharm.* 2000;**195**:179-188.
301. Della Porta G, Falco N, Reverchon E. NSAID Drugs Release from Injectable Microspheres Produced by Supercritical Fluid Emulsion Extraction. *Journal of pharmaceutical sciences.* 2010;**99**:1484-1499.
302. Cantón I, McKean R, Charnley M, Blackwood Ka, Fiorica C, Ryan AJ, MacNeil S. Development of an Ibuprofen-releasing biodegradable PLA/PGA electrospun scaffold for tissue regeneration. *Biotechnol Bioeng.* 2010;**105**:396-408.
303. Ring A, Goertz O, Muhr G, Steinau HU, Langer S. In vivo microvascular response of murine cutaneous muscle to ibuprofen-releasing polyurethane foam. *Int Wound J.* 2008;**5**:464-469.
304. Malaviya AP, Ostor AJ. Rheumatoid arthritis and the era of biologic therapy. *Inflammopharmacology.* 2012;**20**:59-69.
305. Lavi G, Voronov E, Dinarello CA, Apte RN, Cohen S. Sustained delivery of IL-1Ra from biodegradable microspheres reduces the number of murine B16 melanoma lung metastases. *J Control Release.* 2007;**123**:123-130.
306. Huuskonen J, Suuronen T, Miettinen R, van Groen T, Salminen A. A refined in vitro model to study inflammatory responses in organotypic membrane culture of postnatal rat hippocampal slices. *J Neuroinflammation.* 2005;**2**:25.
307. Olinga P, Merema MT, de Jager MH, et al. Rat liver slices as a tool to study LPS-induced inflammatory response in the liver. *J Hepatol.* 2001;**35**:187-194.

308. Smith EL, Locke M, Waddington RJ, Sloan AJ. An ex vivo rodent mandible culture model for bone repair. *Tissue engineering. Part C, Methods.* 2010;**16**:1287-1296.
309. Nikkola L, Seppala J, Harlin A, Ndreu A, Ashammakhi N. Electrospun multifunctional diclofenac sodium releasing nanoscaffold. *J Nanosci Nanotechnol.* 2006;**6**:3290-3295.
310. Attama AA, Reichl S, Muller-Goymann CC. Diclofenac sodium delivery to the eye: in vitro evaluation of novel solid lipid nanoparticle formulation using human cornea construct. *Int J Pharm.* 2008;**355**:307-313.
311. Stellato C. Post-transcriptional and nongenomic effects of glucocorticoids. *Proc Am Thorac Soc.* 2004;**1**:255-263.
312. Bladh LG, Liden J, Pazirandeh A, Rafter I, Dahlman-Wright K, Nilsson S, Okret S. Identification of target genes involved in the antiproliferative effect of glucocorticoids reveals a role for nuclear factor-(kappa)B repression. *Mol Endocrinol.* 2005;**19**:632-643.
313. Brewer JA, Khor B, Vogt SK, Muglia LM, Fujiwara H, Haegele KE, Sleckman BP, Muglia LJ. T-cell glucocorticoid receptor is required to suppress COX-2-mediated lethal immune activation. *Nat Med.* 2003;**9**:1318-1322.
314. Lasa M, Brook M, Saklatvala J, Clark AR. Dexamethasone destabilizes cyclooxygenase 2 mRNA by inhibiting mitogen-activated protein kinase p38. *Mol Cell Biol.* 2001;**21**:771-780.
315. Korhonen R, Lahti A, Hamalainen M, Kankaanranta H, Moilanen E. Dexamethasone inhibits inducible nitric-oxide synthase expression and nitric oxide production by destabilizing mRNA in lipopolysaccharide-treated macrophages. *Mol Pharmacol.* 2002;**62**:698-704.
316. Waters RV, Gamradt SC, Asnis P, Vickery BH, Avnur Z, Hill E, Bostrom M. Systemic corticosteroids inhibit bone healing in a rabbit ulnar osteotomy model. *Acta Orthop Scand.* 2000;**71**:316-321.
317. O'Brien CA, Jia D, Plotkin LI, Bellido T, Powers CC, Stewart SA, Manolagas SC, Weinstein RS. Glucocorticoids act directly on osteoblasts and osteocytes to induce their apoptosis and reduce bone formation and strength. *Endocrinology.* 2004;**145**:1835-1841.
318. Weinstein RS, Jilka RL, Parfitt AM, Manolagas SC. Inhibition of osteoblastogenesis and promotion of apoptosis of osteoblasts and osteocytes by glucocorticoids. Potential mechanisms of their deleterious effects on bone. *J Clin Invest.* 1998;**102**:274-282.
319. Jaiswal N, Haynesworth SE, Caplan AI, Bruder SP. Osteogenic differentiation of purified, culture-expanded human mesenchymal stem cells in vitro. *J Cell Biochem.* 1997;**64**:295-312.
320. Hoes JN, Jacobs JW, Buttgereit F, Bijlsma JW. Current view of glucocorticoid co-therapy with DMARDs in rheumatoid arthritis. *Nat Rev Rheumatol.* 2010;**6**:693-702.
321. Mitchell JA, Akarasereenont P, Thiemermann C, Flower RJ, Vane JR. Selectivity of nonsteroidal antiinflammatory drugs as inhibitors of constitutive and inducible cyclooxygenase. *Proc Natl Acad Sci U S A.* 1993;**90**:11693-11697.
322. Aeberhard EE, Henderson SA, Arabolos NS, Griscavage JM, Castro FE, Barrett CT, Ignarro LJ. Nonsteroidal anti-inflammatory drugs inhibit expression of the inducible nitric oxide synthase gene. *Biochem Biophys Res Commun.* 1995;**208**:1053-1059.
323. Amin AR, Vyas P, Attur M, Leszczynska-Piziak J, Patel IR, Weissmann G, Abramson SB. The mode of action of aspirin-like drugs: effect on inducible nitric oxide synthase. *Proc Natl Acad Sci U S A.* 1995;**92**:7926-7930.

324. Kepka-Lenhart D, Chen LC, Morris SM, Jr. Novel actions of aspirin and sodium salicylate: discordant effects on nitric oxide synthesis and induction of nitric oxide synthase mRNA in a murine macrophage cell line. *J Leukoc Biol.* 1996;**59**:840-846.
325. Salvemini D, Manning PT, Zweifel BS, Seibert K, Connor J, Currie MG, Needleman P, Masferrer JL. Dual inhibition of nitric oxide and prostaglandin production contributes to the antiinflammatory properties of nitric oxide synthase inhibitors. *J Clin Invest.* 1995;**96**:301-308.
326. Kanematsu M, Ikeda K, Yamada Y. Interaction between nitric oxide synthase and cyclooxygenase pathways in osteoblastic MC3T3-E1 cells. *J Bone Miner Res.* 1997;**12**:1789-1796.
327. Tetsuka T, Daphna-Iken D, Srivastava SK, Baier LD, DuMaine J, Morrison AR. Cross-talk between cyclooxygenase and nitric oxide pathways: prostaglandin E2 negatively modulates induction of nitric oxide synthase by interleukin 1. *Proc Natl Acad Sci U S A.* 1994;**91**:12168-12172.
328. Salvemini D, Settle SL, Masferrer JL, Seibert K, Currie MG, Needleman P. Regulation of prostaglandin production by nitric oxide; an in vivo analysis. *Br J Pharmacol.* 1995;**114**:1171-1178.
329. Bakker AC, Joosten LAB, Arntz OJ, Helsen MMA, Bendele AM, vandeLoo FAJ, vandenBerg WB. Prevention of murine collagen-induced arthritis in the knee and ipsilateral paw by local expression of human interleukin-1 receptor antagonist protein in the knee. *Arthritis Rheum.* 1997;**40**:893-900.
330. Cohen S, Hurd E, Cush J, et al. Treatment of rheumatoid arthritis with anakinra, a recombinant human interleukin-1 receptor antagonist, in combination with methotrexate - Results of a twenty-four-week, multicenter, randomized, double-blind, placebo-controlled trial. *Arthritis Rheum.* 2002;**46**:614-624.
331. Donahue KE, Jonas DE, Hansen RA, et al. Drug Therapy for Rheumatoid Arthrits in Adults:An Update. Comparitive Effectiveness Reviews. Vol 55: Agency for Healthcare Research and Quality (US); 2012.
332. Fleischmann R, Iqbal I, Nandeshwar P, Quiceno A. Safety and efficacy of disease-modifying anti-rheumatic agents: focus on the benefits and risks of etanercept. *Drug Saf.* 2002;**25**:173-197.
333. Chang JK, Li CJ, Liao HJ, Wang CK, Wang GJ, Ho ML. Anti-inflammatory drugs suppress proliferation and induce apoptosis through altering expressions of cell cycle regulators and pro-apoptotic factors in cultured human osteoblasts. *Toxicology.* 2009;**258**:148-156.
334. Chang JK, Li CJ, Wu SC, Yeh CH, Chen CH, Fu YC, Wang GJ, Ho ML. Effects of anti-inflammatory drugs on proliferation, cytotoxicity and osteogenesis in bone marrow mesenchymal stem cells. *Biochem Pharmacol.* 2007;**74**:1371-1382.
335. Ho ML, Chang JK, Chuang LY, Hsu HK, Wang GJ. Effects of nonsteroidal anti-inflammatory drugs and prostaglandins on osteoblastic functions. *Biochem Pharmacol.* 1999;**58**:983-990.
336. Utvag SE, Fuskevag OM, Shegarfi H, Reikeras O. Short-term treatment with COX-2 inhibitors does not impair fracture healing. *J Invest Surg.* 2010;**23**:257-261.
337. Adolphson P, Abbaszadegan H, Jonsson U, Dalen N, Sjoberg HE, Kalen S. No effects of piroxicam on osteopenia and recovery after Colles' fracture. A randomized, double-blind, placebo-controlled, prospective trial. *Arch Orthop Trauma Surg.* 1993;**112**:127-130.
338. van Staa TP, Leufkens HG, Cooper C. Use of nonsteroidal anti-inflammatory drugs and risk of fractures. *Bone.* 2000;**27**:563-568.

339. Krischak GD, Augat P, Blakytny R, Claes L, Kinzl L, Beck A. The non-steroidal anti-inflammatory drug diclofenac reduces appearance of osteoblasts in bone defect healing in rats. *Arch Orthop Trauma Surg.* 2007;**127**:453-458.
340. Bo J, Sudmann E, Marton PF. Effect of indomethacin on fracture healing in rats. *Acta Orthop Scand.* 1976;**47**:588-599.
341. Beck A, Krischak G, Sorg T, Augat P, Farker K, Merkel U, Kinzl L, Claes L. Influence of diclofenac (group of nonsteroidal anti-inflammatory drugs) on fracture healing. *Arch Orthop Trauma Surg.* 2003;**123**:327-332.
342. Altman RD, Latta LL, Keer R, Renfree K, Hornicek FJ, Banovac K. Effect of nonsteroidal antiinflammatory drugs on fracture healing: a laboratory study in rats. *J Orthop Trauma.* 1995;**9**:392-400.
343. Diaz-Rodriguez L, Garcia-Martinez O, Morales MA, Rodriguez-Perez L, Rubio-Ruiz B, Ruiz C. Effects of indomethacin, nimesulide, and diclofenac on human MG-63 osteosarcoma cell line. *Biol Res Nurs.* 2012;**14**:98-107.
344. Rahman CV, Smith SJ, Morgan PS, Langmack KA, D.C. M, Rose FR, Shakesheff KM, Grundy RG, Rahman R. Adjuvant chemotherapy for brain tumors delivered via a novel intra-cavity moldable polymer matrix. *Clin Cancer Res.* 2012.
345. Kang Y, Wu J, Yin G, Huang Z, Yao Y, Liao X, Chen A, Pu X, Liao L. Preparation, characterization and in vitro cytotoxicity of indomethacin-loaded PLLA/PLGA microparticles using supercritical CO2 technique. *Eur J Pharm Biopharm.* 2008;**70**:85-97.
346. Ju YM, Yu BZ, West L, Moussy Y, Moussy F. A dexamethasone-loaded PLGA micirospheres/collagen scaffold composite for implantable glucose sensors. *Journal of biomedical materials research. Part A.* 2010;**93A**:200-210.
347. Williams DF. On the mechanisms of biocompatibility. *Biomaterials.* 2008;**29**:2941-2953.
348. Anderson JM, Rodriguez A, Chang DT. Foreign body reaction to biomaterials. *Semin Immunol.* 2008;**20**:86-100.
349. Li L, Qian Y, Jiang C, Lv Y, Liu W, Zhong L, Cai K, Li S, Yang L. The use of hyaluronan to regulate protein adsorption and cell infiltration in nanofibrous scaffolds. *Biomaterials.* 2012;**33**:3428-3445.
350. Roach P, Eglin D, Rohde K, Perry CC. Modern biomaterials: a review - bulk properties and implications of surface modifications. *Journal of materials science. Materials in medicine.* 2007;**18**:1263-1277.
351. Granet C, Miossec P. Combination of the pro-inflammatory cytokines IL-1, TNF-alpha and IL-17 leads to enhanced expression and additional recruitment of AP-1 family members, Egr-1 and NF-kappa B in osteoblast-like cells. *Cytokine.* 2004;**26**:169-177.
352. Harbour ME, Gregory JW, Jenkins HR, Evans BA. Proliferative response of different human osteoblast-like cell models to proinflammatory cytokines. *Pediatr Res.* 2000;**48**:163-168.
353. Zini N, Lisignoli G, Solimando L, Bavelloni A, Grassi F, Guidotti L, Trimarchi C, Facchini A, Maraldi NM. IL1-beta and TNF-alpha induce changes in the nuclear polyphosphoinositide signalling system in osteoblasts similar to that occurring in patients with rheumatoid arthritis: an immunochemical and immunocytochemical study. *Histochemistry and Cell Biology.* 2003;**120**:243-250.
354. Chidgey AP, Layton D, Trounson A, Boyd RL. Tolerance strategies for stem-cell-based therapies. *Nature.* 2008;**453**:330-337.
355. Menendez P, Bueno C, Wang L, Bhatia M. Human embryonic stem cells: potential tool for achieving immunotolerance? *Stem cell reviews.* 2005;**1**:151-158.

356. Vats A, Tolley NS, Bishop AE, Polak JM. Embryonic stem cells and tissue engineering: delivering stem cells to the clinic. *J R Soc Med.* 2005;**98**:346-350.
357. Hmadcha A, Dominguez-Bendala J, Wakeman J, Arredouani M, Soria B. The immune boundaries for stem cell based therapies: problems and prospective solutions. *J Cell Mol Med.* 2009;**13**:1464-1475.
358. Keller G. Embryonic stem cell differentiation: emergence of a new era in biology and medicine. *Genes Dev.* 2005;**19**:1129-1155.

Appendix I – Batch Testing of Serum

Foetal bovine serum (FBS) batch testing was carried out to determine optimal serum for growth and osteogenic differentiation of mESCs and mouse primary calvarial cells.

Methods

Six batches of FBS, from different suppliers, were tested on both cell types. See table AI.1 for sera details. Mouse primary calvarial cells were plated in 6-well tissue culture treated plates and changed to standard primary calvarial osteogenic medium (50 mM BGP and 50 µg/mL ascorbate 2-phosphate) containing each serum type. After 21 days culture in the osteogenic medium, cells were fixed in 10% (*w/v*) formalin and stained with alizarin red S. Mouse embryonic stem cells were induced to form EBs in SNL culture medium containing each of the sera. EBs were dissociated and cells plated in monolayer in gelatin-coated 6-well plates. Cells were cultured for 21 days in osteogenic medium (50 mM BGP, 50 µg/mL ascorbate 2-phosphate, 10 µM dexamethasone), with different groups for each sera.

Table AI.1: Batches of serum for testing.

Sera	Source	Product Code	Lot Number
A	Sigma	F9665	109K3398
B	Sigma	F9665	070M3397
C	BioSera	FB-1001H	S08371S1810
D	BioSera	FB-1001H	S08370S1810
E	PAA	Standard FBS	A15-104
F	PAA	Gold FBS	A15-152

Results

Results of alizarin red staining of the mouse primary calvarial cells can be seen in figure AI.1. Images of staining show that nodules did not form when cells were cultured in serum A or F. Most successful nodule formation was seen in the when cells cultured with serum B and D. Quantification results indicated that serum B would be the optimal serum for osteogenic culture of mouse primary calvarial cells. From these results all further primary calvarial cell culture was performed with serum B, purchased from Sigma-Aldrich, product code F9665, lot number 070M3397.

Results for osteo-mESC staining can be seen in figure AI.2. Cells did not grow in serum A. In serum B and F, cell did stain bright red for calcium deposition, only background staining can be seen. Most successful sera for osteogenic differentiation of mESCs were serum C and D. Serum D, purchased from Biosera, product code FB1001H, lot number S08670S1810. was chosen for all further culture of mESCs.

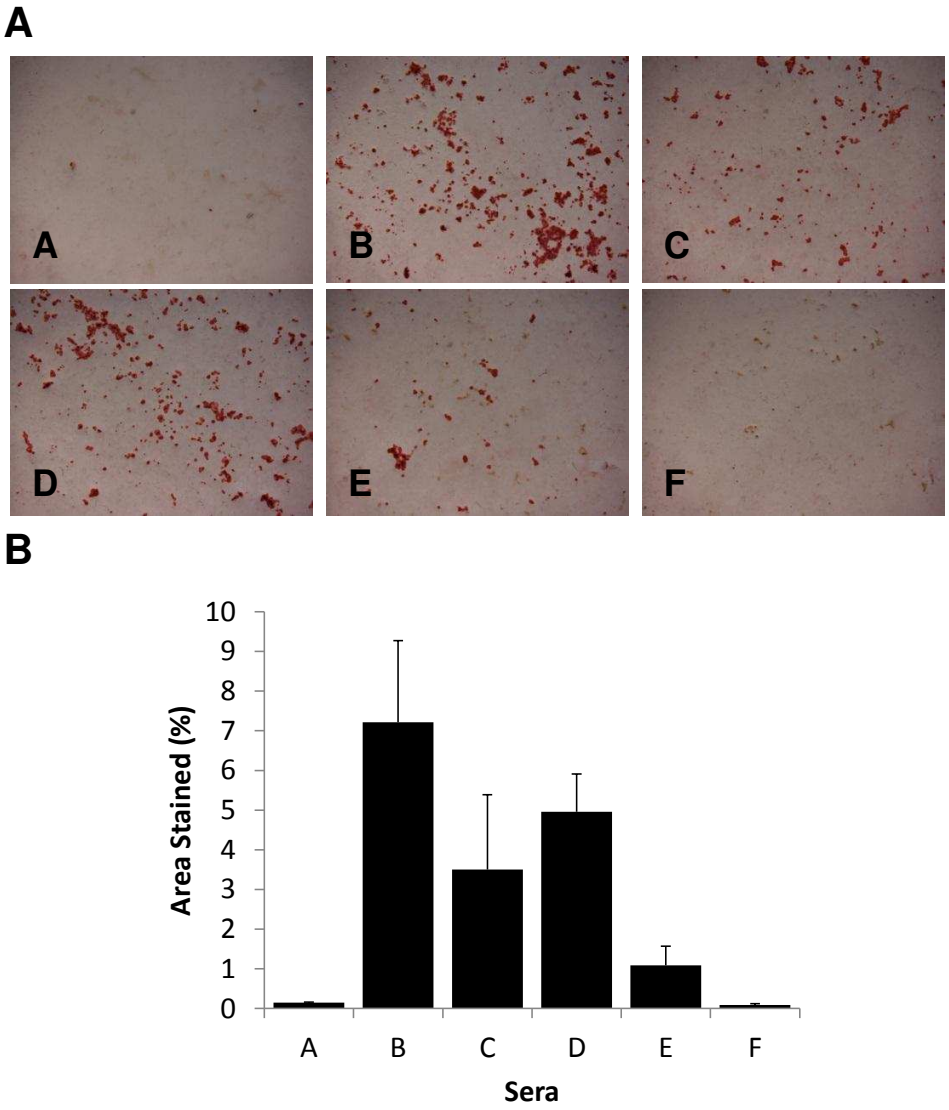

Figure AI.1: Serum batch testing results for mouse primary calvarial cells. (A) alizarin red S staining for bone nodule formation. (B) Quantification of alizarin red staining.

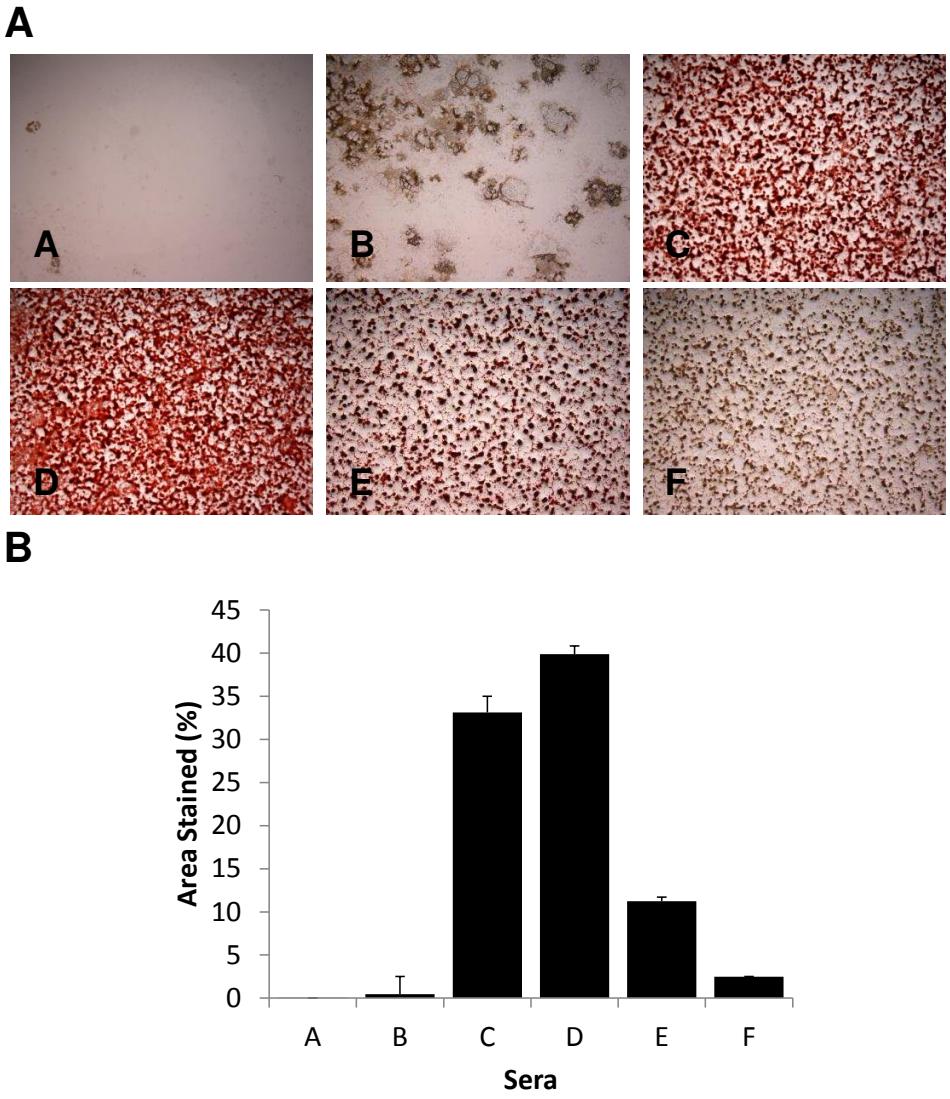

Figure AI.2: Serum batch testing results for osteo-mESCs (A) alizarin red S staining for bone nodule formation. (B) Quantification of alizarin red staining.

Appendix II – Cryopreservation Protocol

Cryopreservation

Cryopreservation of mouse primary calvarial cells, mESCs and SNLs was routinely performed. Cryopreservation medium for all cells consisted of FBS containing 10% (*v/v*) DMSO. In all cases, cells were detached from culture flask surface using trypsin/EDTA treatment, trypsin was inactivated with serum-containing medium and centrifuged (calvarial cells – 300 x g, mESCs and SNLs – 180 x g). The pellet was then resuspended in a small amount of cryopreservation medium and counted. Cells were suspended in the correct volume of cryopreservation medium to achieve a freezing density of 1,000,000 cells/mL for primary calvarial cells and SNLs and 2,000,000 cells/mL for mESCs. Cells were transferred to cryovials and placed into dedicated storage boxes for cryopreservation (CoolCell, Sanyo). These boxes allow the cell suspension to freeze at a consistent rate of -1°C/minute, increasing cell viability upon reanimation. Boxes were placed into a -80°C freezer for 24 hours, before cryovials transferred to liquid nitrogen storage.

Cell Reanimation from Storage

Cells were removed from liquid nitrogen storage and defrosted as rapidly as possible. When reanimating mESCs, immediately after thawing, the cell suspension was transferred to a volume of pre-warmed mESC medium and transferred to an SNL feeder layer for immediate culture. For SNLs and primary calvarial cells, after thawing, cell suspension was transferred to a volume of pre-warmed cell culture medium, centrifuged to remove DMSO, before being resuspended in medium, and transferred to a T75 cm^2 flask for further culture.

Appendix III – Trypan Blue Exclusion

Cell counts were performed using a trypan blue exclusion technique to estimate cell viability. When mixed with a cell suspension, trypan blue will penetrate the non-viable cells due to loss of membrane integrity and stain blue. Viable cells will remain colourless. This can then be seen under a haemocytometer. Equal volumes of 0.5% (*w/v*) trypan blue solution were mixed with a volume of cell suspension and 10 µL transferred to a haemocytometer. The cells were then counted under an inverted light microscope, disregarding the non-viable cells. Number of viable cells could be calculated and plated at the correct cell density for experiments.

Appendix IV – Paraformaldehyde

PFA was used as a cell fixative. To make a 4% (*w/v*) solution, first a 0.2 M phosphate buffer (pH 7.4) was made by dissolving 21.8 g Na_2HPO_4 and 6.4 g NaH_2PO_4 in 1 L distilled water. This was diluted to a 0.1 M solution with distilled water. To make the PFA, 40 g paraformaldehyde powder was added to 1 L of 0.1 M phosphate buffer. This was heated to 60-65°C whilst stirring, until dissolved. Drops of 1 M sodium hydroxide were added until the solution turned clear. The solution was then cooled, tested for pH 7.4 with pH paper and passed through 0.22 µm filters. The solution was aliquoted and stored at -20°C, until use.

Appendix V – PGES Immunocytochemistry

Results for PGES immunostaining can be seen in figure AV.1 (primary calvarial cells) and figure AV.2 (osteo-mESCs). PGES staining can be seen in the primary calvarial cells only when stimulated with proinflammatory cytokines, not in the control culture medium. This occurs at all differentiation timepoints. In osteo-mESC cultures, no PGES in seen in control medium or proinflammatory cytokine medium at day 0 or day 7. PGES staining can be seen to a small amount in day 14 proinflammatory cytokine medium and can be seen in large amounts when stimulated on day 21, in nodule-like areas.

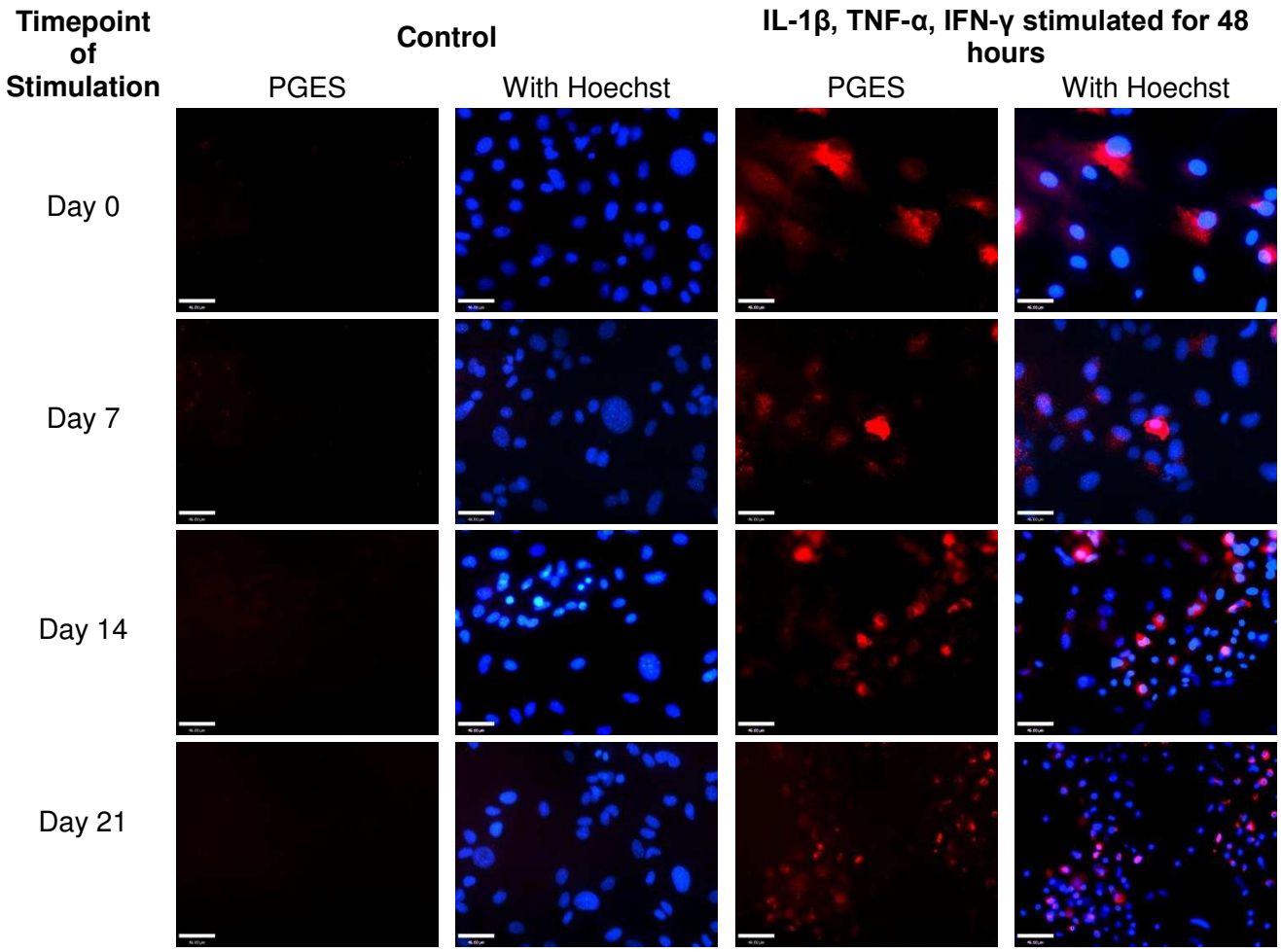

Figure AV.1: PGES expression in primary calvarial cells stimulated with proinflammatory cytokines. Cells were stimulated with IL-1β, TNFα and IFN-γ for 48 hours at either day 0, day 7, day 14 or day 21 of osteogenic culture before fixation. PGES expression in both proinflammatory cytokine stimulated and control cultures was assessed by immunocytochemistry. Representative images shown. Scale bar = 46 μm

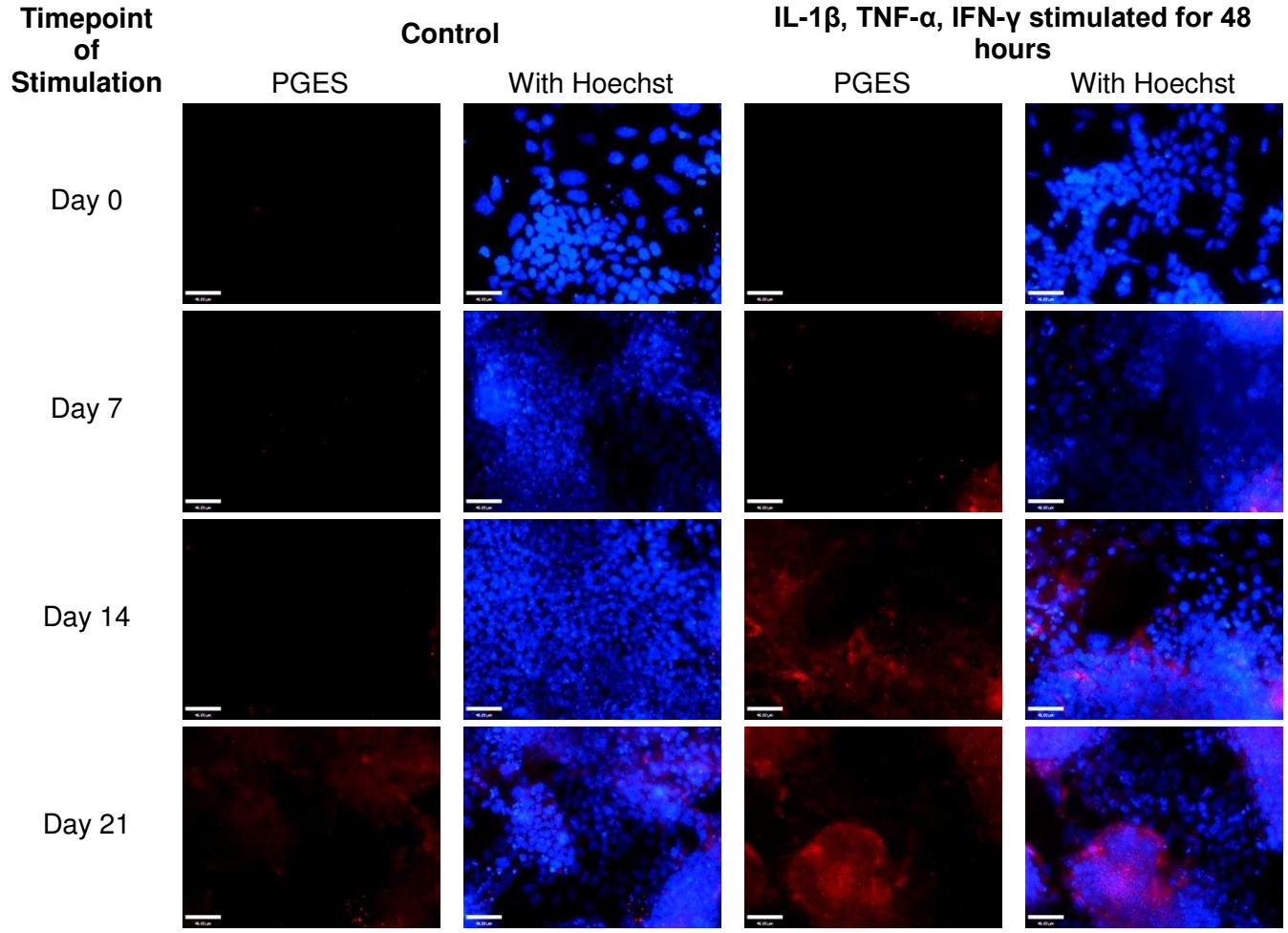

Figure AV.2: PGES expression in osteo-mESCs stimulated with proinflammatory cytokines. Cells were stimulated with IL-1β, TNFα and IFN-γ for 48 hours at either day 0, day 7, day 14 or day 21 of osteogenic culture before fixation. PGES expression in both proinflammatory cytokine stimulated and control cultures was assessed by immunocytochemistry. Representative images shown. Scale bar = 46 μm.

Appendix VI – mESC Conditioned Medium

Full result set showing the effect of mESC CM on viability and NO production of primary calvarial cells, in response to proinflammatory cytokines. Figure AVI.1 A and B show MTS assay results for day 3, day 7 and day 10. Figure AVI.1 C shows non-cumulative nitrite results for day 3, day 7 and day 10 medium collections.

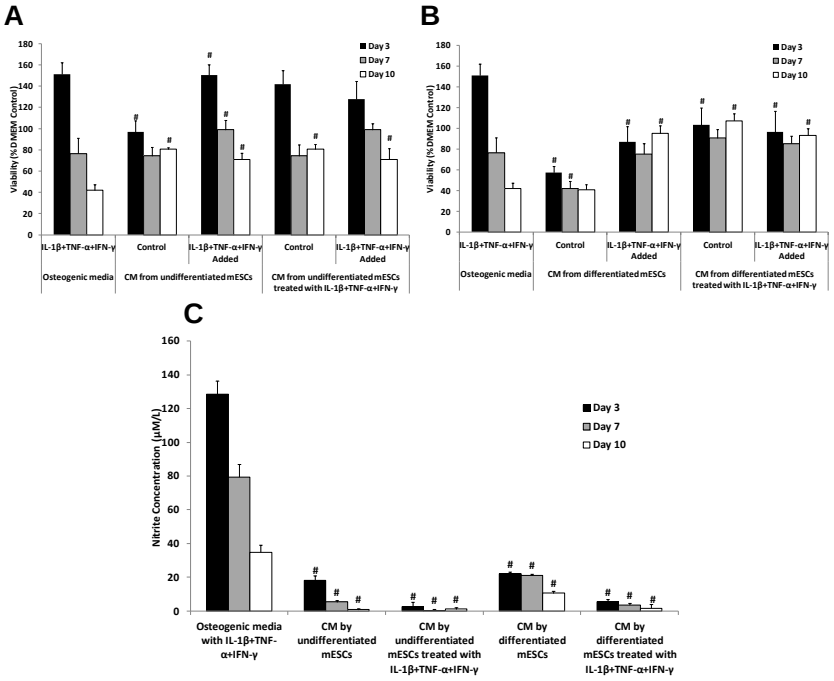

Figure AVI.1: Effect of mESC conditioned medium on primary calvarial cells treated with proinflammatory cytokines. (A and B) Viability of primary calvarial cells over 10 days, in OM with IL-1β, TNF-α and IFN-γ and various CM. (A) CM from undifferentiated mESCs, cultured with and without cytokines, and with and without supplemented cytokines when added to primary calvarial cells. (B) CM from differentiated mESCs, with and without IL-1β, TNF-α and IFN-γ, with and without supplemented cytokines when added to primary calvarial cells. Data shown as percentage of primary calvarial cell viability in control OM. Values shown as mean±SD, n=6, representative of 3 independent experiments. *Statistical significance vs. OM control (p≤0.01) #Statistical significance vs. OM with IL-1β, TNF-α and IFN-γ (p≤0.01). (C)Nitrite production by primary calvarial cells treated with CM from undifferentiated and differentiated mESCs, with and without cytokines. All groups supplemented with IL-1β, TNF-α and IFN-γ when added to primary calvarial cells. Control readings with no proinflammatory cytokines have been subtracted from treated groups. Values shown as mean±SD, n=6, representative of 3 independent experiments. #Statistical significance vs. OM with IL-1β, TNF-α and IFN-γ (p≤0.01).

Appendix VII – Anti-Inflammatory Effect of Prednisolone, Ibuprofen and Piroxicam

Basic validation of the primary calvarial cell inflammation model was carried out using a range of anti-inflammatory mediators. The results for prednisolone, ibuprofen and piroxicam can be seen in figures AVII.1, AVII.2 and AVII.3, respectively. Viability results for prednisolone (Figure AVII.1 A) show that the drug was not toxic to the cells at any concentration. However, prednisolone was only successful at inhibiting the toxic effects of the cytokines at a concentration of 100 µM. Prednisolone was only successful at inhibiting cytokine-induced-NO production at the highest concentration of 100 µM but inhibited cytokine-induced PGE_2 production at all concentrations.

Ibuprofen results (Figure AVII.2) showed the drug was most effective at improving cell viability in the presence of cytokines when at a concentration of 250–500 µM. This also correlated with a reduction in cytokine-induced NO and PGE_2 production.

Piroxicam (Figure AVII.3) was toxic to the cells at a concentration of 500 µM. The most effective results for piroxicam occurred at a concentration of 100 µM. Although, at this concentration cytokine-induced NO production was not inhibited. Piroxicam was a potent inhibitor of PGE_2 production by the primary calvarial cells in the presence of proinflammatory cytokines, across all concentrations.

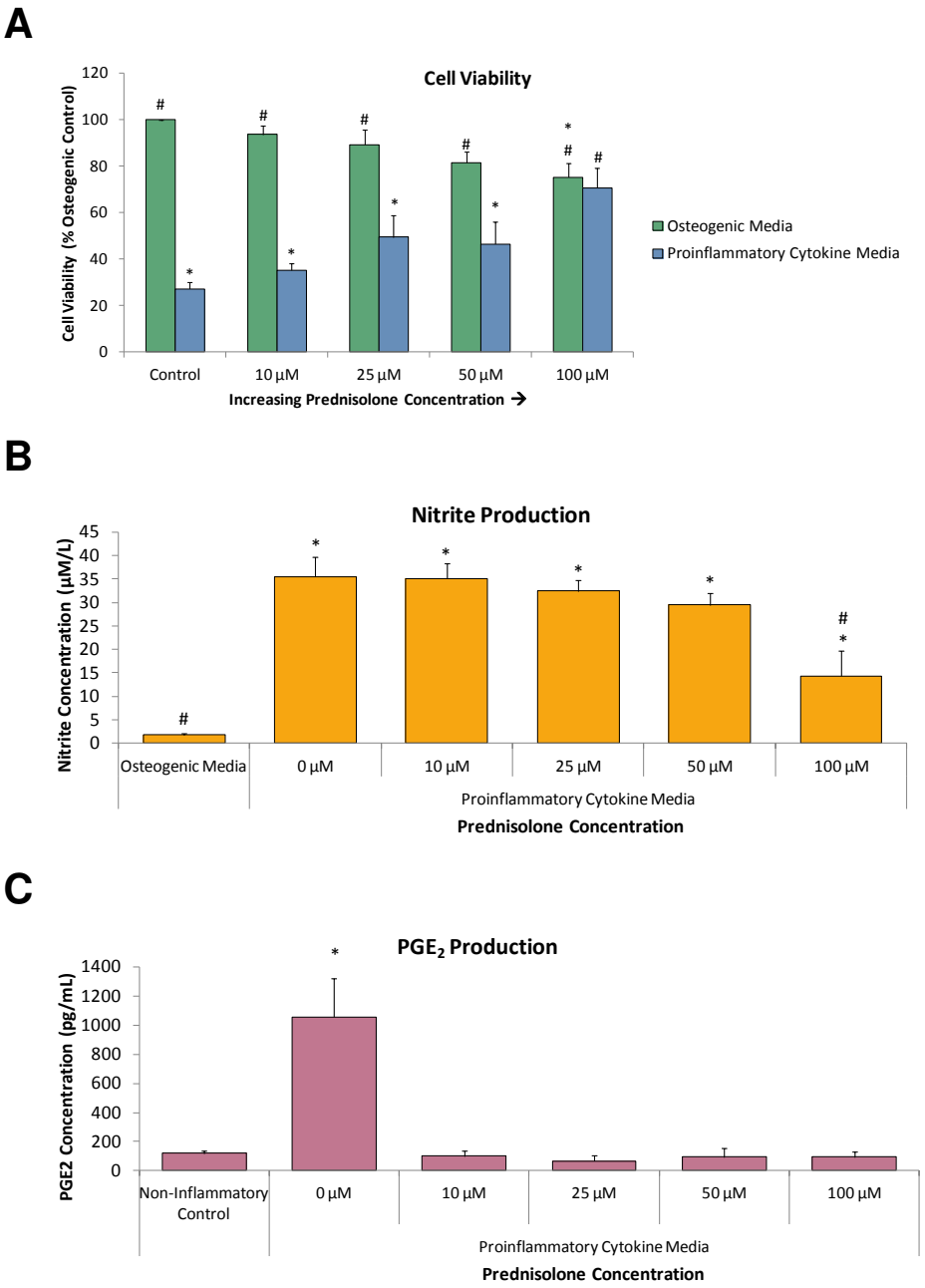

Figure AVII.1: Anti-inflammatory effect of prednisolone. Primary calvarial cells were cultured for 10 days in osteogenic media, before media supplemented with prednisolone and proinflammatory cytokines. (A) Cell viability, determined by MTS assay, after 3 days in either basal osteogenic or proinflammatory cytokine containing osteogenic media, with prednisolone at increasing concentrations. Values are represented as mean±SD, n=6. (B) Nitrite concentration in media after 3 days proinflammatory cytokine and prednisolone treatment. Values are represented as mean±SD, n=6. (C) PGE_2 concentration in media after 3 days proinflammatory cytokine and prednisolone treatment. Values are represented as mean±SD, n=4. #Statistical significance vs. proinflammatory cytokine control (0 ng/mL) ($p \leq 0.05$), *Statistical significance vs. osteogenic control ($p \leq 0.05$).

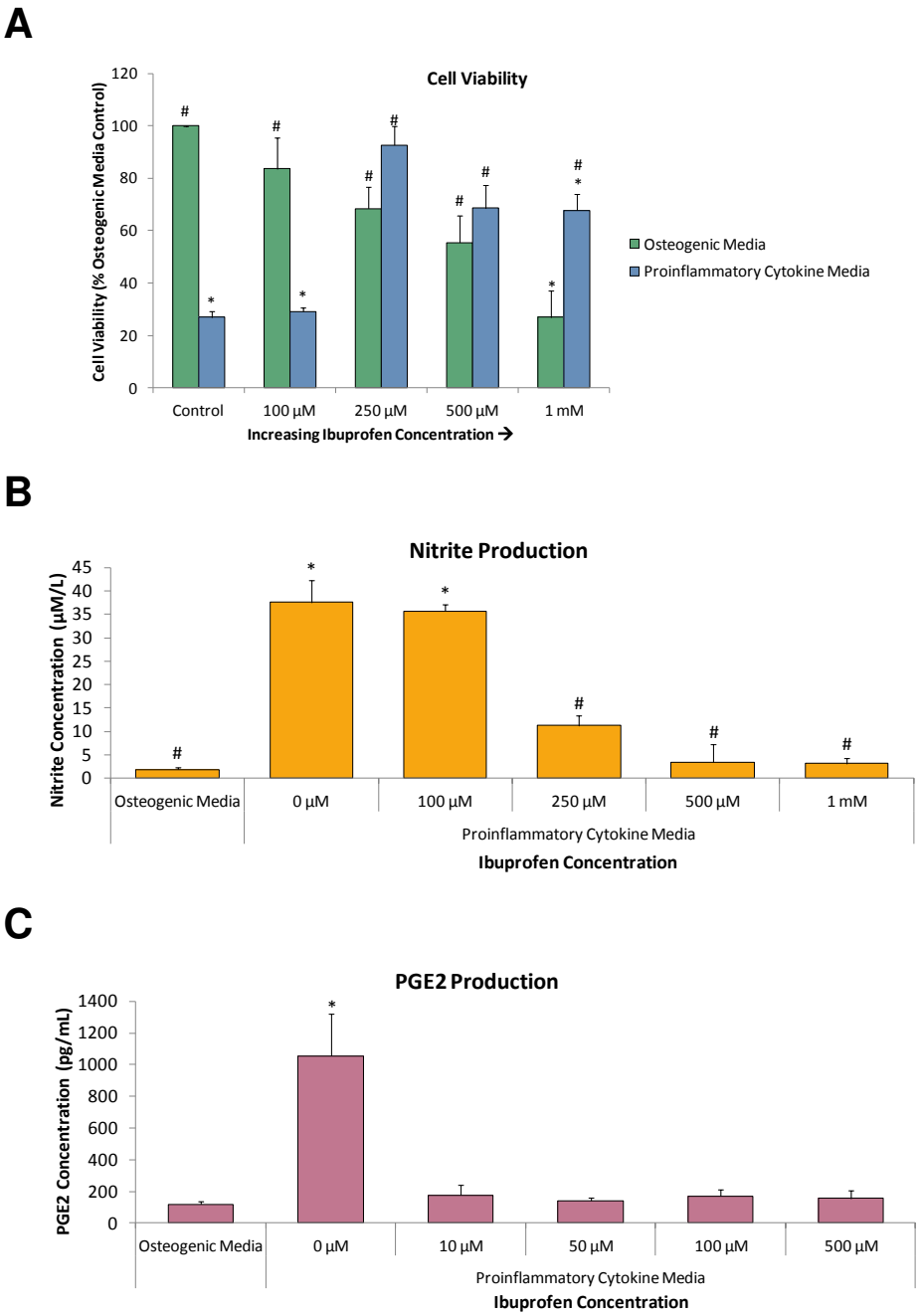

Figure AVII.2: Anti-inflammatory effect of ibuprofen. Primary calvarial cells were cultured for 10 days in osteogenic media, before media supplemented with ibuprofen and proinflammatory cytokines. (A) Cell viability, determined by MTS assay, after 3 days in either basal osteogenic or proinflammatory cytokine containing osteogenic media, with ibuprofen at increasing concentrations. Values are represented as mean±SD, n=6. (B) Nitrite concentration in media after 3 days proinflammatory cytokine and ibuprofen treatment. Values are represented as mean±SD, n=6. (C) PGE_2 concentration in media after 3 days proinflammatory cytokine and ibuprofen treatment. Values are represented as mean±SD, n=4. #Statistical significance vs. proinflammatory cytokine control (0 ng/mL) ($p \leq 0.05$), *Statistical significance vs. osteogenic control ($p \leq 0.05$).

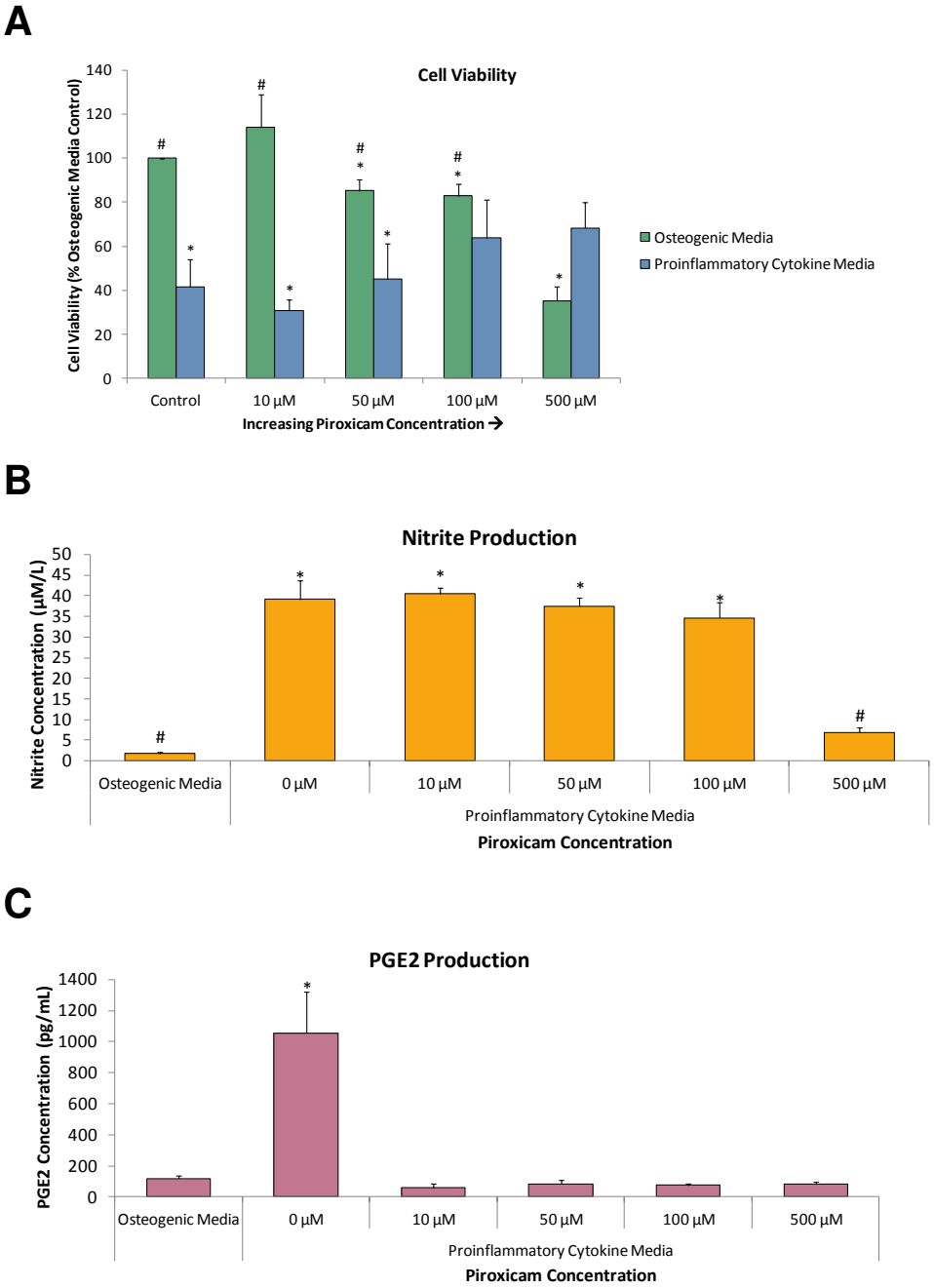

Figure AVII.3: Anti-inflammatory effect of piroxicam. Primary calvarial cells were cultured for 10 days in osteogenic media, before media supplemented with piroxicam and proinflammatory cytokines. (A) Cell viability, determined by MTS assay, after 3 days in either basal osteogenic or proinflammatory cytokine containing osteogenic media, with piroxicam at increasing concentrations. Values are represented as mean±SD, n=6. (B) Nitrite concentration in media after 3 days proinflammatory cytokine and piroxicam treatment. Values are represented as mean±SD, n=6. (C) PGE_2 concentration in media after 3 days proinflammatory cytokine and piroxicam treatment. Values are represented as mean±SD, n=4. #Statistical significance vs. proinflammatory cytokine control (0 ng/mL) ($p \leq 0.05$), *Statistical significance vs. osteogenic control ($p \leq 0.05$).